EXPERIMENTAL INVESTIGATION ON ESTIMATION AND PREDICTION OF SOUND IN PERCUSSIVE DRILLING

THESIS

Submitted in partial fulfillment of the requirements for the degree of

DOCTOR OF PHILOSOPHY

By

SANGSHETTY KIVADE

DEPARTMENT OF MINING ENGINEERING

NATIONAL INSTITUTE OF TECHNOLOGY KARNATAKA

SURATHKAL, MANGALORE - 575 025

OCTOBER 2013

EXPERIMENTAL INVESTIGATION ON ESTIMATION AND PREDICTION OF SOUND IN PERCUSSIVE DRILLING

THESIS

Submitted in partial fulfillment of the requirements for the degree of

DOCTOR OF PHILOSOPHY

By

SANGSHETTY KIVADE

DEPARTMENT OF MINING ENGINEERING

NATIONAL INSTITUTE OF TECHNOLOGY KARNATAKA

SURATHKAL, MANGALORE - 575 025

OCTOBER 2013

DECLARATION
by the Ph.D. Research Scholar

I hereby *declare* that the Research Thesis entitled, **"Experimental Investigation on Estimation and Prediction of Sound in Percussive Drilling"** which is being submitted to the **National Institute of Technology Karnataka, Surathkal** in partial fulfillment of the requirements for the award of the Degree of **Doctor of Philosophy** in **Mining Engineering** is a *bonafide report of the research work carried out by me.* The material contained in this Research Thesis has not been submitted to any University or Institution for the award of any degree.

Sangshetty Kivade

(Register No.: **060410MN06P03**)

Department of Mining Engineering

Place: NITK - Surathkal,

Date: 15/10/2013

C E R T I F I C A T E

This is to certify that the Research Thesis entitled, **"Experimental Investigation on Estimation and Prediction of Sound in Percussive Drilling"** submitted by **Sangshetty Kivade** (Register Number: **060410MN06P03**) as the record of research work carried out by him, is accepted as the Research Thesis Submission in Partial fulfillment of the requirements for the award of degree of **Doctor of Philosophy**.

Research Guides

(Name and Signature with Date and Seal)

Dr. Ch. S. N. Murthy   **Dr. Harsha Vardhan**

Chairman - DRPC

(Signature with Date and Seal)

ACKNOWLEDGEMENT

I take this opportunity to express my sincere thanks to faculty members of Mining Engineering Dept., Mr. Chandrahas Rai, Foreman, and other staff of the Rock mechanics Engineering Laboratory for their assistance and co-operation during conducting the experimental work.

It is a pleasure to express my heartfelt thanks to Mr. Shivalingayya Swamy, Foreman and staff of Mechanical Engineering Department of Basavakalyan Engineeering College, who have helped me in conducting the experimental work and preparing the thesis.

It is also my great pleasure to record the help, inspiration and encouragement that I got from my loving sons Sai Prasad and Shiv Prasad and Spouse Preeti, my parents, brother, my in-laws, and co-brothers, whose patience, I have tested to the limits during my research programme. I am lost at words to express only gratitude to the immeasurable support of my father in-law.

Finally, I wish to thank all other individuals who have helped me directly/indirectly to complete my research work.

<div align="right">SANGSHETTY   KIVADE</div>

Place: NITK
Date: 15/10/2013

ABSTRACT

This research work was taken up with the objectives of developing general prediction models for the determination of uni-axial compressive strength (UCS), abrasivity, tensile strength (TS) and Schmidt rebound number (SRN) for sedimentary and igneous rocks using penetration rate and sound level produced during percussive drilling. To carry out this investigation fabricated pneumatic drill set-up on the laboratory scale was used. In the present work shale, dolomite, sand stone, lime stone and hematite were the sedimentary rocks, whereas dolerite, soda granite, black granite, basalt and gabbros were the igneous rocks used in this investigation.

For all the above mentioned rocks their mechanical properties were determined as per the suggested methods of International Society of Rock Mechanics (ISRM). The laboratory investigation on all the sedimentary and igneous rocks using the drill set-up was carried out to find the penetration rate (mm/s) and sound level (dB (A)) produced by varying air pressure from 392 to 588 kPa, thrust from 100 to 1000 N and with varying drill bits and types (integral chisel drill bit: 30, 34 and 40 mm diameter, threaded (R22) cross drill bit: 35 and 38 mm diameter).

The data generated in the laboratory investigation was utilized for the development of regression models for predicting rock properties like, UCS, abrasivity, TS, and SRN using air pressure, thrust, bit diameter, penetration rate and sound level. Further, regression models were also developed for predicting penetration rate and sound level using air pressure, thrust, bit diameter and rock properties as input parameters.

In a similar way, i.e. utilizing the same input parameters for determining the rock properties and predicting the sound level and penetration rate, Artificial Neural Network (ANN) models were developed. A comparison was made between the results obtained using various regression models developed and the ANN models. Results of this investigation indicate that ANN models are superior over regression models.

Key words: Percussive drill, Sound level, Penetration rate, Air pressure, Thrust, Drill bit types and diameter, Uni-axial compressive strength, Abrasivity, Tensile strength, Schmidt rebound number, Regression models, Artificial Neural Network.

TABLE OF CONTENTS

List of Figures

NOMENCLATURE

ANFIS - Adaptive Neuro-Fuzzy Inference System

ANN - Artificial Neural Network

ANOVA - Analysis of Variance

AP - Air Pressure

ASTM - American Society for Testing and Materials

BD - Bit Diameter

BPNN - Back Propagation Neural Network

CoV - Coefficients of Variation

CRS - Coefficient of Rock Strength

dB (A) - Decibel A-weighted

DF - Degree of Freedom

DTH - Down the Hole Hammer

GA- Genetic Algorithms

HPD - Hearing Protection Devices

ISRM - International Society for Rock Mechanics

MAPE - Mean Absolute Percentage Error

MLP - Multi Layer Perceptron

MLPNN - Multi Layer Perceptron Neural Networks

MR - Multiple Regression

MRA - Multiple Regression Analysis

MS - Mean Square

MSE - Mean Square Error

NIHL - Noise Induced Hearing Loss

PR - Penetration Rate

RBF - Radial Basis Function

RMSE - Root Mean Square Error

SL - Sound Level

SPL - Sound Pressure Level

SRN - Schmidt rebound number

SS - Sum of Square

T - Thrust

traingda - Gradient Descent with Adaptive Learning Back-Propagation
            Algorithm

trainlm - Levenberg-Marquardt Algorithm

trainrp - Resilient Back-Propagation Algorithm

trainscg - Scaled Conjugate Gradient Algorithm

TS - Tensile strength

UCS - Uniaxial compressive strength

VAF - Values Account For

CHAPTER I

INTRODUCTION

Investigations on percussive drilling have been carried out analytically, numerically and experimentally over many years. In percussive drilling, an impact tool continuously rises and drops to generate short duration compressive loads to crush the rock material (Dutta, 1972; Hakalehto, 1972; Schmidt, 1972). In general, a piston driven by compressed air converts its kinetic energy to impact energy by colliding with a steel rod or drill bit. This impact energy is transferred to the steel in the form of a stress wave that travels to the bit rock interface. Part of the energy in the wave goes to the rock, causing failure, and part of the energy is reflected back. The effective stress in breaking rock acts in an axial direction and in a pulsating manner. Thrust is the external force applied to a drill to keep the bit in contact with the rock.

An accurate estimation of drilling rate helps in planning of the rock excavation projects more efficiently. Drilling is the most expensive process and the prediction of penetration rate is very important in mine planning (Onan, and Muftuoglu 1993). Also, one could use the prediction equation to select drill rig type, which is best suited for given conditions. Variables used to predict penetration rate could be classified into three main categories such as, drill bit characteristics, characteristics of rock and operational variables such as air pressure, thrust and bit diameter. However, rock properties such as compressive strength, porosity, density and geological conditions are uncontrollable parameters (McGregor, 1967; Beste et al. 2007). Penetration rate is the progression of the drilling bit into the rock in a certain period of time, which is generally expressed as "mm/s". The phenomenon of percussive drilling is a complex process and is affected by many factors. Bit type and diameter, applied thrust, and flushing of debris are some of the controllable parameters.

Percussive drills have been extensively used in quarries, open pit mines, and construction sites all over the world. Many of the researchers (Powell, 1956; Holdo, 1958; Gorden, 1963; and Walker; 1963) carried out the experimental investigation on noise emitted by pneumatic drills and its control. Percussion drills are the source of

the most serious noise problem in mining activities, due to extremely high noise levels of the order of 114 dB (A) to 122 dB (A) and their widespread use (Bartholoame & Stein 1988). Percussion drills will continue to be widely used to drill small diameter holes in hard rock because no other methods seems to economically available to replace them (Boillat et al.1993). Many studies (Jensen & Visnapuu, 1972; Hawkes et al. 1977a; Hawkes and Burks, 1979; Milette, 1989) were conducted to determine the major noise sources of percussion drills.

According to Powell (1956) the major noise source in pneumatic drill is the driving unit which emits high intensity low frequency noise due to compressed air. Of the total noise energy of pneumatic drill, 87.5% is contributed by the exhaust and the next largest component is the impact between the piston and drill steel (Holdo 1958; Walker 1963; Gorden 1963; Miller 1963; Wallace 1964; Savich 1982; Turner 1986: Aljoe, et al. 1987; and stein and Aljoe 1989). It was suggested by Miller (1963) that efforts should be made to attenuate the sound levels in the frequency range of 500 to 600 Hz and 1500 to 1700 Hz, as most of the sound power is concentrated in these frequency ranges.

Rock engineers widely use the uni-axial compressive strength (UCS) of rocks in designing surface and underground structures. The procedure for measuring this rock strength has been standardized by both the International Society for Rock Mechanics (Brown 1981) and American Society for Testing and Materials (ASTM 1984). Recent trend on estimating UCS from simple laboratory index tests has gained popularity. Various experimental methods and drillability models were developed to determine drillability or to predict penetration rate by various researchers (Fish 1961; Protodyaknov 1962; Paone and Madson 1966; Singh 1969; Paone et al. 1969, Bilgin, 1983, Schneider, 1988, Gehring, 1997, Thuro and Plinninger, 1999).

Further a number of attempts have been made by many researchers to indirectly define various rock properties using different approaches (Vallejo et al., 1989; Cargill and Shakoor 1990; Xu et al., 1990; Singh and Singh, 1993; Chau and Wong, 1996; Grima and Babuska, 1999; Palchik 1999; Tugrul and Zarif 1999; Koncagul and Santi, 1999; Katz et al., 2000; Kahraman, 1999, 2001). Most of these studies have been dealt with simple models relating UCS to Schmidt hammer

rebounds (SHR), UCS to sonic velocity (Vp,) UCS to porosity (n), UCS to point load (PL) and so on.

As regard to estimating the rock properties using sound level produced during drilling, limited publications are available. Rajesh Kumar et al. (2010) carried out a work on field investigation for estimating rock properties using the sound level produced during drilling. In this study, investigation is carried out in a Singareni coal mine (Andhra Pradesh) to estimate some of the rock properties during blast hole drilling.

Neural networks may be used as a direct substitute for auto correlation, multivariable regression, linear regression, trigonometric and other statistical analysis and techniques (Singh et al. 2003). The particular network can be defined by three fundamental components: transfer function, network architecture and learning law (Simpson, 1990). It is essential to define these components, to solve the problem satisfactorily. Neural network consists of a large class of different architectures. Multi Layer Perceptron (MLP) and Radial Basis Function (RBF) are two of the most widely used neural network architecture in literature for classification of regression problems (Loh and Tim, 2000; Kenneth et al. 2001; Cohen and Intrator, 2002, 2003).

Some of the recent research on estimating UCS using Multiple Regression (MR), Artificial Neural Network (ANN) and Adaptive Neuro-Fuzzy Inference System (ANFIS) models was carried out by Yilmaz and Yuksek (2008, 2009). A higher prediction performance of ANFIS over MR and ANN models was reported by Yilmaz and Yuksek (2009). Majdi and Beiki (2010) used Genetic Algorithms (GA) in design and optimizing the Back Propagation Neural Network (BPNN) structure and applied the GA-ANN to predict the modulus of deformation of rock masses. In general, the models developed are successful in predicting the mechanical properties of rocks with index properties.

From the above it is clear that extensive work has been carried out with regard to noise control of pneumatic drills, mathematical models for estimating the rock properties using stepwise linear regression analysis, MRA, ANN, ANFIS, BPNN, GA, GA-ANN, etc.

In view of the above, it is felt that investigation using percussive drilling machine which is widely used in the mining (underground mine, opencast mine) and

mineral (Iron ore mine) industries in production operations can help in estimating rock properties also. Noise measurements were carried out in open space (outdoor location) to reduce the effect of reflecting noise. In this laboratory investigation, total five drill bits were used. Three integral steel chisel bits with 30, 34, and 40 mm in diameter and 42, 43, and 62 cm in length and two threaded (R22) type bits with 35 and 38 mm in diameter and 58 and 57.5 cm in length of chisel and cross geometry were used. These bits were selected from among the available sizes were used (Department of Mining Engineering, NITK, Surathkal). An attempt has been made in this investigation to determine the rock properties vis-à-vis sound level using of fabricated pneumatic drill set-up on the laboratory scale. Also, developing various models for the prediction of UCS, abrasivity, tensile strength (TS) and Schmidt rebound number (SRN) for rocks considered using penetration rate and sound level produced during percussive drilling and prediction of penetration rate and sound level for a given air pressure, thrust and bit-rock combination using multiple regression analysis. In this study, artificial neural network models were also developed to predict the rock properties of sedimentary and igneous rock, by using penetration rate and sound level produced during drilling and prediction of penetration rate and sound level for a given air pressure, thrust and bit-rock combination. The developed models were checked using various prediction performance indices and compared with the artificial neural network (ANN) and traditional statistical model of MR (multiple regression).

CHAPTER II

LITERATURE REVIEW

2.1 General

Considering the wide spread use of percussive rock drilling, many investigators (Selim and Bruce, 1970; Dutta, 1972; Schmidt, 1972; Pandey et al. 1991) have reported excellent findings over a long period of time covering theoretical/numerical and experimental aspects. However, in view of the complexity in the percussive drilling operation, some of the investigations (Schmidt, 1972; Paone et al. 1966; Pandey et al. 1991) were related to the laboratory simulated studies, experimental as well as numerical studies incorporating the mechanism of percussive drilling, such as indentation of the bit into the rock.

Percussive drilling has been studied experimentally, numerically and analytically over many years (USBM mines and quarries of Minnesota, Wisconsin and Michigan). In percussive drilling, an impact tool continuously rises and drops to generate short duration compressive loads to crush the rock material at the bit-rock interface. In general, a piston driven by compressed air or hydraulic drilling converts its kinetic energy into impact energy by colliding with a steel rod or drill bit. This impact energy is transferred to the steel in the form of a stress wave that travels to the bit rock interface. Part of the energy in the wave goes to the rock, causing failure, and part of the energy is reflected back. The effective stress in breaking the rock acts in an axial direction and in a pulsating manner (Kennedy and Bruce 1990). A thrust force may be applied to keep the bit in contact with the rock.

Selim and Bruce (1970) carried out percussive drilling experiments on nine types of rocks in the laboratory (USBM). Two drill rigs were used in the experiments. The drill rig included in this study was 6.67 cm bore jackleg type. The drill was backstroke rifle-bar-rotation machine and the bit diameter was confined to 3.81 cm cross bits. They correlated the penetration rate with compressive strength, tensile strength, Shore hardness, apparent density, static and dynamic, Young's modulus, shear modulus, coefficient of rock strength (CRS) and percentage of quartz and established linear predictive equations.

Hustrulid and Fairhust (1971a; 1971b; and 1972a; 1972b) first carried out a detailed theoretical and experimental study of the percussive drilling of rock. Then, they applied the model to actual percussive drilling. Hakalehto (1972) reported the res ults of actual percussive drilling experiments. He stated that penetration rate depends primarily on the energy used to fracture the rock under the drill bit. Though the energy which is transmitted elastically to the rock is generally estimated to be negligible, in some rock types under this investigation the elastic energy is a considerable amount of the total energy transferred to the rock.

Dutta (1972) developed a theory of percussive bit penetration. In developing this theory he assumed that a mathematical model which is based on some of his experimental observations. Schmidt (1972) reported the performance characteristics of two percussive drills mounted on a truck in 25 rock types. The drill included in this study was a standard drifter having a bore diameter of 6.67 cm. The bit type was H-thread carbide and bit diameter was 5.08 cm. Schmidt correlated the penetration rate with compressive strength, tensile strength, Shore hardness, density, static and dynamic Young's modulus, shear modulus, longitudinal velocity, shear velocity and Poisson's ratio. He found that only compressive strength and above mentioned properties highly correlated with it, such as tensile strength and Young's modulus, exhibited good correlations with penetration rate.

Pathinkar and Misra (1980) concluded that conventional rock properties such as compressive strength, tensile strength, specific energy, shore hardness and Mohr's hardness do not individually give good correlation with the penetration rate of percussive drilling. Lundeberg (1982) carried out detailed investigation on stress wave mechanics of percussive drilling and developed a microcomputer simulation program. Miranda and Mello-Mendes (1983) stated that rock drillability definition based on Vickers micro hardness and specific energy seems to point to a logical selection scheme for the most adequate rock drilling equipment based only on rock laboratory tests. Lundberg (1985) microcomputer simulation studies of a percussive drill (Atlas Copco1038 HD) have shown that the predicted values of a drill stresses, efficiency, coefficient of restitution of the hammer and forces acting on the rock compare well with exact theoretical results.

Howarth et al. (1986) carried out percussion drilling tests on 10 sedimentary and crystalline rocks. The percussion drilling tool was a 37.7mm wedge indenter (tungsten carbide insert) located on the end of a drill steel that was driven by an Atlas Copco571 RH compressed-air-powered percussion drill with water flushing. They correlated the penetration rate with rock properties and found that bulk density, compressive strength, apparent porosity, P-wave velocity and Schmidt hammer value exhibit strong relationships with the penetration rate. Howarth and Rowland (1987) also developed a quantitative measure of rock texture-the texture coefficient. They found a close relation between the texture coefficient and percussion drill penetration rates. Niyazi Bilim (2011) investigated the relationship between mechanical properties and penetration rates of natural stones and their drillability rate. Also found that relation between uni-axial compressive strength value and penetration rate.

2.2 Noise Emitted by Rock Drills and its Control

Many of the researchers carried out the experimental investigation on noise emitted by rock drills and its control. Holdo (1958) carried out a study pertaining to the energy consumed by rock drill noise. The results of the study show that the impact noise is 110 dB (A) (10 μw/cm²). Of the total noise from the rock drill, the impact noise contributed to 12.5% and the exhaust noise to 87.5%. Of the total useful effect delivered by a rock drill the noise energy was only 0.08%. It was said that, if only the exhaust noise existed, the total noise value would be 70μw/cm² corresponding to 118.4 dB (A). Therefore, the first step in noise control program of rock drill should be to reduce the exhaust noise as it produces most of the noise. The study also indicated that the silencer can reduces the noise from rock drill from 119 dB (A) to 113 dB (A). In other words, the noise with silencer can be reduced by 60μw/cm². Therefore, it can be said that the silencer removes about 75% of the total noise energy, which would otherwise be produced by standard rock drill. If consideration is given only to the exhaust noise, the silencer reduces from 70μw/cm² to 10μw/cm², which is 1/7 of the original value. In terms of decibels, the reduction was around seven times. Therefore, of the noise energy produced by the outlet, the silencer removes about 85%. When the rock drill is fitted with a silencer, the noise produced by the impacts and the exhaust

air has the same intensity i.e.10 µw/cm² which is equivalent to 110 dB (A) each and which added together, makes 20µw/cm².

Fischer (1962) made an attempt to control the noise of percussive rock drills. The study revealed that, for heavy mounted rock drills external mufflers can be used, mounted on or just behind the drill or mounted at the suitable place on the rig and connected to the exhaust port by means of hoses. It was reported that in doing so noise reduction of 8 to 10 dB (A) could be obtained. In other words, the exhaust noise can be totally eliminated. It was also stated that, this reduction in the noise level could be achieved without any observable reduction in the penetration rate. Further, it was reported that similar construction could be used for pusher leg drills. However, such an arrangement would influence the handling of the rock drill, which means that it must increase neither its weight nor its dimensions to maintain the drilling rate. To overcome this problem, doubled muffler cylinder was developed and it consists of an outer aluminum cylinder providing an expansion chamber and protecting the inner steel cylinder with large number of small exhaust holes arranged in a special pattern. It was indicated that this design does not increase the weight and the rock drill was quite easy to handle as the standard rock drill. The noise of the rock drill was reduced from 118dB (A) (64µw/cm²) to 109 dB (A) (8 µw/cm²). The substantial noise reduction was reported to be achieved with very small reduction in the penetration rate that is about 5% only. It was stated that further noise reduction was obtainable only at the cost of increased weight and space or further reduction in the drilling rate.

Miller (1963) carried out a laboratory study on noise produced by pneumatic rock drills. The results of the study showed that, the efforts to attenuate the noise levels should be concentrated in the frequency ranges of 500 to 600 Hz and 1500 to 7000 Hz as most of the sound power occurs in these frequency ranges. Further, the study also indicated that, from 40 to 100 Hz the noise is due to the impact between the piston and drill steel and between the drill steel and the rock, 100 to 2000 Hz is due to exhausting of the air from the exhaust port and above 2000 Hz is due to resonance of the steel parts of the drill and that of the drill steel. It was also stated that attenuation of the sound levels of the noise generated by the exhaust ports and the steel parts of

the drill is required in order to lower the intensity of the noise generated, by a pneumatic rock drill, to a level that would preclude possible damage to hearing.

Walker (1963) made an attempt to control the noise in percussive rock drills. It was indicated in the study that, noise level generated was found to decrease slightly after the drill steel penetrated the rock. It was also reported that, for each kg/cm² reduction in compressed air pressure, the sound level decreases by 1.0 to 3.0 dB (A). It was suggested that some design modification in pneumatic drill for noise reduction and considerable sound level reduction in pneumatic drills could be achieved by eliminating two large exhaust openings and substituting rows of holes around the circumference of the cylinder. It was reported that, as the piston travels down the cylinder, it will first pass two rows of holes, opening them to exhaust and then opens the third row of larger holes and thus noisy air flow is avoided. A 75 % reduction in the total mass energy has been reported by this design modification. The sound level measurement on pneumatic drill equipped with a muffler being operated in an underground roadway, revealed noise reduction of 17 dB (A) in the frequency range of 150-300 Hz at the operator's position. It was also reported that the penetration rate does not increase or decrease significantly by using a muffler.

Gorden (1963) attempted to reduce the high frequency noise due to vibration of the drill steel using rubber collars on the drill rod. However, this method was not successful as the heat generated due to internal friction deteriorated both the material of the collar and resulted in the bending of the rod. Reynolds (1964) highlighted the importance of exhaust hose for noise reduction in pneumatic drills. According to Reynolds, for better noise reduction, the hose should be extended out of the immediate working place using one or two bends and with the end pointed away from the driller. The problem of ice being formed inside the hose at the point where the hose was attached to the exhaust was overcome by using drilling water as a heat source and passing it through a jacket around the exhaust on its way to the back head of the drill. It was concluded that for adequate protection of drilling crew against noise, mufflers should be used for reduction of the low frequency exhaust noise along with suitable ear defenders to guards against high frequency mechanical noise.

Wallace (1964) carried out a study on rock drill noise. In this study, a summary of the elements of rock drill noise was presented. The effect of noise decay with distance both on surface and underground applications was discussed in this study. Further, the effects of mufflers on rock drills were demonstrated and their limitations were discussed. It was reported that, a change in the surroundings produces a substantial change in the characteristics of noise. When the drill is being operated outdoors on level ground with few obstructions; the intensity of the noise diminishes with distance. For moderate distances, the average slope is about 1.3dB/ft. The worst conditions, noise wise, are found in a small underground drift or raise that is free from timbering. Small volume and hard reflecting walls fill the work area with a "diffuse sound field" where the sound waves were reflected and re-reflected so much that little change in noise level was noticed with distance. The average decay was only about 0.3dB/ft. Further it was stated that, worn-out bits and the amount of drill rod confined in the hole cause minor variations in high frequency noises. The effect of distance on the noise spectrum was that of absorption of the high frequency noises.

Chester et al. (1964) carried out an experimental investigation (USBM) to determine the effect of the shape of a pneumatic rock drill exhaust muffler on its efficiency, and the origin and reduction of exit noise from the mufflers. Tests of mufflers of three different shapes proved that the shape was not critical and that a muffler could be incorporated into the shell of the drill. Petal diffusers were said to be beneficial in reducing exit noise but they add another projection to the machine. It was said that, increasing the number of exit openings while maintaining the same area of exit opening has a markedly beneficial effect on the exit noise and appears to be the most satisfactory treatment.

Lemay (1972) carried out a study, the use of sound suppression hose, having spiral square ribs and specially designed to trap sound, moisture and oil in the air. It was suggested that, the hose should be of 5 cm diameter and should be made of material which is not affected by oil or moisture. Also it should be flexible enough and should hold its roundness and could be used in lengths of 7.6 m and 15.3 m with a muffler attached. This will dissipate the cool fog and oil saturated air to a safe

distance from the immediate working area. It was stated that, the encased urethane assembly enclosed in an outer casing and surrounded by a pressurized air barrier would further reduce the noise. Weber (1972) discussed the noise suppression of rock drills. It was suggested that, unless pneumatic drills and drill steels are completely encased, low frequency exhaust and high frequency machine noise could not be reduced below 85 dB (A) along the whole range of the octave band of about 30 Hz to 8 KHz. It was reported that, low frequency noise was reduced approximately by 75% or by about 6 dB (A) due to exhaust modification.

Savich and Wylie (1975) made an attempt to investigate the noise attenuation in rock drills. The study revealed that, every problem in noise and vibration control involves a source, a path and a receiver. About 90% of the drill noise was said to be due to the energy released from the exhaust air. This noise is produced due to turbulence and pulsation of high-pressure air. It was reported that, the noise produced by rock drills could be reduced by the successful application of devices such as lead-off hoses on the exhaust and the use of mufflers. It was suggested that, the best way to reduce noise from rock drills was through engineering control and proper design of the noise source. Visnapuu and Jensen (1975) from USBM carried out an experimental investigation on noise attenuation in rock drill. It was suggested in the study to design a close-fitting case muffler around the drill body. The inner part of the case was made up of metallic honeycomb skeleton filled with Visco-elastic absorber. The idea was to muffle and absorb the exhaust and the drill body noise. It was stated that, the drill steel resonance noise was reduced by a constrained layer treatment consisting of a tubular metal cover bonded to the outside of the rod by Visco-elastic filler. Further, it was stated that, damping alloy components were also developed to reduce the metallic resonance noise. Incorporation of all the above modifications reduced the A-weighted sound level from 115 to 97dB (A) while drilling in granite stone. Schliesing (1978) made an attempt to attenuate noise from rock drills. It was suggested that, replacement of normal steel collared rod by a plastic collared rod in pneumatic drills could bring down the A-weighted sound level by 2 dB (A) .It was stated that, the drill noise could be further reduced by muffling the hammer using

telescopic tube for the rods and using borehole mouth seal. The A-weighted sound level was found to decrease further 4 dB (A) with treatment.

Savich (1982) made an attempt to investigate the abatement of noise and vibration in Canadian Mining Industry. It was indicated in the study that, the noise and vibration problem would be concerned with: source, path and receiver. The study reported the development of the redesign of machines to reduce self-generated noise and vibration or the design of a new machine. A change in technology also changes the economic factors of production and productivity. However, path modification was one of the major methods of protection from noise and vibration. It was suggested that, ear protector was a basic form of protection. It was capable of reducing noise levels by 10 to 45 dB (A). It was reported that, noise produced by rock drills, could be reduced by successful application of devices such as lead-off hoses on the exhaust and use of mufflers. Further it was said that, the best way of reducing the noise from rock drill was through engineering control and proper design of the noise source.

Aljoe (1984) conducted a study on quieted percussion drills. It was reported in the study that, the sound levels of pneumatic drills at the operators' position of the order of 112 to 114 dB (A) was due to the exhaust and 105 to 110 dB (A) was due to the drill steel vibrations. The drill steel vibration noise was said to be due to the transverse stress waves generated by the steel. It was stated that these transverse waves result from off-center impacts worn drill chucks and bent drill steels. Redesign of the pneumatic drill was also discussed which includes independent rotation, valve less operation, muffler enclosure, shroud tube and redesigned controls. A-weighted sound level of 104 dB (A) (with shroud tube) and 107 dB (A) (without shroud tube) was reported for pneumatic drills from underground tests. It was stated that, noise control using concentric drill steels, which consists of an inner pulse transmission rod and an outer torque tube reduce the noise level significantly. The inner rod transmits percussive energy to the bit but does not rotate, while the torque tube supplies rotation and acts as a shroud tube to attenuate the noise produced by the inner rod. The torque tube is acoustically isolated from the inner rod by button-like rubber inserts. The inner rod is solid, and flushing air or water from the hole passes through the annulus

between the rod and the tube. Sound level measurement using concentric drill steels was not performed as it was still under prototype construction stage.

Bartholomae (1994) reported on an in-the-hole drill concept for noise control associated with percussive type drills. The concept eliminated the drill rod as a stress transfer mechanism so that the percussive motor was located just behind the drill bit. The motor is pushed into the borehole by using a drill pipe. The percussion motor rotates the drill bit to transmit the drill feed force. The noise reduction principle of the "in-the-hole" drill involved an operational effect. Once the borehole was started, the high energy noise from the percussive tool was contained entirely within the borehole, with the rock mass acting as an acoustic enclosure. This design was significantly different from standard percussive drills, in which the major noise producing components (drill hammer, drill steel, and air exhaust) were located outside the borehole. Laboratory testing for noise related to this concept showed that noise levels significantly decreased, by 4 dB (A) (4 ft. into rock). However, mechanical difficulties associated with water leaks, percussion motor, etc. related to the drill eliminated any further testing. Future plans in this regard were to address the mechanical problems associated with the new design, since noise level reduction did show promise.

Champoux, et al. (1994) followed a method for determining the contribution of both longitudinal and flexural waves related to the radiation of noise associated with percussive type drill steel rods. The authors determined that in order to reduce the noise produced by the steel rod, one must understand significant aspects of the noise generation mechanism. Lesage, et al. (1997) adopted an experimental approach to characterize the vibro-acoustic behavior of percussion drill steel rods under real operating conditions and laboratory controlled conditions. The contribution of longitudinal and flexural vibration related to noise generation was provided. The testing concluded that the bending waves within the drill steel were mainly responsible for the largest portion of noise radiation and the contribution of longitudinal waves to the noise radiation was found to be negligible.

Reeves (2005) conducted a study on the assessment of noise controls commonly used on jumbo drills and bolters in underground metal mines of Western

United States. It was indicated in the study that, the noise control measures most commonly applied to drills and bolters were windshields, sound absorbing material and hydraulic motor covers. These controls were evaluated on machines at underground metal mines to determine the extent of noise reduction by each control. The results indicate that absorbing material has very little effect on the noise levels. The noise reduction attributable to the motor covers was dependent on the material used to create the cover. Properly installed windshields were the most consistent control. It was suggested that when applying noise control measures, care should be taken to use the right product for the job. In the study conducted, 13 mm thick rubber conveyor belt mats and 6.35 mm thick Plexiglas motor covers reduced motor noise because they are barrier materials, which was the correct choice for the application.

The study showed that sound absorbing material was much more effective when backed by a noise barrier. It was stated that hydraulic motor covers on the face drills and roof bolters were not necessary as the noise levels produced by the uncovered motors were below 85dB (A), much lower than the levels produced by other noise generating mechanisms to which the operator would be exposed. The study revealed that the use of absorptive materials in the operators' area slightly reduces the sound levels of the machines working underground. The windshields reduced the noise reaching the operator during the drilling / bolting cycle. The generated noise from the aforementioned processes was of relatively high frequency in content. Therefore, windshield provides a protective barrier between the noise source and the operator. Care should be taken to seal the gaps in the windshield and between the windshield and the structure of the machine.

Harper and O'Brien (2006) conducted a study (platinum mine) on the prediction of underground drilling noise. The study reported the development of a simple spreadsheet-based model to provide an indication of the anticipated sound pressure level (SPL) distribution in an underground environment under free field conditions. Application of the model to various types of rock drills showed that at high drilling rates the effective use of simple muff type hearing protection devices (HPD) was sufficient to eliminate noise induced hearing loss (NIHL) compensation, provided such devices were used correctly at all times. It was also stated that, the

current model was specific to a stopping operation and would require further calibration for application to other underground environments such as development ends and shaft sinking.

2.2.1 Estimating the Rock Properties Using Sound Level Produced During Drilling

Very limited publications are available on estimating the rock properties using sound level produced during drilling. Vardhan and Murthy (2007) carried out an experimental investigation of jack hammer drill noise with drilling in rocks of different compressive strength. They investigated the influence of mechanical properties of rocks on sound level due to drilling in rocks. Vardhan et al. (2009) carried out a research work, estimating the rock properties based on the sound level produced during pneumatic drilling. In this investigation, same data was utilized which was obtained by Vardhan and Murthy (2007). Rajesh Kumar et al. (2010) carried out a work on field investigation for estimating rock properties using the sound level produced during drilling. In this study, the authors carried out an investigation in a coal mine to estimate some of the rock properties during blast hole drilling. They reported that a detailed study could not be taken up in the field as it was difficult to get wide range of rocks with varying compressive strength and therefore, it was also difficult to determine the sound level produced.

2.2.2 Determination of Drillability of Rock and Their Relation with Rock Properties Using Statistical Analysis

The physico-mechanical properties of rocks are the most important parameters in the design of underground workings and in the classification of rocks for engineering purposes. The measurement of rock strength has been standardized by both the International Society for Rock Mechanics (ISRM 1981) and the American Society for Testing and Materials (ASTM 1984).

Various experimental methods and drillability models were developed to determine drillability or to predict penetration rate. Fish (1961) found out that there is a linear relation between the rate of force applied to drill to penetration rate and the uniaxial compressive strength of some sedimentary rocks. Protodyaknov (1962)

developed drop tests and described the coefficient of rock strength (CRS) used as a measure of the resistance of rock impact. Paone and Madson (1966) observed that there was an exponential relation between penetration rate and uniaxial compressive strength (UCS) and tensile strength. Singh (1969) showed that compressive strength was not directly related to the drilling rate of a drag bit. Paone et al. (1969) conducted a study on percussion drilling in the field on nine hard abrasive rocks. They concluded that shore hardness, tensile strength, uniaxial compressive strength and static young's modulus correlated with the penetration rates of percussive drills. Better correlation was obtained by using the CRS and it was stated that no single property of rock was completely satisfactory as a predictor of penetration rate.

Selim and Bruce (1970) developed a penetration rate model for percussive drilling using stepwise linear regression analysis. The model pertains to function of the drill power and the physical properties of the rocks penetrated. Statistical regression was then used to analyze the relationship between the dimensionless groups. The equations developed by this method were in line with others findings. Schmidt (1972) who studied 25 different types of rock with hammer drilling machine examined the relation between the penetration rate and tensile strength, density, shore hardness, static and dynamic young's modulus, compressive strength, longitudinal velocity and shear modulus. It was observed that only compressive strength and those properties highly correlated with it, such as tensile strength and young's modulus exhibited good correlations with penetration rate. Tadanand and Unger (1975) developed an equation that showed good correlations with actual penetration rates of percussive drills, and concluded that CRS shows it's usefulness in predicting penetration rate with higher reliability than other rock properties. Pathinkar and Misra (1980) concluded that conventional rock properties such as UCS, Brazilian Tensile Strength (TS), specific energy, shore hardness, and Mohr's hardness do not individually give good correlation with penetration rate in percussive drilling. They developed a good correlation between penetration rate and a set of rock properties, but the relation was complex. Rabia and Brook (1980) used the modified test apparatus of Protodyakonov to determine the rock impact hardness number and developed an empirical equation for predicting drilling rates for both down the hole

hammer (DTH) and drifter drills. Leighton et al (1982) developed a rock quality index which was the rate of the pressure strength to progression rate, and used them successfully in an open-pit copper mine (Canada) in the arrangement of loosening holes and determination of the amount of explosives to be used.

Miranda and Mello-Mendes (1983) stated that rock drillability definition based on Vickers microhardness and specific energy seems to point to a logical selection scheme for the most adequate rock drilling equipment based only on laboratory tests of the rocks. Howarth et al. (1986) correlated penetration rate with rock properties and observed that compressive strength, apparent porosity, bulk density and P-wave velocity exhibit strong relations with penetration rate. However, correlations between Schmidt hammer value, penetration rate and dry compressive strength were not strong. They concluded that porosity can influence drillabillty, since high porosity is likely to assist the formation of fracture paths and networking of such paths.

Recent trend on estimating UCS from simple laboratory index tests has gained impor-tance as they are easy and don't require regular samples. Many researchers have indirectly defined various rock properties using different approaches for predicting UCS from non-destructive testing methods such as sound velocity, porosity and density. A great number of attempts have been made to predict uni-axial compressive strength (UCS) of intact rocks (Vallejo et al. 1989; Xu et al. 1990; Singh and Singh 1993; Chau and Wong 1996; Koncagul and Santi 1999; Grima and Babuska 1999; Katz et al. 2000; Kahraman 2001). Most of these studies have dealt with simple models relating to UCS to Schmidt hammer rebounds (SHR), UCS to sonic velocity (Vp,) UCS to porosity (n), UCS to point load (PL) and so on. Within this study, different rock types have been tested according to ISRM suggested methods. These tests consist of unconfined compressive strength test, point load index test, Schmidt hammer hardness test, and sound velocity and each rock type has been subjected to the aforementioned four tests and their average values, standard deviations and Coefficients of Variation (CoV) from each test were calculated accordingly. Coefficient of variation has been calculated by dividing standard deviations by average values.

Pandey et al. (1991) correlated the shear strength, compressive strength, tensile strength, and Protodykonov Index with the penetration rate value obtained from a microbit drilling test and found logarithmic relations. Kahraman and Mulazimoglu (1999) observed that the performance of a drilling is dependent on drillability of rock, work organization, and technical characteristics of the drilling. It is very important that rotation speed, pressure, torque, and impact frequency called operational parameters are to be applied according to formation characteristics. Kahraman (1999) conducted a study on rotary blast hole drills using the data obtained from field observations and developed a model for the prediction of penetration rates using a multiple regression. The indicated results show that the parameters that significantly affect penetration rate of rotary blast hole drills were bit diameter, compressive strength, weight on bit, and rotational speed. Kahraman et al. (2000) developed a mathematical penetration rate model for rotary drills and defined a new drillability index from force-penetration curves of indentation tests. They also correlated this drillability index and found significant correlations with p-wave velocity, elastic modulus, point load index, Schmidt hammer value, tensile strength, impact strength, compressive strength, and density.

Kahraman (2002) statistically investigated the relationships between three different methods of brittleness and both drillability and borability using the raw data obtained from the experimental works of different researchers. The obtained result shows that there is no correlation between the brittleness values and penetration rate of diamond drills. However, strong correlations were found between the brittleness values and penetration rate of rotary drills obtained from tensile strength and compressive strength of the rocks.

Kahraman et al. (2003) found that point load strength, tensile strength, uniaxial compressive strength and Schmidt hammer value are the dominant rock properties affecting the penetration rate of percussive drills. Yenice et al. (2009) studied the relation between drillability index of marbles (DRI) and their physical, mechanical and texture characteristics. As a result, they determined significant relations between density of the marble, its tensile strength, hardness, uniaxial compressive strength and DRI. Rajesh Kumar et al. (2011) carried out a detailed

investigation for the prediction of compressive strength, tensile strength, and porosity of sedimentary rocks using sound level produced during rotary drilling. A general prediction model was developed and investigation was carried out to find out the relationship between sound level produced during drilling and the physical properties of sedimentary rocks.

2.2.3 Artificial Neural Network and Multiple Regression Analysis Its Application in Indirect Estimation of Rock Properties

Neural networks are a powerful technique to solve many real world problems. They have the ability to learn from experience in order to improve their performance and to adapt themselves to changes in the environment. In addition to that they are able to deal with incomplete information or noisy data and can be very effective especially in situations where it is not possible to define the rules or steps that lead to the solution of a problem.

Artificial neural network (ANN) models are suitable for complex problems where many factors influence the mechanism and the result. In this technique many competing correlations can be examined using massive parallel networks composed of many computational elements connected by links of variable weights (Kalogirou 2000). Neural networks may be used as a direct substitute for auto correlation, multivariable regression, linear regression, trigonometric and other statistical analysis and techniques (Singh et al. 2003). Neural networks, with their remarkable ability to derive a general solution from complicated or imprecise data, can be used to extract patterns and detect trends that are too complex to be noticed either by humans or other computer techniques. The particular network can be defined by three fundamental components: transfer function, network architecture, and learning law (Simpson 1990). It is essential to define these components, to solve the problem satisfactorily. Neural networks consist of a large class of different architectures. Multi Layer Perceptron (MLP) and Radial Basis Function (RBF) are two of the most widely used neural network architectures in the literature for classification or regression problems (Loh and Tim 2000; Kenneth et al. 2001; Cohen and Intrator 2002, 2003).

Multi layer perceptron neural networks (MLPNN) are dominantly used. In a MLPN network, input units are connected to the first layer of hidden units which are further connected to the units of the second hidden layer. The units of the last hidden layer are connected to the output units. The multi-layer feed-forward networks are usually employed as the predictors of the unknown functional relation. The hidden layers may be defined as a black box, which performs the necessary transformations of the input data so that the target output data can be obtained.

To overcome the inaccuracy resulting from the application of empirical methods, it is necessary to adopt newly developed scientific concepts (Lu Y 2005). In this regard, ANN approach can effectively be used to predict ground vibration due to blasting. Yilmaz and Yuksek (2008, 2009) carried out research on estimating UCS using Multiple Regression (MR), ANN and adaptive neuro-fuzzy inference system (ANFIS) models. It was reported a higher prediction performance of ANFIS over MR and ANN models. RBF neural network is based on supervised learning. RBF networks were independently proposed by many researchers and are a popular alternative to the MLP. RBF networks are also good at modeling nonlinear data and can be trained in one stage rather than using an iterative process as in MLP and also learn the given application quickly (Venkatesan and Anitha, 2006). Majdi and Beiki (2010) used Genetic Algorithms (GA) in design and optimizing the Back Propagation Neural Network (BPNN) structure and applied the GA-ANN to predict the modulus of deformation of rock masses. In general, the models developed in this study are successful in predicting the mechanical properties of rocks with index properties. However, there have been a few attempts found in the literature about the identification of the parameters and functions which play a vital role in defining strength properties of rocks with regard to the aforementioned rock properties.

A neural network does not force the predicted value to be a mean value, thus preserving and using the existing variance of the measured data. Because of ANN's ability to learn and generalize interactions among many variables, ANN technology has been reported to be very useful in modelling the rock material behaviour. Study indicated that ANN technology is more powerful than conventional statistical techniques.

CHAPTER III

OBJECTIVES AND SCOPE OF THE PRESENT INVESTIGATION

3.1 Objectives of the Present Investigation

The aim of this investigation was to elucidate, through a fairly extensive laboratory experimentation carried out on a variety of rock types, the influence of various drill machine parameters i.e. air pressure (392, 441, 490, 539 and 588 kPa), thrust, (100 to 1000 N) and bit diameter and types (integral 30, 34 and 40 mm and threaded R22 type 35 and 38 mm) and different mechanical properties of rock such as uni-axial compressive strength (UCS), abrasivity, tensile strength (TS), and Schmidt rebound number (SRN) on the performance of percussive drilling i.e. penetration rate and sound level produced during pneumatic drilling.

The objectives of the present research work are given below:

(1) Investigation of various pneumatic drill machine parameters with different mechanical properties on penetration rate and sound level on a variety of rocks through laboratory studies.

(2) Development of mathematical and artificial neural network models for prediction of sound level, penetration rate and rock properties using percussive drilling.

3.2 Scope of the Work

To fulfill the above objectives the following scopes under the present research work have been identified.

(1) To establish a relationship between machine parameters on penetration rate and sound level.

(2) To correlate various mechanical properties such as UCS, abrasivity, TS, and SRN of sedimentary and igneous rocks, with penetration rate and sound level produced during pneumatic drilling.

(3) Based on the results of laboratory investigation, development of mathematical equations for the UCS, abrasivity, TS, and SRN for rocks considered (sedimentary and igneous) using penetration rate and sound level produced during drilling.

(4) Development of artificial neural network (ANN) models to predict the rock properties of sedimentary and igneous rocks using penetration rate and sound level produced during drilling. Also, prediction of penetration rate and sound level for a given air pressure, thrust and bit-rock combination.

(5) Evaluation of developed models using various prediction performance indices and comparison of the results obtained using ANN with of Multiple Regression Analysis (MRA).

The details of parametric variations investigated are given in Table 3.1.

Table 3.1 Details of parametric variations investigated

Parameters	Variables
I Laboratory investigations	
A. Drilling Experiments	

(a) Bit parameters
   (i) Bit type
   (ii) Bit geometry
   (iii) Bit diameter
	Integral steel, Threaded (R22)
	Chisel, and Cross
	30, 34, and 40 mm (integral) and 35 and 38 mm
	 (threaded R22 type)

(b) Operational parameters
   (i) Thrust
   (ii) Operating air
      pressure
	Ten magnitudes (100, 200, 300, 400, 500, 600, 700, 800, 900, and 1000 N)
	Five magnitudes (392, 441, 490, 539, and 588 kPa)

(c) Rock parameters
   (i) Type
   (ii) Rock properties
      considered
	Shale, Dolomite, Sandstone, Limestone, Hematite, Dolerite, Soda granite, Black granite, Basalt, Gabbros
	Uniaxial compressive strength (UCS), Abrasivity, Tensile strength (TS) and Schmidt rebound number(SRN)

(d) Measured parameters	Sound level (dB (A)), and Penetration rate (mm/s)

CHAPTER IV

DESIGN OF EXPERIMENTAL SET-UP/ FABRICATION, INSTRUMENTATION AND METHODOLOGY

4.1 General

The primary objective of the present study is to establish the influence of machine parameters (thrust and air pressure) and various mechanical properties of rocks on the performance of percussive drilling (sound level and penetration rate). Extensive experiments in this regard have been conducted in the laboratory on ten different widely varying types of rocks collected from Indian mines.

4.2 Design of Experimental Set up for Laboratory Investigation

4.2.1 Brief Description of the Percussive Drill Machine

A jackhammer drill is a compressed air operated machine. The drill weighs 10 to 30 kg and is hand held. It can drill holes with diameter varying from 25 to 40 mm. It can be used to drill both vertical and horizontal holes up to 3 m depth. Drilling with the pneumatic drill consists essentially in the drill delivering blows against the bottom of the holes and lifting the rock cuttings.

4.2.2 Design of experimental set-up

In the laboratory of Department of Mining Engineering, NITK, Surathkal, all the sound level measurements were conducted on a commercially used jackhammer drill machine (Atlas Copco, RH658L) operated by compressed air with suitable arrangement made to measure applied thrust and air pressure. It is extensively used in underground hard rock excavation (underground mine eg. Hatti gold mine and opencast mine eg. Iron ore mine) and quarries (eg. Limestone mine). The important specifications of the jackhammer drill used were:

- Weight of the jackhammer drill machine (28 Kgs)

- Number of blows per minute – 2200

- Type of drill rod – Integral drill steel and Threaded (R22) type with tungsten carbide drill bit

- Recommended maximum air pressure – 589.96 kPa

- Bit geometry – Chisel and Cross

A lubricator of capacity 0.5 litre and a pressure gauge range (0 to 28 Kg/cm^2) with a least count of 49 kPa were provided between the compressor and jackhammer drill machine to lubricate the various components and to regulate the air pressure supplied to the drill machine, respectively. A percussive drill setup using the jackhammer to drill vertical holes was fabricated similar to that given by Vardhan and Murthy (2007) to carry out the drilling experiments for sound level measurement on a laboratory scale (Fig.4.1). The base plate of the set-up consists of two 12.5 mm thick I- sections (flange width–1 cm and height–30 cm) welded together all along the center, which was firmly grouted to the concrete floor with the help of four numbers of 3.8 cm diameter anchored bolts. Two circular guiding columns of 60 mm diameter, 1175 cm long, and 55 cm apart were secured firmly to the base plate. The vertical position of the two columns was maintained with the help of a top plate (3.8 cm in thick, 13 cm width and 62.5 cm length). On the top of the base plate holes of 25.4 mm diameter were drilled at close intervals on two opposite sides for accommodating different sizes of rock blocks (up to 500 mm cube). With the help of two numbers of mild steel plates (1 cm in thick, 7.5 cm width and 61 cm length) on the top of the rock block and four numbers of 25.4 mm bolts, placed at the four corners, the rock block was firmly held on the base plate.

The jackhammer was firmly clamped at its top and bottom with the help of four numbers of semi- circular mild steel clamps, which were in turn bolted firmly to four numbers of mild steel bushes for frictionless vertical movement of the unit over the two guiding columns of the setup. In order that the top and bottom clamps work as one unit, they were firmly connected with the help of four numbers of vertical mild steel strips (1.3 cm thick, 5 cm width and 50 cm length) on each side of the jackhammer. For increasing the vertical thrust, two vertical mild steel strips (1.3 cm in thick, 5 cm width and 32 cm length) were bolted to the top and bottom clamps. On this strip, dead weights made up of mild steel blocks (16 cm diameter, 3.5 cm in thick; and 12.5 cm diameter, 3.5 cm in thick) as per the requirement were fixed with the help of nut and bolt arrangements.

For conducting drilling experiments at low thrust level (less than the dead-weight of drill machine assembly), a counter-weight assembly was fabricated. For this

purpose a steel wire rope (0.65 cm in diameter) was clamped to the top of the jackhammer unit, which in turn passed through the pulley arrangements located at the plate of the setup. A rigid frame was firmly grouted to the shop floor at a distance of 86 cm from the experimental setup. The steel wire rope from the experimental setup was made to pass over the pulley mounted on the rigid frame. At the other end of the rope, a plate was fixed for holding the counter-weights. The dead-weight of jackhammer drill machine and accessories for vertical drilling was 637 N. With the help of counter-weight arrangement, it was possible to achieve a desired thrust value of as low as 100 N. Similarly, through the arrangement of increasing the thrust level, it was possible to achieve a thrust value as high as 1000 N.
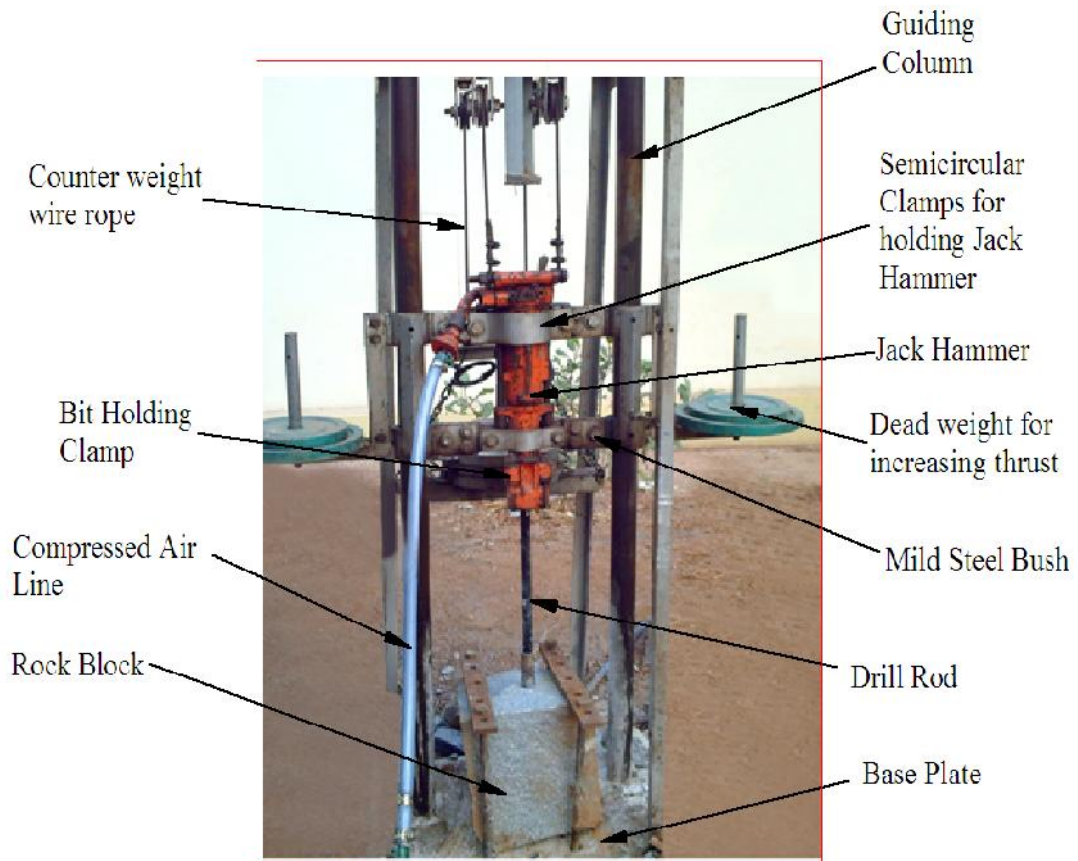
Fig. 4.1 Jackhammer drill setup for drilling vertical holes in rock samples

4.3 Instrumentation for Determining Rock Properties

The rock properties of all the rock samples used in this investigation were measured in the Rock Mechanics Laboratory of Department of Mining Engineering, NITK, Surathkal.

4.3.1 Uniaxial Compression Testing Machine

Uniaxial compressive strength is one of the most important mechanical properties of rock material used in excavation projects. AIM-317E-Mu micro-controlled compression testing machine was used for the measurement of uniaxial compressive strength as shown in Fig. 4.2. It has an intelligent pace rate controller, motorized pumping unit and loading unit with maximum loading capacity of 2,000 kN. The uniaxial compression strength of the rock specimens was determined as per International Society of Rock Mechanics (ISRM) suggested methods (Brown, 1981).

Fig. 4.2 AIM-317E-Mu Compression testing machine (AIMIL, New Delhi)

4.3.2 Los Angeles Abrasion Testing Set-up

Abrasion test measures the resistance of rock to wear. This test includes wear when subjected to an abrasive material, wear in contact with metal and wear produced by contact between the rocks. The abrasivity of rock samples was determined in accordance with the ISRM suggested methods (Brown, 1981). For this purpose, Los Angele's abrasion test apparatus was used (Fig. 4.3).

Fig.4.3 Los Angeles abrasion test apparatus (HEICO, New Delhi)

4.3.3 Brazilian Tensile Strength Testing Machine

Rocks generally have a low tensile strength which is due to the existence of micro cracks in the rock. The existence of micro cracks may also be the cause of rock failing suddenly in tension with a small strain. The tensile strength of rock was obtained from Brazilian test loading frame with 100 kN capacity, having a base and a cross-head joined together with two solid pillars with nuts (Fig. 4.4).

Fig. 4.4 Tensile strength testing machine (AIMIL, New Delhi)

At the top, the pillars have long threads for height adjustment and on the base a 100 kN hydraulic jack is centrally fixed between the pillars. This jack has an integral pumping unit and oil reservoir. A 100 kN capacity pressure gauge is fixed to the jack for indicating the load on the specimen and also an operating handle is provided with the jack.

4.3.4. Schmidt Hammer

Schmidt hammer hardness test is very valuable for a preliminary stage of designing a structure. This test is quick, cheap and non-destructive. Schmidt hammer was originally developed for measuring the strength of hardened concrete (Schmidt, 1951), but it can also be correlated with rock compressive strength (Miller, 1965; Barton and Choubey, 1977).
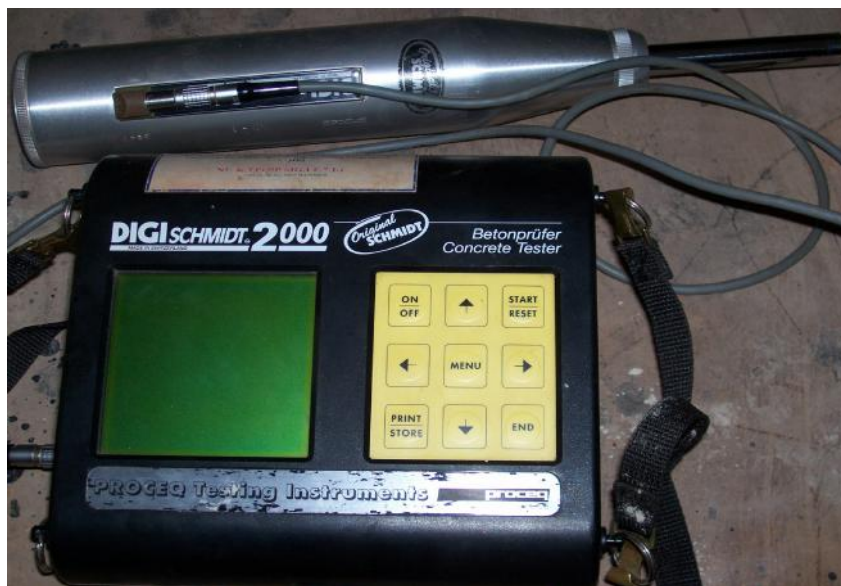
Fig.4.5. Digi Schmidt 2000 hammer hardness tester (Proceq SA, Switzerland)

The device consists of spring loaded steel mass that is automatically released against a plunger when the hammer is pressed against the rock surface. A small sliding pointer indicates the rebound of the hammer on a graduated scale. The principle of the test is based on the absorption of part of the spring-released energy through plastic deformation of the rock surface, while the remaining elastic energy causes the actual rebound of the hammer. The distance traveled by the mass, expressed as a percentage of the initial extension of the spring, is called the rebound

number (Kolaiti and Papadopoulus, 1993). This method is an index test which provides strength and deformability characteristics of rocks, but there are certain limitations concerning its application (Yılmaz, and Sendir, 2002). Fig. 4.5 shows the Digi Schmidt 2000 hammer used in this investigation.

4.4 Instrumentation for Sound Level Measurement

Sound pressure levels were measured with a CENTER make Model 320, IEC 651 Type II sound level meter. The instrument was equipped with a CENTER make windscreen for minimizing the sound effect produced from wind, ½ inch electret condenser microphone, digital display, time weighting and level ranges. The microphone and the preamplifier assembly were mounted directly on the sound level meter. The sound level meter was calibrated before taking up any measurement using an acoustic calibrator available in the institute. For all measurements, the sound level meter was hand-held. The instrument was set to measure A- weighted sound levels in the range of 30 dB (A) to 130 dB (A). Fig. 4.6 shows the Model 320, IEC 651 Type II sound level meter used in this investigation.

Fig.4.6. Model 320, IEC 651 Type II sound level meter

4.5 METHODOLOGY

4.5.1. Determination of Rock Property

The mechanical tests were carried out in the laboratory according to test standards suggested by International Society of Rock Mechanics (ISRM) methods (Brown, 1981).

4.5.2 Uniaxial Compressive Strength

Compressive strength is one of the most important mechanical properties of rock material, used in blast hole design. To determine the UCS of the rock samples, 54 mm diameter NX size core specimens, having a length-to-diameter ratio of 2.5:1 were prepared as suggested by ISRM standards (Brown, 1981). Each block was represented by at least three core specimens. The oven dried and NX size core specimens were tested by using a microcontroller compression testing machine. The average results of uniaxial compressive strength values of different rocks were arrived from the set of three measurements.

4.5.3 Abrasivity of Rock Specimens

The abrasivity of rock samples was also determined in accordance with the International Society of Rock Mechanics (ISRM) suggested methods. For this purpose, Los Angeles abrasion apparatus was used. The abrasion test requires two different sizes of rock samples i.e., 19.0-13.2 mm and 13.2–9.5 mm. One set of test samples of (1250±10) grams was prepared so that they pass through a sieve of 19.0 mm and are retained on a sieve of 13.2 mm. Another set of test samples of (1250 ±10) grams was prepared so that they pass through a sieve of 13.2 mm and retained on a 9.5 mm sieve. Both the test samples were placed in the Los Angeles abrasion testing machine. The abrasive charge consists of cast-iron spheres approximately 48 mm in diameter and each weighing between 390-445 grams. The machine is rotated at a speed of 20–30 revolution/minute for a period of 15 minutes. The material is then discharged from the machine and sieved on a 1.7 mm sieve. The material retained on the sieve is weighed. The abrasion resistance is calculated using the relation,

Abrasion resistance or Abrasivity = Loss in weight of the samples/original weight of the samples i.e. 5000 ± 20 gm) x 100%.

4.5.4 Tensile Strength

Tensile strength of rock was obtained from Brazilian test. To determine the tensile strength of the rock samples, 54 mm diameter NX-size core specimens, having a length less than 27 mm were prepared as suggested by ISRM standards (Brown, 1981). The cylindrical surfaces were made free of any irregularities across the thickness. End faces were made flat to within 0.25 mm and parallel to within 0.25°. The specimen was wrapped around its periphery with one layer of masking tape and loaded into the Brazilian tensile test apparatus across its diameter. Load was applied continuously at a constant rate so that failure occurred within 15-30 seconds. Three specimens of the same sample were tested and the average results of Brazilian tensile strength of different rocks were obtained.

4.5.5 Schmidt Rebound Number

Collected different rock block samples of sedimentary and igneous from different localities (Andhra Pradesh, Karnataka, Maharashtra and Rajasthan) of India were used to determine the Schmidt hardness. The rock samples having an approximate dimension of 30 cm × 20 cm × 20 cm were prepared, and the test surfaces of all specimens were smoothened and polished. Schmidt hammer hardness test were carried out in the laboratory according to the ISRM (1981a) suggested method. Schmidt hammer was held vertically and 5 impacts were carried out at each point, and peak rebound value was recorded. The test was repeated at least two times on any rock type and average value was recorded as rebound number. The hammer orientation was chosen in the same direction of the stress application in uniaxial compressive strength tests.

4.6 Experimental Procedure/ Methodology of Sound Level Measurement

The rock samples were kept on the base plate and clamped with properly bolt and nut. So that rock block is not moved while drilling. The drill rod attached to the chuck of the drill machine and the bit tip is made to touch the rock block (Fig.4.1). Initially collaring was done before starting drilling a hole in the rock. Air pressure

was varied from 392, 441, 490, 539 and 588 kPa and for each air pressure, thrust is varied from 100 N to 1000 N with an increment of 100 N on each rock sample. Noise measurements were carried out in open space (outdoor location) to reduce the effect of reflecting noise. In this laboratory investigation, total five drill bits were used. Three integral steel chisel bits with 30, 34, and 40 mm diameter and 42, 43, and 62 cm length and two threaded (R22) type bits with 35 and 38 mm diameter and 58 and 57.5 cm length of chisel and cross geometry were used. These bits were selected from among the available sizes. Fig. 4.7 shows the drill bits used in laboratory drilling experiments.

For each air pressure and thrust combination holes were drilled in each rock and sound level measurements were carried out. For each air pressure and thrust mentioned above, the A-weighted equivalent continuous sound level was measured (30 sec each at all the measurement locations and for a particular bit-rock combinations) by holding the sound level meter at a distance of 15 cm from the drill rod, drill bit, exhaust, and operator's position. Similarly, the A-weighted equivalent continuous sound level was measured at the operator's position refers to the position of the operator's ear, which was at a height of 1.7 m from the ground level and 0.75 m from the center of the experimental set up. Depth of the hole drilled was measured after the drilling operation in each rock block using vernier scale. The duration of drilling was recorded using a stop-watch and thereafter the penetration rate was determined from the depth of the hole drilled (mm) and the duration of drilling (s).

Fig. 4.7 Drill Bits used in laboratory drilling experiments (Integral and threaded)

4.7 Rock Samples Used in the Investigation

In this investigation, different types of sedimentary (shale, dolomite, sandstone, limestone, and hematite), and igneous rocks (dolerite, soda granite, black granite, basalt, and gabbros) were collected from different localities (Andhra Pradesh, Karnataka, Maharashtra and Rajasthan) of India taking care of variety of strength. During sample collection, each block was inspected for macroscopic defects so that it provides test specimens free of fractures and joints. Sound level measurement on pneumatic drill set up was carried out for 10 different rock samples. The size of the rock blocks was approximately 30 cm × 20 cm × 20 cm. A view of some of the rock blocks used in laboratory drilling experiments is shown in Fig. 4.8.

Fig. 4.8 View of some of the Rock Blocks used in laboratory drilling experiments
(Integral chisel and threaded cross bit)

 CHAPTER V

RESULTS OF EXPERIMENTAL INVESTIGATION

5.1 General

The results of various mechanical properties investigated for all the rock types are listed in Table 5.1. The primary objective of the present study was to establish the influence of operational parameters such as air pressure, thrust, bit type and diameter and mechanical properties such as uni-axial compressive strength (UCS), abrasivity, tensile strength (TS), Schmidt rebound number (SRN) of rocks on the performance of percussive drilling i.e. penetration rate (mm/s) and also the sound level (dB (A)) produced.

Table 5.1 Mechanical properties of rocks investigated

Sl no	Rock types	Uniaxial compressive strength (MPa)	Abrasivity (%)	Tensile strength (MPa)	Schmidt rebound number
1	Shale	30.8	15.2	4.37	570
2	Dolomite	38.9	16.7	4.83	602
3	Sandstone	63.6	17.3	5.76	621
4	Limestone	68.1	18.8	6.39	667
5	Hematite	73.6	19.5	6.84	703
6	Dolerite	81.2	20.1	7.57	722
7	Soda granite	98.4	20.5	9.13	733
8	Black granite	112.3	21.4	10.69	756
9	Basalt	119.8	22.5	11.30	767
10	Gabbros	129.7	23.8	12.85	790

5.2 Experimental Investigations on Penetration Rate of Percussive Drill

5.2.1 Influence of Air pressure on Penetration Rate

A. Integral Drill Bit

The penetration rate in various rocks (sedimentary and igneous) at different air pressures and thrust combinations is given in Table 5 of Appendix I. The influence of air pressure (392 to 588 kPa) on penetration rate for integral drill bit of 30 mm diameter at different thrust levels varying from 100 N to 1000 N with an increment of 100 N for sedimentary and igneous rocks is shown in Figure 5.1a & 5.1b (Appendix II). It was observed that, the penetration rate increased with increase in air pressure.

The penetration rate increased linearly when the air pressure is increased at lower thrust levels and non-linearly at higher thrust levels. The penetration rate varied from 0.44 to 1.27 and 0.90 to 3.75 mm/sec for air pressures of 392 and 588 kPa at different thrust levels varying from 100 N to 1000 N with an increment of 100 N for soft rock (shale) to hard rock (gabbros). Similar results were obtained at air pressures of 441, 490 and 539 kPa and are given separately for all the bit-rock combinations. Further similar type of results were also observed for drill bit diameters of 34 and 40 mm respectively for all 10 rocks considered and are given in Table 5.2a.

It was also observed that, with increase in air pressure from 392 to 588 kPa, the penetration rate increased from 0.20 to 2.99 mm/sec, 0.25 to 2.75 mm/sec and 0.29 to 2.45 mm/sec for integral drill bit diameters of 30, 34, and 40 mm for all the rocks considered (Table 5 of Appendix I).

At lower air pressures and given thrust, due to improper contact of bit with the rock, the penetration rate is low and at higher air pressures and for a given thrust, the impact energy increases and hence penetration rate is increased. Impact energy is proportional to the air pressure in percussive drilling. However, it is observed that beyond 588 kPa air pressure, there is no appreciable increase in penetration rate and curve is becoming asymptotic to the x-axis. Further, beyond air pressure of 588 kPa, if air pressure is increased, there is a danger of breaking of the drill rod due to more vibrations and flexural strains developed in the drill rod. This is also the true maximum recommended air pressure of jack hammer drills.

For all integral and threaded drill bits used in the present investigation, optimum penetration rate (mm/s) obtained was at a thrust of 400 N at air pressures of 392 and 441 kPa; at a thrust of 500 N at air pressures of 490 kPa; at a thrust of 600 N at air pressures of 539 kPa and at a thrust of 700 N at air pressures of 588 kPa for all the bit-rock combinations considered in case of sedimentary rocks. Similarly, optimum penetration rate (mm/s) was obtained at a thrust of 500 N at air pressures of 392 and 441 kPa; at a thrust of 600 N at air pressures of 490 kPa; at a thrust of 700 N at air pressures of 539 kPa and at a thrust of 800 N at air pressures of 588 kPa for all the bit-rock combinations considered in case of igneous rocks. The thrust at which optimum penetration rate was obtained for different rocks at different air pressures is shown as "Bold" in Table 5 for integral drill bit (Appendix I).

B. Threaded (R22) Drill Bit

The penetration rate in various rocks (sedimentary and igneous) at different air pressures and thrust combinations is given in Table 10 of Appendix I. The influence of air pressure (392 to 588 kPa) on penetration rate for threaded drill bit of 35 mm diameter at different thrust levels varying from 100 N to 1000 N with an increment of 100 N for sedimentary and igneous rocks is shown in Figure 5.2a & 5.2b (Appendix II). It was observed that, the penetration rate increased with increase in air pressure. The penetration rate increased linearly when the air pressure is increased at lower thrust levels and non-linearly at higher thrust levels. The penetration rate varied from 0.26 to 0.41 and 0.23 to 0.47 mm/sec for air pressures of 392 and 588 kPa at different thrust levels varying from 100 N to 1000 N with an increment of 100 N for soft rock (shale) to hard rock (gabbros). Similar results were obtained at air pressures of 441, 490 and 539 kPa and given separately in Table 5.2b for all the bit-rock combinations. Results of similar nature were also observed for drill bit diameter of 38 mm for all 10 rocks considered and are given in Table 5.2b.

It was also observed that, with increase in air pressure from 392 to 588 kPa, the penetration rate increased from 0.16 to 1.9 mm/sec and 0.12 to 1.8 mm/sec for threaded drill bit diameter of 38 mm for all the rocks considered (Table 10 of Appendix I).

It was observed that, penetration rate was higher in integral drills than threaded drill bit because of energy losses at joints in case of threaded drill bits. Air pressure and thrust were found to have a significant effect on the penetration rate for all the bit rock combinations considered in case of integral and threaded drill bits. The thrust at which optimum penetration rate was obtained for different rocks at different air pressures is shown as "Bold" in Table 10 for threaded drill bits (Appendix I).

5.2.2 Influence of Thrust on Penetration Rate

A. Integral Drill Bit

The penetration rate in various rocks (sedimentary and igneous) at different air pressures and thrust combinations is given in Table 5 of Appendix I. The influence of thrust (100 to 1000 N) on penetration rate for integral drill bit of 30 mm diameter with varying air pressure (392, 441, 490, 539 and 588 kPa) for different sedimentary and igneous rocks are shown in Figure 5.3a & 5.3b (Appendix II). It was observed that

penetration rate was less at lower thrust levels, for any given pressure and penetration rate increased to optimum thrust level beyond which the penetration rate was decreasing even though the thrust is increased. This is because excessive thrust was given; so that the drill bit was not made to complete the return stroke and if the thrust was further increased, the bit may reach the **"stall"** condition. However, due to inadequate number of rock samples, the experiment were not conducted till the stall condition is reached for all the bit-rock combinations considered.

The penetration rate increased linearly when the air pressure is increased at lower thrust levels and non-linearly at higher thrust levels. Air pressure and thrust were found to have a significant impact on the penetration rate in percussive drill for all the bit rock combinations considered.

- The penetration rate varied from 0.44 to 1.38, 0.37 to 1.31 and 0.30 to 0.70 mm/sec, for air pressure of 392 kPa at different thrust levels varying from 100 N to 1000 N with an increment of 100 N for soft rock (shale) to hard rock (gabbros) for drill bit diameters of 30, 34 and 40 mm respectively.

- It is observed from Fig. 5.4a & 5.4b (Appendix II) that penetration rate increased with increase in thrust, reaches the optimum level and then starts decreasing, at very high thrust level.

- The penetration rate varied from 0.90 to 3.95, 0.73 to 3.62 and 0.59 to 2.85 mm/sec for air pressure of 588 kPa at different thrust levels varying from 100 N to 1000 N with an increment of 100 N for soft rock (shale) to hard rock (gabbros) for drill bit diameters of 30, 34 and 40 mm respectively.

- The thrust at which optimum penetration rate was obtained for different rocks at different air pressures is shown as "Bold" in Table 5 for integral drill bit (Appendix I).

B. Threaded (R22) Drill Bit

The penetration rate in various rocks (sedimentary and igneous) at different air pressures and thrust combinations is given in Table 10 of Appendix I. The influence of thrust (100 to 1000 N) on penetration rate for threaded drill bit of 35 mm diameter

with varying air pressure (392, 441, 490, 539 and 588 kPa) for different sedimentary and igneous rocks are shown in Figure 5.5a & 5.5b (Appendix II). It is observed that, the penetration rate increased with the increase of thrust up to an optimum value beyond which, the penetration rate decreased with the increase in the values of thrust. In general, it was also observed that optimum penetration rate is different for different air pressures for a given bit-rock combinations. Very high thrusts do not result in high penetration rate even at higher operating air pressures.

Penetration rate varied from 0.26 to 0.59 and 0.23 to 0.62 mm/s for air pressure of 392 kPa and 0.48 to 2.17 and 0.43 to 1.99 mm/s for air pressure of 588 kPa at different thrust levels varying from 100 N to 1000 N with an increment of 100 N for soft rock (shale) to hard rock (gabbros). It is observed from Fig. 5.6a & 5.6b (Appendix II) that penetration rate increased with increase in thrust, reaches the optimum level and then starts decreasing for all the bit-rock combinations. The thrust at which optimum penetration rate was obtained for different rocks at different air pressures is shown as "Bold" in Table 10 for threaded drill bit (Appendix I).

5.2.3 Influence of Rock Properties on Penetration rate

A. Influence of Uni-axial Compressive Strength (UCS)

The uni-axial compressive strength (UCS) values of different rocks tested are given in Table 5.1. To study the influence of UCS on penetration rate, the penetration rate was taken (from Table 5 and 10 of Appendix I) at air pressure of 588 kPa and at optimum thrust of 700 N for sedimentary and 800 N for igneous rocks for all bit-rock combinations (both integral and threaded) considered as shown in Figure 5.7a and 5.7b (Appendix II).

It was observed that, with increase in UCS, the penetration rate decreases non-linearly for all the rocks considered. The rocks having more compressive strength offer more resistance to penetration. Hence, there is a decrease in penetration rate as the UCS increases for both sedimentary (soft rock) and igneous (hard rock) rocks.

B. Influence of Abrasivity

The abrasivity values of different rocks tested are given in Table 5.1. To study the influence of abrasivity on penetration rate, the penetration rate was taken (from Table 5 and 10 of Appendix I) at air pressure of 588 kPa and at optimum thrust of

700 N for sedimentary and 800 N for igneous rocks for all bit-rock combination considered as shown in Figure 5.8a and 5.8b (Appendix II).

The rocks having more abrasivity results in more bit wear and results in decrease in penetration rate. Hence as the abrasivity of rock increases, penetration rate decreases non-linearly for all rocks considered. It was observed that, abrasivity was more predominant property of rock which affects the penetration rate in percussive drilling. Hence, there is a decrease in penetration rate as the abrasivity increases for both sedimentary (soft rock) and igneous (hard rock) rocks.

5.2.4 Influence of Bit Diameter on Penetration Rate

A. Integral Drill Bit

The influence of bit diameter (30, 34 and 40 mm) on penetration rate was also analyzed. This analysis was done by measuring penetration rate at air pressure of 588 kPa at different thrust levels varying from 100 N to 1000 N with an increment of 100 N for different sedimentary and igneous rocks. This is shown in Figure 5.9a & 5.9b (Appendix II). It was observed that with an increase in bit diameter, penetration rate decreases for all the bit-rock combination considered. A small diameter bit has to remove a smaller volume of rock in drilling a hole of given length than a bit of larger diameter.

For a given air pressure and thrust combination of integral drill bit, the force exerted at the bit rock interface is same. However, the area of contact will be increasing as the bit diameter increases, which results in decrease in energy available for penetration because E = F/A.

where E = Energy developed (Joules)

F = Force exerted at bit-rock interface (N)

A = area of the bit (mm^2)

Variation in penetration from shale (soft rock) to gabbros (hard rock) at different thrust levels varying from 100 N to 1000 N with an increment of 100 N for different air pressures for integral drill bit diameters of 30, 34 and 40 mm is given in Table 5.2 a.

B. Threaded (R22) Drill Bit

Find the influence of bit diameter (35 and 38 mm) on penetration rate, the penetration rate was taken at air pressure of 588 kPa at different thrust levels varying from 100 N to 1000 N with an increment of 100 N for different sedimentary and igneous rocks are shown in Figure 5.10a & 5.10b (Appendix II). It was observed that with an increase in bit diameter, penetration rate decreases for all the bit-rock combination considered. A small diameter bit has to remove a smaller volume of rock in drilling a hole of given length than a bit of larger diameter.

Integral steel chisel bit achieves more penetration rate than threaded (R22) type bit because of energy losses at joints in all the rocks considered for a given bit-rock combination. Variation in penetration from shale (soft rock) to gabbros (hard rock) at different thrust levels varying from 100 N to 1000 N with an increment of 100 N for different air pressures for threaded drill bit diameters of 35 and 38 mm is given in Table 5.2 b.

5.3 Rock Properties vis-à-vis on Sound Level Produced by Percussive Drill

5.3.1 Rock Properties and Sound Level -At Operator's Position

A. Integral Drill Bit

The influence of bit diameter on sound level at operator's position using integral drill bit are shown in Fig.5.11a & 5.11b (Appendix II). It was observed that, with increase in bit diameters, air pressure and thrust, the sound level also increased for all the rocks tested.

The A-weighted equivalent continuous sound level at operator's position for sedimentary and igneous rocks at various thrust and air pressure is given in Table 1 of Appendix I for integral drill bit diameters of 30, 34 and 40 mm. It is seen that, for the entire bit-rock combinations, the sound level increases with the increase of thrust up to a certain value beyond which there is a gradual decrease in the sound level. In general it is observed that maximum sound level is different for different air pressures at operators position for a given bit-rock combination as shown in Fig 5.12a & 5.12b (Appendix II).

The sound level increased linearly when the air pressure is increased at lower thrust levels and non-linearly at higher thrust levels. At lower air pressure and given

thrust, due to improper contact of bit with the rock, the sound level is low and at higher air pressures and given thrust, the impact energy increases and hence an increase in sound level. Impact energy is proportional to the air pressure in percussive drilling. However, it is observed that beyond 588 kPa air pressure, there is no appreciable increase in sound level and curve is becoming asymptotic to the x-axis. However, beyond air pressure of 588 kPa, there is a danger of breaking of the drill rod due to more vibrations and flexural strains developed in the drill rod. This is also the true maximum recommended air pressure of jack hammer drills. Air pressure and thrust were found to have a significant impact on the sound level in percussive drill for all the bit rock combinations considered.

Fig. 5.13a & 5.13b (Appendix II) shows the sound level with varying drill bit diameter and thrust keeping the operating air pressure constant at 392 kPa for different rocks at operator's position. It is also observed that, an increase in the sound level is associated with increase in bit diameters for all the rocks from shale to gabbros. It is clearly seen that, the sound level increases with increase in thrust, reaches maximum at a certain thrust level (400 N for sedimentary rock and 500 N for igneous rock) and then it starts decreasing. The sound level variation was observed from shale (minimum sound level) to gabbros (maximum sound level) as 2.9 to 3.8, 3.2 to 3.9 & 2.8 to 4.0 dB (A) for drill bit diameters of 30, 34 and 40 mm respectively.

It was observed that sound level was low at lower thrust levels, for any given pressure and it increased up to optimum thrust level, beyond which the sound level was decreasing even though the thrust is increased. This is because, at higher thrust, the drill bit was not able to complete the return stroke and may reach the **"stall"** condition. However, due to lack of rock samples, the experiment were not conducted till the stall condition is reached for all the bit-rock combinations considered.

Fig. 5.14a & 5.14b (Appendix II) shows the variation in sound level for drill bit diameters of (30, 34 and 40 mm) and thrust (100 to 1000 N) keeping the operating air pressure constant at 588 kPa at operator's position for different rocks. It is observed from Fig. 5.14a & 5.14b (Appendix II) that sound level increases with increase in thrust, reaches the maximum level at thrust of 700 N for sedimentary rock and 800 N for igneous rock and then starts decreasing. The increase in sound level from shale (minimum sound level) to gabbros (maximum sound level) was 2.5 to 2.9,

2.7 to 3.0 and 2.6 to 2.9 dB (A) for drill bit diameters of 30, 34 and 40 mm respectively. The maximum sound level (dB (A)) obtained (both integral and threaded drill bit) for sedimentary rock in the present investigation was at air pressures of 392 and 441 kPa and at 400 N, 490 kPa at 500 N, 539 kPa at 600 N and 588 kPa at 700 N for all the rock blocks tested. Similarly, maximum sound level for igneous rocks was also at air pressures of 392 and 441 kPa at 500 N, 490 kPa at 600 N, 539 kPa at 700 N and 588 kPa at 800 N for all the rock blocks tested. The maximum sound level for different rock blocks at different air pressures is shown as "Bold" in Table 1 of Appendix I for integral drill bit.

It was observed that, with increase in air pressure from 392 to 588 kPa, the sound level increases by 1.0 to 3.0 dB, 1.4 to 2.6 dB and 1.3 to 3.5 dB (A) for integral drill bit diameters of 30, 34 and 40 mm for all the rocks considered for a given bit-rock combination.

To study the influence of UCS on sound level, the sound level was taken (from Table 1 and 6 of Appendix I) at air pressure of 588 kPa and at optimum thrust of 700 N for sedimentary and 800 N for igneous rocks for all bit-rock combinations (both integral and threaded) considered as shown in Figure 5.15a and 5.15b (Appendix II).

It was observed that, with increase in UCS, the sound level increases non-linearly for all rocks considered. The rocks having more compressive strength offer more resistance. Hence, there is an increase in sound level as the UCS increases for both sedimentary (soft rock) and igneous (hard rock) rocks for the entire bit-rock combinations.

The abrasivity values of different rocks tested are given in Table 5.1. To study the influence of abrasivity on sound level, the sound level was taken (from Table 1 and 6 of Appendix I) at air pressure of 588 kPa and at optimum thrust of 700 N for sedimentary and 800 N for igneous rocks for all bit-rock combination considered as shown in Figure 5.16a and 5.16b (Appendix II).

The rocks having more abrasivity results in more bit wear and increase in sound level. Hence with increase in abrasivity of rocks, sound level increases non-linearly for all rocks considered. It was observed that, abrasivity was more predominant property of rock which affects the sound level in percussive drilling.

Hence, there is an increase in sound level as the abrasivity increases for both sedimentary (soft rock) and igneous (hard rock) rocks for all the bit-rock combination considered.

B. Threaded (R22) Drill Bit

The A-weighted equivalent continuous sound level (dB (A)) for sedimentary and igneous rocks at various thrust and air pressure values at operators position is given in Table 6 of Appendix I for threaded (R22) drill bit of diameters 35 and 38 mm. The Influence of thrust (100 to 1000 N) on A-weighted sound level at operator's position at air pressure of 392 and 588 kPa with varying drill bit diameters of 35 and 38 mm for different sedimentary and igneous rocks is shown in Figure 5.17a & 5.17b to 5.18a & 5.18b (Appendix II). Similar trends were observed, for the entire bit-rock combinations as in the case of integral drill bit.

The increase in sound level from shale (minimum sound level) to gabbros (maximum sound level) was 2.9 to 3.4 and 3.2 to 3.5 dB (A) for air pressure of 392 kPa and 2.5 to 3.0 and 2.4 to 3.2 dB (A) for air pressure of 588 kPa. The optimum sound level for different rocks at different air pressures is shown as "Bold" in Table 6 of Appendix I for threaded drill bit.

It was observed that, sound level was higher in integral drills than threaded drill bit because of higher energy losses at joints. Air pressure and thrust were found to have a significant impact on the sound level for all the bit rock combinations considered in case of integral and threaded drill bits.

It was also observed that, with, increase in air pressure from 392 to 588 kPa, the sound level increased by 1.5 to 3.5 dB (A) and 1.8 to 3.7 dB (A) for threaded drill bit diameters of 35 and 38 mm respectively for all the rocks considered for a given bit-rock combinations.

5.3.2 Rock Properties and Sound level -At Exhaust
A. Integral Drill Bit

The A-weighted equivalent continuous sound level for sedimentary and igneous rocks at exhaust and for various thrust and air pressure values is given in Table 2 of Appendix I. Influence of thrust (100 to 1000 N) on A-weighted sound level at exhaust position at constant air pressure of 588 kPa with varying integral bit

diameter (30, 34 and 40 mm) is shown in Figure 5.19a & 5.19b (Appendix II). It is observed that, an increase in the sound level is associated with increase in bit diameters for all the rocks from shale to gabbros. It is clearly seen that, the sound level increases with increase in thrust, reaches maximum and then it starts decreasing as explained in Section 5.3.1A. A significant increase in the sound level with an increase in the UCS and abrasivity is observed for different rocks near the exhaust. Influence of UCS on A-weighted sound level at exhaust position at given air pressure of 588 kPa with integral and threaded drill bit for five different sedimentary and igneous rocks at thrust of 700 N and 800 N is shown in Figure 5.20a & 5.20b (Appendix II). It was observed that, with increase in UCS, bit diameter and thrust, the sound level also increases for all the rocks tested.

It was observed that, with increase in air pressure from 392 to 588 kPa, the sound level increased by 1.5 to 4.0 dB, 2.0 to 4.2 dB (A) and 1.6 to 3.7 dB (A) for integral drill bit diameters of 30, 34 and 40 mm respectively for all the rocks considered for a given bit-rock combinations.

Influence of abrasivity on A-weighted sound level at exhaust position at given air pressure of 588 kPa with integral and threaded drill bits for five different sedimentary and igneous rocks at thrust of 700 N and 800 N is shown in Figure 5.21a & 5.21b (Appendix II). It was observed that, with increase in abrasivity, bit diameter and thrust, the sound level also increases for all the rocks tested.

Similar results were obtained with integral drill bit diameters of 34 and 40 mm. The increase in sound level from shale to gabbros for a particular bit-rock combination at 100 to 1000 N thrust for different air pressures are given in Table 5.3a.

B. Threaded Drill Bit

The A-weighted equivalent continuous sound level for sedimentary and igneous rocks at exhaust and for various thrust and air pressure values is given in Table 7 of Appendix I. Influence of thrust (100 to 1000 N) on A-weighted sound level at exhaust position at constant air pressure of 588 kPa with varying threaded bit diameter (35 and 38 mm) is shown in Figure 5.22a & 5.22b (Appendix II). It is observed that, an increase in the sound level is associated with increase in bit diameters for all the rocks tested. It was also observed that, sound level was more in

integral drills than threaded drill bit because of energy losses at joints. Similar trends were observed for influence of UCS and abrasivity on sound level, as in the case of integral drill bit. Results of similar type were obtained with drill bit diameter of 38 mm threaded. Increase in sound level from shale to gabbros at different thrust levels (100 to 1000 N) for different air pressures are given in Table 5.3b. The same trend was observed at exhaust position for different values of thrust and air pressure for different rock samples. It was observed that, with increase in UCS and abrasivity, the sound level increase non-linearly for all rocks considered as shown in Figure 5.20a & 5.20b and 5.21a & 5.21b (Appendix II). The rocks having more compressive strength offer more resistance. Hence, there is an increase in sound level as the UCS increases for both sedimentary (soft rock) and igneous (hard rock) rocks.

It was observed that, with increase in air pressure from 392 to 588 kPa, the sound level increased by 1.8 to 4.2 dB (A) and 2.0 to 4.0 dB (A) for threaded drill bit diameters of 35 and 38 mm respectively for all the rocks considered for a given bit-rock combinations.

5.3.3 Rock Properties and Sound level-Near Drill Bit

A. Integral Drill Bit

The A-weighted equivalent continuous sound level for sedimentary and igneous rocks near drill bit and for various thrust and air pressure values is given in Table 3 of Appendix I. Influence of thrust (100 to 1000 N) on A-weighted sound level near drill bit at constant air pressure of 588 kPa with varying integral bit diameters (30, 34 and 40 mm) is shown in Figure 5.23a and 5.23b (Appendix II). It is observed that, an increase in the sound level is associated with increase in bit diameters and for all the rocks from shale to gabbros. It is clearly seen that, the sound level increased with increase in thrust, reaches maximum and then it starts decreasing as explained in Section 5.3.1A. The influence of thrust (100 to 1000 N) on A-weighted Leq sound level at all the measurement locations at drill bit diameter of 30 mm and air pressure of 392 kPa for different rock samples is shown in Fig. 5.24a & 5.24b (Appendix II). An increase in the sound level was observed at each thrust and air pressure with an increase in the compressive strength and abrasivity for different rocks near the drill bit.

It was observed that, with increase in air pressure from 392 to 588 kPa, the sound level increased by 1.6 to 3.4 dB (A), 2.0 to 3.7 dB (A) and 1.8 to 3.9 dB (A) for integral drill bit diameters of 30, 34 and 40 mm respectively for all the rocks considered for a given bit-rock combinations.

Influence of UCS on A-weighted sound level near drill bit at given air pressure of 588 kPa with integral and threaded drill bit for five different sedimentary and igneous rocks at thrust of 700 N and 800 N is shown in Figure 5.25a & 5.25b (Appendix II). It was observed that, with increase in UCS, bit diameter and thrust, the sound level also increases for all the rocks tested. Influence of abrasivity on A-weighted sound level near drill bit at given air pressure of 588 kPa with integral and threaded drill bit for five different sedimentary and igneous rocks at thrust of 700 N and 800 N is shown in Figure 5.26a & 5.26b (Appendix II). It was observed that, with increase in abrasivity, bit diameter and thrust, the sound level also increased for all the rocks tested.

This shows that an increase in the UCS and abrasivity of rock increases the sound level significantly. Air pressure and thrust were observed to have a significant impact on the sound level, as the trend of change in the sound level at various bit-rock combinations as well as thrust and air pressure values at all the measurement locations is similar.

B. Threaded Drill Bit

The A-weighted equivalent continuous sound level for sedimentary and igneous rocks near drill bit and for various thrust and air pressure values is given in Table 8 of Appendix I. Influence of thrust (100 to 1000 N) on A-weighted sound level near drill bit at constant air pressure of 588 kPa with varying threaded bit diameter (35 and 38 mm) is shown in Figure 5.27a & 5.27b (Appendix II). It is observed from the figure that, an increase in the sound level with increase in bit diameters for all the rocks tested is observed and is similar to that of Section 5.3.2B. Similar trends were observed, for the entire bit-rock combinations as in the case of integral drill bit.

The A-weighted equivalent continuous sound level near drill bit for rocks at various thrust and air pressure is given in Table 8 of Appendix I. Similar trends were observed for influence of UCS and abrasivity on sound level, as in the case of integral

drill bit. Results of similar nature were obtained with drill bit diameter of 38 mm threaded. Increase in sound level from shale to gabbros at different thrust levels (100 to 1000 N) for different air pressures are given in Table 5.3b. The same trend was observed near drill bit for different values of thrust and air pressure for different rock samples. It was observed that, with increase in UCS and abrasivity, the sound level increase non-linearly for all rocks considered as shown in Figure 5.25a & 5.25b (Appendix II) and 5.26a & 5.26b (Appendix II). The rocks having more compressive strength offer more resistance. Hence, there is an increase in sound level as the UCS increases for both sedimentary (soft rock) and igneous (hard rock) rocks. The rocks having more abrasivity results in more bit wear and results in increase in sound level. Hence as the abrasivity of rock increases, sound level increases non-linearly for all the rocks considered. It was observed that, abrasivity was more predominant property of rock which affects the sound level in percussive drilling. Hence, there is an increase in sound level as the abrasivity increases for both sedimentary (soft rock) and igneous (hard rock) rocks.

It was observed that, with, increase air pressure from 392 to 588 kPa, the sound level increased by 1.4 to 3.6 dB (A) and 1.2 to 3.5 dB (A) for threaded drill bit diameters of 35 and 38 mm respectively for all the rocks considered for a given bit-rock combinations.

5.3.4 Rock properties and Sound level-Near Drill Rod
A. Integral Drill Bit

The A-weighted equivalent continuous sound level near drill rod for sedimentary and igneous rocks at various thrust and air pressure is given in Table 4 of Appendix I. The A-weighted Leq sound level was measured by holding the sound level meter near the drill rod at a height of 20 cm above the surface of the rock block and at a distance of 15 cm from the drill rod. Influence of thrust (100 to 1000 N) on A-weighted sound level near drill rod at constant air pressure of 588 kPa with varying integral bit diameters (30, 34 and 40 mm) is shown in Figure 5.28a & 5.28b (Appendix II). It is observed that, an increase in the sound level is associated with increase in bit diameters for all the rocks from shale to gabbros. It is clearly seen that, the sound level increases with increase in thrust, reaches maximum and then it starts

decreasing as explained in Section 5.3.1A. The influence of thrust (100 to 1000 N) on A-weighted Leq sound level at all the measurement locations at constant drill bit diameter of 30 mm and constant air pressure of 588 kPa for different rock samples is shown in Fig. 5.29a & 5.29b (Appendix II). It was found that, sound level increases with the increase in air pressure and thrust for all the bit rock combinations. Variation in sound level from shale to gabbros at 100 to 1000 N thrust for different air pressures at all the measurement locations for integral drill bit is given separately in Table 5.3a.

It was observed that, with increase in air pressure from 392 to 588 kPa, the sound level increased by 1.4 to 3.5 dB (A), 1.8 to 3.8 dB (A) and 1.6 to 3.0 dB (A) for integral drill bit diameters of 30, 34 and 40 mm respectively for all the rocks considered for a given bit-rock combinations. Influence of UCS on A-weighted sound level near drill rod at given air pressure of 588 kPa with integral and threaded drill bit for five different sedimentary and igneous rocks at thrust of 700 N and 800 N is shown in Figure 5.30 a & 5.30b (Appendix II). It was observed that, with increase in UCS, bit diameter and thrust, the sound level also increased for all the rocks tested. Influence of abrasivity on A-weighted sound level near drill rod at given air pressure of 588 kPa with integral and threaded drill bit for five different sedimentary and igneous rocks at thrust of 700 N and 800 N is shown in Figure 5.31a & 5.31b (Appendix II). It was observed that, with increase in abrasivity, bit diameter and thrust, the sound level also increased for all the rocks tested.

Sound level near the drill rod is comparatively higher than that near the drill bit, exhaust and the operators position for a given operating parameters and bit-rock combinations used for integral and threaded bits. This is due to increased vibrations in the drill rod. For both integral and threaded drill bits, the sound level increases with increase in the bit diameter. Further, integral steel chisel bit gives higher sound level than threaded bit in all the rocks considered for a given bit-rock combination. Air pressure and thrust were found to have a significant impact on the sound level produced by percussive drill for all the bit rock combinations considered.

B. Threaded Drill Bit

The A-weighted equivalent continuous sound level near drill rod for sedimentary and igneous rocks at various thrust and air pressure is given in Table 9 of Appendix I. Influence of thrust (100 to 1000 N) on A-weighted sound level near drill

rod at constant air pressure of 588 kPa with varying threaded bit diameter (35 and 38 mm) is shown in Figure 5.32a & 5.32b (Appendix II). It is observed from the figure that, an increase in the sound level is associated with increase in bit diameters for all the rocks tested and as explained in Section 5.3.2B. The influence of thrust (100 to 1000 N) on A-weighted Leq sound level at all the measurement locations at constant drill bit diameter of 35 mm and constant air pressure of 588 kPa for different rock samples is shown in Fig. 5.33a & 5.33b (Appendix II). It was found that, sound level increases with increase in air pressure and thrust for all the bit rock combinations. Similar results were obtained with drill bit diameter of 38 mm threaded. Increase in sound level from shale to gabbros at different thrust levels (100 to 1000 N) for different air pressures are given in Table 5.3b. The same trend was observed near drill rod for different values of thrust and air pressure for different rock samples. It was observed that, with increase in UCS and abrasivity, the sound level increase non-linearly for all rocks considered as shown in Figure 5.30a & 5.30b and 5.31a & 5.31b (Appendix II) and as explained in Section 5.3.3B. It was observed that, with increase in air pressure from 392 to 588 kPa, the sound level increased by 1.7 to 3.5 dB (A) and 2.0 to 3.7 dB (A) for threaded drill bit diameters of 35 and 38 mm respectively for all the rocks considered for a given bit-rock combinations.

Table 5.2a Variation in penetration rate from shale to gabbros at 100 to 1000 N thrust for different air pressures for integral drill bit diameters of 30, 34 and 40 mm

Drill bit diameter (mm)	Air pressure (kPa)				
	392	441	490	539	588
	Penetration rate (mm/s)				
30	0.44-1.27	0.50-1.55	0.58-2.40	0.71-3.08	0.90-3.75
34	0.37-1.22	0.52-1.47	0.57-0.97	0.66-1.65	0.73-3.42
40	0.30-0.75	0.36-0.80	0.44-1.51	0.51-2.16	0.59-2.64

Table 5.2b Variation in penetration rate from shale to gabbros at 100 to1000 N thrust for different air pressures for threaded drill bit diameters of 35 and 38 mm

Drill bit diameter (mm)	Air pressure (kPa)				
	392	441	490	539	588
	Penetration rate (mm/s)				
35	0.26-0.41	0.31-0.67	0.34-1.08	0.4.0-1.49	0.48-1.60
38	0.23-0.47	0.25-0.70	0.31-1.11	0.37-1.44	0.43-1.56

Table 5.3a Increase in sound level from shale to gabbros at 100 to 1000 N thrust for different air pressures at all the measurement locations for integral drill bit

Measurement locations	Drill bit diameter (mm)	Air pressure (kPa)				
		392	441	490	539	588
		A-weighted sound level (dB (A))				
Operators position	30	2.9-3.8	2.8-3.7	3.0-3.7	3.1-3.5	2.5-2.9
	34	3.2-3.9	3.2-4.0	2.9-3.7	3.0-3.4	2.7-3.0
	40	2.8-4.0	3.1-4.2	2.8-3.3	2.8-3.2	2.6-2.9
Exhaust position	30	3.6-4.1	3.4-4.1	3.0-3.5	3.1-3.6	2.8-3.5
	34	3.5-3.9	3.5-4.0	3.1-3.5	3.0-3.5	3.0-3.5
	40	3.3-4.1	3.3-3.9	3.2-3.8	2.9-3.3	2.7-3.4
Near drill Bit	30	3.1-3.5	3.0-3.3	3.0-3.3	3.0-3.4	3.0-3.2
	34	3.2-3.7	2.6-3.0	3.1-3.4	2.9-3.3	2.6-3.1
	40	3.0-3.7	2.8-3.4	2.9-3.2	2.1-2.7	2.5-2.8
Near drill rod	30	3.3-3.8	2.7-3.3	2.8-3.8	3.0-3.4	2.9-3.3
	34	3.2-3.7	2.9-3.9	2.6-3.2	2.8-3.4	2.8-3.1
	40	3.1 3.5	2.8-3.7	2.7-3.3	2.9-4.1	2.1-2.8

Table 5.3b Increase in sound level from shale to gabbros at 100 to 1000 N thrust for different air pressures at all the measurement locations for threaded drill bit

Measurement locations	Drill bit diameter (mm)	Air pressure (kPa)				
		392	441	490	539	588
		A-weighted sound level (dB (A))				
Operators Position	35	2.9-3.4	3.2-3.9	2.9-3.6	3.2-3.6	2.5-3.0
	38	3.2-3.5	3.1-3.7	2.8-3.7	3.0-3.6	2.4-3.2
Exhaust Position	35	3.1-4.2	3.0-4.0	3.0-3.5	3.2-3.5	2.8-3.5
	38	3.2-4.3	3.0-3.8	3.1-3.6	3.1-3.7	2.9-3.7
Near drill Bit	35	3.1-3.8	2.9-3.5	3.2-3.6	3.0-3.6	2.6-2.9
	38	3.3-3.7	2.8-3.6	2.9-3.5	3.1-3.5	2.4-2.7
Near drill rod	35	3.4-3.9	3.2-4.1	2.9-3.6	3.0-3.7	3.0-3.5
	38	3.5–4.0	3.0-3.5	3.1-3.6	3.1-3.7	3.2-3.7

5.4 Summary of Results and Discussion

1. For all the bit-rock combinations, the penetration rate and sound level increased up to a certain value of thrust (air pressures of 392 and 441 kPa at 400 N, 490 kPa at 500 N, 539 kPa at 600 N and 588 kPa at 700 N in case of sedimentary rocks and 392 and 441 kPa at 500 N, 490 kPa at 600 N, 539 kPa at 700 N and 588 kPa at 800 N in case of igneous rocks) beyond which it decreases gradually with increase in thrust (air pressures of 392 and 441 kPa at 500 N, 490 kPa at 600 N, 539 kPa at 600 N and 588 kPa at 800 N in case of sedimentary rocks and 392 and 441 kPa at 600 N, 490 kPa at

700 N, 539 kPa at 800 N and 588 kPa at 900 N in case of igneous rocks). The maximum value of penetration rate and sound level also varies with the air pressure for a given bit-rock combination. Both at lower and higher thrust levels, the penetration rate and sound levels are lower. Air pressure and thrust were found to have a significant impact on penetration rate and sound level produced by percussive drill for all the bit- rock combinations considered.

2. The penetration rate decreases with increase in the bit diameter for both integral and threaded drill bits. Further, integral steel chisel bit gives higher penetration rate than threaded bit because of energy losses at joints in all the rocks considered for a given bit-rock combination.

3. The penetration rate and sound level increases as the air pressure increases. At lower air pressure and thrust level, the drill steel bounces back indicating improper contact of the bit with the rock.

4. Sound level increases and penetration rate decreases with increase in uni-axial compressive strength and abrasivity for all bit rock combinations. Further, sound level near the drill rod is comparatively higher than that near the drill bit, exhaust and the operators position for a given operating parameters and bit-rock combinations used for integral and threaded bits. This is due to increased vibrations in the drill rod.

CHAPTER – VI

MULTIPLE REGRESSION ANALYSIS

6.1 General

Regression analysis is the statistical methodology for predicting values of one or more dependent variables from a collection of (independent) variables. Multiple regressions are widely used for identifying the relationship between dependent variable and several predictor variables. This method works best when there are complex interactions between various factors. It is a powerful modeling technique Yilmaz, and Yuksek, 2009). Multiple regression and Analysis of variance (ANOVA) techniques were used, in order to establish the predictive models among the parameters obtained in this research work. For modeling and analysis Minitab 15 software for windows was used (NITK Laboratory).

6.2 Multiple Regression Analysis (MRA)

Generally the purpose of multiple regression analysis is to learn more about the relationship between several predictor variables and a dependent or criterion variable. The performance of the model depends on a large number of factors that act and interact in a complex manner. The mathematical modeling of penetration rate and sound level produced during drilling is influenced by many factors. Therefore, a detailed process representation anticipates a second order model. ANOVA was carried out to find out which input parameter significantly affects the desired response. To facilitate the experiments and measurement, five important parameters were considered in the present study. They are: air pressure in kPa (A), drill bit diameter in mm (B), thrust in N (C), equivalent sound level produced during drilling in dB (D), and penetration rate in mm/sec (E). The responses considered are uni-axial compressive strength (UCS), Schmidt rebound number (SRN), tensile strength (TS) and abrasivity. The mathematical models for the mechanical properties with parameters under consideration can be expressed as

$$Y = f(x_1, x_2, x_3, ...) + \in \qquad\qquad \text{------------ (6.1)}$$

where Y represents the response and x_1, x_2, x_3 are the independent process

variables and $\in$ is fitting error (Srivastava, 2002). The second order polynomial equation used to represent response surface for the factor is given by

$$Y = b_0 + \sum_{i=1}^{n} b_i x_i + \sum_{i=1}^{n} b_{ij} x_i^2 + \sum_{\substack{i=1 \\ i<j}}^{n} b_{ij} x_i x_j + \in \qquad \text{--------------- (6.2)}$$

When there is a curvature in the response surface the first-order model is insufficient. A second order model is useful in approximating a portion of the true response surface with parabolic curvature. The second-order model includes all the terms in the first-order model, plus all quadratic terms like $b_{11} x_{1i}^2$ and all cross product terms like $b_{13}\, x_{1i}\, x_{3j}$. The second-order model is flexible, because it can take a variety of functional forms and approximates the response surface locally. Therefore, this model is usually a good estimation of the true response surface (Myer and Montgomery 2002).

In order to compare all the reasonable regression models, a backward elimination procedure was used as the screening procedure. Then the predictor variable having the absolute smallest t statistic was selected. If the t statistic was not significant at the selected level (95% confidence interval), the predictor variable under consideration was removed from the model and the regression analysis was performed using a regression model containing all the remaining predictor variables. If the t statistic was significant, the model was selected. The procedure was continued by removing one predictor variable at a time from the model. The screening was stopped when the predictor variable remaining in the model could not be removed further from the system (Rajesh Kumar et al. 2011).

6.3 Regression Modeling

For developing the regression model, results of Table 5.1 Chapter V and Table 1 to 10 of Appendix I were used. For each combination of drill bit diameter, air pressure and thrust, a total of 150 sets of test conditions were arrived for integral drill bits. A 150 set of test conditions was arrived considering the machine parameters as given below:

(a) Integral drill bit diameters of 30, 34, and 40 mm,

(b) Air pressure of 392, 441, 490, 539 and 588 kPa

(c) Thrust from 100, 200, 300, 400, 500, 600, 700, 800, 900 and 1000 N,

Therefore, as can be seen, the total test conditions from the above is 3 (drill bits) × 5(air pressure values) × 10(Thrust values) which gives a value of 150. Further, penetration rate and sound level (A-weighted) during drilling for 5 types of sedimentary rocks were carried out which makes the total test as 150 × 5 = 750. Therefore a total of 750 test values were used for developing the regression model for integral drill bit.

Similarly, for each combination of drill bit diameter, air pressure and thrust, a total of 100 sets of test conditions were arrived. A 100 set of test conditions was arrived considering the machine parameters as given below:

(a) Threaded (R22) drill bit diameters of 35 and 38 mm,

(b) Air pressure of 392, 441, 490, 539 and 588 kPa

(c) Thrust from 100, 200, 300, 400, 500, 600, 700, 800, 900 and 1000 N,

Therefore, as can be seen, the total test conditions from the above is 2 (drill bits) × 5(air pressure values) × 10(Thrust values) which gives a value of 100. Further, penetration rate and sound level (A-weighted) during drilling for 5 types of sedimentary rocks were carried out which makes the total test as 100 × 5= 500. Therefore a total of 500 test values were used for developing the regression model for threaded drill bit.

Though sound level measurements were taken at operator's position, exhaust position, near drill bit and near drill rod separately, for developing the model, arithmetic average values of sound level for all the above mentioned positions were used for each condition.

In this work, mathematical models were developed for the prediction of uni-axial compressive strength (UCS), abrasivity, tensile strength (TS) and Schmidt rebound number (SRN) for the rocks considering penetration rate and sound level produced during percussive drilling. Further, mathematical models were also developed for the prediction of penetration rate and sound level for a given air pressure, thrust and bit-rock combinations. Ten different types of rocks (5 sedimentary and 5 igneous) were used.

6.3.1 Development of Mathematical Models for the Prediction of Rock Properties Using Penetration Rate and Sound Level

6.3.1.1 Models to Predict Rock Properties of Sedimentary and Igneous Rock Using Integral Drill Bit

The nomenclature of various variables are: air pressure in kPa (A), drill bit diameter in mm (B), thrust in N (C), equivalent sound level produced during drilling in dB (D), and penetration rate in mm/s (E).

A. Prediction of Uni-axial Compressive Strength (UCS) of Sedimentary and Igneous Rocks

Prediction of UCS of sedimentary rocks is:

$$\text{UCS}=-89080.5-12.14{\times}A-213.64{\times}B+0.4864{\times}C+1585.22{\times}D-756.84{\times}E-0.0005924{\times}A^2$$
$$-0.079{\times}B^2+0.000056{\times}C^2-7.04364{\times}D^2-4.054{\times}E^2-0.013{\times}A{\times}B+0.10825{\times}A{\times}D+1.8764$$
$$\times B{\times}D-1.4215{\times}B{\times}E-0.00464{\times}C{\times}D+6.7686{\times}(D{\times}E) \qquad \text{--------------- (6.3)}$$

Prediction of UCS of igneous rocks is:

$$\text{UCS}=-83527.6-12.643{\times}A-142.034{\times}B-0.054{\times}C+1449.9{\times}D-514.3{\times}E-0.000799{\times}A^2$$
$$+0.0796{\times}B^2+0.0000427{\times}C^2-6.2724{\times}D^2-3.33{\times}E^2-0.0089{\times}A{\times}B+0.1113{\times}A{\times}D+0.0196$$
$$02{\times}A{\times}E+1.147{\times}B{\times}D-1.175{\times}B{\times}E+4.42{\times}D{\times}E \qquad \text{---------------- (6.4)}$$

Significance of regression co-efficient of UCS is given in Table 6.1a, which also shows t-value and p-value. The final ANOVA table of the reduced quadratic model for UCS is shown in Table 6.1b. This table also represents degree of freedom (DF), mean square (MS), sum of squares (SS), F-value and P-values associated with factors. As seen from Table 6.1c, for sedimentary rocks, the selected model explains 91.37% of the total variation in the observed UCS tests where as Table 1c of Appendix III, the selected models explains 92.65% of the total variation in the observed UCS tests for igneous rock. Figure 6.1(A) shows the cross correlation of predicted and experimentally determined values of UCS for Eq. 6.3.

Table6.1a. Significance of regression coefficients for estimation of UCS

Model terms for UCS	Parameter Estimate (Coefficients)	t-value	p-value
Constant	-89080.5	101.104	0.000
A	-12.1389	-18.998	0.000
B	-213.640	-46.255	0.000
C	0.486380	-5.030	0.000
D	1585.22	61.194	0.000
E	-756.841	-21.250	0.000
A^2	-0.000592423	-9.532	0.000
B^2	-0.0787186	-3.957	0.000
C2	0.0000560729	6.818	0.000
D^2	-7.04364	-23.593	0.000
E^2	-4.05369	-12.343	0.000
A×B	-0.0128222	-11.969	0.000
A×D	0.108252	17.828	0.000
B×D	1.87636	18.253	0.000
B×E	-1.42147	-15.537	0.000
C×D	-0.00464411	-5.562	0.000
D×E	6.76863	15.714	0.000

Table6.1b Analysis of variance (ANOVA) for the selected quadratic model for estimation of UCS

Source of variations	Degree of freedom	Sum of squares	Mean Squares	F-Value	P-Value
Model	16	197252	12328.2	496.38	0.000
Linear	5	179234	30599.4	1232.03	0.000
Square	5	4185	2945.7	118.60	0.000
Interaction	6	13833	2305.5	92.83	0.000
Residual Error	733	18205	24.8		
Total	749	215457			

Table 6.1c. Model summary for dependent variable (UCS)

R²Value	R² Predicted	R² Adjusted	Standard Error
91.55	91.16	91.37	4.9836

B. Prediction of Abrasivity of Sedimentary and Igneous Rock

Prediction of abrasivity of sedimentary rock is:

Abrasivity=-4369.81-0.7035×A-10.047×B+0.0293×C+77.18×D-22.633×E-0.0000455 ×A^2+0.00000374×C^2-0.339×D^2-0.211097×E^2-0.00062×A×B+0.00625×A×D+0.0024 ×A×E+0.085×B×D-0.0752×B×E-0.000283×C×D+0.199×D×E   --------------- (6.5)

Prediction of abrasivity of igneous rock is:

Abrasivity=-3141.22-0.57492×A-4.21367×B+53.8855×D+27.47×E-0.0000512×A^2+0.00672519×B^2-0.228714×D^2+0.312527×E^2-0.000230658×A×B+0.0050787×A×D+0.0046414×A×E+0.030306×B×E-0.26447×D×E   -------------- (6.6)

   Significance of regression co-efficient of abrasivity is given in Table 6.2a, which also shows t-value and p-value. The final ANOVA table of the reduced quadratic model for abrasivity is shown in Table 6.2b. This table also represents degree of freedom (DF), mean square (MS), sum of squares (SS), F-value and P-values ass associated with factors. As seen from Table 6.2c, for sedimentary rocks, the selected model explains 93.88% of the total variation in the observed abrasivity tests where as Table 2c of Appendix III the selected models explains 94.39% of the total variation in the observed abrasivity tests for igneous rock. Figure 6.1(B) shows the cross correlation of predicted and experimentally determined values of abrasivity for Eq.6.5.

Table 6.2a Significance of regression coefficients for estimation of abrasivity

Model terms for abrasivity	Parameter Estimate (Coefficients)	t-value	p-value
Constant	-4369.81	532.693	0.000
A	-0.703251	-18.174	0.000
B	-10.0468	-54.112	0.000
C	0.0293172	-3.736	0.000
D	77.1760	66.953	0.000
E	-22.6329	-26.922	0.000
A^2	-0.0000454451	-9.602	0.000
C^2	3.73934E-06	5.933	0.000
D^2	-0.338803	-14.370	0.000
E^2	-0.211097	-8.518	0.000
A×B	-0.000618172	-7.154	0.000
A×D	0.00624992	12.852	0.000
A×E	0.00240005	5.708	0.000
B×D	0.0851653	12.043	0.000
B×E	-0.0752275	-12.012	0.000
C×D	-0.000282976	-4.442	0.000
D×E	0.198571	5.408	0.000

Table 6.2b Analysis of variance (ANOVA) for the selected quadratic model for estimation of abrasivity

Source of variations	Degree of freedom	Sum of squares	Mean Squares	F-Value	P-Value
Model	16	1644.32	102.770	719.61	0.000
Linear	5	1560.24	227.128	1590.38	0.000
Square	4	16.31	9.991	69.96	0.000
Interaction	7	67.77	9.681	67.79	0.000
Residual Error	733	104.68	0.143		
Total	749	1749.00			

Table 6.2c. Model summary for dependent variable (abrasivity)

R²Value	R² Predicted	R² Adjusted	Standard Error
94.01	93.74	93.88	0.3779

C. Prediction of Tensile Strength of Sedimentary and Igneous Rocks

Prediction of tensile strength of sedimentary rock is:

$$TS=-2981.62-0.431354\times A-6.12\times B+0.0194\times C+47.59\times D-13.165\times E-0.000027\times A^2+$$
$$0.00000273\times C^2-0.209\times D^2-0.13452\times E^2-0.00038\times A\times B+0.0038\times A\times D+0.001528\times A\times E$$
$$+ 0.052\times B\times D-0.045\times B\times E-0.0002\times C\times D+0.116\times D\times E \qquad \text{------------------ (6.7)}$$

Prediction of tensile strength of igneous rock is:

$$TS=-2702.98-1.17604\times A-12.26\times B-0.00525\times C+130.415\times D-26.18\times PR-0.000078\times A^2$$
$$+0.00926\times B^2+0.0000042\times C^2-0.5618\times D^2-0.1485\times E^2-0.00076\times A\times B+0.0104\times A\times D+$$
$$0.0034\times A\times E+0.097\times B\times D-0.0874\times B\times E+0.214\times D\times E \qquad \text{--------------- (6.8)}$$

Significance of regression co-efficient of tensile strength is given in Table 6.3a, which also shows t-value and p-value. The final ANOVA table of the reduced quadratic model for tensile strength is shown in Table 6.3b. This table also represents degree of freedom (DF), mean square (MS), sum of squares (SS), F-value and P-values associated with factors. As seen from Table 6.3c, for sedimentary rocks, the selected model explains 95.20% of the total variation in the observed tensile strength tests where as Table 3c of Appendix III the selected models explains 92.82%.of the total variation in the observed t tests for igneous rock. Figure 6.1(C) shows the cross correlation of predicted and experimentally determined values of tensile strength for Eq. 6.7.

Table 6.3a Significance of regression coefficients for estimation of tensile strength

Model terms for tensile strength	Parameter Estimate (Coefficients)	t-value	p-value
Constant	-2981.62	311.873	0.000
A	-0.431354	-21.805	0.000
B	-6.11682	-60.998	0.000
C	0.0194231	-5.513	0.000
D	47.5896	76.758	0.000
E	-13.1650	-29.248	0.000
A^2	-0.0000270070	-10.627	0.000
C^2	0.00000272590	8.056	0.000
D^2	-0.208659	-16.482	0.000
E^2	-0.134515	-10.109	0.000
A×B	-0.000380258	-8.196	0.000
A×D	0.00382270	14.640	0.000
A×E	0.00152753	6.766	0.000
B×D	0.0518579	13.657	0.000
B×E	-0.0449607	-13.371	0.000
C×D	-0.000190412	-5.567	0.000
D×E	0.115820	5.875	0.000

Table 6.3b Analysis of variance (ANOVA) for the selected quadratic model for estimation of tensile strength

Source of variations	Degree of freedom	Sum of squares	Mean Squares	F-Value	P-Value
Model	16	612.704	38.2940	930.13	0.000
Linear	5	580.200	84.1733	2044.49	0.000
Square	4	6.917	3.9045	94.84	0.000
Interaction	7	25.586	3.6551	88.78	0.000
Residual Error	733	30.178	0.0412		
Total	749	642.882			

Table 6.3c Model summary for dependent variable (tensile strength)

R²Value	R² Predicted	R² Adjusted	Standard Error
95.31	95.08	95.20	0.2029

D. Prediction of Schmidt Rebound Number of Sedimentary and Igneous Rocks

Prediction of SRN for sedimentary rock is:

$$SRN = -5324.46 - 6.46646 \times A - 27.5013 \times B + 52.871 \times D + 1058.3 \times E - 0.001122 \times A^2 + 0.271 \times B^2 + 0.05714 \times A \times D + 0.17905 \times A \times E - 9.9 \times D \times E$$ -------------- (6.9)

Prediction of SRN for igneous rock is:

SRN=-4924.01-12.9616×A-126.43×B-0.059989×C+1381.03×D-29.0512×E-0.000978

9×A^2+0.13046×B^2+0.000048454×C^2-5.9181×E^2-0.0075394×A×B+0.11412×A×D+

0.062508×A×E+0.97385×B×E-0.776766×B×E   ---------------- (6.10)

Significance of regression co-efficient of Schmidt rebound number (SRN) is given in Table 6.4a, which also shows t-value and p-value. The final ANOVA table of the reduced quadratic model for SRN is shown in Table 6.4b. This table also represents degree of freedom (DF), mean square (MS), sum of squares (SS), F-value and P-values ass associated with factors. As seen from Table 6.4c, for sedimentary rocks, the selected model explains 93.57% of the total variation in the observed SRN tests where as Table 4c of Appendix III the selected models explains 94.08% of the total variation in the observed abrasivity tests for igneous rock. Figure 6.1 (D) shows the cross correlation of predicted and experimentally determined values of SRN for Eq. 6.9.

Table 6.4a Significance of regression coefficients for estimation of SRN

Model Terms for SRN	Parameter Estimate (Coefficients)	t-value	p-value
Constant	-5324.46	619.771	0.000
A	-6.46646	-19.196	0.000
B	-27.5013	-63.071	0.000
D	52.8708	81.916	0.000
E	1058.30	-66.236	0.000
A^2	-0.00112240	-8.019	0.000
B^2	0.270809	6.930	0.000
A×D	0.0571377	6.972	0.000
A×E	0.179050	17.904	0.000
D×E	-9.90189	-14.978	0.000

6.4b. Analysis of variance (ANOVA) for the selected quadratic model for estimation of SRN

Source of variations	Degree of freedom	Sum of squares	Mean Squares	F-Value	P-Value
Model	9	1563317	173702	1211.91	0.000
Linear	4	1504927	360092	2512.35	0.000
Square	2	8315	8112	56.60	0.000
Interaction	3	50075	16692	116.46	0.000
Residual Error	740	106063	143		
Total	749	1669380			

6.4c. Model summary for dependent variable (SRN)

R²Value	R² Predicted	R² Adjusted	Standard Error
93.65	93.48	93.57	11.97

6.3.1.2 Models to Predict Rock Properties for Sedimentary and Igneous rock Using Threaded Drill Bit

A. Prediction of UCS of Sedimentary and Igneous Rocks

Prediction of UCS of sedimentary is:

$UCS=-126905-13.7812\times A-243.5\times B-0.10618\times C+2253.5\times D-182\times E-0.0005459\times A^2$ $+0.000091514\times C^2-9.9825\times D^2-13.45\times E^2-0.0094529\times A\times B-0.0000373\times A\times C+0.1213\times$ $A\times D+2.08\times B\times D-2.08\times B\times E+6.08\times D\times E$ ---------------- (6.11)

Prediction of UCS of igneous rock is:

$UCS=-90586.8-12.82\times A-157.15\times B-0.10284\times C+1576.58\times D-699.4\times E-0.001012\times A^2$ $+0.0000781\times C^2-6.8423\times D^2-5.9982\times E^2-0.00528\times A\times B+0.1135\times A\times D+0.064492\times A\times E$ $+1.31\times B\times D-1.484\times B\times E+5.92\times D\times E$ ---------------- (6.12)

Significance of regression co-efficient of UCS is given in Table 6.5a, which also shows t-value and p-value. The final ANOVA table of the reduced quadratic model for UCS is shown in Table 6.5b. This table also represents degree of freedom (DF), mean square (MS), sum of squares (SS), F-value and P-values ass associated with factors. As seen from Table 6.5c, for sedimentary rocks, the selected model explains 90.52% of the total variation in the observed UCS tests where as Table 5c of Appendix III the selected models explains 94.42% of the total variation in the observed UCS tests for igneous rock. As seen, the selected model explains 90.52% of the total variation in the observed UCS tests. Figure 6.2(A) shows the cross correlation of predicted and experimentally determined values of UCS for Eq. 6.11.

Table 6.5a Significance of regression coefficients for estimation of UCS

Model Terms for UCS	Parameter Estimate (Coefficients)	t-value	p-value
Constant	-126905	79.572	0.000
A	-13.7812	-16.010	0.000
B	-243.502	-15.948	0.000
C	-0.106183	-9.172	0.000
D	2253.51	58.751	0.000
E	-1816.01	-10.981	0.000
A^2	-0.000545896	-6.861	0.000
C^2	0.0000915136	8.387	0.000
D^2	-9.98249	18.775	0.000
E^2	-13.4468	-13.802	0.000
A×B	-0.00945287	-3.079	0.002
A×C	-0.0000373365	-2.048	0.041
A×D	0.121322	14.169	0.000
B×D	2.08173	7.993	0.000
B×E	-2.07452	-6.284	0.000
D×E	16.0747	15.920	0.000

Table 6.5b Analysis of variance (ANOVA) for the selected quadratic model for estimation of UCS

Source of variations	Degree of freedom	Sum of squares	Mean Squares	F-Value	P-Value
Model	15	130430	8695.3	318.64	0.000
Linear	5	117547	22655.9	830.22	0.000
Square	4	2162	2513.1	92.09	0.000
Interaction	6	10721	1786.9	65.48	0.000
Residual Error	484	13208	27.3		
Total	499	143638			

Table 6.5c Model summary for dependent variable (UCS)

R²Value	R² Predicted	R² Adjusted	Standard Error
90.80	90.19	90.52	5.22389

B. Prediction of Abrasivity of Sedimentary and Igneous Rocks

Prediction of abrasivity of sedimentary rock is:

Abrasivity = -6068.94-0.762115×A-9.561×B-0.0090004×C+106.7×D-78.9×E-0.0000398×A^2+0.0000065846×C^2-0.466125×D^2-0.7829×E^2+0.006545×A×D+0.002845×A×E+0.0794×B×D-0.106×B×E+0.69×D×E   --------------- (6.13)

Prediction of abrasivity of igneous rock is:

Abrasivity = -1985.97-0.464933×A-0.196998×B-0.0071309×C+32.7951×D+65.4225 ×E-0.0000688005×A^2+0.00000543476×C^2-0.133516×D^2+0.199613×E^2+0.00419554 ×A ×D+0.0105524×A×E-0.597676×D×E   ---------------- (6.14)

Significance of regression co-efficient of abrasivity is given in Table 6.6a, which also shows t-value and p-value. The final ANOVA table of the reduced quadratic model for abrasivity is shown in Table 6.6b. This table also represents degree of freedom (DF), mean square (MS), sum of squares (SS), F-value and P-values ass associated with factors. As seen from Table 6.6c, for sedimentary rocks, the selected model explains 92.59% of the total variation in the observed abrasivity tests where as Table 6c of Appendix III the selected models explains 94.86% of the total variation in the observed abrasivity tests for igneous rock. Figure 6.2(B) shows the cross correlation of predicted and experimentally determined values of abrasivity for Eq.6.13.

Table 6.6a Significance of regression coefficients for estimation of abrasivity

Model Terms for abrasivity	Parameter Estimate (Coefficients)	t-value	p-value
Constant	-6068.94	354.777	0.000
A	-0.762115	-19.129	0.000
B	-9.56106	-17.693	0.000
C	-0.00900041	-10.693	0.000
D	106.677	66.562	0.000
E	-78.8803	-16.999	0.000
A^2	-0.0000398191	-6.295	0.000
C^2	0.00000658464	9.553	0.000
D^2	-0.466125	-10.378	0.000
E^2	-0.782914	-10.829	0.000
A×D	0.00654484	9.514	0.000
A×E	0.00284457	3.442	0.001
B×D	0.0794382	4.161	0.000
B×E	-0.105892	-4.031	0.000
D×E	0.690123	7.759	0.000

Table 6.6b Analysis of variance (ANOVA) for the selected quadratic model for estimation of abrasivity

Source of variations	Degree of freedom	Sum of squares	Mean Squares	F-Value	P-Value
Model	14	1082.03	77.288	446.42	0.000
Linear	5	1024.14	165.117	953.73	0.000
Square	4	16.98	10.267	59.30	0.000
Interaction	5	40.92	8.183	47.27	0.000
Residual Error	485	83.97	0.173		
Total	499	1166.00			

Table 6.6c Model summary for dependent variable (abrasivity)

R²Value	R² Predicted	R² Adjusted	Standard Error
92.80	92.35	92.59	0.4161

C. Prediction of Tensile Strength (TS) of Sedimentary Rocks

Prediction of tensile strength of sedimentary rock is:

$TS = -5315.61 - 0.465205 \times A - 5.8254 \times B - 0.00566588 \times C + 64.1346 \times D - 46.855 \times E - 0.0000268415 \times A^2 + 0.0000049174 \times C^2 - 0.2803 \times D^2 - 0.5282 \times E^2 - 0.0000021364 \times A \times C + 0.0040094 \times A \times D + 0.0025 \times A \times E + 0.048436 \times B \times D - 0.0657808 \times B \times E + 0.4099 \times D \times E$ --------- (6.15)

Prediction of tensile strength of igneous rock is:

$TS = -3652.91 - 1.15494 \times A - 9.4762 \times B - 0.0117914 \times C + 125.839 \times D - 3.13058 \times E - 0.00010605 \times A^2 + 0.0000089524 \times C^2 - 0.539424 \times D^2 - 0.339815 \times E^2 + 0.010129 \times A \times D + 0.0107874 \times A \times E + 0.0765331 \times B \times D - 0.0880001 \times B \times E$ ---------------- (6.16)

Significance of regression co-efficient of tensile strength is given in Table 6.7a, which also shows t-value and p-value. The final ANOVA table of the reduced quadratic model for tensile strength is shown in Table 6.7b. This table also represents degree of freedom (DF), mean square (MS), sum of squares (SS), F-value and P-values ass associated with factors. As seen from Table 6.7c, for sedimentary rocks, the selected model explains 93.85% of the total variation in the observed tensile strength tests where as Table 7c of Appendix III the selected models explains 94.27%.of the total variation in the observed t tests for igneous rock. Fig. 6.2(C) shows the cross correlation of predicted and experimentally determined values of TS for Eq. 6.15.

Table 6.7a Significance of regression coefficients for estimation of Tensile strength

Model Terms for TS	Parameter Estimate (Coefficients)	t-value	p-value
Constant	-5315.61	311.873	0.000
A	-0.465205	-21.805	0.000
B	-5.82542	-60.998	0.000
C	-0.00566588	-5.513	0.000
D	64.1346	76.758	0.000
E	-46.8550	-29.248	0.000
A^2	-2.68415E-05	-10.627	0.000
C^2	4.91744E-06	8.056	0.000
D^2	-0.280304	-16.482	0.000
E^2	-0.528206	-10.109	0.000
A×C	-2.13637E-06	-8.196	0.000
A×D	0.00400944	14.640	0.000
A×E	0.00251050	6.766	0.000
B× D	0.0484361	13.657	0.000
B×E	-0.0657808	-13.371	0.000
D×E	0.409913	5.875	0.000

Table 6.7b Analysis of variance (ANOVA) for the selected quadratic model for estimation of (TS)

Source of variations	Degree of freedom	Sum of squares	Mean Squares	F-Value	P-Value
Model	15	403.017	26.8678	508.54	0.000
Linear	5	381.295	61.2748	1159.77	0.000
Square	4	6.463	2.9974	56.73	0.000
Interaction	6	15.258	2.5430	48.13	0.000
Residual Error	484	25.571	0.0528		
Total	499	428.588			

Table 6.7c Model summary for dependent variable (TS)

R²Value	R² Predicted	R² Adjusted	Standard Error
94.03	93.62	93.85	0.2298

D. Prediction of Schmidt Rebound Number of Sedimentary and Igneous Rocks

Prediction of SRN of sedimentary rock is:

SRN=-6637.07-11.0269×A-6.5858×B-0.272977×C+33.126×D+537.38×E-

0.00119814×A^2+0.00023784×C^2-14.1324×E^2-0.00010715×A×C+0.0958692×A×D

+0.222843×A×E-5.30945×D×E ---------------- (6.17)

Prediction of SRN of igneous rock is:

SRN=-2905.42-11.4728×A-69.8878×B-0.136037×C+1138.4×D+477.523×E-0.00129
59×A^2+0.000103554×C^2-4.81711×D^2+0.101723×A×D+0.161958×A×E+0.54606×B×
D-4.80393×D×E   ---------------- (6.18)

　　　　Significance of regression co-efficient of Schmidt rebound number (SRN) is given in Table 6.8a, which also shows t-value and p-value. The final ANOVA table of the reduced quadratic model for SRN is shown in Table 6.8b. This table also represents degree of freedom (DF), mean square (MS), sum of squares (SS), F-value and P-values ass associated with factors. As seen from Table 6.8c, for sedimentary rocks, the selected model explains 93.16% of the total variation in the observed SRN tests where as Table 8c of Appendix III the selected models explains 94.23% of the total variation in the observed SRN tests for igneous rock. Figure 6.8(D) shows the cross correlation of predicted and experimentally determined values of STN for Eq. 6.17.

Table 6.8a Significance of regression coefficients for estimation of SRN

Model Terms for SRN	Parameter Estimate (Coefficients)	t-value	p-value
Constant	-6637.07	550.568	0.000
A	-11.0269	-22.961	0.000
B	-6.58580	-23.727	0.000
C	-0.272977	-12.155	0.000
D	33.1261	91.222	0.000
E	537.381	-14.163	0.000
A^2	-0.00119814	-8.397	0.000
C^2	0.000237840	11.384	0.000
E^2	-14.1324	-8.830	0.000
A×C	-1.07146E-04	-2.790	0.005
A×D	0.0958692	8.729	0.000
A×E	0.222843	10.779	0.000
D×E	-5.30945	-4.769	0.000

Table 6.8b Analysis of variance (ANOVA) for the selected quadratic model for estimation of (SRN)

Source of variations	Degree of freedom	Sum of squares	Mean Squares	F-Value	P-Value
Model	12	1410268	117522	927.35	0.000
Linear	5	1341602	255318	2014.68	0.000
Square	3	27231	7304	57.64	0.000
Interaction	4	41436	10359	81.74	0.000
Residual Error	804	101890	127		
Total	816	1512158			

Table 6.8c Model summary for dependent variable (SRN)

R²Value	R² Predicted	R² Adjusted	Standard Error
93.26	93.04	93.16	11.26

6.4 Development of Mathematical Models for the Prediction of Penetration Rate and Sound Level for a given Air Pressure, Thrust and Bit-Rock Combination

Earlier many researchers in the course of their investigation predicted and developed mathematical models using rock properties i.e. UCS, TS, SRN, porosity, and density etc. In this investigation, multiple regression analysis was used to predict and develop mathematical models for penetration rate and sound level.

In this mathematical model, sound level (dB) and penetration rate (mm/sec) were considered as response variables. After determining the coefficients, the mathematical models were developed and are given in equations (6.19) to (6.26). All the data was used to generate the regression equations for the prediction of penetration rate (PR) and sound level (SL). Six important parameters were considered in the laboratory investigation, viz; air pressure in kPa (A), drill bit diameter in mm (B), thrust in N (C), uniaxial compressive strength in MPa (D), abrasivity in % (E) and tensile strength in MPa (F) which are input parameters. The responses are penetration rate (mm/s) and equivalent continuous sound level (dB) produced during drilling.

Mathematical models were developed for the prediction of sound level and penetration rate by using multiple regression analysis (MRA) for integral bit diameters of 30, 34 and 40 mm and threaded (R22) bit diameters of 35 and 38 mm for

varying air pressure (i.e. 392, 441, 490, 539 and 588 kPa) and thrust (100 to 1000 N) which are given below:

6.4.1 Mathematical models for Sedimentary and Igneous Rocks Using Integral Drill Bit

Mathematical models for the sound level and penetration rate were developed for sedimentary and igneous rocks, during percussive drilling using rock properties such as UCS, abrasivity, and tensile strength.

A. Prediction of sound level of sedimentary rock is:

$SL = 105.021 + 0.0123074 \times A + 0.0259454 \times B + 0.00492772 \times C - 0.093533 \times D + 0.656426 \times E - 1.65747 \times F - 0.00000698122 \times A^2 - 0.0031 \times B^2 - 0.00000558674 \times C^2 + 0.00167952 \times D^2 + 0.0001154 \times A \times B + 0.00000474665 \times A \times C + 0.0000283763 \times A \times D$ ---------------- (6.19)

B. Prediction of sound level of igneous rock is:

$SL = 112.712 + 0.00848458 \times A + 0.0907237 \times B + 0.00589917 \times C - 0.00000588889 \times C^2 + 0.00000333354 \times A \times C$ ---------------- (6.20)

Significance of regression co-efficient of sound level is given in Table 6.9a, which also shows t-value and p-value. The final ANOVA table of the reduced quadratic model for sound level is shown in Table 6.9b. This table also represents degree of freedom (DF), mean square (MS), sum of squares (SS), F-value and P-values ass associated with factors. As seen from Table 6.9c, for sedimentary rocks, the selected model explains 96.06% of the total variation in the observed sound level tests where as Table 9c of Appendix III the selected models explains 95.93% of the total variation in the observed sound level tests for igneous rock. Figure 6.3(A) shows the cross correlation of predicted and experimentally determined values of sound level for Eq.6.19.

Table 6.9a Significance of regression coefficients for estimation of sound level

Model Terms for sound level	Parameter Estimate (Coefficients)	t-value	p-value
Constant	105.021	595.452	0.000
A	0.0123074	82.203	0.000
B	0.259454	47.515	0.000
C	0.00492772	37.420	0.000
D	-0.0935333	2.886	0.004
E	0.656426	3.586	0.000
F	-1.65747	-2.304	0.022
A^2	-6.98122E-06	-3.297	0.001
B^2	-0.00310000	-4.096	0.000
C^2	-5.58674E-06	-47.725	0.000
D^2	0.00167952	3.769	0.000
A×B	0.000115400	3.864	0.000
A×C	4.74665E-06	11.107	0.000
A×D	-2.83763E-05	-3.918	0.000

Table 6.9b Analysis of variance (ANOVA) for the selected quadratic model for estimation of (sound level)

Source of variations	Degree of freedom	Sum of squares	Mean Squares	F-Value	P-Value
Regression	13	991.88	76.298	1406.02	0.000
Linear	6	857.67	141.671	2610.70	0.000
Square	4	125.87	31.467	579.88	0.000
Interaction	3	8.34	2.779	51.21	0.000
Residual Error	736	39.94	0.054		
Total	749	1031.82			

6.9c Model summary for dependent variable (sound level)

R²Value	R² Predicted	R² Adjusted	Standard Error
96.13	95.99	96.06	0.2329

C. Prediction of Penetration Rate of Sedimentary Rock is:

PR=0.0879242+0.0111569×A-0.246978×B+0.0070986×C-0.0000100938×A^2+0.003057×B^2-0.00000760976×C^2+0.0000103687×A×C-0.0000546415×B×C   --------- (6.21)

D. Prediction of Penetration Rate of Igneous Rock is:

PR=1.32215+0.000985088×A-0.0272657×B+0.00399512×C-0.00000495972×C^2+0.0000000522404×A×C   ----------------- (6.22)

Significance of regression co-efficient of penetration rate is given in Table 6.9a, which also shows t-value and p-value. The final ANOVA table of the reduced quadratic model for penetration rate is shown in Table 6.9b. This table also represents degree of freedom (DF), mean square (MS), sum of squares (SS), F-value and P-values ass associated with factors. As seen from Table 6.9c, for sedimentary rocks, the selected model explains 89.30% of the total variation in the observed sound level tests where as Table 10c of Appendix III the selected models explains 86.18% of the total variation in the observed penetration rate tests for igneous rock. Fig. 6.3(B) shows the cross correlation of predicted and experimentally determined values of penetration rate for Eq.6.21.

Table 6.10a Significance of regression coefficients for estimation of penetration rate of sedimentary rock

Model Terms for penetration rate	Parameter Estimate (Coefficients)	t-value	p-value
Constant	0.0879242	92.556	0.000
A	0.0111569	39.072	0.000
B	-0.246978	-20.821	0.000
C	0.00709864	43.926	0.000
A^2	-1.00938E-05	-3.282	0.001
B^2	0.00305720	2.780	0.006
C^2	-7.60976E-06	-44.745	0.000
A×C	1.03687E-05	16.700	0.000
B×C	-5.46415E-05	-5.219	0.000

Table 6.10b Analysis of variance (ANOVA) for the selected quadratic model for estimation of (penetration rate)

Source of variations	Degree of freedom	Sum of squares	Mean Squares	F-Value	P-Value
Regression	8	716.90	89.612	782.37	0.000
Linear	3	450.40	148.505	1296.55	0.000
Square	3	231.44	77.145	673.53	0.000
Interaction	2	35.06	17.532	153.07	0.000
Residual Error	741	84.87	0.115	2.50	0.000
Total	749	801.77			

Table 6.10c Model summary for dependent variable (penetration rate)

R²Value	R² Predicted	R² Adjusted	Standard Error
89.41	89.196	89.30	0.3384

6.4.2 Mathematical Models for Sedimentary and Igneous Rocks using Threaded Drill Bit

A. Prediction of Sound Level for Sedimentary Rock is:

$SL = 108.373 + 0.0181872 \times A + 0.0768 \times B + 0.00563859 \times C - 0.12938 \times D + 2.07887 \times E - 7.11371 \times F - 0.00000437318 \times A^2 - 0.00000517348 \times C^2 + 0.00373915 \times D^2 + 0.00000265059 \times A \times C - 0.000168535 \times A \times D - 0.00113795 \times A \times E - 0.00414492 \times A \times F$ ---------- (6.23)

B. Prediction of Sound Level of Igneous Rock is:

$SL = 109.413 - 0.00115996 \times A + 0.0736 \times B + 0.00652005 \times C + 0.324432 \times D + 1.17027 \times E + 0.684527 \times F + 0.00000105908 \times A^2 - 0.00000547045 \times C^2 - 0.002179 \times D^2 + 0.0000011453 \times A \times C$ ---------- (6.24)

Significance of regression co-efficient of sound level is given in Table 6.11a, which also shows t-value and p-value. The final ANOVA table of the reduced quadratic model for sound level is shown in Table 6.11b. This table also represents degree of freedom (DF), mean square (MS), sum of squares (SS), F-value and P-values ass associated with factors. As seen from Table 6.11c, for sedimentary rocks, the selected model explains 96.50% of the total variation in the observed sound level tests where as Table 11c of Appendix III the selected models explains 96.67% of the total variation in the observed SRN tests for igneous rock. Figure 6.4(A) shows the cross correlation of predicted and experimentally determined values of sound level 3.

Table 6.11a Significance of regression coefficients for estimation of sound level

Model Terms for sound level	Parameter Estimate (Coefficients)	t-value	p-value
Constant	108.373	573.674	0.000
A	0.0181872	52.706	0.000
B	0.0768	13.206	0.000
C	0.00563859	41.046	0.000
D	-0.12938	7.393	0.000
E	2.07887	8.104	0.000
F	-7.11371	-6.888	0.000
A^2	-0.00000437318	-2.014	0.045
C^2	-0.00000517348	-43.096	0.000
D^2	0.00373915	8.183	0.000
A×C	0.00000265059	6.048	0.000
A×D	-0.000168535	-3.478	0.001
A×E	-0.00113795	-2.215	0.027
A×F	0.00414492	2.699	0.007

Table 6.11b Analysis of variance (ANOVA) for the selected quadratic model for estimation of (sound level)

Source of variations	Degree of freedom	Sum of squares	Mean Squares	F-Value	P-Value
Regression	13	524.606	40.3543	1060.69	0.000
Linear	6	448.330	55.8120	1466.99	0.000
Square	3	73.361	24.4537	642.75	0.000
Interaction	4	2.914	0.7286	19.15	0.000
Residual Error	486	18.490	0.0380		
Total	499	543.096			

Table 6.11c Model summary for dependent variable (sound level)

R²Value	R² Predicted	R² Adjusted	Standard Error
96.60	96.40	96.50	0.1950

C. Prediction of Penetration Rate of Sedimentary Rock is:

$$PR=0.114853+0.00124027\times A-0.0326267\times B+0.0032204\times C-0.00000562561\times C^2+0.00000879134\times A\times C \qquad \text{---------- (6.25)}$$

D. Prediction of Penetration Rate of Igneous Rock is:

$$PR=1.4592+0.03255\times A-0.042497\times B+0.00927668\times C-0.175622\times D+0.25718\times E-0.69617\times F-0.0000040735\times C^2+0.0012389\times D^2+0.000005568\times A\times C+0.000052476\times A\times D-0.00172338\times A\times E-0.000042546\times C\times D-0.0003417\times C\times E+0.000522208\times C\times F \text{ ------ (6.26)}$$

Significance of regression co-efficient of penetration rate is given in Table 6.12a, which also shows t-value and p-value. The final ANOVA table of the reduced quadratic model for penetration rate is shown in Table 6.12b. This table also represents degree of freedom (DF), mean square (MS), sum of squares (SS), F-value and P-values ass associated with factors. As seen from Table 6.12c, for sedimentary rocks, the selected model explains 92.86% of the total variation in the observed sound level tests where as Table 12c of Appendix III the selected models explains 91.43% of the total variation in the observed penetration rate tests for igneous rock. Fig. 6.4(B) shows the cross correlation of predicted and experimentally determined values of penetration rate for Eq. 6.25.

Table 6.12a Significance of regression coefficients for estimation of penetration rate of sedimentary rock is

Model Terms for penetration rate	Parameter Estimate (Coefficients)	t-value	p-value
Constant	0.114853	144.757	0.000
A	0.00124027	46.795	0.000
B	-0.0326267	-5.440	0.000
C	0.00322040	42.779	0.000
C^2	-0.00000562561	-45.435	0.000
A×C	0.00000879134	19.449	0.000

Table 6.12b Analysis of variance (ANOVA) for the selected quadratic model for estimation of (penetration rate)

Source	Degree of Freedom	Sum of square	Mean square	F-value	P-value
Regression	5	262.749	52.5497	1298.39	0.000
Linear	3	163.890	54.6300	1349.79	0.000
Square	1	83.549	83.5493	2064.33	0.000
Interaction	1	15.309	15.3093	378.26	0.000
Residual Error	494	19.994	0.0405		
Total	499	282.742			

Table 6.12c Model summary for dependent variable (penetration rate)

R²Value	R² Predicted	R² Adjusted	Standard Error
92.93	92.77	92.86	0.2011

6.5 Performance Prediction of the Derived Models

The coefficient of correlation between the measured and predicted values is a good indicator to check the prediction performance of the model. In this study, values account for (VAF) (Eq.6.27) and root mean square error (RMSE) (Eq.6.28) indices were calculated to control the performance of the prediction capacity of predictive model developed in the study (Alvarez and Babuska 1999; Finol et al. 2001; Gokceoglu 2002; Yilmaz and Yuksek 2008, 2009).

$$VAF = \left[1 - \frac{var(y - y')}{var(y)} \right] \times 100 \qquad \text{------------------ (6.27)}$$

$$RMSE = \sqrt{\frac{1}{N} \sum_{i=1}^{N} (y - y')^2} \qquad \text{------------------ (6.28)}$$

Where y and y´ are measured and predicted values, respectively. The calculated

indices are given in Table 6.13. If the VAF is 100 and RMSE is 0, then the model will be excellent. Mean absolute percentage error (MAPE) which is a measure of accuracy in a fitted series value in statistics was also used to check the prediction performances of the models. The constructed models were checked using various prediction performance indices. Consequently, it is possible to say that the constructed models can be used for practical purposes. The use of soft computing will also may provide new approaches and methodologies, and minimize the potential inconsistency of correlations. MAPE usually expresses accuracy as a percentage (Eq.6.29).

$$\text{MAPE} = \frac{1}{N}\left[\frac{\text{Ai - Pi}}{\text{Ai}}\right] \times 100 \qquad \text{------------------- (6.29)}$$

Where Ai is the actual value and Pi is the predicted value. The obtained values of RMSE, VAF and MAPE, are given in Table 6.13 to 6.18.

Using the developed regression models for sedimentary and igneous rocks, performance prediction indices were calculated and are given in Table 6.13 and 6.14 for integral and threaded drill bit. From the table it is observed that, for sedimentary and igneous rocks, developed model for predicting Schmidt rebound number is less efficient when compared to all other models as it has low VAF value. Also, performance prediction indices of penetration rate and sound level were calculated and are given in Table 6.15, 6.16, 6.17 and 6.18 for integral and threaded drill bit.

Significance of regression co-efficient and ANOVA table, cross correlation graph between predicted and measured (UCS, abrasivity, tensile strength, SRN, sound level and penetration rate) for igneous rocks using integral and threaded drill bit is given in Appendix III.

6.6 Summary

(1) Multiple regression analysis was performed, in order to establish the predictive models among the parameters obtained in the study. The performance prediction values showed that the multiple regression models are good tools for minimizing the uncertainties and potential inconsistency of the correlations.

(2) The empirical relationship developed is not aimed at replacing the ISRM suggested testing methods, but rather as a quick and easy method to estimate the

UCS, abrasivity, TS and SRN of sedimentary and igneous rocks reported in this investigation.

(3) The population of the analyzed data is relatively limited in this study. Therefore, the practical outcome of the proposed equations would be very valuable, when the data are considered along with the interpretation based on the engineering experiences, with acceptable accuracy, at the preliminary stage of design.

(4) In this chapter, experiment data were used to develop the regression models for prediction of various rock properties.

(5) By using backward elimination method regression equations were developed for individual responses.

(6) Prediction indices were calculated for the developed models so that, these values may be used to compare the performance of the developed model with other indirect investigations.

Table 6.13 Statistical analysis of mechanical properties of sedimentary and igneous rocks for integral drill bit diameters of 30, 34, and 40 mm

Rock type	Rock properties	R^2 Value	RMSE	VAF	MAPE
Sedimentary rocks	Uniaxial compressive strength	0.9155	4.93	93.55	6.45
	Abrasivity	0.9401	0.3737	94.18	5.82
	Tensile strength	0.9531	0.2006	94.15	5.85
	Schmidt Rebound Number	0.9365	11.89	92.32	7.68
Igneous rocks	Uniaxial compressive strength	0.9280	4.56	95.35	4.65
	Abrasivity	0.9449	0.3172	94.65	5.35
	Tensile strength	0.9298	0.4811	96.72	3.28
	Schmidt Rebound Number	0.9419	5.8574	93.55	5.45

Table 6.14 Statistical analysis of mechanical properties of sedimentary and igneous rocks for threaded (R22) drill bit diameters of 35 and 38 mm

Rock type	Rock Properties	R^2 Value	RMSE	VAF	MAPE
Sedimentary rocks	Uniaxial compressive strength	0.9080	5.140	92.166	7.834
	Abrasivity	0.9280	0.4120	92.787	7.213
	Tensile strength	0.9403	0.2261	93.757	6.243
	Schmidt Rebound Number	0.9326	12.09	91.053	8.947
Igneous rocks	Uniaxial compressive strength	0.9459	7.50	92.690	7.31
	Abrasivity	0.9498	0.3028	93.678	6.322
	Tensile strength	0.9442	0.4318	94.534	5.466
	Schmidt Rebound Number	0.9436	5.75	92.568	7.432

Table 6.15 Statistical analysis of sound level for sedimentary and igneous rocks for integral drill bit diameters of 30, 34, and 40 mm

Rock type	MRA	R^2 Value	RMSE	VAF	MAPE
Sedimentary rocks	Sound level	0.9613	0.2476	94.218	5.782
Igneous rocks	Sound level	0.9599	0.4200	94.64	5.36

Table 6.16 Statistical analysis of sound level for sedimentary and igneous rocks for threaded (R22) drill bit diameters of 35 and 38 mm

Rock type	MRA	R^2 Value	RMSE	VAF	MAPE
Sedimentary rocks	Sound level	0.9660	0.2704	93.33	6.67
Igneous rocks	Sound level	0.9674	0.4200	94.638	5.362

Table 6.17 Statistical analysis of penetration rate for sedimentary and igneous rocks for integral drill bit diameters of 30, 34, and 40 mm

Rock type	MRA	R^2 Value	RMSE	VAF	MAPE
Sedimentary rocks	Penetration rate	0.8941	0.2210	93.892	6.108
Igneous rocks	Penetration rate	0.8647	0.2380	95.106	4.894

Table 6.18 Statistical analysis of penetration rate for sedimentary and igneous rocks for threaded (R22) drill bit diameter of 35 and 38 mm

Rock type	MRA	R^2 Value	RMSE	VAF	MAPE
Sedimentary rocks	Penetration rate	0.9293	0.2386	93.129	6.871
Igneous rocks	Penetration rate	0.9166	0.2870	94.175	5.825
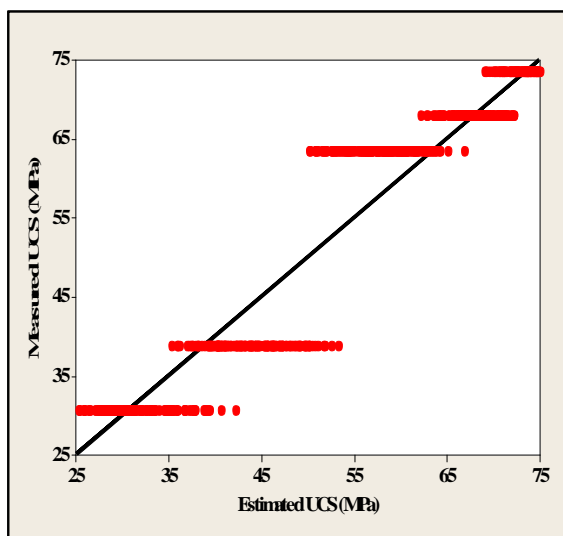
(A)
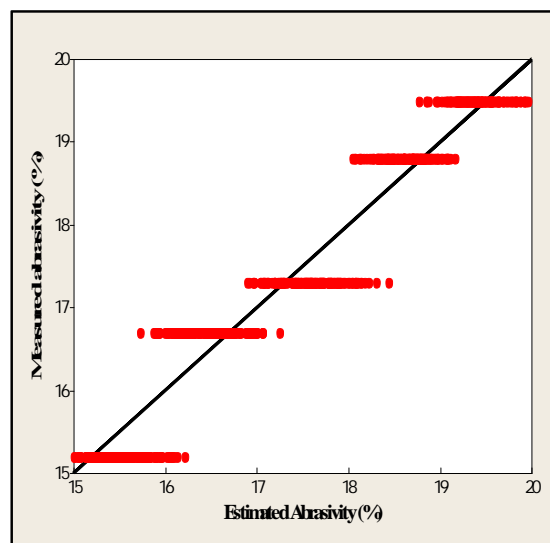
(B)
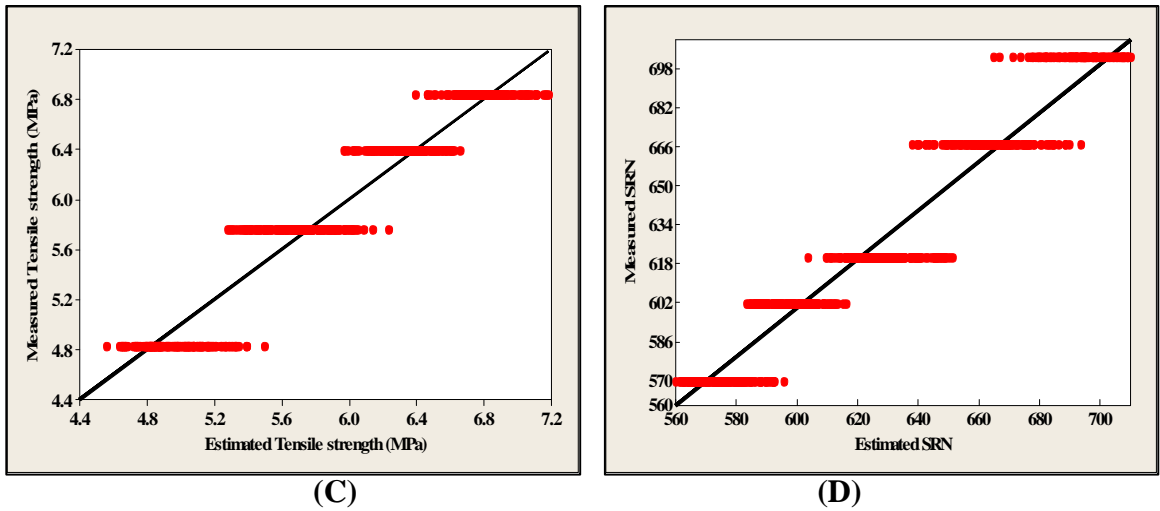
Fig. 6.1 Cross correlation graph between predicted and measured for sedimentary rocks using integral drill bit
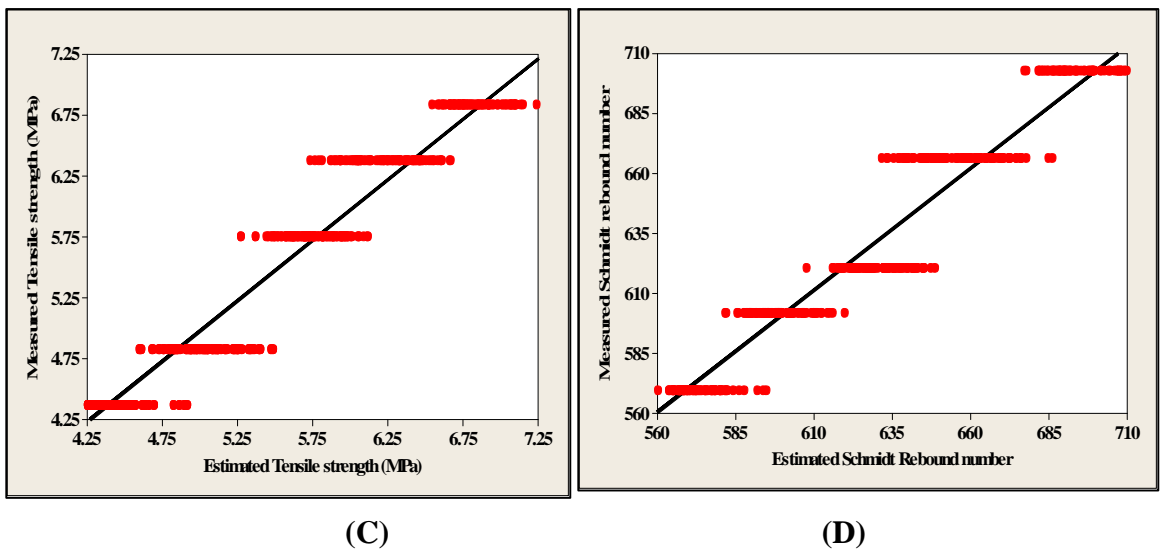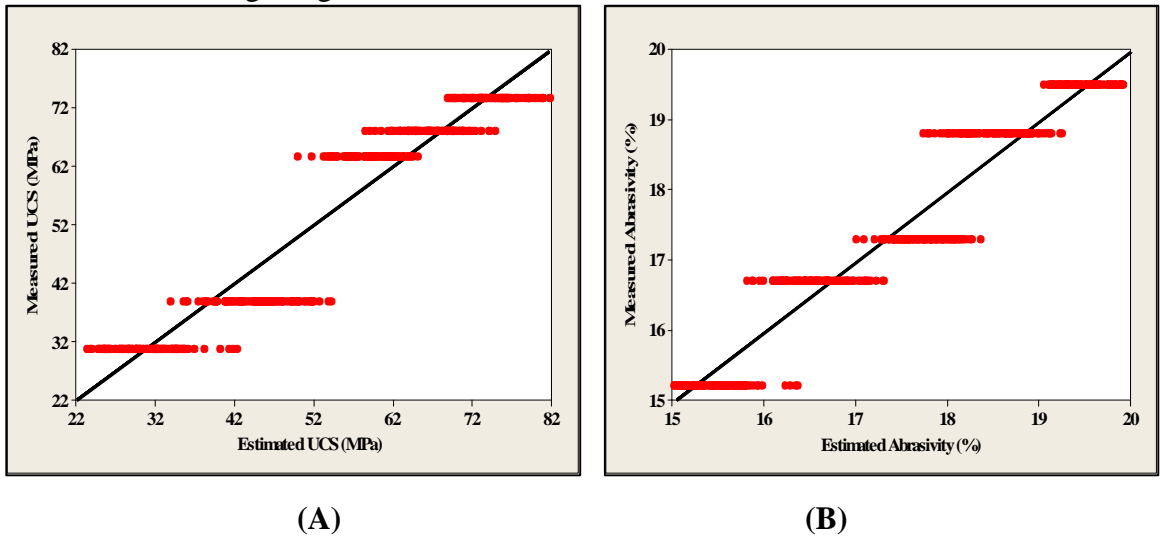
Fig. 6.2 Cross correlation graph between predicted and measured for sedimentary rocks using threaded drill bit

(A)   **(B)**
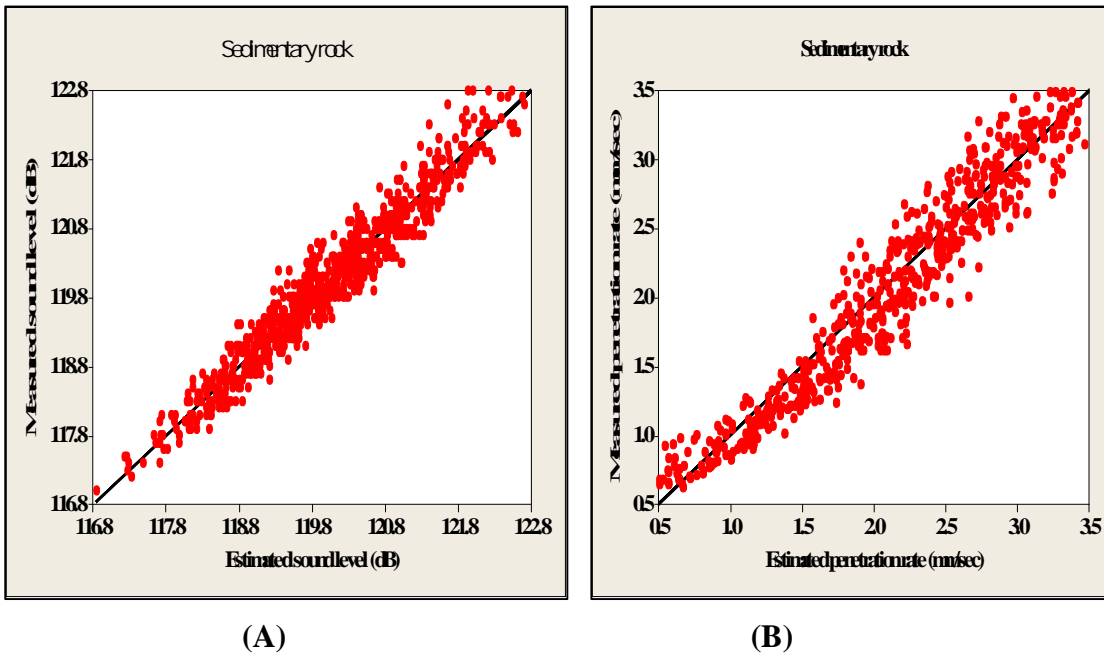
Fig. 6.3 Cross correlation graph between predicted and measured for sedimentary
rocks using integral drill bit

(A)   **(B)**
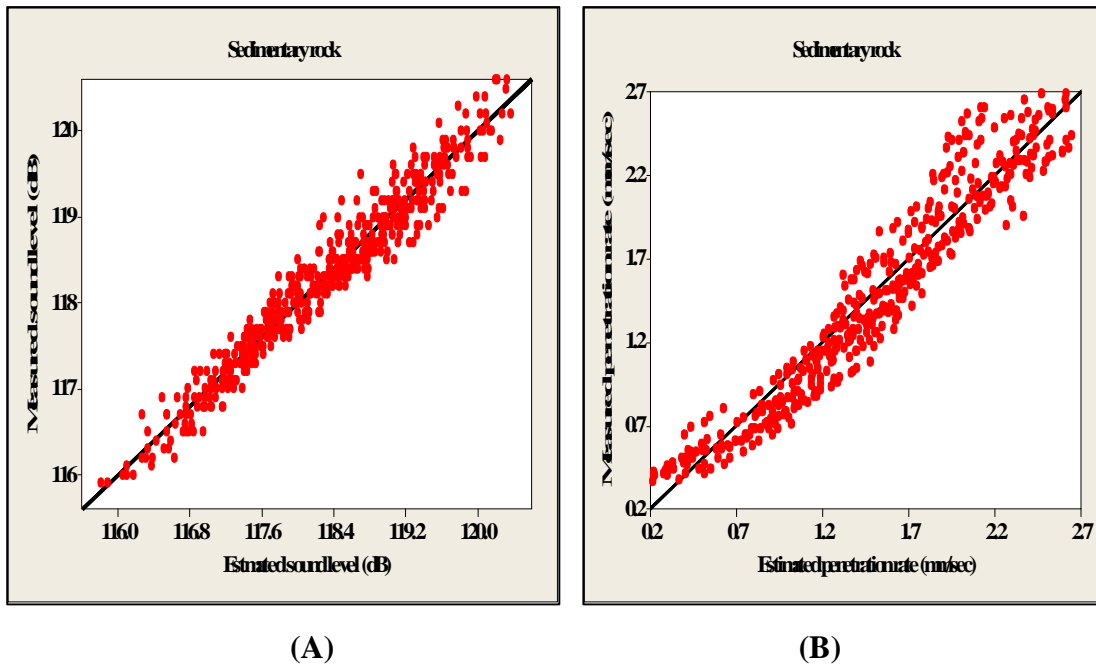
Fig. 6.4 Cross correlation graph between predicted and measured for sedimentary
rocks using threaded drill bit

CHAPTER – VII

ARTIFICIAL NEURAL NETWORKS (ANN)

7.1 Introduction

Neural network is a powerful technique to solve many real-world problems. It has the quality of adaptability to the changes in the environment which results in the improvement in its performance. In addition to this they are able to deal with incomplete information or noisy data (Singh et al., 2003) and are very effective especially in situations when it is not possible to define the rules or steps that lead to the solution of a problem.

Artificial neural networks (ANNs), or shortly, neural networks (NN) have been used for finding out the structure and functionality of biological, nature of human brain. Therefore, ANN is found to be more flexible and suitable than other modeling methods (Zhang et al., 1997). ANN is based on the neural architectures of the human brain (Haykin, 1994), and is described as group of simple processing units, known as neurons (nodes), that are arranged in parallel layers that are connected to each other by weighted connections. By virtue of hidden layers of neurons that lie between the input and output layers of the network, and the nonlinear activation functions that are used to translate nodal input into output, ANN provides linear and nonlinear modeling without the requirement of preliminary information and assumption as to the relationship between input and output variables. This provides ANN an advantage over other statistical and conventional prediction methods such as logistic regression and numerical methods, in which nonlinear interactions among variables must be modeled in explicit functional form (Tu, 1996). ANN trained with feed-forward back-propagation algorithm has been studied extensively and applied successfully in various areas, such as automotives (Majors et al., 2002), banking (Arzum and Yalcin, 2007), electronics (Bor-ren and Hof, 2003), finance (Xiaotian et al., 2008), industry (Cheginia et al., 2008), oil and gas (Peranbur and Preechayasomboon, 2002), and robotics (Huang et al., 2008). Most of the ANNs

contain three layers: input, output and hidden layer. Generally, there are various types of ANN techniques for example feed forward network, radial basis network, generalized regression network and recurrent neural network.

Neural networks may be used as a direct substitute for auto correlation, linear regression, trigonometric, multivariable regression, and other statistical analyses and techniques (Singh et al., 2003). Neural networks, with their remarkable ability to derive meaning from complicated or imprecise data, can be used to extract patterns and detect trends that are too complex to be noticed by either humans or other computer techniques (Yilmaz, and Yuksek, 2008). Rumelhart and McClelland (1986) reported that the main characteristics of ANN include large-scale parallel distributed processing, continuous nonlinear dynamics, collective computation, high fault-tolerance, self-organization, self-learning, and real-time treatment. When a data stream is analyzed using a neural network, it is possible to detect important predictive patterns that were not previously apparent to a non-expert. Thus, the neural network can act as an expert. The particular network can be defined using three fundamental components: transfer function, network architecture and learning law (Simpson, 1990). It is essential to define these components to solve the problem satisfactorily.

Neural networks consist of a large class of different architectures. Multi Layer Perceptron (MLP) and Radial Basis Function (RBF) are two of the most widely used neural network architectures in literature for classification or regression problems (Cohen and Intrator, 2002, 2003; Kenneth, et al., 2001; Loh and Tim, 2000). Both types of neural network structures are good for pattern classification problems.

One of the most important aspects of neural networks is the learning process. The learning process of a neural network can be viewed as reshaping a sheet of metal, which represents the output (range) of the function being mapped. The training set (domain) acts as energy required to bend the sheet of metal such that it passes through predefined points. However, the metal, by its nature, will resist such reshaping (Lee, et al., 2005). So the network will attempt to find a low energy configuration (i.e. a flat/non-wrinkled shape) that satisfies the constraints (training data). Learning cycle in ANN model is as shown in Figure 7.1 (Magali and Paul 2003).
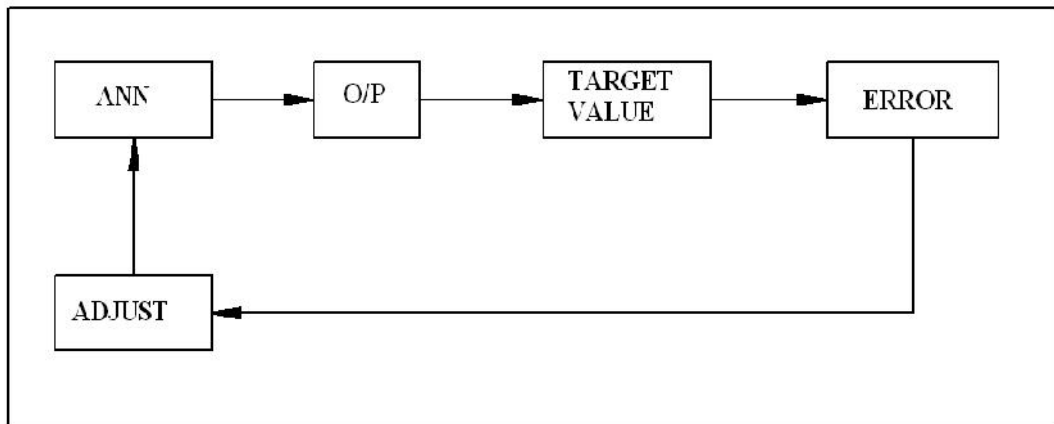
Fig. 7.1 Learning cycle in ANN model

Learning methods in neural networks (Rumelhart, and McClelland, 1986) can be broadly classified into two types. They are

a. Supervised learning

b. Unsupervised learning

In supervised learning, both the inputs and the outputs are provided. The network then processes the inputs and compares its resulting outputs against the desired outputs. Errors are then propagated back through the system, causing the system to adjust the weights which control the network. This process occurs over and over as the weights are continually tweaked. The set of data which enables the training is called the "training set." During the training of a network the same set of data is processed many times as the connection weights are ever refined.

In the unsupervised learning, the network is provided with inputs but not with desired outputs. The system itself must then decide what features it will use to group the input data. This is also known as self organized or adaptation.

In this study, feed forward networks namely MLP have been used to develop the prediction model of rock properties and penetration rate and sound level.

7.2 Multi Layer Perceptron (MLP)

Multi Layer Perceptron (MLP) network models are the popular network architectures used in most of the research applications in medicine, engineering,

mathematical modeling, etc. In MLP, the weighted sum of the inputs and bias term are passed to activation level through a transfer function to produce the output, and the units are arranged in a layered feed-forward topology called Feed Forward Neural Network (Venkatesan and Anitha, 2006). To achieve higher level of computational capabilities, a more complex structure of neural network is required. Multilayer neural network distinguishes itself from the single layer network by having one or more hidden layers. In this multilayer structure, the input nodes pass the information to the units in the first hidden layer, and then the outputs from the first hidden layer are passed to the next layer, and so on. Multilayer network can also be viewed as a cascading of groups of single-layer networks. The level of complexity in computing can be seen by the fact that many single-layer networks are combined into this multilayer network. The designer of an artificial neural network should consider how many hidden layers are required, depending on the complexity in desired computation.

The multilayer feed-forward network is the most commonly used network architecture with the back propagation algorithm. Back propagation networks, and multilayered perceptrons, in general, are feed forward networks with distinct input, output, and hidden layers. The units function basically like perceptrons, except that the transition (output) rule and the weight update (learning) mechanism are more complex.

Back Propagation

Back-propagation Neural Network (BPNN) algorithm is widely used in solving many practical problems. The BPNN learns by calculating the errors of the output layer to find the errors in the hidden layers. Due to this ability of Back-Propagating, it is highly suitable for problems in which no relationship is found between the output and inputs. Due to its flexibility and learning capabilities, it has been successfully implemented in wide range of applications (Lee et al. 2005). A Back-Propagation network consists of at least three layers of units: an input layer, at least one intermediate hidden layer, and an output layer. Typically, units are

connected in a feed-forward fashion with input units fully connected to units in the hidden layer and hidden units fully connected to units in the output layer.

The input pattern is presented to the input layer of the network. These inputs are propagated through the network until they reach the output units. This forward pass produces the actual or predicted output pattern. Because back propagation is a supervised learning algorithm, the desired outputs are given as part of the training vector. The actual network outputs are subtracted from the desired outputs and an error signal is produced. This error signal is then the basis for the back propagation step, whereby the errors are passed back through the neural network by computing the contribution of each hidden processing unit and deriving the corresponding adjustment needed to produce the correct output. The connection weights are then adjusted and the neural network has just "learned" from an experience. Once the network is trained, it will provide the desired output for any of the input patterns.

Steps of the Back propagation algorithm

Step 1: Obtain a set of training patterns.

Step 2: Set up neural network model: No. of I/P neurons, hidden neurons, & O/P neurons

Step 3: Set learning rate   and momentum rate

Step 4: Initialize all connection W_{ji}, W_{kj} and bias weights ${}_j$ ${}_k$ to random values.

Step 5: Set minimum error, E_{min}

Step 6: Start training by applying input patterns one at a time and propagate through the layers then calculate total error.

Step 7: Back propagate error through output and hidden layer and adapt weights.

Step 8: Back propagate error through hidden and input layer and adapt weights.

Step 9: Check it Error $< E_{min}$

If not repeat Steps 6-9. If yes stop training.

7.3 Multi Layer Perceptron (MLP) Modeling

Artificial neural network model is developed by using the experimental data based on multi layer perceptron. In order to develop a best possible MLP architecture based on good generalization ability and a compact structure, different training algorithms were compared. Detailed procedure used for developing the optimized MLP model for sedimentary rock type is given. Similar procedure is employed and results were obtained also for other types of rock.

Steady state experimental data were used for ANN modeling. Out of 750 data, approximately 70% (525 data) were used in the training and remaining 225 data were employed for testing the models. Air pressure, bit diameter, thrust, penetration rate and A-weighted equivalent sound level were used as the input parameters. These input parameters cover the entire problem domain under study and are effective in their prediction. Rock properties such as UCS, Abrasivity, SRN, and tensile strength, were the output parameters for the model. A schematic representation of the ANN model is shown in Fig. 7.2.

Similarly, air pressure, thrust, bit diameter, and rock properties were used as the input parameters. Sound level and penetration rate, were the output parameters for the model. The architecture of the neural network model is shown in Fig.7.3.

To ensure that each input provides an equal contribution in the ANN, the inputs to the model were pre-processed and scaled into a common numeric range (0, 1). A network with three hidden layer was used with a sigmoid activation function in the hidden layer and output layer.

The number of empirical equations obtained from the conventional statistical techniques for assessing the rock properties. The major demerit of statistical relations (e.g. regression analysis) is the prediction of mean values only. Consequently, low experimental values are overestimated, while high experimental values are underestimated. A neural network does not force the predicted value to be a mean value, thus preserving and using the existing variance of the measured data. Because of ANN's ability to learn and generalize interactions among many variables, artificial

neural networks technology has been reported to be very useful in modelling the rock material behaviour. Study indicated that ANN technology is more powerful than conventional statistical techniques in predicting penetration rate, sound level and rock properties.
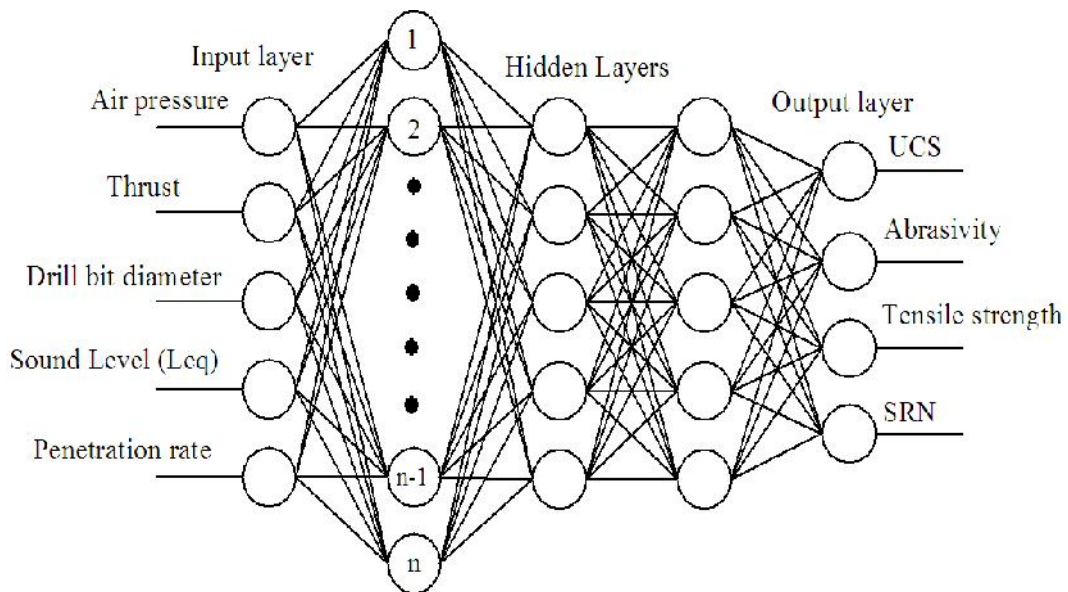
Fig.7.2 Neural network architecture of 5 input neurons and four output neurons with three hidden layers.
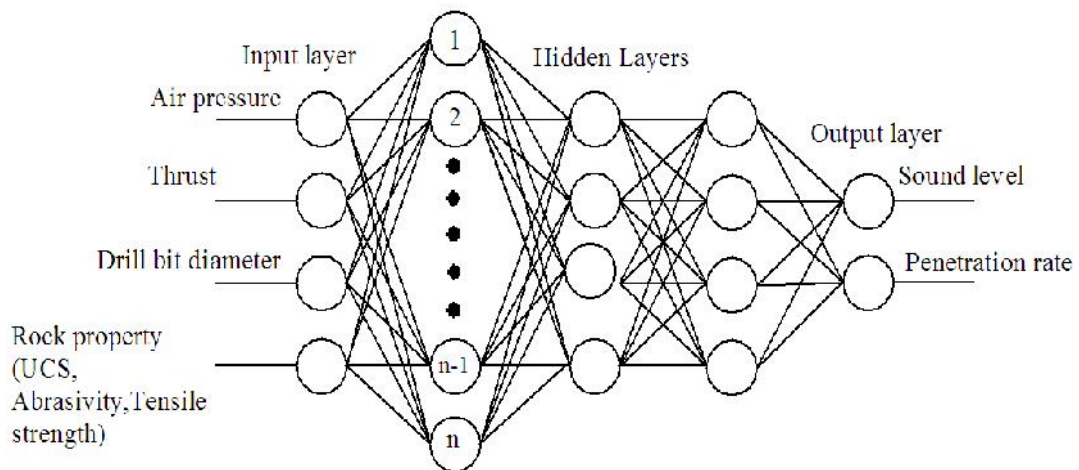
Fig.7.3 Neural network architecture of four input neurons and two output neurons with three hidden layers

The Muti-Layer-Perceptron (MLP) network was implemented using Matlab Neural Network Toolbox (MatLab 2010). The network was trained using four

different back-propagation training algorithms namely, Resilient Back-propagation algorithm (*trainrp*), Scaled Conjugate Gradient algorithm (*trainscg*), Gradient descent with adaptive learning back-propagation algorithm (traingda) and Levenberg-Marquardt algorithm (*trainlm*). The output of the network was compared with the desired output at each presentation and the error was computed. This error was then back-propagated to the network and used for adjusting the weights in such a way that the error decreased with iteration. Mean square errors (MSE) of 1.0e-5, a minimum gradient of 1.0e-5 and maximum number of epochs of 2000 were used. The training process would stop if any of these conditions has met. For each of the training algorithms, a number of trials were conducted initially to fix the number of neurons in the hidden layer. The number of neurons for which MSE is minimum, was selected as the optimum number of neurons in the hidden layer.

The architecture and performances of the network using different training algorithms are given in Table 7.1b. It is clear from Table 7.1b; that, trainlm converges faster than all other training algorithms as the number of epochs as well as the time taken for convergence is less. The variation of MSE with the number of neurons in the hidden layer for trainlm algorithm is shown in Figure 7.4. From the Figure 7.4, it can be observed that for the performance model, when the number of neurons in the hidden layer was (13, 10, 7) increased the error was 0.0001 and it decreased as the number of neurons in the hidden layer (7, 4, 2) was decreased and reached maximum of 0.000132 and on increasing the number of neurons further, MSE gradually increased. Training results based on the 5-3-4 configuration, training and testing data error of sedimentary rock is shown in Figure 7.5 to 7.8.

Similar type observations were made for other architecture and performances of the network using different training algorithms of threaded drill bit (Table 7.3 a and 7.3b) and sound level and penetration rate for integral and threaded drill bit (Table 7.2a & 7.2b, 7.4a & 7.4b)
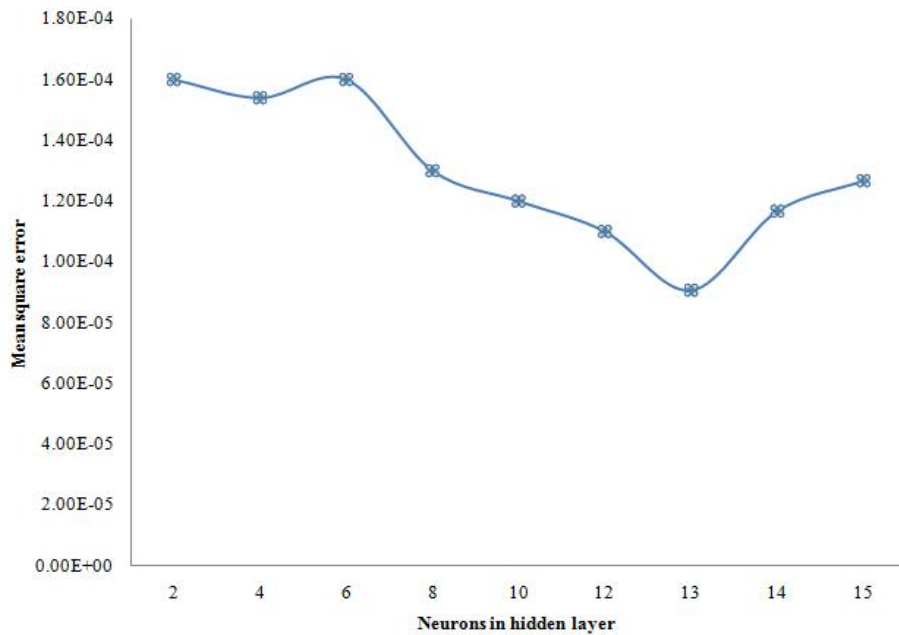
Figure 7.4 Variation of MSE with the number of neurons in the hidden layer for trainlm algorithm

Comparison of performance of the developed model of MRA and ANN for sedimentary rocks using integral and threaded drill bit is as shown in Figure 7.9 to 7.12 and also comparison of performance of the developed model of MRA and ANN for igneous rocks using integral and threaded drill bit is as shown in Figure 1 to 4 in Appendix IV.

7.4 Performance Prediction of the Model

Trained networks were tested for performance. The performances of the networks were evaluated using Values Account For (VAF) and Root Mean Square Error (RMSE) indices (Alvarez and Babuska 1999, Finol *et al.* 2001, Gokceoglu 2002, Yilmaz and Yuksek 2008, 2009). VAF, RMSE and MAPE can be computed using Equations (7.1, 7.2 and 7.3) respectively.

$$VAF = \left[1 - \frac{var(y - y')}{var(y)} \right] \times 100 \qquad -------------------- (7.1)$$

$$RMSE = \sqrt{\frac{1}{N} \sum_{i=1}^{N} (y - y')^2} \qquad -------------------- (7.2)$$

87

$$\text{MAPE} = \frac{1}{N}\left[\frac{\text{Ai - Pi}}{\text{Ai}}\right] \times 100 \qquad \text{----------------------- (7.3)}$$

The networks performance for different training algorithms is shown in Table 7.1a. It is clear from the table, VAF values are maximum. RMSE and MAPE values are minimum for the network using train algorithm when compared to the other models for both training and testing data. VAF values were 95.576%, 94.284%, 96.215% and 93.317% for UCS, Abrasivity, tensile strength and SRN respectively, whereas for the test data these values were 90.567%, 91.324%, 92.253% and 89.137 respectively. Further the RMSE values were 0.1530, 0.0316, 0.0172 and 1.689 for UCS, Abrasivity, tensile strength and SRN respectively for the training data, whereas for the test data these values were 0.1813, 0.0349, 0.0199 and 5.043 respectively for the test data. MAPE values for the training data were 4.424%, 5.216%, 3.785% and 6.683% for UCS, Abrasivity, tensile strength and SRN respectively, whereas, the corresponding values for the testing data were 9.433%, 8.676%, 7.468% and 10.629%. Hence the MLP model with trainlm algorithm can be effectively used as a predictor of rock properties based on sound level produced during drilling. Also, performance prediction indices of different training algorithm for mechanical properties of sedimentary rocks using integral and threaded drill bit is given in Table 7.1a, 7.1b, 7.3a and 7.3b of Appendix IV and performance of different training algorithm for sound level and penetration rate of sedimentary rocks using integral and threaded drill bit is given in Table 7.2a, 7.2b, 7.4a and 7.4b.

Variation in sound level with mechanical properties of rocks using integral drill bit diameter of 30, 34 and 40 mm for sedimentary rocks are shown in Figure 7.13 (A to D). Experimental mean values and ANN predicted mean values using trainlm algorithm for sedimentary rocks using integral drill bit diameters of 30, 34 and 40 mm are shown in Figure 7.14 (A to D).

Performance prediction indices of different training algorithm for mechanical properties of igneous rocks using integral and threaded drill bit is given in Table 1a, 1b, 2a and 2b of Appendix IV and performance of different training algorithm for

sound level and penetration rate of igneous rocks using integral and threaded drill bit are given in Table 3a, 3b, 4a and 4b of Appendix IV.

Comparison of performance of the developed model of MRA and ANN for mechanical properties of igneous rocks using integral and threaded drill bit are given in Table 5a and 5b and comparison of performance indices of MRA and ANN for sound level and penetration rate of igneous rock using integral and threaded drill bit are given in Table 5c, 5d of Appendix IV. The variation in sound level produced during drilling with various rock properties for igneous rocks for integral drill bit diameters of 30, 34 and 40 mm are shown in Figure 5 (A to D). Experimental mean values and ANN predicted mean values using trainlm algorithm for igneous rocks using integral drill bit diameters of 30, 34 and 40 mm are shown in Figure 6 (A to D) of Appendix IV.

7.5 Comparison of ANN and Regression Models

The best architecture in each of the ANN methods has been compared with the regression method. The results of comparison are given in Table 7.5a to 7.5d for sedimentary rocks using integral and threaded drill bit. Similar comparison were made for igneous rocks using integral and threaded drill bit are given in Table 5a to 5d of Appendix IV.

7.6 Summary

(1) MLP model have been developed for prediction of the rock properties.

(2) MLP has fixed architecture where the number of hidden neurons was determined by trial and error method. Network was trained using different types of Back-propagation algorithm such as trainrp, trainscg, traingda, trainlm.

(3) Performances of the algorithm for different categories of rocks were compared in terms of VAF, RMSE, and MAPE values. For MLP model trainlm algorithm preferred better than other algorithm and hence it is recommended.

(4) ANN methods have been compared with MRA
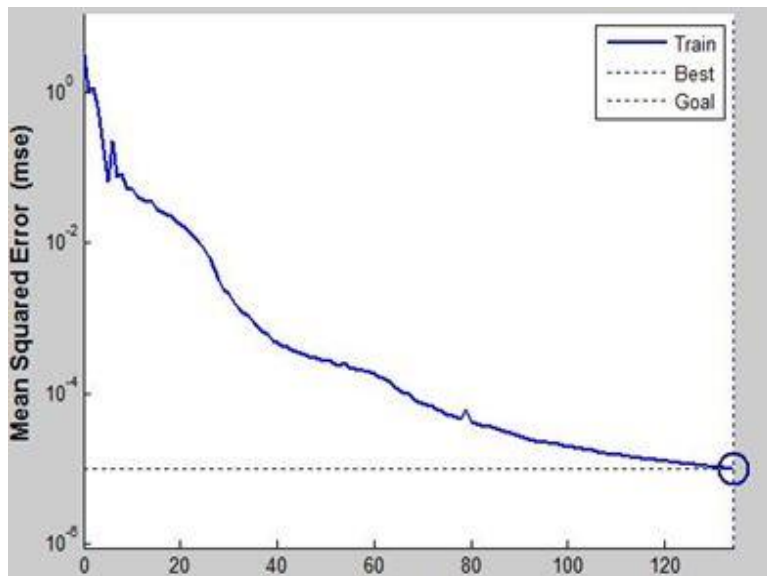
Figure7.5 Training results based on the 5-3-4 configuration
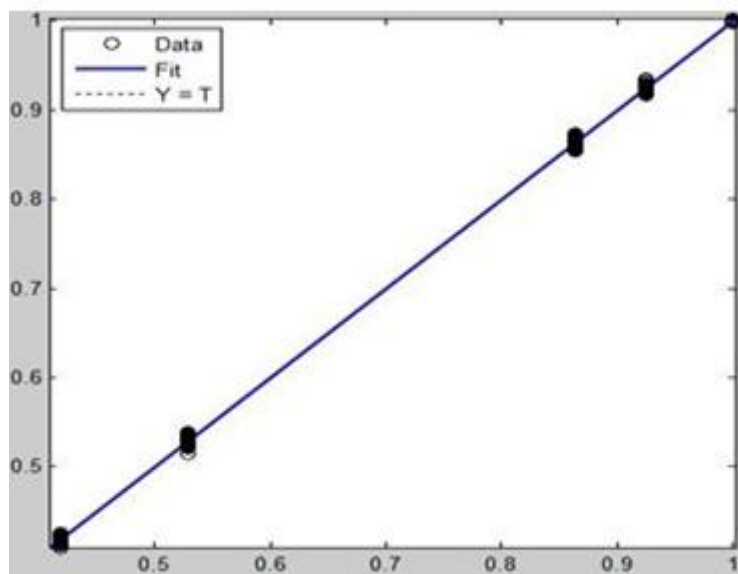
Figure 7.6 Training results based on the 5-3-4 configuration
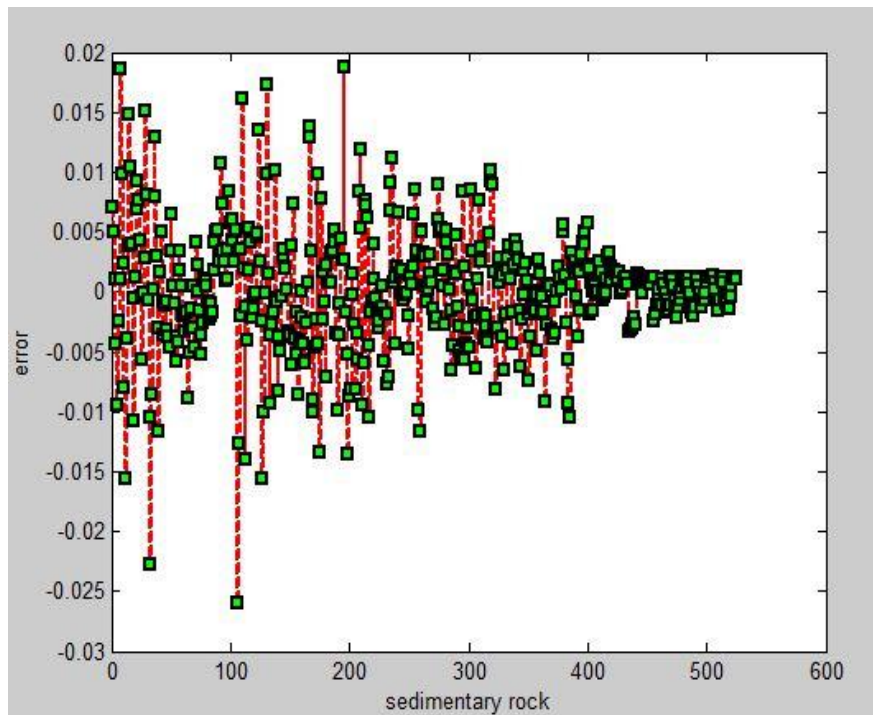
Fig.7.7 Training data error of sedimentary rock
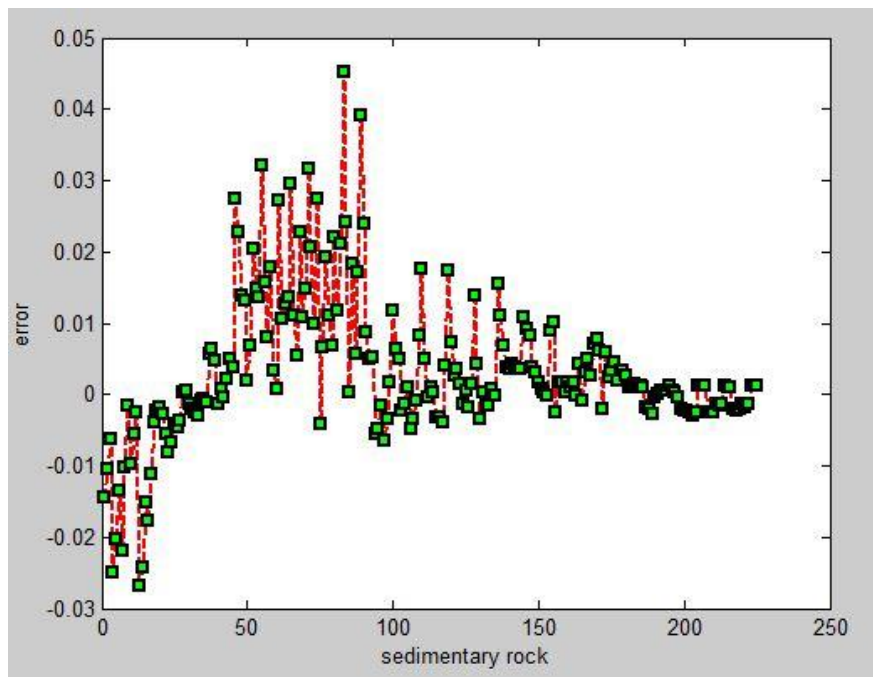
Fig.7.8 Testing data error of sedimentary rock

Table 7.1a Performance prediction indices of different training algorithms for sedimentary rock using integral drill bit

			UCS	Abrasivity	Tensile strength	SRN
traingda	Training data	VAF	85.169	84.219	87.627	81.985
		RMSE	4.85	2.191	2.374	3.2
		MAPE	14.831	15.781	12.373	18.015
	Testing data	VAF	83.625	82.605	84.567	79.578
		RMSE	6.314	3.498	4.634	5.678
		MAPE	16.375	17.395	15.433	20.422
trainrp	Training data	VAF	87.782	86.329	88.769	83.856
		RMSE	0.2325	0.0611	0.0233	2.22
		MAPE	12.218	13.671	11.231	16.144
	Testing data	VAF	86.918	84.932	87.098	81.547
		RMSE	0.4348	0.1919	0.0458	5.33
		MAPE	13.082	15.068	12.902	18.453
trainscg	Training data	VAF	88.675	89.524	89.635	84.957
		RMSE	0.2392	0.0615	0.0289	2.2156
		MAPE	11.325	10.476	10.365	15.043
	Testing data	VAF	87.427	87.873	88.618	82.043
		RMSE	0.4833	0.0956	0.0529	5.69
		MAPE	12.573	12.127	11.382	17.957
trainlm	Training data	VAF	95.576	94.284	96.215	93.317
		RMSE	0.1530	0.0316	0.0172	1.689
		MAPE	4.424	5.216	3.785	6.683
	Testing data	VAF	90.567	91.324	92.253	89.137
		RMSE	0.1813	0.0349	0.0199	5.043
		MAPE	9.433	8.676	7.468	10.629

Table 7.1b Performance of different training algorithm for sedimentary rock using integral drill bit

Training algorithm	Network architecture	Number of epochs	Time taken for convergence (sec)	Mean square error
trainrp	5,13,10,7,4	94	03	0.00000982
trainlm	5,13,10,7,4	11	01	0.00000969
trainscg	5,13,10,7,4	2000	48	0.0000126
traingda	5,13,10,7,4	20000	27	0.0530

Table 7.2a Performance prediction indices of different training algorithms for sedimentary rock using integral drill bit

			Penetration rate	Sound level
traingda	Training data	VAF	86.912	88.764
		RMSE	2.182	2.106
		MAPE	13.088	11.236
	Testing data	VAF	84.187	86.456
		RMSE	3.968	4.832
		MAPE	15.813	13.544
trainrp	Training data	VAF	87.234	89.691
		RMSE	0.0531	0.0413
		MAPE	12.766	10.309
	Testing data	VAF	85.296	86.873
		RMSE	0.2191	0.0365
		MAPE	14.704	13.127
trainscg	Training data	VAF	89.617	90.918
		RMSE	0.0535	0.0298
		MAPE	10.383	9.082
	Testing data	VAF	87.328	88.839
		RMSE	0.0762	0.0615
		MAPE	12.672	11.161
trainlm	Training data	VAF	94.379	95.687
		RMSE	0.0382	0.0191
		MAPE	5.621	4.313
	Testing data	VAF	92.974	93.109
		RMSE	0.0298	0.0219
		MAPE	7.026	6.891

Table 7.2b Performance of different training algorithm for sedimentary rock using integral drill bit

Training algorithm	Network architecture	Number of epochs	Time taken for convergence (sec)	Mean square error
trainrp	4,13,10,7,2	205	04	0.0000133
trainlm	4,13,10,7,2	11	02	0.0000132
trainscg	4,13,10,7,2	2000	47	0.0000135
traingda	4,13,10,7,2	2000	27	0.0000679

Table 7.3a Performance prediction indices of different training algorithms for
sedimentary rock using threaded (R22) bit

			UCS	Abrasivity	Tensile strength	SRN
traingda	Training data	VAF	83.261	83.912	86.275	82.856
		RMSE	4.93	2.293	2.465	3.132
		MAPE	16.739	16.088	13.725	17.144
	Testing data	VAF	82.516	81.016	84.976	80.527
		RMSE	6.412	3.596	4.727	5.875
		MAPE	17.484	18.984	15.024	19.473
trainrp	Training data	VAF	85.456	86.342	87.987	84.326
		RMSE	0.2562	0.0675	0.0254	2.432
		MAPE	14.544	13.658	12.013	15.674
	Testing data	VAF	84.376	85.142	86.342	83.657
		RMSE	0.4523	0.2215	0.0642	5.562
		MAPE	15.624	14.858	13.658	16.343
trainscg	Training data	VAF	86.458	87.486	88.342	85.316
		RMSE	0.2483	0.0693	0.0312	2.2831
		MAPE	13.542	12.514	11.658	14.684
	Testing data	VAF	85.231	86.487	87.295	83.387
		RMSE	0.4978	0.1231	0.0695	5.982
		MAPE	14.769	13.513	12.705	16.613
trainlm	Training data	VAF	92.874	93.167	93.978	91.376
		RMSE	0.1723	0.0432	0.0197	1.864
		MAPE	7.126	6.833	6.022	8.624
	Testing data	VAF	90.654	92.897	93.125	90.478
		RMSE	0.1996	0.0458	0.0231	5.289
		MAPE	9.346	7.103	6.875	9.522

Table 7.3b Performance of different training algorithm for sedimentary rock using
threaded bit

Training algorithm	Network architecture	Number of epochs	Time taken for convergence (sec)	Mean square error
trainrp	5,13,10,7,4	22	06	0.00000578
trainlm	5,13,10,7,4	624	07	0.00000999
trainscg	5,13,10,7,4	2000	37	0.0000470
traingda	5,13,10,7,4	2000	22	0.00632

Table 7.4a Performance prediction indices of different training algorithms for sedimentary rock using threaded drill bit

			Penetration rate	Sound level
traingda	Training data	VAF	84.912	86.764
		RMSE	2.182	2.112
		MAPE	15.088	13.236
	Testing data	VAF	83.187	85.456
		RMSE	4.012	3.897
		MAPE	16.813	14.544
trainrp	Training data	VAF	85.234	87.691
		RMSE	0.0591	0.0654
		MAPE	14.766	12.309
	Testing data	VAF	83.296	86.473
		RMSE	0.2292	0.0395
		MAPE	16.704	13.527
trainscg	Training data	VAF	88.617	88.918
		RMSE	0.0585	0.0312
		MAPE	11.383	11.082
	Testing data	VAF	86.328	87.839
		RMSE	0.0862	0.0721
		MAPE	13.672	12.161
trainlm	Training data	VAF	93.379	95.687
		RMSE	0.0426	0.0285
		MAPE	6.621	4.313
	Testing data	VAF	91.974	92.109
		RMSE	0.0324	0.0256
		MAPE	8.026	7.891

Table 7.4b Performance of different training algorithm for sedimentary rock using threaded drill bit

Training algorithm	Network architecture	Number of epochs	Time taken for convergence (sec)	Mean square error
trainrp	4,13,10,7,2	79	02	0.00000927
trainlm	4,13,10,7,2	07	01	0.00000733
trainscg	1413,10,7,2	435	09	0.00001
traingda	16,13,10,7,2	2000	26	0.00159

Table 7.5a Comparison of performance of the developed model of MRA and ANN
for sedimentary rock using integral drill bit

	Rock property	RMSE	VAF	MAPE
MRA	Uniaxial compressive strength	4.93	93.550	6.45
	Abrasivity	0.3737	94.180	5.82
	Tensile strength	0.2006	94.150	5.85
	Schmidt rebound number	11.89	92.320	7.68
ANN	Uniaxial compressive strength	0.1530	95.576	4.424
	Abrasivity	0.0316	94.284	5.216
	Tensile strength	0.0172	96.215	3.785
	Schmidt rebound number	1.689	93.317	6.683

Table 7.5b Comparison of performance of the developed model of MRA and ANN
for sedimentary rock using integral drill bit

		RMSE	VAF	MAPE
MRA	Sound level	0.2476	94.218	5.782
	Penetration rate	0.2210	93.892	6.108
ANN	Sound level	0.0191	95.687	4.313
	Penetration rate	0.0382	94.379	5.621

Table 7.5c Comparison of performance of the developed model of MRA and ANN
for sedimentary rock using threaded drill bit

	Rock property	RMSE	VAF	MAPE
MRA	Uniaxial compressive strength	5.140	92.166	7.834
	Abrasivity	0.4120	92.787	7.213
	Tensile strength	0.2261	93.757	6.243
	Schmidt rebound number	12.09	91.053	8.947
ANN	Uniaxial compressive strength	0.1723	92.874	7.126
	Abrasivity	0.0432	93.167	6.833
	Tensile strength	0.0197	93.978	6.022
	Schmidt rebound number	1.864	91.376	8.624

Table 7.5d Comparison of performance of the developed model of MRA and **ANN**
for sedimentary rock using threaded drill bit

		RMSE	VAF	MAPE
MRA	Sound level	0.2704	93.33	6.67
	Penetration rate	0.2386	93.129	6.871
ANN	Sound level	0.0285	95.687	4.313
	Penetration rate	0.0426	93.379	6.621
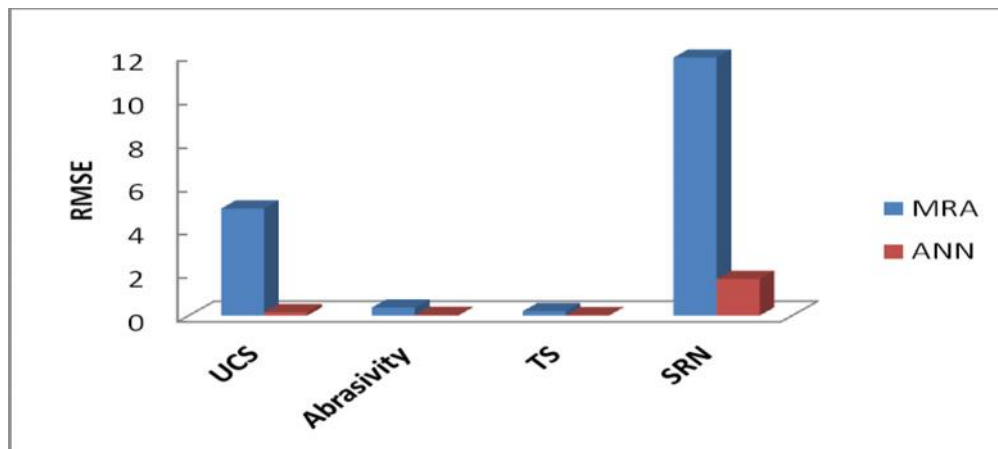
(A)
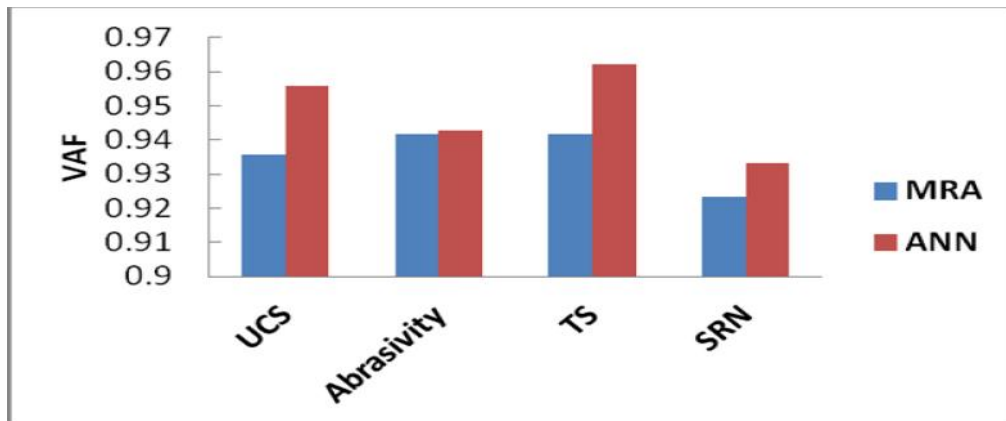
(B)
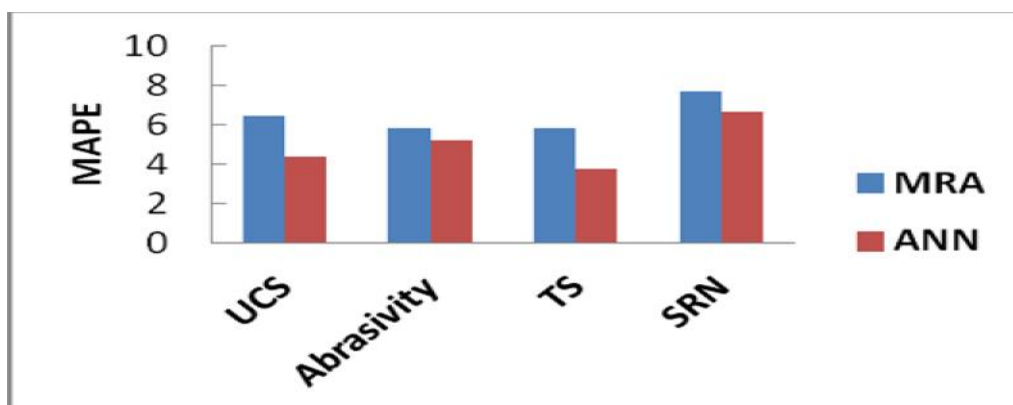
(C)

Fig. 7.9 Performance indices of: (A) RMSE (B) VAF and (C) MAPE of MRA and ANN for sedimentary rock using integral drill bit
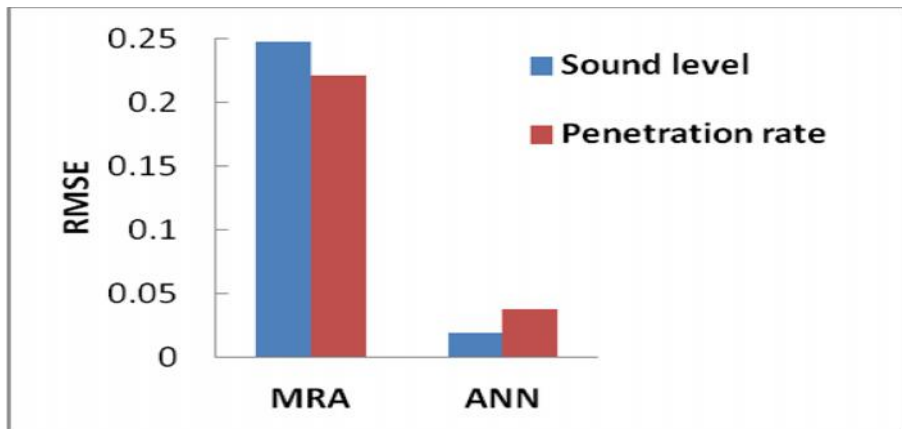
(A)
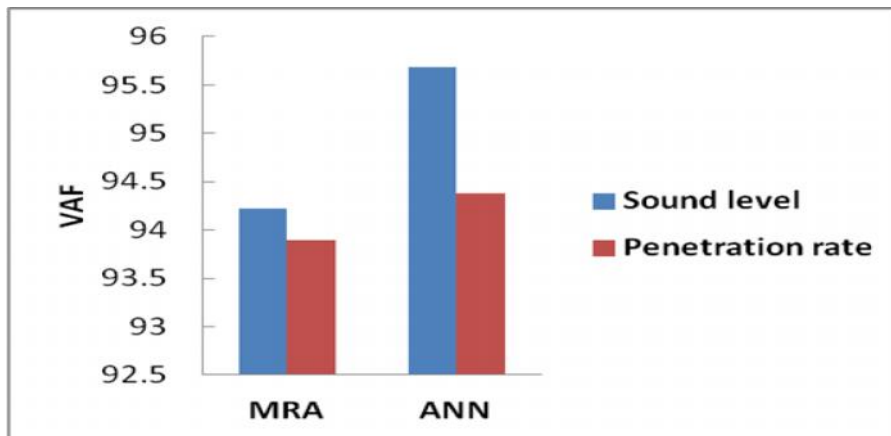
(B)
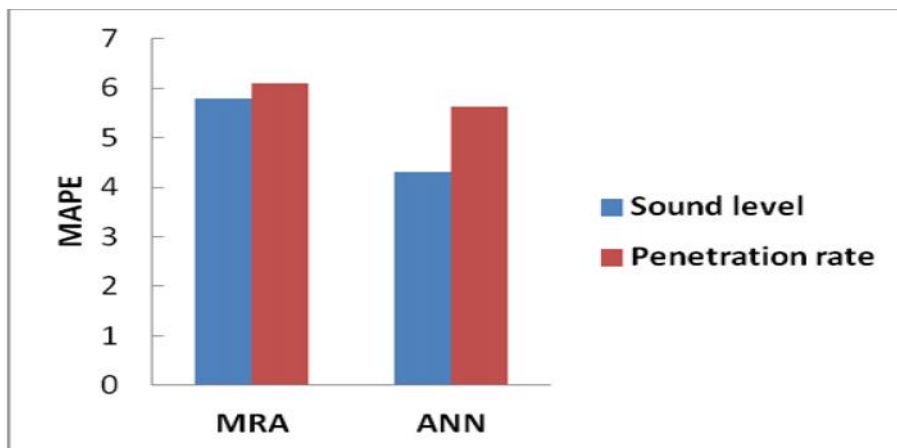
(C)

Fig. 7.10 Performance indices of: (A) RMSE (B) VAF and (C) MAPE of MRA and ANN for sedimentary rock using integral drill bit
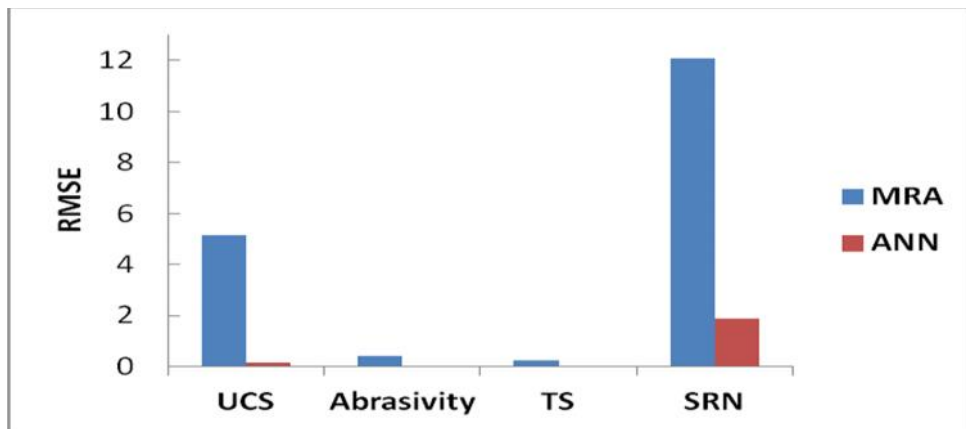
(A)
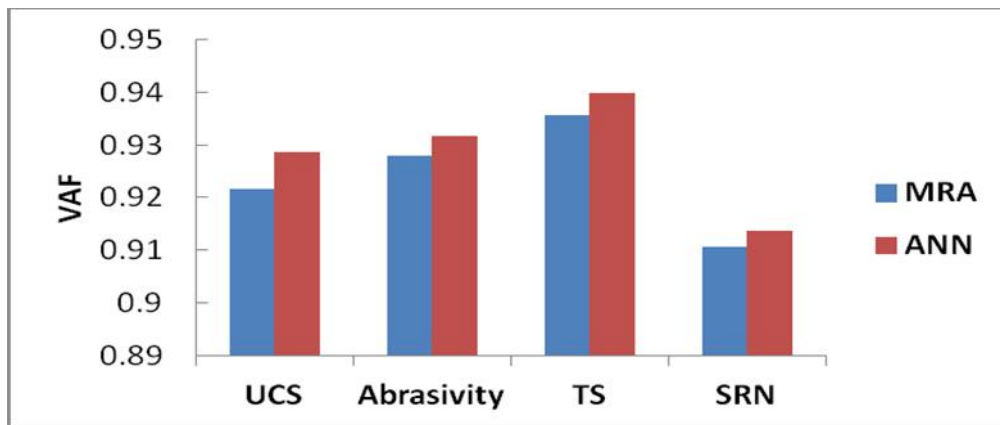
(B)
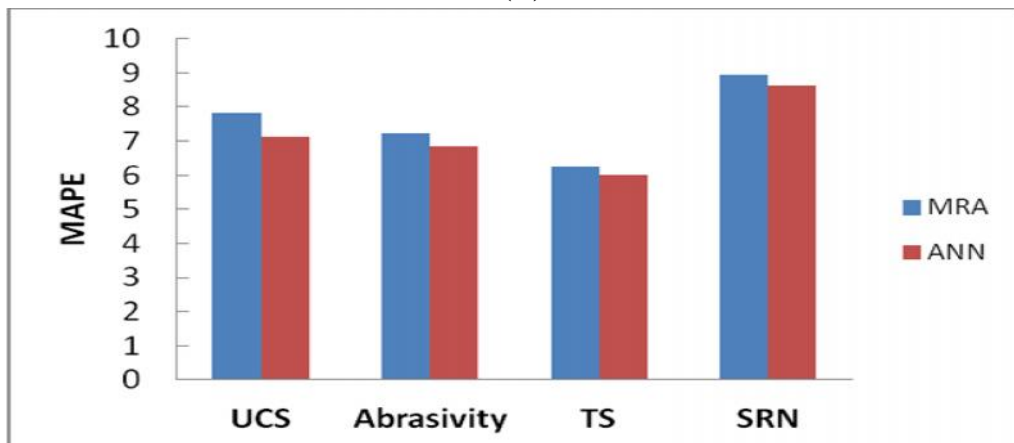
(C)

Fig. 7.11 Performance indices of: (A) RMSE (B) VAF and (C) MAPE of MRA and ANN for sedimentary rock using threaded drill bit
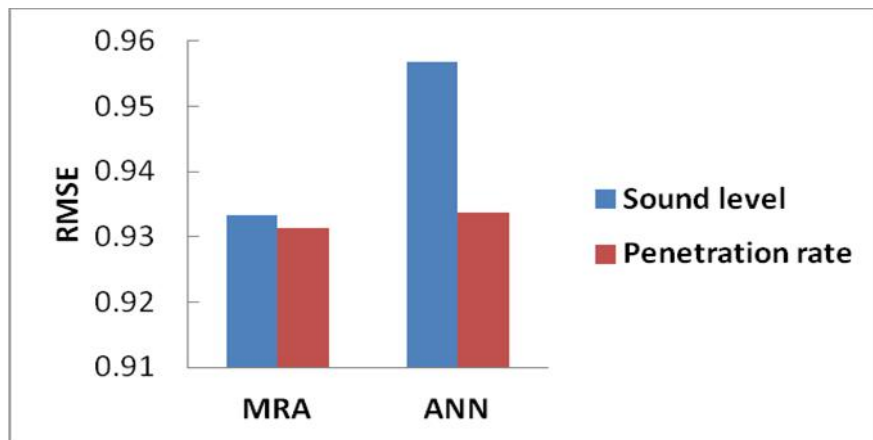
(A)
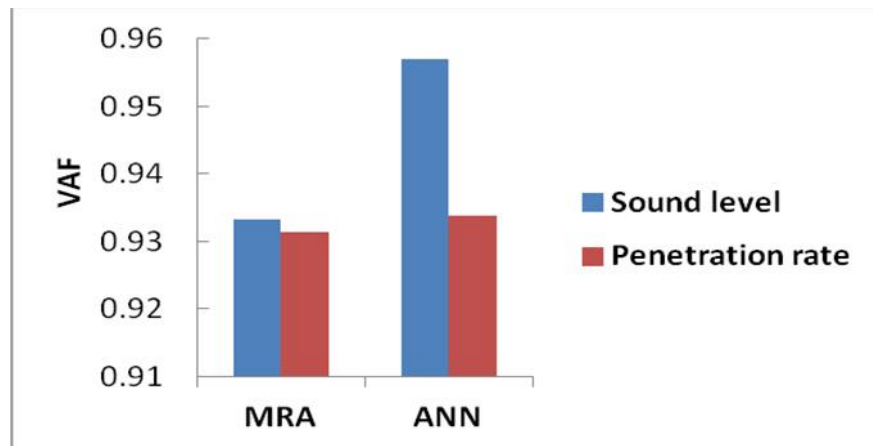
(B)
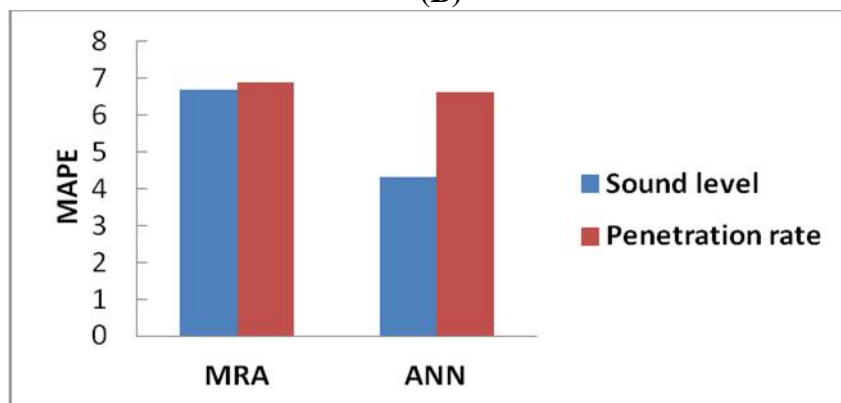
(C)

Fig. 7.12 Performance indices of: (A) Root mean square error (RMSE) (B) value account for (VAF) and (C) Mean absolute percentage error (MAPE) of multiple regression analysis (MRA) and artificial neural network (ANN) for sedimentary rock using threaded drill bit

(A) **(B)**

(C) **(D)**
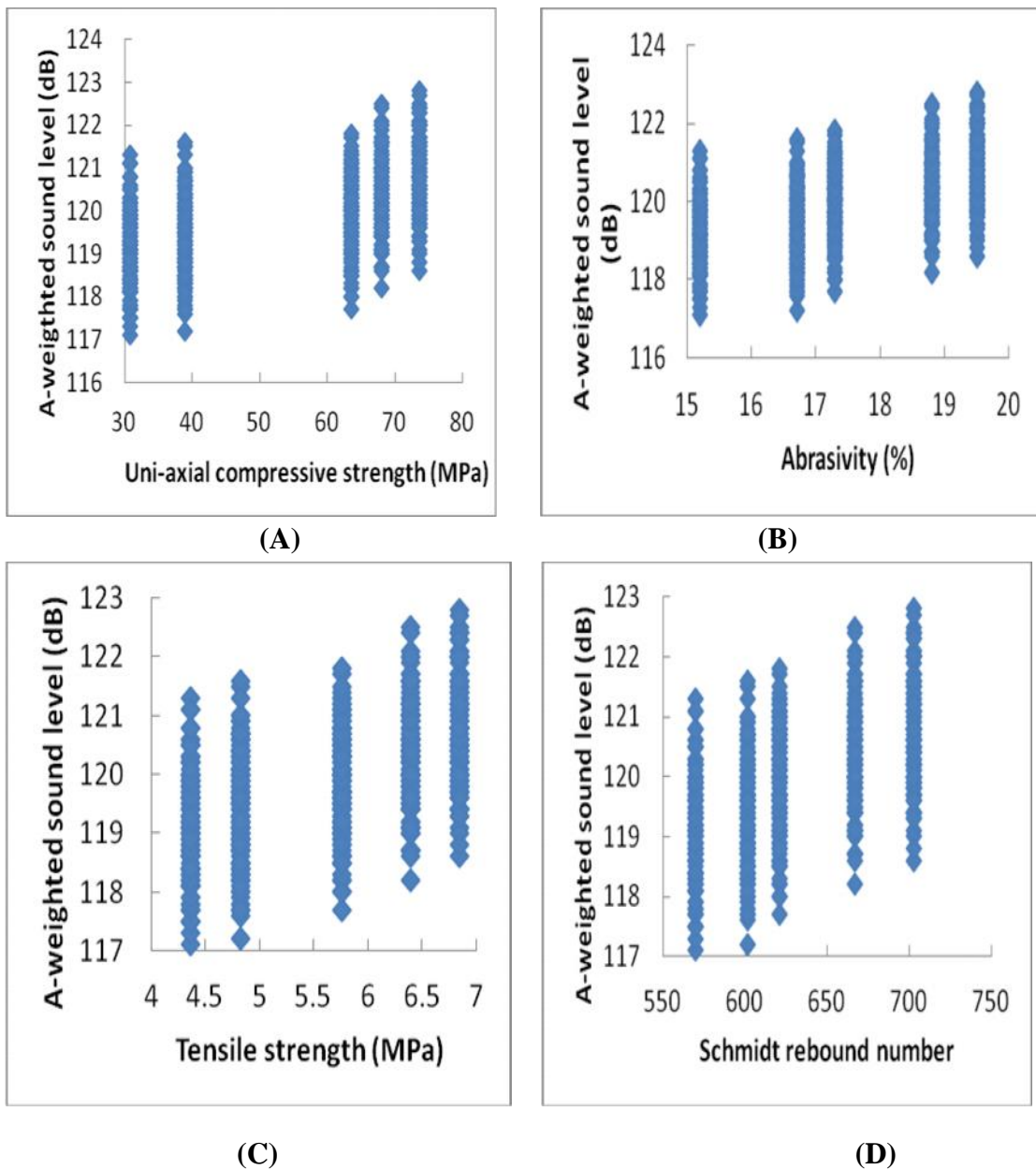
Fig.7.13 Variation of sound level with various rock properties of sedimentary rocks using integral drill bit diameters of 30, 34 mm
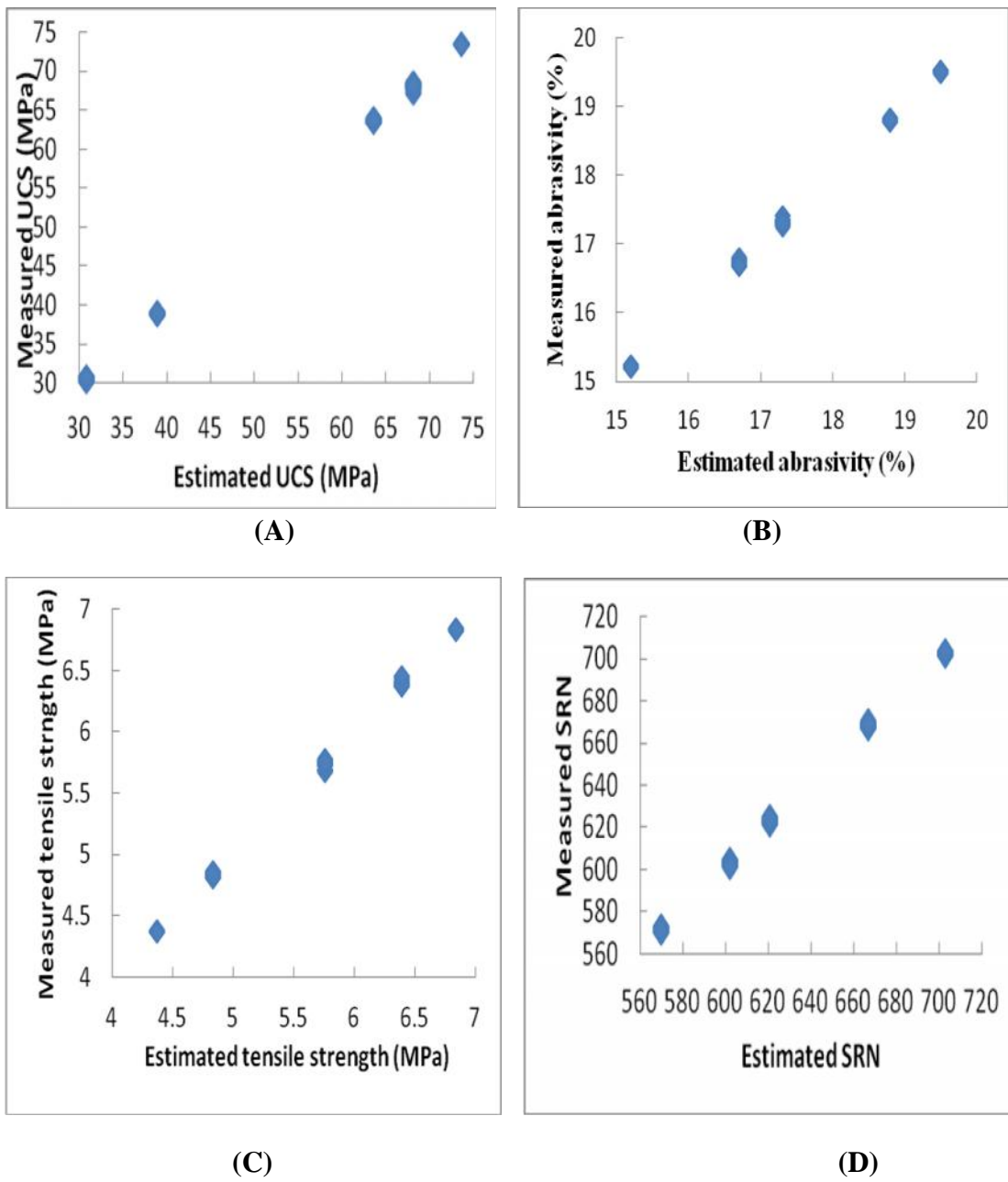
Fig. 7.14 Experimental mean values and ANN predicted mean values using trainlm algorithm for sedimentary rock using integral drill bit

CHAPTER - VIII

CONCLUSIONS AND SCOPE FOR FURTHER WORK

8.1 Conclusions

In the present investigation, machine parameters (air pressure, thrust and bit diameter), penetration rate and equivalent sound level produced during drilling were used to predict various rock properties. Mechanical properties of various rocks were measured in the laboratory by ISRM suggested methods. Experiments were conducted using percussive drill with different types of bit diameter (integral and threaded), air pressure and thrust. For all the conditions, penetration rate and equivalent sound levels were recorded. The experimental results were used to develop the prediction models using multiple regression and ANN techniques. The conclusions drawn from the experimental and modeling studies are as follows:

1. For all the bit-rock combinations, the penetration rate and sound level increased up to an optimum value of thrust beyond which it decreases gradually with increase in the thrust. The maximum value of penetration and sound level also varies with the air pressure for a given bit-rock combination. Both at lower and higher thrust levels, the penetration rate and sound levels are lower. Air pressure and thrust were found to have a significant impact on penetration rate and sound level produced by percussive drill for all the bit-rock combinations considered.

2. The penetration rate decreases with increase in the bit diameter for both integral and threaded drill bits. Further, integral steel chisel bit gives higher penetration rate than threaded bit because of energy losses at joints in all the rocks considered for a given bit-rock combination.

3. Sound level increases and penetration rate decreases with increase in uni-axial compressive strength and abrasivity for all bit rock combinations. Further, sound level near the drill rod is comparatively higher than that near the drill bit, exhaust and the operators position for a given operating parameters and bit-rock combinations used for integral and threaded bits. This is due to increased vibrations in the drill rod.

4. Multiple regression models were developed, for prediction of various rock properties which shows statistically meaningful relationships with high prediction performances between rock properties and operational parameters (air pressure, thrust and bit diameter) of the drill machine along with penetration rate and equivalent sound level. The performance prediction values showed that the multiple regression models are good tools for minimizing the uncertainties and potential inconsistency of the correlation. The empirical relationship developed is not aimed at replacing the ISRM suggested testing methods, but rather as a quick and easy method to estimate the mechanical properties of rock.

5. Multi-layer perceptron neural network was trained using trainrp, traingdx, trainscg and trainlm algorithms which are different means of implementing back propagation algorithms and their performances were compared in terms of RMSE, VAF and MAPE values. trainlm algorithms showed better performance than all other algorithms in the prediction of all the rock properties and sound level and penetration rate.

6. A comparison of multiple regression model and MLP model using trainlm algorithm revealed that, MLP model gave better performance than multiple regression technique with lower RMSE and MAPE values and higher prediction accuracy (VAF) value for all the prediction variables.

7. The ability to adapt or continue learning is another important advantage of rock parameters prediction because training data are limited and new cases are continuously encountered. For this reason, the use of neural network may provide new approaches and methodologies, and minimize the potential inconsistency of correlations.

8.2 Scope for Further Work

1. In the present investigation only sedimentary and igneous rocks are considered. Rock properties (UCS, abrasivity, TS, SRN) and penetration rate and sound levels are measured. Mathematical models are developed to predict penetration rate and sound level from rock properties and machine parameters and vice-versa. In this investigation only 10 rocks (5 sedimentary and 5 igneous rocks) were considered, in future work more number of rocks can be considering for a better prediction. Further studies may be carried out on other types of rocks.

2. In the present investigation only integral and threaded drill bits were used. This work can be further extended by carrying out studies using spherical button, conical button and taper type drill bits.

3. This work can be extended by carrying out field investigation using the available drilling machines in the mine and using those data for development of prediction models. The developed models can be directly used in the field to predict rock properties.

4. In the present study only machine parameters, rock properties (uni-axial compressive strength, abrasivity, tensile strength and Schmidt rebound number), penetration rate and sound level are considered during the development of the prediction models. This work can be extended by using other physico-mechanical properties also for the development of the prediction models.

5. In the present study, regression and ANN modeling techniques are used. However, other techniques like Adaptive Neuro Fuzzy Inference System (ANFIS), Radial Basis Function (RBF), Fuzzy Logic modeling may be tried. Also, other analysis tools like Fast Fourier Transformer (FFT) can be used.

Table 1 A-weighted equivalent continuous sound level at operator's position for rock at various air pressures and thrust (sedimentary rock) for integral drill bit.

Air pressure (kPa)	Thrust (N)	A-weighted equivalent continuous sound level (dB)														
		Shale			Dolomite			Sand stone			Lime stone			Hematite		
		Drill bit diameter in (mm)														
		30	34	40	30	34	40	30	34	40	30	34	40	30	34	40
392	100	116.1	116.4	116.8	116.3	116.7	117..0	116.6	116.9	117.3	117.0	117.2	117.4	117.3	117.5	117.7
	200	116.4	116.7	117.1	116.6	116.9	117.3	116.8	117.2	117.5	117.3	117.4	117.7	117.5	117.7	117.9
	300	116.7	116.7	117.3	117.0	117.2	117.5	117.2	117.5	117.8	117.5	117.7	118.0	117.8	118.0	118.2
	400	**117.1**	**117.3**	**117.6**	**117.3**	**117.5**	**117.8**	**117.5**	**117.9**	**118.1**	**117.8**	**118.1**	**118.3**	**118.2**	**118.3**	**118.5**
	500	116.8	117.1	117.4	117.1	117.3	117.6	117.3	117.6	117.9	117.6	117.8	118.1	117.9	118.1	118.3
	600	116.5	116.8	117.2	116.8	117.0	117.4	117.1	117.3	117.7	117.3	117.6	117.9	117.7	117.8	118.1
	700	116.3	116.6	116.9	116.6	116.8	117.1	116.9	117.1	117.4	117.1	117.4	117.6	117.4	117.6	117.8
	800	116.1	116.4	116.7	116.3	116.6	116.9	116.7	116.8	117.2	116.9	117.1	117.4	117.2	117.3	117.6
	900	115.8	116.2	116.4	116.0	116.4	116.6	116.3	116.6	117.0	116.6	116.8	117.2	116.9	117.1	117.4
	1000	115.6	115.9	116.2	115.8	116.1	116.4	116.1	116.3	116.7	116.4	116.5	116.9	116.7	116.8	117.1
441	100	116.4	116.6	117.1	116.6	117.0	117.3	116.8	117.3	117.6	117.2	117.5	117.8	117.5	117.8	118.1
	200	116.6	116.8	117.4	116.9	117.3	117.5	117.1	117.5	118.0	117.4	117.8	118.2	117.8	118.2	118.4
	300	116.9	117.2	117.6	117.1	117.5	117.8	117.4	117.8	118.3	117.7	118.1	118.5	118.1	118.5	118.7
	400	**117.3**	**117.5**	**117.9**	**117.5**	**117.8**	**118.2**	**117.8**	**118.4**	**118.7**	**118.1**	**118.6**	**118.9**	**118.5**	**118.8**	**119.1**
	500	117.1	117.3	117.7	117.3	117.6	117.9	117.6	118.1	118.5	117.9	118.4	118.7	118.2	118.6	118.9
	600	116.8	117.0	117.4	117.0	117.3	117.7	117.4	117.9	118.2	117.6	118.2	118.4	118.0	118.4	118.7
	700	116.6	116.8	117.2	116.8	117.1	117.4	117.1	117.6	117.9	117.4	117.9	118.1	117.7	118.1	118.4
	800	116.4	116.6	116.9	116.5	116.9	117.2	116.8	117.4	117.7	117.1	117.7	117.9	117.5	117.9	118.2
	900	116.1	116.3	116.7	116.3	116.6	116.9	116.6	117.1	117.4	116.8	117.3	117.6	117.2	117.6	117.9
	1000	115.9	116.1	116.4	116.1	116.4	116.7	116.4	116.9	117.0	116.6	117.1	117.3	116.9	117.4	117.6

490	100	116.8	117.4	118.0	117.2	117.6	118.2	117.7	118.2	118.5	118.0	118.4	118.8	118.3	118.8	119.2
	200	117.2	117.6	118.2	117.5	117.8	118.4	117.8	118.5	118.9	118.2	118.7	119.2	118.6	119.1	119.6
	300	117.5	117.8	118.5	117.8	118.0	118.7	118.0	118.8	119.3	118.4	119.0	119.6	118.8	119.3	120.0
	400	117.8	118.2	118.8	118.0	118.3	119.0	118.3	119.0	119.6	118.6	119.3	120.0	119.0	119.6	120.3
	500	**118.0**	**118.5**	**119.1**	**118.3**	**118.6**	**119.3**	**118.6**	**119.3**	**119.9**	**118.9**	**119.7**	**120.4**	**119.3**	**120.0**	**120.6**
	600	117.7	118.2	118.9	118.1	118.4	119.1	118.4	119.1	119.7	118.7	119.5	120.1	119.1	119.8	120.4
	700	117.5	118.0	118.6	117.9	118.2	118.9	118.1	118.8	119.4	118.4	119.3	119.9	118.7	119.5	120.1
	800	117.3	117.7	118.4	117.7	117.1	118.7	117.9	118.5	119.2	118.1	119.1	119.7	118.5	119.3	119.9
	900	117.0	117.4	118.1	117.3	116.8	118.4	117.6	118.3	118.8	117.9	118.8	119..3	118.3	119.0	119.7
	1000	116.6	117.1	117.7	117.0	116.5	118.1	117.4	118.0	118.5	117.6	118.6	119.1	118.0	118.8	119.4
539	100	117.1	117.6	118.2	117.5	117.9	118.5	117.9	118.4	119.0	118.3	118.7	119.1	118.8	119.2	119.6
	200	117.4	117.8	118.4	117.8	118.1	118.8	118.2	118.6	119.2	118.7	119.1	119.5	119.0	119.5	119.9
	300	117.8	118.2	118.8	118.0	118.4	119.0	118.4	118.9	119.4	118.9	119.3	119.9	119.2	119.9	120.1
	400	118.1	118.4	119.0	118.2	118.6	119.2	118.7	119.1	119.7	119.0	119.5	120.3	119.5	120.4	120.5
	500	118.3	118.6	119.3	118.6	118.8	119.5	118.8	119.5	119.9	119.2	119.7	120.7	119.7	120.8	120.9
	600	**118.6**	**119.0**	**119.6**	**118.9**	**119.2**	**119.8**	**119.1**	**119.8**	**120.2**	**119.6**	**119.9**	**121.1**	**119.9**	**121.2**	**121.4**
	700	118.4	118.8	119.3	118.7	119.0	119.5	118.9	119.5	120.0	119.3	119.7	120.8	119.7	120.9	121.1
	800	118.2	118.6	119.1	118.5	118.8	119.3	118.7	119.3	119.8	119.1	119.5	121.6	119.5	120.7	120.8
	900	117.9	118.3	118.9	118.2	118.5	119.1	118.4	119.0	119.5	118.8	119.2	120.3	119.3	120.4	120.6
	1000	117.6	118.1	118.6	118.0	118.3	118.9	118.2	118.8	119.3	118.6	119.0	120.0	119.0	120.2	120.4
588	100	117.8	118.3	118.7	118.0	118.4	119.0	118.3	118.8	119.4	118.8	119.1	119.5	119.2	119.6	120.0
	200	118.0	118.5	119.0	118.4	118.6	119.2	118.6	119.1	119.6	119.0	119.4	119.9	119.4	120.0	120.3
	300	118.4	118.7	119.2	118.7	118.9	119.5	118.9	119.3	119.9	119.3	119.7	120.3	119.6	120.3	120.7
	400	118.7	119.1	119.4	119.1	119.3	119.9	119.3	119.6	120.2	119.7	120.1	120.7	119.9	120.6	121.1
	500	118.9	119.3	119.7	119.3	119.5	120.3	119.5	120.0	120.5	119.8	120.4	121.1	120.2	120.8	121.4
	600	119.3	119.5	120.1	119.7	119.9	120.6	119.9	120.5	120.9	120.1	120.8	121.5	120.6	121.1	121.8
	700	**119.6**	**120.0**	**120.4**	**120.0**	**120.4**	**121.0**	**120.4**	**120.9**	**121.4**	**120.6**	**121.2**	**121.9**	**121.0**	**121.5**	**122.2**
	800	119.4	119.7	120.2	119.8	120.2	120.7	120.1	120.7	121.1	120.4	120.7	121.4	120.8	121.3	121.9
	900	119.1	119.4	120.0	119.4	119.9	120.4	119.9	120.4	120.8	120.1	120.3	121.0	120.6	121.0	121.5
	1000	118.9	119.2	119.7	119.1	119.6	120.1	119.6	120.2	120.5	119.8	120.0	120.8	120.3	120.8	121.1

Table 1(Cont….): A-weighted equivalent continuous sound level at operator's position for rocks at various air pressures and thrust (igneous rock) for integral drill bit.

Air pressure (kPa)	Thrust (N)	A-weighted equivalent continuous sound level (dB)														
		Dolerite			Soda granite			Black granite			Basalt			Gabbros		
		Drill bit diameter (mm)														
		30	34	40	30	34	40	30	34	40	30	34	40	30	34	40
392	100	117.5	118.1	118.5	118.2	118.3	118.8	118.6	118.8	119.5	118.8	119.4	119.8	119.0	119.6	120.1
	200	118.0	118.4	118.9	118.5	118.6	119.1	119.0	119.2	119.9	119.2	119.6	120.1	119.5	119.8	120.3
	300	118.5	118.9	119.3	119.0	119.2	119.4	119.3	119.6	120.3	119.4	119.8	120.4	119.8	120.2	120.6
	400	118.9	119.3	119.7	119.2	119.5	120.0	119.7	120.0	120.7	119.9	120.3	120.8	120.2	120.6	121.0
	500	**119.3**	**119.7**	**120.1**	**119.5**	**119.8**	**120.4**	**120.0**	**120.3**	**121.0**	**120.3**	**120.7**	**121.2**	**120.6**	**121.0**	**121.4**
	600	119.1	119.4	119.9	119.3	119.6	120.1	119.8	120.1	120.7	120.0	120.5	120.9	120.4	120.7	121.2
	700	118.8	119.1	119.7	119.1	119.3	119.9	119.5	119.8	120.5	119.8	120.3	120.7	120.2	120.5	121.0
	800	118.6	118.9	119.4	118.8	119.1	119.6	119.3	119.6	120.3	119.6	120.1	120.5	119.9	120.3	120.7
	900	118.3	118.6	119.2	118.5	118.8	119.4	119.1	119.3	120.1	119.3	119.9	120.3	119.6	120.1	120.5
	1000	118.1	118.4	119.0	118.3	118.6	119.2	118.8	119.1	119.9	119.0	119.6	120.1	119.4	119.8	120.3
441	100	117.8	118.3	118.7	118.5	118.8	119.2	118.7	119.0	119.7	119.0	119.6	120.0	119.3	119.8	120.3
	200	118.4	118.7	119.1	118.8	119.2	119.6	119.3	119.4	120.1	119.4	119.8	120.3	119.8	120.1	120.6
	300	118.7	119.1	119.5	119.2	119.6	119.9	119.5	119.8	120.5	119.7	120.2	120.7	120.0	120.5	121.0
	400	119.1	119.5	119.9	119.4	119.8	120.3	119.8	120.2	120.8	120.1	120.6	121.1	120.4	120.9	121.5
	500	**119.5**	**119.9**	**120.3**	**119.7**	**120.2**	**120.7**	**120.2**	**120.6**	**121.3**	**120.4**	**120.9**	**121.4**	**120.8**	**121.3**	**121.9**
	600	119.3	119.7	120.1	119.5	119.9	120.5	120.0	120.3	121.0	120.2	120.7	121.1	120.6	121.0	121.6
	700	119.0	119.4	119.9	119.2	119.7	120.4	119.7	120.1	120.7	120.0	120.5	120.9	120.4	120.8	121.4
	800	118.8	119.1	119.6	119.0	119.4	120.2	119.5	119.8	120.5	119.8	120.3	120.7	120.1	120.5	121.1
	900	118.5	118.9	119.4	118.7	119.2	119.9	119.3	119.5	120.3	119.5	120.1	120.5	119.9	120.3	120.9
	1000	118.3	118.6	119.2	118.5	119.0	119.7	119.0	119.3	120.1	119.2	119.9	120.3	119.6	120.1	120.6

490	100	118.7	119.1	119.4	119.1	119.5	119.6	119.3	119.8	120.3	119.6	120.0	120.6	119.8	120.3	120.8
	200	119.0	119.4	119.6	119.3	119.7	119.8	119.5	120.2	120.5	120.0	120.4	120.8	120.2	120.6	121.0
	300	119.2	119.7	120.1	119.5	119.9	120.3	119.8	120.4	120.8	120.1	120.6	121.1	120.5	120.9	121.3
	400	119.5	119.9	120.3	119.7	120.1	120.5	120.0	120.6	121.0	120.4	120.9	121.3	120.7	121.2	121.6
	500	119.7	120.2	120.6	119.9	120.4	120.8	120.3	120.8	121.3	120.6	121.0	121.5	120.9	121.6	121.8
	600	**119.9**	**120.6**	**121.0**	**120.2**	**120.8**	**121.3**	**120.6**	**121.1**	**121.5**	**120.9**	**121.4**	**121.8**	**121.1**	**121.8**	**122.0**
	700	119.6	120.4	120.7	120.0	120.6	121.0	120.4	120.8	121.2	120.6	121.1	121.6	120.8	121.6	121.8
	800	119.4	120.2	120.4	119.7	120.4	120.8	120.1	120.6	121.0	120.4	120.8	121.3	120.6	121.4	121.6
	900	119.1	119.8	120.1	119.5	120.1	120.5	119.9	120.3	120.7	120.2	120.6	121.0	120.4	121.1	121.4
	1000	118.9	119.6	119.9	119.1	119.8	120.2	119.7	120.0	120.4	120.0	120.3	120.8	120.2	120.8	121.0
539	100	119.0	119.4	119.8	119.3	119.8	120.2	119.6	120.0	120.5	120.0	120.3	120.8	120.2	120.6	121.0
	200	119.2	119.8	120.2	119.6	120.2	120.4	119.8	120.4	120.7	120.3	120.6	121.2	120.6	120.8	121.4
	300	119.6	120.2	120.5	119.9	120.4	120.7	120.1	120.7	120.9	120.5	120.9	121.4	120.8	121.1	121.6
	400	119.8	120.5	120.7	120.2	120.7	121.0	120.5	121.0	121.2	120.9	121.2	121.6	121.1	121.4	121.8
	500	120.1	120.8	121.1	120.4	121.0	121.4	120.8	121.2	121.6	121.1	121.4	121.8	121.3	121.6	122.0
	600	120.3	121.1	121.3	120.7	121.3	121.6	121.0	121.5	121.8	121.3	121.6	122.0	121.5	122.0	122.2
	700	**120.5**	**121.3**	**121.6**	**120.9**	**121.5**	**121.8**	**121.2**	**121.8**	**122.0**	**121.5**	**122.0**	**122.2**	**121.8**	**122.2**	**122.4**
	800	120.3	121.0	121.4	120.6	121.3	121.6	121.0	121.6	121.8	121.3	121.9	122.0	121.6	122.0	122.2
	900	120.1	120.9	121.2	120.3	121.1	121.4	120.8	121.3	121.6	121.0	121.6	121.8	121.4	121.8	122.0
	1000	119.8	120.7	121.0	120.0	120.9	121.2	120.4	121.1	121.4	120.6	121.2	121.6	121.1	121.5	121.8
588	100	119.4	119.8	120.2	119.6	120.2	120.6	120.0	120.4	120.9	120.4	120.8	121.2	120.7	121.0	121.4
	200	119.7	120.1	120.5	119.9	120.4	120.7	120.3	120.6	121.3	120.6	121.0	121.5	121.0	121.3	121.7
	300	119.9	120.4	120.7	120.2	120.7	121.1	120.5	120.9	121.5	120.9	121.2	122.8	121.2	121.5	122.0
	400	120.1	120.7	120.9	120.4	121.0	121.5	120.8	121.1	121.7	121.1	121.5	122.0	121.5	121.7	122.2
	500	120.5	121.0	121.2	120.7	121.3	121.8	121.1	121.4	122.0	121.4	121.8	122.3	121.8	122.0	122.5
	600	120.7	121.2	121.4	121.0	121.6	122.2	121.3	121.8	122.4	121.6	122.0	122.6	122.0	122.3	122.8.
	700	120.9	121.4	121.7	121.2	121.8	122.4	121.5	122.0	122.6	121.8	122.2	122.8	122.2	122.6	123.0
	800	**121.1**	**121.6**	**122.1**	**121.4**	**122.0**	**122.6**	**121.7**	**122.2**	**122.8**	**122.0**	**122.4**	**123.0**	**122.4**	**122.8**	**123.2**
	900	120.7	121.3	121.9	121.2	121.7	122.2	121.4	121.8	122.5	121.6	122.2	122.7	122.0	122.5	122.9
	1000	120.5	121.1	121.7	120.8	121.4	121.9	121.0	121.6	122.2	121.3	122.0	122.4	121.7	122.2	122.6

Table 2 A-weighted equivalent continuous sound level at exhaust for rocks at various air pressures and thrust (sedimentary rock) for integral drill bit.

Air pressure (kPa)	Thrust (N)	A-weighted equivalent continuous sound level (dB)														
		Shale			Dolomite			Sand stone			Lime stone			Hematite		
		Drill bit diameter in (mm)														
		30	34	40	30	34	40	30	34	40	30	34	40	30	34	40
392	100	116.5	117.0	117.6	116.8	117.2	117.8	117.1	117.5	118.2	118.0	118.2	118.6	118.4	118.8	119.0
	200	116.7	**117.3**	117.9	117.1	117.5	118.1	117.4	117.7	118.5	118.3	118.4	118.9	118.7	119.1	119.3
	300	116.9	117.6	118.1	117.3	117.7	118.4	117.7	118.0	118.7	118.5	118.7	119.2	119.0	119.4	119.5
	400	**117.2**	**117.8**	**118.3**	**117.6**	**118.1**	**118.6**	**117.9**	**118.3**	**119.0**	**118.8**	**119.0**	**119.4**	**119.2**	**119.7**	**119.9**
	500	117.0	117.5	118.1	117.4	117.8	118.3	117.7	118.0	118.8	118.6	118.8	119.1	119.0	119.4	119.7
	600	116.8	117.3	117.8	117.1	117.6	118.1	117.4	117.8	118.6	118.3	118.5	118.9	118.7	119.2	119.5
	700	116.5	117.0	117.6	116.9	117.4	117.8	117.2	117.6	118.3	118.1	118.3	118.6	118.5	118.9	119.2
	800	116.3	116.8	117.3	116.6	117.1	117.6	116.9	117.3	118.1	117.8	118.0	118.4	118.3	118.7	119.0
	900	116.1	116.5	117.1	116.4	116.9	117.3	116.7	117.1	117.9	117.6	117.8	118.1	118.1	118.5	118.7
	1000	115.9	116.3	116.8	116.1	116.6	117.1	116.5	116.8	117.6	117.4	117.6	117.9	117.8	118.3	118.5
441	100	117.0	117.3	117.9	117.3	117.8	118.4	118.0	118.5	119.1	118.6	118.9	119.4	118.7	119.1	119.6
	200	117.2	117.6	118.1	117.6	118.1	118.7	118.2	118.7	119.4	118.8	119.2	119.7	119.1	119.4	119.9
	300	117.6	117.8	118.4	118.0	118.3	119.0	118.6	119.1	119.7	119.2	119.5	120.1	119.4	119.8	120.3
	400	**117.8**	**118.2**	**118.7**	**118.3**	**118.6**	**119.4**	**118.9**	**119.4**	**119.9**	**119.4**	**119.8**	**120.4**	**119.8**	**120.2**	**120.6**
	500	117.5	118.0	118.5	118.0	118.4	119.2	118.7	119.2	119.6	119.1	119.6	120.2	119.5	120.0	120.3
	600	117.3	117.7	118.2	117.8	118.1	119.0	118.4	118.9	119.4	118.9	119.4	119.8	119.3	119.7	120.1
	700	117.0	117.5	118.0	117.6	117.9	118.8	118.2	118.7	119.1	118.6	119.1	119.7	119.0	119.5	119.8
	800	116.8	117.2	117.7	117.3	117.7	118.5	117.9	118.5	118.9	118.4	118.9	119.5	118.8	119.3	119.7
	900	116.5	116.9	117.5	117.1	117.4	118.1	117.7	118.2	118.6	118.1	118.6	119.2	118.5	119.0	119.4
	1000	116.3	116.7	117.3	116.9	117.0	117.9	117.4	117.9	118.4	117.8	118.4	119.0	118.3	118.8	119.2

490	100	118.0	118.3	119.0	118.4	118.9	119.4	118.7	119.4	119.0	119.2	119.6	120.3	119.4	120.0	120.3
	200	118.2	118.6	119.3	118.6	119.1	119.6	119.0	119.7	120.3	119.5	119.9	120.6	119.7	120.4	120.7
	300	118.5	119.0	119.5	118.9	119.3	120.0	119.2	120.0	120.5	119.7	120.1	120.8	119.9	120.7	121.0
	400	118.9	119.2	119.9	119.1	119.5	120.2	119.6	120.3	120.8	119.8	120.5	121.4	120.2	120.9	121.4
	500	**119.2**	**119.5**	**120.2**	**119.4**	**119.9**	**120.4**	**119.8**	**120.5**	**121.0**	**120.1**	**120.7**	**121.6**	**120.5**	**121.2**	**121.8**
	600	119.0	119.3	119.9	119.2	119.6	120.1	119.5	120.3	120.7	119.9	120.4	121.3	120.3	121.0	121.5
	700	118.7	119.0	119.7	118.9	119.4	119.9	119.3	120.0	120.5	119.7	120.2	121.1	120.1	120.7	121.3
	800	118.5	118.8	119.4	118.7	119.1	119.7	119.0	119.8	120.3	119.4	119.9	120.8	119.8	120.5	121.1
	900	118.2	118.5	119.2	118.4	118.9	119.4	118.8	119.6	120.0	119.1	119.6	120.6	119.6	120.2	120.8
	1000	117.9	118.3	118.9	118.2	118.6	119.2	118.6	119.3	119.8	118.9	119.4	120.3	119.4	120.0	120.5
539	100	118.3	118.7	119.0	118.7	119.2	119.7	119.1	119.5	120.3	119.6	120.7	120.5	119.8	120.4	120.8
	200	118.6	119.0	119.5	118.9	119.4	120.0	119.5	119.9	120.6	119.8	120.3	120.8	120.2	120.8	121.1
	300	119.0	119.3	119.8	119.2	119.7	120.2	119.7	120.2	120.8	120.0	120.5	121.2	120.4	121.0	121.4
	400	119.3	119.5	120.2	119.6	119.9	120.4	119.9	120.5	121.1	120.2	120.7	121.5	120.7	121.3	121.7
	500	119.7	119.8	120.5	119.9	120.1	120.7	120.1	120.7	121.3	120.4	120.9	121.9	120.9	121.6	122.0
	600	**119.9**	**120.2**	**120.7**	**120.1**	**120.5**	**120.9**	**120.3**	**121.0**	**121.6**	**120.7**	**121.2**	**122.1**	**121.1**	**121.8**	**122.2**
	700	119.6	120.0	120.6	119.8	120.2	120.7	120.0	120.8	121.4	120.4	121.0	121.8	120.8	121.5	122.0
	800	119.4	119.7	120.3	119.6	120.0	120.5	119.8	120.6	121.1	120.1	120.7	121.6	120.6	121.3	121.7
	900	119.2	119.5	120.1	119.4	119.7	120.2	119.6	120.3	120.9	119.9	120.5	121.3	120.3	121.0	121.5
	1000	118.9	119.2	119.8	119.1	119.5	119.8	119.3	120.1	120.6	119.7	120.3	121.0	120.1	120.8	121.2
588	100	118.6	119.0	119.5	119.1	119.6	120.1	119.4	120.2	120.7	119.8	120.4	120.8	120.3	120.7	121.1
	200	119.1	119.2	119.8	119.5	119.9	120.3	119.7	120.4	120.9	120.1	120.6	121.0	120.5	121.0	121.5
	300	119.4	119.6	120.3	119.8	120.1	120.7	119.9	120.6	121.2	120.4	120.8	121.4	120.8	121.4	121.8
	400	119.7	119.9	120.6	120.2	120.4	121.0	120.3	120.9	121.4	120.8	121.3	121.7	121.2	121.7	122.1
	500	120.1	120.3	121.0	120.4	120.7	121.4	120.6	121.1	121.7	121.0	121.6	122.0	121.4	121.9	122.5
	600	120.5	120.9	121.3	120.7	121.0	121.7	120.9	121.5	122.0	121.2	121.8	122.2	121.7	122.2	122.8
	700	**120.8**	**121.2**	**121.6**	**121.1**	**121.5**	**122.0**	**121.3**	**121.7**	**122.3**	**121.5**	**122.0**	**122.6**	**122.0**	**122.5**	**123.0**
	800	120.6	120.9	121.4	120.8	121.2	121.8	121.0	121.4	122.1	121.3	121.7	122.4	121.7	122.3	122.7
	900	120.3	120.7	121.1	120.6	121.0	121.5	120.8	121.2	121.8	121.0	121.5	122.1	121.4	122.0	122.5
	1000	120.0	120.4	120.8	120.3	120.7	121.3	120.5	120.9	121.5	120.7	121.2	121.8	121.2	121.7	122.2

Table 2 (Cont….): A-weighted equivalent continuous sound level at exhaust for rocks at various air pressures and thrust (igneous rock) for integral drill bit.

Air pressure (kPa)	Thrust (N)	A-weighted equivalent continuous sound level (dB)														
		Dolerite			Soda granite			Black granite			Basalt			Gabbros		
		Drill bit diameter (mm)														
		30	34	40	30	34	40	30	34	40	30	34	40	30	34	40
392	100	118.4	118.6	119.0	119.0	119.3	119.5	119.4	119.7	120.2	119.6	120.0	120.5	120.1	120.5	120.9
	200	118.7	119.0	119.3	119.4	119.5	119.8	119.8	120.1	120.4	120.0	120.3	120.7	120.4	120.9	121.3
	300	118.9	119.3	119.6	119.7	119.8	120.0	120.1	120.3	120.7	120.4	120.6	121.0	120.8	121.2	121.6
	400	119.2	119.5	120.0	120.1	120.2	120.3	120.3	120.7	120.9	120.6	121.0	121.4	121.1	121.5	121.8
	500	**119.5**	**119.8**	**120.3**	**120.4**	**120.5**	**120.7**	**120.7**	**121.0**	**121.3**	**121.0**	**121.3**	**121.7**	**121.3**	**121.7**	**122.1**
	600	119.3	119.6	120.0	120.2	120.3	120.4	120.5	120.8	121.0	120.8	121.1	121.4	121.0	121.4	121.8
	700	119.0	119.4	119.8	120.0	120.0	120.2	120.2	120.5	120.8	120.5	120.8	121.2	120.8	121.2	121.6
	800	118.8	119.1	119.6	119.7	119.8	120.0	120.0	120.3	120.6	120.3	120.6	121.0	120.6	120.9	121.4
	900	118.6	118.8	119.3	119.4	119.6	119.7	119.7	120.1	120.3	120.0	120.3	120.7	120.3	120.4	121.1
	1000	118.4	118.6	119.1	119.2	119.3	119.5	119.4	119.8	120.1	119.7	120.1	120.4	120.0	120.2	120.9
441	100	118.9	119.4	119.8	119.5	119.7	120.2	119.7	120.0	120.7	120.1	120.5	121.0	120.4	120.8	121.2
	200	119.3	119.7	120.2	119.7	120.1	120.5	120.1	120.3	121.1	120.4	120.8	121.3	120.8	121.2	121.5
	300	119.6	120.1	120.4	120.0	120.4	120.8	120.4	120.7	121.3	120.7	121.1	121.6	121.0	121.5	121.9
	400	120.0	120.3	120.7	120.4	120.6	121.3	120.6	121.0	121.6	121.1	121.5	121.8	121.4	121.9	122.1
	500	**120.3**	**120.7**	**120.9**	**120.7**	**121.0**	**121.5**	**121.0**	**121.4**	**121.9**	**121.4**	**121.8**	**122.3**	**121.7**	**122.1**	**122.5**
	600	120.0	120.5	120.6	120.5	120.7	121.3	120.7	121.2	121.6	121.2	121.6	122.0	121.5	121.8	122.3
	700	119.8	120.2	120.4	120.3	120.4	121.1	120.5	121.0	121.4	120.9	121.3	121.8	121.2	121.6	122.0
	800	119.6	120.0	120.2	120.0	120.2	120.8	120.3	120.7	121.1	120.7	121.0	121.5	120.9	121.3	121.7
	900	119.3	119.7	119.8	119.7	119.9	120.6	120.1	120.5	120.9	120.4	120.8	121.3	120.7	121.1	121.5
	1000	119.1	119.4	119.6	119.4	119.7	120.3	119.9	120.2	120.6	120.2	120.5	121.0	120.4	120.7	121.2

	100	119.9	120.3	120.7	120.2	120.4	120.8	120.5	121.0	121.4	120.7	121.2	121.6	121.0	121.4	121.8
	200	120.2	120.5	121.1	120.4	120.6	121.1	120.7	121.3	121.7	121.2	121.6	121.9	121.4	121.8	122.1
	300	120.4	120.8	121.3	120.6	121.0	121.4	121.0	121.7	121.9	121.4	121.9	122.2	121.7	122.1	122.3
	400	120.6	121.2	121.5	120.9	121.3	121.8	121.2	122.0	122.2	121.6	122.1	122.4	121.9	122.4	122.6
490	500	120.9	121.5	121.9	121.1	121.7	122.1	121.5	122.2	122.4	121.8	122.2	122.6	122.2	122.6	122.8
	600	**121.1**	**121.7**	**122.2**	**121.4**	**122.1**	**122.4**	**121.8**	**122.4**	**122.6**	**122.1**	**122.6**	**122.8**	**122.5**	**122.8**	**123.0**
	700	120.8	121.4	122.0	121.0	121.8	122.2	121.6	122.1	122.3	121.9	122.3	122.6	122.2	122.5	122.8
	800	120.6	121.2	121.7	120.8	121.6	121.9	121.3	122.0	122.1	121.7	122.0	122.4	122.0	122.3	122.5
	900	120.3	120.9	121.5	120.5	121.3	121.7	121.0	121.7	121.9	121.5	121.8	122.2	121.7	122.0	122.2
	1000	120.1	120.7	121.2	120.2	121.1	121.4	120.8	121.4	121.6	121.2	121.6	121.9	121.4	121.8	122.0
	100	120.2	120.5	121.0	120.5	121.0	121.4	120.8	121.2	121.7	121.2	121.6	122.0	121.4	121.8	122.3
	200	120.5	120.8	121.3	120.8	121.2	121.7	121.0	121.5	121.9	121.5	121.9	122.3	121.6	122.0	122.5
	300	120.8	121.2	121.7	121.0	121.5	121.9	121.4	121.7	122.2	121.7	122.1	122.5	121.9	122.3	122.7
	400	121.0	121.5	122.0	121.3	121.7	122.3	121.7	122.0	122.5	122.0	122.4	122.8	122.2	122.6	123.0
539	500	121.2	121.8	122.2	121.5	122.0	122.5	122.0	122.2	122.8	122.2	122.7	123.0	122.4	122.9	123.2
	600	121.4	122.2	122.5	121.8	122.4	122.7	122.2	122.5	123.0	122.5	122.9	123.2	122.7	123.2	123.4
	700	**121.7**	**122.5**	**122.7**	**122.1**	**122.7**	**122.9**	**122.5**	**122.8**	**123.2**	**122.7**	**123.1**	**123.4**	**123.0**	**123.4**	**123.6**
	800	121.5	122.2	122.4	121.9	122.5	122.7	122.1	122.6	122.9	122.5	122.8	123.1	122.8	123.1	123.3
	900	121.2	121.9	122.2	121.7	122.2	122.5	121.9	122.4	122.7	122.2	122.6	122.9	122.5	122.9	123.1
	1000	120.8	121.7	121.9	121.4	121.9	122.2	121.6	122.1	122.4	122.0	122.4	122.7	122.3	122.7	122.9
	100	120.7	121.1	121.5	121.0	121.4	121.8	121.3	121.7	122.2	121.7	122.2	122.7	122.1	122.5	122.9
	200	121.0	121.3	121.7	121.3	121.7	122.1	121.6	121.9	122.5	121.9	122.4	122.9	122.3	122.7	123.1
	300	121.2	121.6	122.0	121.5	121.9	122.4	121.8	122.1	122.7	122.2	122.7	123.1	122.5	123.0	123.3
	400	121.5	122.0	122.3	121.7	122.2	122.6	122.1	122.4	123.0	122.5	122.9	123.3	123.7	123.2	123.5
588	500	121.8	122.3	122.5	122.0	122.4	122.8	122.3	122.6	123.2	122.7	123.1	123.6	123.9	123.4	123.7
	600	122.1	122.6	122.7	122.2	122.6	123.0	122.5	122.8	123.4	122.9	123.3	123.7	123.1	123.6	123.8
	700	122.5	122.8	123.0	122.4	122.8	123.2	122.7	123.0	123.6	123.1	123.5	123.8	123.3	123.7	123.9
	800	**122.7**	**122.9**	**123.2**	**122.5**	**123.0**	**123.1**	**122.9**	**123..2**	**123.7**	**123.2**	**123.6**	**123.9**	**123.4**	**123.8**	**124.0**
	900	122.4	122.7	122.9	122.3	122.7	122.9	122.6	123.0	123.5	122.9	123.4	123.7	123.1	123.6	123.8
	1000	122.1	122.4	122.7	122.0	122.5	122.6	122.3	122.7	122.2	122.6	123.1	123.5	122.8	123.4	123.6

Table 3 A-weighted equivalent continuous sound level near drill bit for rocks at various air pressures and thrust (sedimentary rock) for integral drill bit.

Air pressure (kPa)	Thrust (N)	A-weighted equivalent continuous sound level (dB)														
		Shale			Dolomite			Sand stone			Lime stone			Hematite		
		Drill bit diameter in (mm)														
		30	34	40	30	34	40	30	34	40	30	34	40	30	34	40
392	100	117.4	117.8	118.3	117.5	118.0	118.6	118.2	118.6	119.1	118.5	119.1	119.5	119.1	119.5	119.9
	200	117.6	118.0	118.6	118.1	118.2	118.8	118.6	119.0	119.4	118.9	119.4	119.9	119.4	119.9	120.3
	300	118.2	118.3	118.9	118.4	118.6	119.0	119.1	119.5	119.8	119.3	119.8	120.2	119.6	120.3	120.6
	400	**118.5**	**118.7**	**119.1**	**118.8**	**119.1**	**119.4**	**119.3**	**119.8**	**120.2**	**119.6**	**120.2**	**120.6**	**120.1**	**120.7**	**121.0**
	500	118.3	118.4	118.8	118.6	118.8	119.2	119.0	119.6	119.9	119.4	119.9	120.4	119.8	120.5	120.8
	600	118.1	118.2	118.6	118.4	118.6	119.0	118.8	119.4	119.7	119.1	119.7	120.3	119.6	120.3	120.5
	700	117.8	118.0	118.4	118.1	118.3	118.7	118.6	119.1	119.5	118.9	119.4	120.1	119.3	120.0	120.3
	800	117.6	117.7	118.1	117.9	118.1	118.5	118.4	118.8	119.3	118.7	119.1	119.8	119.1	119.8	120.1
	900	117.3	117.5	117.9	117.7	117.9	118.3	118.1	118.6	119.0	118.4	118.9	119.7	118.9	119.7	119.8
	1000	117.1	117.3	117.5	117.1	117.7	118.1	117.8	118.3	118.8	118.1	118.7	119.5	118.6	119.4	119.6
441	100	117.7	118.2	118.8	118.0	118.5	119.0	118.4	118.8	119.3	119.0	119.4	119.8	119.3	119.9	120.4
	200	118.1	118.5	119.0	118.4	118.7	119.2	118.7	119.1	119.7	119.4	119.8	120.2	119.7	120.2	120.7
	300	118.4	118.9	119.2	118.7	119.0	119.5	119.1	119.5	120.0	119.7	120.1	120.5	120.0	120.6	121.1
	400	**118.8**	**119.1**	**119.5**	**119.0**	**119.3**	**119.8**	**119.3**	**119.7**	**120.4**	**120.1**	**120.4**	**120.8**	**120.3**	**121.0**	**121.4**
	500	118.5	118.9	119.3	118.8	119.1	119.6	119.0	119.4	120.2	119.8	120.2	120.6	120.0	120.8	121.2
	600	118.3	118.7	119.0	118.5	118.9	119.3	118.8	119.2	120.0	119.6	119.9	120.4	119.8	120.6	121.0
	700	118.1	118.4	118.8	118.3	118.6	119.1	118.6	118.9	119.7	119.3	119.7	120.2	119.6	120.4	120.7
	800	117.8	118.1	118.6	118.1	118.4	118.9	118.3	118.7	118.5	119.1	119.4	119.9	119.4	120.1	120.4
	900	117.6	117.9	118.3	117.8	118.2	118.6	118.1	118.4	118.3	118.9	119.2	119.7	119.1	119.9	120.1
	1000	117.4	117.6	118.1	117.6	117.9	118.3	117.8	118.2	118.0	118.7	119.0	119.4	118.8	119.6	119.9

	100	118.5	118.7	119.5	119.0	119.4	120.2	119.4	119.8	120.3	119.6	120.0	120.4	119.9	120.3	120.7
	200	118.9	119.2	119.6	119.4	119.7	120.4	119.7	120.1	120.6	120.0	120.5	120.8	120.2	120.7	121.0
	300	119.2	119.5	119.8	119.7	120.1	120.6	119.9	120.4	120.9	120.4	120.9	121.1	120.6	121.2	121.4
	400	119.6	119.9	120.0	119.9	120.3	121.0	120.2	120.7	121.1	120.7	121.2	121.5	120.9	121.4	121.7
490	**500**	**119.8**	**120.2**	**120.4**	**120.3**	**120.7**	**121.3**	**120.6**	**121.1**	**121.5**	**121.1**	**121.5**	**121.8**	**121.3**	**121.7**	**122.0**
	600	119.5	120.0	120.1	120.1	120.4	121.1	120.4	120.8	121.3	120.9	121.3	121.5	121.1	121.5	121.7
	700	119.3	119.8	119.9	119.8	120.2	120.9	120.3	120.6	121.1	120.7	121.1	121.3	120.8	121.3	121.5
	800	119.1	119.5	119.7	119.6	120.0	120.7	120.1	120.4	120.9	120.4	120.8	121.1	120.5	121.0	121.2
	900	118.8	119.3	119.4	119.4	119.7	120.4	119.9	120.1	120.7	120.2	120.6	120.9	120.3	120.8	121.0
	1000	118.6	119.1	119.2	119.2	119.5	120.3	119.7	119.9	120.6	119.9	120.4	120.6	120.1	120.6	120.8
	100	119.0	119.5	120.1	119.4	119.8	120.3	119.8	120.3	120.6	120.1	120.5	120.9	120.5	120.9	121.3
	200	119.2	119.8	120.3	119.7	120.0	120.6	120.2	120.6	121.2	120.5	120.9	121.3	120.8	121.3	121.5
	300	119.5	120.1	120.5	120.1	120.2	120.9	120.5	120.9	121.4	120.8	121.2	121.6	121.1	121.5	121.7
	400	119.8	120.3	120.7	120.3	120.5	121.2	120.8	121.1	121.7	121.2	121.6	121.8	121.5	121.8	122.0
539	500	120.2	120.5	120.9	120.5	120.8	121.5	121.0	121.3	121.9	121.4	121.8	122.1	121.8	122.1	122.3
	600	**120.5**	**120.9**	**121.2**	**120.8**	**121.2**	**121.8**	**121.2**	**121.5**	**122.1**	**121.7**	**122.0**	**122.4**	**122.0**	**122.3**	**122.6**
	700	120.3	120.6	120.9	120.6	120.9	121.6	120.9	121.3	121.8	121.5	121.7	122.2	121.7	122.1	122.4
	800	120.1	120.4	120.7	120.4	120.7	121.4	120.7	121.0	121.5	121.3	121.5	122.0	121.5	121.9	122.2
	900	119.8	120.2	120.4	120.2	120.5	121.2	120.5	120.8	121.3	121.0	121.3	121.7	121.3	121.6	121.9
	1000	119.6	119.9	120.2	119.9	120.2	121.0	120.2	120.6	121.0	120.8	121.0	121.5	121.0	121.3	121.7
	100	119.3	119.8	120.4	119.6	120.0	120.6	120.1	120.6	121.1	120.5	120.9	121.3	120.8	121.2	121.7
	200	119.7	120.1	120.7	119.9	120.3	120.8	120.4	120.8	121.4	120.7	121.3	121.7	121.0	121.6	122.0
	300	120.0	120.4	121.1	120.2	120.5	121.0	120.6	121.1	121.6	121.1	121.5	122.0	121.3	121.8	122.2
	400	120.2	120.8	121.3	120.4	120.8	121.4	120.9	121.4	121.8	121.4	121.8	122.2	121.7	122.1	122.5
588	500	120.6	121.1	121.5	120.7	121.2	121.7	121.2	121.6	122.2	121.6	122.0	122.4	122.0	122.4	122.7
	600	120.9	121.4	121.8	121.1	121.6	122.0	121.4	121.9	122.4	121.9	122.2	122.7	122.2	122.6	123.0
	700	**121.2**	**121.7**	**122.2**	**121.4**	**121.9**	**122.4**	**121.7**	**122.2**	**122.7**	**122.1**	**122.4**	**122.9**	**122.5**	**122.9**	**123.2**
	800	121.0	121.4	121.9	121.2	121.7	122.1	121.5	121.9	122.5	121.8	122.2	122.6	122.3	122.7	122.9
	900	120.8	121.2	121.7	121.0	121.4	121.9	121.3	121.6	122.2	121.6	122.0	122.4	122.1	122.4	122.7
	1000	120.5	121.0	121.4	120.8	121.2	121.7	121.0	121.4	122.0	121.4	121.7	122.2	121.8	122.2	122.4

Table 3(Cont….): A-weighted equivalent continuous sound level near drill bit for rocks of at various air pressures and thrust (igneous rock) for integral drill bit.

Air pressure (kPa)	Thrust (N)	A-weighted equivalent continuous sound level (dB)														
		Dolerite			Soda granite			Black granite			Basalt			Gabbros		
		Drill bit diameter in (mm)														
		30	34	40	30	34	40	30	34	40	30	34	40	30	34	40
392	100	119.3	119.7	120.1	119.6	120.0	120.5	120.0	120.4	120.9	120.2	120.7	121.1	120.5	120.9	121.3
	200	119.7	120.1	120.5	119.9	120.2	120.7	120.4	120.6	121.2	120.5	121.1	121.4	120.7	121.3	121.5
	300	120.0	120.3	120.8	120.2	120.6	121.1	120.7	121.0	121.6	120.9	121.4	121.7	121.1	121.5	121.8
	400	120.3	120.6	121.1	120.4	121.0	121.4	121.1	121.3	121.9	121.3	121.6	122.1	121.4	121.8	122.2
	500	**120.5**	**121.0**	**121.3**	**120.8**	**121.3**	**121.6**	**121.4**	**121.6**	**122.1**	**121.6**	**121.9**	**122.2**	**121.7**	**122.1**	**122.4**
	600	120.2	120.7	121.0	120.6	121.1	121.3	121.2	121.2	121.8	121.4	121.6	122.0	121.5	121.9	122.1
	700	120.0	120.5	120.8	120.4	120.8	121.1	121.0	121.0	121.6	121.1	121.4	121.8	121.2	121.6	121.9
	800	119.7	120.3	120.6	120.1	120.6	120.9	120.7	120.8	121.4	120.9	121.1	121.5	121.0	121.4	121.7
	900	119.5	120.0	120.4	119.9	120.4	120.7	120.5	120.6	121.2	120.7	120.9	121.3	120.8	121.2	121.5
	1000	119.2	119.8	120.1	119.7	121.0	120.4	120.3	120.5	121.0	120.5	120.8	121.0	120.6	121.0	121.2
441	100	119.7	120.1	120.5	120.0	120.6	120.8	120.2	120.8	121.1	120.4	121.0	121.4	120.8	121.2	121.6
	200	120.1	120.4	120.9	120.3	120.8	121.2	120.5	121.1	121.4	120.7	121.3	121.6	121.1	121.5	122.0
	300	120.4	120.8	121.2	120.7	121.2	121.5	120.8	121.5	121.7	121.0	121.7	121.9	121.3	121.9	122.2
	400	120.6	121.1	121.5	120.9	121.4	121.7	121.0	121.7	122.0	121.2	122.0	122.2	121.5	122.2	122.5
	500	**120.9**	**121.3**	**121.8**	**121.2**	**121.7**	**122.0**	**121.4**	**122.0**	**122.2**	**121.6**	**122.2**	**122.5**	**121.8**	**122.4**	**122.7**
	600	120.7	121.0	121.6	121.0	121.4	121.8	121.2	121.7	122.0	121.3	121.9	122.3	121.6	121.1	122.4
	700	120.5	120.8	121.4	120.7	121.2	121.5	120.9	121.5	121.8	121.1	121.7	122.1	121.4	120.9	122.2
	800	120.2	120.6	121.1	120.5	121.0	121.3	120.7	121.3	121.6	120.9	121.5	121.8	121.1	120.7	122.0
	900	120.0	120.3	120.9	120.3	120.7	121.1	120.4	121.0	121.3	120.6	121.4	121.6	120.9	120.4	121.7
	1000	119.8	120.1	120.7	120.0	120.5	120.8	120.2	120.8	121.1	120.4	121.2	121.4	120.7	120.2	121.5

490	100	120.3	120.7	121.1	120.8	121.3	121.5	121.1	121.6	121.8	121.3	121.8	122.2	121.5	122.1	122.4
	200	120.6	121.1	121.3	121.1	121.5	121.8	121.3	121.8	122.1	121.6	122.0	122.4	121.8	122.3	122.6
	300	121.0	121.3	121.5	121.3	121.8	122.0	121.5	122.0	122.4	122.0	122.4	122.7	122.1	122.6	122.8
	400	121.3	121.6	121.8	121.6	122.0	122.3	122.8	122.3	122.6	122.2	122.6	122.9	122.4	122.9	123.0
	500	121.6	121.8	122.0	121.8	122.2	122.5	122.0	122.6	122.8	122.5	122.9	123.1	123.7	123.1	123.2
	600	**121.9**	**122.1**	**122.3**	**122.1**	**122.4**	**122.6**	**122.4**	**122.8**	**123.0**	**122.6**	**123.1**	**123.2**	**122.9**	**123.3**	**123.4**
	700	121.7	121.8	122.2	121.9	122.1	122.3	121.1	122.6	122.7	122.4	122.8	123.1	122.6	123.1	123.2
	800	121.4	121.6	122.0	121.6	121.9	122.1	121.9	122.4	122.5	122.2	122.6	122.9	122.4	122.9	122.9
	900	121.2	121.4	121.7	121.4	121.7	121.9	121.7	122.1	122.2	121.9	122.4	122.6	122.1	122.6	122.7
	1000	121.0	121.2	121.5	121.1	121.4	121.7	121.5	121.9	122.0	121.7	122.1	122.4	121.9	122.2	122.4
539	100	120.7	121.1	121.5	121.1	121.5	121.9	121.3	121.8	122.2	121.6	122.1	122.5	122.0	122.4	122.8
	200	121.0	121.3	121.7	121.3	121.8	122.1	121.6	122.1	122.5	121.8	122.4	122.8	122.3	122.7	123.1
	300	121.2	121.6	122.0	121.6	122.0	122.4	121.8	122.5	122.7	122.0	122.6	123.0	122.5	123.1	123.4
	400	121.5	121.9	122.2	121.8	122.3	122.6	122.1	122.7	123.0	122.3	122.9	123.3	122.7	123.4	123.6
	500	121.7	122.2	122.4	122.1	122.6	122.8	122.4	123.0	123.2	122.6	123.3	123.5	123.0	123.6	123.8
	600	122.1	122.5	122.7	122.4	122.8	123.0	122.7	123.2	123.4	122.9	123.5	123.7	123.2	124.8	123.9
	700	**122.3**	**122.7**	**123.0**	**122.6**	**123.0**	**123.3**	**122.9**	**123.4**	**123.6**	**123.1**	**123.7**	**123.9**	**123.4**	**124.0**	**124.1**
	800	122.0	122.5	122.8	122.3	122.7	123.1	122.6	123.2	123.3	122.8	123.4	123.7	123.1	123.7	123.8
	900	121.8	122.2	122.5	122.1	122.5	122.8	122.4	123.0	123.1	122.6	123.2	123.4	122.9	123.5	123.6
	1000	121.6	122.0	122.3	121.8	122.2	122.6	122.1	122.7	122.9	122.4	122.9	123.2	122.7	123.2	123.3
588	100	121.0	121.2	121.7	121.4	121.8	122.2	121.7	122.2	122.7	122.0	122.5	123.0	122.5	122.9	123.2
	200	121.3	121.5	121.9	121.7	122.2	122.5	122.0	122.4	122.9	122.5	122.8	123.2	122.8	123.1	123.4
	300	121.5	121.8	122.3	122.0	122.4	122.8	122.3	122.7	123.1	122.8	123.0	123.4	123.1	123.3	123.6
	400	121.7	122.1	122.5	122.2	122.7	123.2	122.5	123.0	123.4	123.2	123.2	123.6	123.5	123.4	123.8
	500	122.1	122.4	122.7	122.3	123.0	123.5	122.8	123.2	123.6	123.4	123.5	123.8	123.7	123.6	124.0
	600	122.3	122.7	123.0	122.5	123.2	123.7	123.0	123.4	123.8	123.6	123.7	124.0	123.9	124.8	124.2
	700	122.6	123.0	123.3	122.8	123.4	123.8	123.2	123.6	123.9	123.8	123.9	124.2	124.0	124.0	124.3
	800	**122.8**	**123.2**	**123.5**	**123.0**	**123.5**	**123.9**	**123.3**	**123.7**	**124.0**	**123.9**	**124.1**	**124.4**	**124.2**	**124.3**	**124.5**
	900	122.5	122.7	123.2	122.7	123.3	123.7	123.0	123.5	123.8	123.7	123.8	124.1	123.9	123.7	124.2
	1000	122.3	122.5	123.0	122.4	123.0	123.4	122.8	123.2	123.5	123.4	123.5	123.8	123.5	123.6	124.0

Table 4 A-weighted equivalent continuous sound level near drill rod for rocks at various thrust and air pressures (sedimentary rock) for integral drill bit.

Air pressure (kPa)	Thrust (N)	A-weighted equivalent continuous sound level (dB)														
		Shale			Dolomite			Sand stone			Lime stone			Hematite		
		Drill bit diameter in (mm)														
		30	34	40	30	34	40	30	34	40	30	34	40	30	34	40
392	100	117.6	118.2	118.7	117.7	118.3	118.9	118.5	119.0	119.6	118.9	119.3	119.8	119.3	119.6	120.0
	200	118.0	118.3	118.9	118.2	118.5	119.2	118.7	119.2	119.8	119.5	119.8	120.1	120.0	120.2	120.3
	300	118.3	118.7	119.3	118.6	118.9	119.4	118.9	119.5	120.1	119.9	120.3	120.5	120.2	120.4	120.7
	400	**118.6**	**119.0**	**119.5**	**118.9**	**119.2**	**119.7**	**119.3**	**119.7**	**120.4**	**120.2**	**120.6**	**120.8**	**120.5**	**120.7**	**121.0**
	500	118.4	118.8	119.3	118.7	119.0	119.5	119.0	119.4	120.2	119.8	120.4	120.6	120.3	120.5	120..8
	600	118.2	118.5	119.1	118.4	118.8	119.3	118.8	119.2	120.0	119.6	120.2	120.4	120.1	120.3	120.6
	700	117.9	118.3	118.8	118.2	118.5	119.0	118.6	119.0	119.7	119.3	120.0	120.1	119.9	120.1	120.3
	800	117.7	118.1	118.6	117.9	118.2	118.8	118.4	118.7	119.5	119.1	119.7	119.8	119.6	119.9	120.1
	900	117.5	117.9	118.4	117.7	118.0	118.6	118.1	118.5	119.3	118.9	119.5	119.6	119.4	119.6	119.8
	1000	117.2	117.7	118.1	117.5	117.8	118.3	117.9	118.4	119.0	118.7	119.3	119.4	119.1	119.4	119.6
441	100	118.3	118.7	119.2	118.5	118.8	119.4	118.7	119.2	119.7	119.3	119.7	120.1	119.5	120.0	120.6
	200	118.5	118.9	119.5	118.8	119.0	119.6	119.1	119.6	119.9	119.6	120.1	120.4	119.7	120.4	120.9
	300	119.9	119.2	119.8	119.3	119.5	119.8	119.5	119.9	120.2	120.0	120.4	120.8	120.0	120.7	121.1
	400	**119.2**	**119.6**	**120.0**	**119.6**	**119.8**	**120.2**	**119.8**	**120.2**	**120.6**	**120.2**	**120.6**	**121.1**	**120.4**	**121.0**	**121.5**
	500	119.0	119.3	119.7	119.4	119.6	119.9	119.6	120.0	120.3	120.0	120.3	120.9	120.2	120.8	121.3
	600	118.8	119.1	119.5	119.2	119.4	119.7	119.4	119.8	120.1	119.7	120.1	120.7	120.0	120.6	121.2
	700	118.6	118.8	119.2	118.9	119.1	119.4	119.1	119.6	119.8	119.5	119.8	120.5	119.7	120.4	120.9
	800	118.3	118.6	118.9	118.7	118.8	119.2	118.9	119.3	119.5	119.3	119.6	120.2	119.5	120.1	120.7
	900	118.1	118.3	118.7	118.4	118.6	118.9	118.6	119.0	119.3	119.0	119.4	120.0	119.2	119.8	120.5
	1000	117.9	118.1	118.4	118.1	118.3	118.6	118.3	118.8	119.1	118.8	119.1	119.7	118.9	119.5	120.2

490	100	119.1	119.5	120.0	119.3	119.7	120.4	119.5	120.2	120.7	119.7	120.3	120.8	120.5	120.9	121.3
	200	119.3	119.8	120.2	119.5	120.0	120.6	119.8	120.4	120.9	120.1	120.9	121.2	120.8	121.3	121.7
	300	119.5	120.0	120.4	119.8	120.3	120.9	120.2	120.7	121.2	120.4	121.1	121.5	121.0	121.7	122.1
	400	119.8	120.4	120.7	120.0	120.5	121.1	120.5	121.1	121.5	120.7	121.5	121.7	121.4	122.0	122.3
	500	**120.0**	**120.7**	**121.0**	**120.2**	**120.8**	**121.4**	**120.8**	**121.4**	**121.9**	**121.1**	**121.7**	**122.1**	**121.7**	**122.3**	**122.5**
	600	119.7	120.5	120.8	119.9	120.6	121.1	120.6	121.2	121.6	120.8	121.5	121.8	121.5	122.0	122.3
	700	119.5	120.3	120.5	110.7	120.4	120.9	120.4	121.0	121.3	120.6	121.3	121.6	121.3	121.8	122.1
	800	119.3	120.0	120.3	119.5	120.2	120.7	120.1	120.8	121.1	120.4	121.0	121.4	121.0	121.6	120.8
	900	119.0	119.8	120.1	119.2	120.0	120.4	119.9	120.5	120.9	120.1	120.8	121.1	120.8	121.4	120.6
	1000	118.7	119.5	110.8	118.9	119.7	120.1	119.7	120.3	120.6	119.9	120.5	120.9	120.5	121.1	120.4
539	100	119.3	119.9	120.2	119.7	120.2	120.7	120.1	120.5	121.0	120.5	120.9	121.3	120.8	121.2	121.6
	200	119.5	120.0	120.4	119.9	120.4	121.0	120.4	120.7	121.2	120.7	121.1	121.7	121.1	121.5	121.9
	300	119.7	120.2	120.8	120.2	120.6	121.2	120.7	121.0	121.4	121.0	121.4	122.0	121.4	121.7	122.1
	400	120.2	120.4	121.0	120.6	120.8	121.4	120.9	121.4	121.6	121.2	121.6	122.2	121.6	122.0	122.4
	500	120.5	120.7	121.4	120.8	121.1	121.6	121.2	121.6	121.9	121.4	121.9	122.5	121.9	122.4	122.7
	600	**120.8**	**121.1**	**121.7**	**121.0**	**121.4**	**121.9**	**121.4**	**122.0**	**122.3**	**121.7**	**122.3**	**122.8**	**122.1**	**122.7**	**123.1**
	700	120.6	120.8	120.5	120.7	121.2	121.7	121.1	121.8	122.0	121.5	122.0	122.6	121.8	122.5	122.8
	800	120.4	120.6	120.2	120.5	121.0	121.4	120.9	121.6	121.7	121.3	121.8	122.4	121.5	122.3	122.6
	900	120.1	120.4	120.0	120.3	120.8	121.3	120.7	121.3	121.5	121.0	121.5	122.1	121.3	122.0	122.3
	1000	119.8	120.2	119.8	120.0	120.4	121.0	120.4	121.0	121.2	120.7	121.3	121.8	121.1	121.7	122.0
588	100	119.8	120.2	120.7	120.0	120.5	121.0	120.4	120.8	121.4	120.9	121.2	121.8	121.3	121.7	122.1
	200	120.1	120.4	120.9	120.4	120.7	121.3	120.7	121.0	121.7	121.2	121.5	122.0	121.5	122.0	122.3
	300	120.4	120.6	121.2	120.7	120.9	121.6	120.9	121.3	122.0	121.6	121.7	122.4	121.8	122.2	122.6
	400	120.8	120.9	121.5	120.9	121.2	121.8	121.1	121.5	122.2	121.9	122.0	122.6	122.2	122.6	122.8
	500	121.1	121.4	121.8	121.3	121.5	122.1	121.5	121.8	122.4	122.2	122.2	122.9	122.4	122.8	123.1
	600	121.4	121.6	122.2	121.5	121.8	122.5	121.7	122.1	122.6	122.4	122.5	123.1	122.7	123.1	123.5
	700	**121.6**	**121.9**	**122.5**	**121.8**	**122.2**	**122.8**	**122.1**	**122.5**	**122.9**	**122.7**	**122.8**	**123.4**	**123.0**	**123.4**	**123.8**
	800	121.3	121.7	122.7	121.6	121.9	122.6	121.8	122.3	122.7	122.4	122.6	123.1	122.8	123.2	123.4
	900	121.0	121.4	122.4	121.4	121.7	122.4	121.5	122.0	122.4	122.2	122.4	122.8	122.5	122.9	123.2
	1000	120.8	121.2	122.1	121.1	121.5	122.2	121.3	121.7	122.2	121.9	122.1	122.5	122.3	122.6	122.8

Table 4(Cont…): A-weighted equivalent continuous sound level near drill rod for rocks at various air pressures and thrust (igneous rock) for integral drill bit.

Air pressure (kPa)	Thrust (N)	A-weighted equivalent continuous sound level (dB)															
		Dolerite			Soda granite			Black granite			Basalt			Gabbros		
		Drill bit diameter in (mm)														
		30	34	40	30	34	40	30	34	40	30	34	40	30	34	40
392	100	119.5	119.9	120.3	120.1	120.6	120.8	120.4	120.7	121.2	120.7	121.2	121.7	120.9	121.4	121.9
	200	120.0	120.2	120.7	120.4	120.8	121.1	120.6	121.0	121.5	121.1	121.6	121.9	121.4	121.7	122.1
	300	120.4	120.6	121.0	120.7	121.1	121.3	121.0	121.4	121.9	121.5	121.8	122.2	121.7	122.1	122.5
	400	120.6	120.9	121.3	121.1	121.5	121.7	121.3	121.6	122.2	121.8	122.1	122.6	122.1	122.4	122.8
	500	**121.0**	**121.3**	**121.5**	**121.3**	**121.8**	**121.9**	**121.6**	**122.0**	**122.4**	**122.0**	**122.4**	**122.8**	**122.3**	**122.7**	**123.0**
	600	120.8	121.0	121.3	121.0	121.6	121.6	121.4	121.7	122.1	121.8	122.0	122.5	122.1	122.5	122.7
	700	120.6	120.8	121.0	120.8	121.3	121.3	121.2	121.5	121.9	121.5	121.7	122.3	121.8	122.2	122.4
	800	120.3	120.5	120.8	120.5	121.1	121.1	120.0	121.3	121.7	121.3	121.5	122.1	121.5	122.0	122.2
	900	120.1	120.3	120.5	120.3	120.8	120.9	119.7	121.0	121.5	121.1	121.3	121.8	121.3	121.7	122.0
	1000	119.8	120.0	120.3	120.1	120.6	120.6	119.4	120.8	121.2	120.9	121.1	121.4	121.0	121.4	121.6
441	100	119.7	120.3	120.8	120.2	120.7	121.1	120.6	121.3	121.5	120.8	121.7	121.8	121.2	121.8	122.0
	200	120.6	120.7	121.0	120.9	121.1	121.4	121.0	121.8	121.8	121.3	122.1	122.2	121.6	122.2	122.4
	300	120.8	121.0	121.3	121.2	121.5	121.7	121.3	122.1	122.2	121.7	122.3	122.5	121.9	122.6	122.9
	400	121.0	121.3	121.5	121.4	121.8	122.1	121.7	122.4	122.5	122.0	122.7	122.7	122.4	122.9	123.2
	500	**121.3**	**121.7**	**121.9**	**121.6**	**122.0**	**122.3**	**122.0**	**122.6**	**122.8**	**122.3**	**123.0**	**123.0**	**122.6**	**123.2**	**123.4**
	600	121.0	121.5	121.7	121.3	121.7	122.0	121.8	122.3	122.6	122.0	122.8	122.8	122.3	123.0	123.1
	700	120.8	121.3	121.4	121.1	121.5	121.8	121.5	122.1	122.3	121.8	122.6	122.5	122.0	122.8	122.9
	800	120.5	121.0	121.2	120.8	121.3	121.6	121.1	121.8	122.0	121.5	122.3	122.1	121.8	122.6	122.6
	900	120.3	120.7	120.9	120.5	121.0	121.3	120.8	121.5	121.6	121.3	122.0	121.9	121.6	122.3	122.4
	1000	120.0	120.4	120.7	120.2	120.7	120.9	120.5	121.1	121.4	120.9	121.6	121.6	121.2	122.0	122.1

490	100	120.8	121.0	121.4	121.3	121.5	121.6	121.4	121.7	122.2	121.7	122.2	122.5	121.9	122.3	122.7
	200	121.2	121.4	121.7	121.5	121.7	121.9	121.6	122.3	122.5	122.0	122.5	122.9	122.3	122.7	123.0
	300	121.5	121.8	122.1	121.7	122.0	122.3	121.9	122.5	122.9	122.4	122.7	123.2	122.6	123.0	123.4
	400	121.7	122.2	122.4	122.0	122.4	122.6	122.2	122.8	123.0	122.7	123.0	123.4	122.8	123.3	123.6
	500	121.9	122.5	122.7	122.2	122.7	123.0	122.4	123.0	123.3	122.9	123.2	123.6	123.1	123.5	123.9
	600	**122.2**	**122.8**	**123.0**	**122.5**	**123.0**	**123.3**	**122.7**	**123.2**	**123.5**	**123.1**	**123.4**	**123.9**	**123.4**	**123.7**	**124.1**
	700	122.0	122.5	122.8	122.3	122.8	123.1	122.4	122.9	123.2	122.9	123.1	123.7	123.2	123.4	124.9
	800	121.7	122.3	122.6	122.1	122.6	122.9	122.2	122.7	123.0	122.6	122.8	123.5	123.0	123.2	124.6
	900	121.5	122.1	122.3	121.8	122.3	122.6	121.9	122.4	122.8	122.4	122.6	123.2	122.7	123.0	124.4
	1000	121.3	121.8	122.0	121.6	122.1	122.5	121.7	122.1	122.6	122.2	122.3	123.0	122.5	122.7	124.1
539	100	121.2	121.6	122.0	121.6	121.8	122.2	121.8	122.0	122.5	122.0	122.4	122.9	122.3	122.7	123.1
	200	121.4	121.9	122.4	121.8	122.2	122.5	122.0	122.3	122.8	122.4	122.7	123.2	122.6	123.1	123.4
	300	121.7	122.3	122.7	122.1	122.5	122.9	122.5	122.7	123.1	122.7	123.0	123.4	122.9	123.4	123.6
	400	122.0	122.6	122.9	122.4	122.9	123.0	122.9	123.0	123.4	123.1	123.4	123.7	123.2	123.6	123.9
	500	122.3	122.8	123.1	122.7	123.2	123.3	123.0	123.4	123.7	123.3	123.7	124.0	123.5	123.9	124.2
	600	122.5	123.0	123.5	122.9	123.5	123.7	123.2	123.7	123.9	123.5	123.9	124.2	123.7	124.1	124.4
	700	**122.8**	**123.3**	**123.7**	**123.1**	**123.8**	**124.0**	**123.5**	**124.0**	**124.2**	**123.8**	**124.2**	**124.4**	**124.0**	**124.4**	**124.5**
	800	122.6	123.0	123.4	122.8	123.6	123.8	123.3	123.8	124.0	123.5	123.9	124.1	123.8	124.2	124.3
	900	122.3	122.8	123.2	122.6	123.4	123.6	123.1	123.6	123.8	123.3	123.7	123.9	123.5	123.9	124.1
	1000	122.1	122.5	123.0	122.4	123,1	123.4	122.8	123.3	123.6	123.1	123.5	123.8	123.2	123.6	123.9
588	100	121.7	122.0	122.5.	122.0	122.4	122.8	122.2	122.6	123.0	122.6	123.0	123.2	123.1	123.3	123.5
	200	122.0	122.4	122.7	122.2	122.6	123.0	122.4	122.8	123.3	123.0	123.5	123.5	123.3	123.6	123.7
	300	122.2	122.7	123.0	122.4	123.0	123.3	122.7	123.1	123.5	123.3	123.7	123.7	123.6	123.8	123.9
	400	122.4	123.0	123.3	122.6	123.4	123.6	123.0	123.5	123.8	123.6	123.9	123.9	123.8	124.0	124.1
	500	122.6	123.3	123.6	122.8	123.7	123.9	123.2	123.8	124.0	123.8	124.0	124.1	124.0	124.1	124.3
	600	122.8	123.5	123.7	123.1	123.8	124.1	123.4	124.0	124.2	124.0	124.2	124.3	124.1	124.3	124.4
	700	123.0	123.7	123.8	123.3	123.9	124.2	123.6	124.1	124.3	124.1	124.3	124.4	124.3	124.4	124.5
	800	**123.2**	**123.8**	**124.0**	**123.4**	**124.0**	**124.3**	**123.7**	**124.3**	**124.4**	**124.3**	**124.4**	**124.5**	**124.4**	**124.5**	**124.6**
	900	122.9	123.6	123.8	123.2	123.8	124.0	123.4	124.0	124.2	123.8	124.2	124.3	124.1	124.3	124.4
	1000	122.6	123.3	123.5	123.0	123.5	123.7	123.2	123.7	123.8	123.4	123.9	124.0	123.7	124.0	124.2

Table 5 Penetration rate (mm/sec) for rocks at various air pressures and thrust (sedimentary rock) for integral drill bit.

Air pressure (kPa)	Thrust (N)	A-weighted equivalent continuous sound level (dB)														
		Shale			Dolomite			Sand stone			Lime stone			Hematite		
		Drill bit diameter in (mm)														
		30	34	40	30	34	40	30	34	40	30	34	40	30	34	40
392	100	0.64	0.54	0.43	0.6	0.51	0.41	0.56	0.46	0.37	0.49	0.41	0.36	0.45	0.40	0.33
	200	1.25	1.11	0.72	1.01	0.94	0.69	0.95	0.81	0.68	0.91	0.71	0.65	0.80	0.69	0.62
	300	1.62	1.50	1.10	1.54	1.34	1.003	1.46	1.19	0.99	1.37	1.07	0.93	1.21	1.14	0.90
	400	**2.15**	**2.04**	**1.35**	**2.03**	**1.84**	**1.32**	**1.93**	**1.60**	**1.26**	**1.83**	**1.56**	**1.24**	**1.61**	**1.33**	**1.23**
	500	1.71	1.66	0.98	1.65	1.48	0.96	1.57	1.22	0.89	1.44	1.18	0.87	1.23	0.36	0.86
	600	1.41	1.34	0.71	1.37	1.27	0.69	1.31	0.94	0.63	1.17	0.91	0.61	0.96	0.68	0.58
	700	1.23	1.17	0.55	1.20	0.96	0.53	1.14	0.87	0.47	1.01	0.75	0.47	0.77	0.52	0.43
	800	1.03	0.98	0.49	1.05	0.79	0.37	0.93	0.60	0.32	0.84	0.58	0.30	0.59	0.35	0.25
	900	0.84	0.66	0.39	0.74	0.48	0.29	0.66	0.34	0.25	0.56	0.33	0.23	0.32	0.28	0.18
	1000	0.53	0.49	0.37	0.52	0.31	0.22	0.47	0.21	0.16	0.35	0.18	0.15	0.20	0.16	0.12
441	100	0.72	0.70	0.50	0.68	0.57	0.48	0.66	0.53	0.44	0.56	0.46	0.38	0.50	0.43	0.37
	200	1.42	1.22	0.91	1.21	1.06	0.88	1.18	0.90	0.80	1.05	0.86	0.78	0.94	0.81	0.77
	300	1.94	1.80	1.28	1.83	1.54	1.25	1.82	1.40	1.23	1.63	1.38	1.21	1.49	1.18	1.19
	400	**2.54**	**2.38**	**1.68**	**2.45**	**2.01**	**1.67**	**2.41**	**1.89**	**1.70**	**2.19**	**1.80**	**1.68**	**2.04**	**1.62**	**1.66**
	500	2.13	2.00	1.27	2.06	1.64	1.28	2.05	1.51	1.32	1.83	1.43	1.29	1.67	1.24	1.22
	600	1.86	1.23	1.08	1.78	1.57	1.04	1.78	1.25	1.02	1.58	1.15	1.00	1.41	0.97	0.95
	700	1.67	1.21	0.73	1.41	1.98	0.86	1.63	1.09	0.84	1.41	1.09	0.81	0.95	0.61	0.58
	800	1.51	1.16	0.72	1.46	1.00	0.67	1.56	0.92	0.78	1.25	0.82	0.69	0.78	0.55	0.42
	900	1.36	1.21	0.64	1.19	0.78	0.42	1.19	0.66	0.43	0.98	0.55	0.42	0.63	0.49	0.36
	1000	1.11	0.97	0.49	1.04	0.62	0.36	1.01	0.49	0.30	0.80	0.39	0.26	0.5	0.24	0.21

490	100	0.82	0.77	0.60	0.78	0.68	0.58	0.7	0.64	0.55	0.65	0.53	0.47	0.56	0.48	0.46
	200	1.74	1.37	1.06	1.60	1.15	1.01	1.47	1.14	0.95	1.20	0.94	0.88	1.08	0.90	0.86
	300	2.42	2.01	1.55	2.35	1.85	1.52	1.92	1.71	1.42	1.81	1.51	1.26	1.67	1.43	1.25
	400	3.16	2.44	2.13	3.01	2.29	2.05	2.61	2.16	1.96	2.38	2.04	1.68	2.22	1.98	1.65
	500	**3.58**	**3.08**	**2.56**	**3.49**	**2.85**	**2.51**	**3.28**	**2.72**	**2.41**	**2.88**	**2.58**	**2.12**	**2.75**	**2.47**	**2.09**
	600	3.12	3.00	2.13	3.09	2.44	2.31	2.91	2.40	2.03	2.47	2.19	1.21	2.36	2.09	1.71
	700	2.81	2.91	1.84	2.78	2.13	1.82	2.64	2.08	1.74	2.14	1.86	1.53	2.07	1.80	1.42
	800	2.63	1.84	1.68	2.59	1.94	1.64	2.46	1.87	1.55	1.93	1.67	1.35	1.88	1.62	1.25
	900	2.47	1.75	1.50	2.38	1.72	1.47	2.27	1.64	1.38	1.72	1.65	1.14	1.66	1.43	1.06
	1000	2.2	1.66	1.21	2.11	1.43	1.17	1.98	1.35	1.08	1.43	1.18	0.86	0.98	1.16	0.84
539	100	0.98	0.88	0.68	0.88	0.76	0.67	0.75	0.73	0.63	0.74	0.61	0.55	0.63	0.51	0.53
	200	1.85	1.61	1.20	1.67	1.45	1.18	1.53	1.35	1.12	1.39	1.15	0.99	1.19	0.96	0.94
	300	2.54	2.36	1.74	2.40	2.04	1.71	2	1.95	1.66	1.98	1.71	1.58	1.78	1.48	1.46
	400	3.28	2.85	2.25	3.1	2.58	2.23	2.66	2.49	2.17	2.59	2.28	2.15	2.35	1.97	1.95
	500	3.71	3.64	2.88	3.53	3.28	2.85	3.39	3.11	2.73	3.18	2.76	2.66	2.83	2.45	2.40
	600	**4.18**	**3.70**	**3.21**	**4.08**	**3.51**	**3.18**	**3.52**	**3.31**	**3.09**	**3.45**	**3.19**	**2.88**	**3.22**	**2.70**	**2.82**
	700	3.80	3.62	2.14	3.69	3.13	2.80	3.13	2.94	2.700	3.04	2.80	2.50	2.84	2.30	2.44
	800	3.51	3.53	2.54	3.38	3.05	2.53	2.86	2.66	2.42	2.75	2.51	2.23	2.55	2.02	2.17
	900	3.30	2.44	2.35	3.18	2.58	2.34	2.70	2.50	2.25	2.57	2.33	2.08	2.37	1.85	1.99
	1000	3.15	2.39	2.18	2.99	2.52	2.16	2.55	2.33	2.09	2.33	2.17	1.60	2.13	1.66	1.79
588	100	1.18	0.96	0.78	1.00	0.88	0.76	0.96	0.84	0.73	0.84	0.71	0.63	0.73	0.58	0.56
	200	2.10	1.82	1.48	1.88	1.65	1.42	1.81	1.54	1.32	1.54	1.33	1.18	1.36	1.07	1.11
	300	2.74	2.58	1.98	2.61	2.44	1.95	2.55	2.34	1.88	2.29	1.95	1.75	1.94	1.67	1.66
	400	3.36	3.15	2.60	3.25	3.05	2.50	3.15	2.95	2.49	2.91	2.41	2.32	2.56	2.34	2.18
	500	3.96	3.78	3.18	3.85	3.65	3.15	3.75	3.55	3.08	3.46	3.09	2.82	3.09	2.75	2.61
	600	4.51	4.35	3.56	4.35	4.16	3.52	4.20	3.98	3.32	3.91	3.35	3.26	3.41	3.01	2.88
	700	**5.00**	**4.62**	**3.79**	**4.69**	**4.39**	**3.75**	**4.48**	**4.26**	**3.63**	**4.18**	**3.61**	**3.53**	**3.69**	**3.29**	**3.16**
	800	4.54	4.20	3.35	4.23	4.05	3.33	4.05	3.82	3.24	3.77	3.45	3.19	3.58	3.2	3.03
	900	4.22	3.75	3.04	3.91	3.62	3.00	3.72	3.51	2.94	3.48	2.89	2.82	2.96	2.67	2.42
	1000	3.98	3.64	2.82	3.72	3.50	2.79	3.54	2.29	2.75	3.21	2.7	2.64	2.71	2.38	2.14

Table 5(Cont…): Penetration rate (mm/sec) for rocks at various air pressures and thrust (igneous rock) for integral drill bit.

Air pressure (kPa)	Thrust (N)	A-weighted equivalent continuous sound level (dB)														
		Dolerite			Soda granite			Black granite			Basalt			Gabbros		
		Drill bit diameter in (mm)														
		30	34	40	30	34	40	30	34	40	30	34	40	30	34	40
392	100	0.40	0.37	0.32	0.36	0.35	0.31	0.33	0.30	0.21	0.28	0.22	0.19	0.20	0.17	0.13
	200	0.73	0.69	0.6	0.69	0.65	0.58	0.63	0.56	0.37	0.46	0.38	0.36	0.38	0.35	0.22
	300	1.16	1.11	0.88	1.12	1.09	0.83	0.95	0.83	0.55	0.75	0.53	0.48	0.57	0.52	0.38
	400	1.58	1.52	1.18	1.46	1.34	1.00	1.31	1.16	0.75	0.83	0.68	0.61	0.68	0.65	0.53
	500	**2**	**1.86**	**1.65**	**1.85**	**1.65**	**1.50**	**1.6**	**1.45**	**0.92**	**0.95**	**0.82**	**0.79**	**0.77**	**0.73**	**0.65**
	600	1.52	1.34	1.21	1.32	1.24	1.09	1.22	1.04	0.54	0.55	0.47	0.42	0.52	0.48	0.42
	700	1.18	1.0	0.8	0.98	0.85	0.78	0.83	0.78	0.53	0.52	0.42	0.39	0.38	0.35	0.31
	800	1.01	0.88	0.69	0.88	0.78	0.71	0.71	0.56	0.51	0.48	0.38	0.35	0.3	0.26	0.24
	900	0.81	0.72	0.58	0.77	0.62	0.55	0.61	0.48	0.42	0.36	0.35	0.32	0.22	0.18	0.14
	1000	0.68	0.43	0.36	0.56	0.43	0.41	0.42	0.35	0.31	0.29	0.27	0.25	0.16	0.14	0.11
441	100	0.48	0.41	0.36	0.42	0.39	0.35	0.36	0.34	0.24	0.32	0.25	0.23	0.22	0.18	0.14
	200	0.85	0.79	0.75	0.78	0.75	0.71	0.71	0.66	0.43	0.55	0.44	0.39	0.41	0.37	0.25
	300	1.36	1.16	1.14	1.18	1.15	1.13	1.08	0.95	0.66	0.86	0.68	0.65	0.60	0.55	0.40
	400	1.65	1.61	1.59	1.57	1.56	1.54	1.44	1.33	0.82	1.00	0.82	0.78	0.70	0.68	0.57
	500	**2.26**	**2.05**	**1.92**	**1.96**	**1.92**	**1.79**	**1.74**	**1.61**	**1.05**	**1.12**	**1.00**	**0.95**	**0.81**	**0.77**	**0.72**
	600	1.78	1.32	1.26	1.41	1.27	1.21	1.31	1.07	0.68	0.75	0.66	0.61	0.55	0.52	0.47
	700	1.45	1.01	0.96	1.1	0.98	0.92	1.03	0.82	0.64	0.67	0.61	0.55	0.48	0.37	0.33
	800	1.19	1.10	1.04	1.01	1.11	1.05	0.98	0.66	0.59	0.6	0.55	0.40	0.39	0.29	0.28
	900	0.99	0.92	0.87	0.88	0.82	0.80	0.83	0.78	0.50	0.51	0.45	0.38	0.32	0.26	0.25
	1000	0.78	0.71	0.68	0.69	0.69	0.66	0.65	0.65	0.78	0.41	0.76	0.71	0.19	0.17	0.13

490	100	0.50	0.46	0.44	0.48	0.45	0.43	0.41	0.37	0.28	0.36	0.33	0.28	0.24	0.2	0.16
	200	0.98	0.89	0.82	0.91	0.86	0.80	0.77	0.74	0.49	0.65	0.59	0.48	0.44	0.38	0.28
	300	1.56	1.38	1.23	1.42	1.36	1.19	1.18	1.05	0.72	0.95	0.90	0.75	0.65	0.62	0.42
	400	2.10	1.84	1.61	1.81	1.72	1.58	1.55	1.47	1.03	1.21	1.10	0.95	0.77	0.72	0.6
	500	2.54	2.27	2.02	2.19	2.09	1.96	1.86	1.81	1.40	1.37	1.32	1.07	0.87	0.81	0.76
	600	**2.83**	**2.43**	**2.10**	**2.4**	**2.28**	**2.04**	**2.26**	**2.13**	**1.95**	**1.67**	**1.45**	**1.28**	**0.95**	**0.90**	**0.85**
	700	2.38	2.09	1.76	2.03	1.91	1.68	1.62	1.58	1.54	1.31	1.09	0.92	0.59	0.54	0.49
	800	2.14	1.92	1.57	1.88	1.76	1.51	1.47	1.44	1.39	1.17	0.93	0.77	0.44	0.40	0.32
	900	1.95	1.86	1.42	1.82	1.81	1.35	1.3	1.25	1.18	0.9	0.77	0.61	0.42	0.24	0.17
	1000	1.76	1.81	1.28	1.4	1.44	1.20	0.86	1.11	1.02	0.63	0.62	0.47	0.25	0.15	0.11
539	100	0.59	0.56	0.49	0.56	0.53	0.48	0.46	0.42	0.36	0.39	0.35	0.31	0.27	0.22	0.17
	200	1.16	1.07	0.94	1.12	1.06	0.93	0.83	0.80	0.68	0.65	0.64	0.57	0.47	0.42	0.31
	300	1.72	1.66	1.42	1.68	1.65	1.40	1.33	1.21	1.09	1.06	0.99	0.91	0.66	0.63	0.51
	400	2.28	2.19	1.89	2.21	2.16	1.80	1.61	1.59	1.45	1.37	1.25	1.12	0.80	0.73	0.68
	500	2.68	2.65	2.29	2.49	2.48	2.14	1.9	1.83	1.71	1.55	1.48	1.25	0.9	0.85	0.80
	600	3.01	2.95	2.58	2.82	2.76	2.38	2.29	2.28	2.20	1.83	1.73	1.48	0.97	0.92	0.90
	700	**3.26**	**3.14**	**2.88**	**3.06**	**2.95**	**2.68**	**2.78**	**2.58**	**2.42**	**2.02**	**1.93**	**1.75**	**1.05**	**1.06**	**1.02**
	800	2.84	2.55	2.31	2.55	2.43	2.10	2.34	2.01	1.85	1.48	1.35	1.08	0.68	0.65	0.60
	900	2.2	1.88	1.83	1.92	1.58	1.46	1.51	1.35	1.24	1.02	0.77	0.02	0.54	0.25	0.20
	1000	1.98	1.46	1.20	1.51	1.22	0.86	1.22	0.78	0.73	0.78	0.48	0.27	0.41	0.14	0.12
588	100	0.69	0.62	0.55	0.64	0.58	0.53	0.55	0.48	0.43	0.42	0.37	0.34	0.28	0.23	0.19
	200	1.24	1.17	1.09	1.18	1.15	1.07	0.93	0.88	0.83	0.75	0.70	0.63	0.50	0.45	0.37
	300	1.82	1.75	1.65	1.78	1.70	1.61	1.446	1.38	1.25	1.12	1.10	0.95	0.67	0.61	0.58
	400	2.48	2.31	2.15	2.41	2.25	2.10	1.71	1.58	1.51	1.44	1.40	1.20	0.82	0.77	0.73
	500	2.90	2.68	2.58	2.7	2.56	2.43	2.1	1.99	1.95	1.65	1.58	1.35	0.92	0.90	0.83
	600	3.28	3.07	2.86	3.02	2.86	2.67	2.46	2.42	2.36	1.93	1.85	1.62	1	0.95	0.91
	700	3.31	3.12	2.94	3.14	2.88	2.75	2.85	2.51	2.30	2.14	1.87	1.48	1.12	0.98	0.94
	800	**3.48**	**3.32**	**3.14**	**3.26**	**3.11**	**2.95**	**2.9**	**2.64**	**2.51**	**2.19**	**2.08**	**1.85**	**1.15**	**1.10**	**1.06**
	900	3	2.71	2.55	2.6	2.43	2.35	2.15	2.10	1.93	1.61	1.54	1.30	0.95	0.92	0.86
	1000	2.78	2.18	2.08	2.11	1.93	1.87	1.6	1.54	1.43	1.33	1.30	1.003	0.83	0.82	0.78

Table 6 A-weighted equivalent continuous sound level at operator's position at various thrust and air pressures (sedimentary rock) for threaded drill bit.

Air Pressure (kPa)	Thrust (N)	A-weighted equivalent continuous sound level (dB)									
		Shale		Dolomite		Sand stone		Lime stone		Hematite	
		Drill bit diameter in (mm)									
		35	38	35	38	35	38	35	38	35	38
392	100	114.5	114.9	114.8	115.1	115.4	115.7	116.0	116.4	116.2	116.6
	200	115.0	115.2	115.3	115.5	115.7	115.9	116.4	116.7	116.6	116.8
	300	115.4	115.6	115.8	115.0	116.1	116.3	116.7	116.9	117.1	117.3
	400	**115.7**	**115.9**	**116.0**	**115.2**	**116.5**	**116.7**	**117.1**	**117.3**	**117.4**	**117.6**
	500	115.5	115.6	115.7	114.9	116.3	116.5	116.8	117.0	117.0	117.2
	600	115.2	115.4	115.5	114.6	116.1	116.2	116.4	116.8	116.7	116.9
	700	114.8	115.1	115.2	114.4	115.8	116.0	116.2	116.5	116.5	116.7
	800	114.6	114.8	115.0	114.1	115.6	115.7	115.9	116.2	116.2	116.4
	900	114.3	114.6	114.8	113.9	115.2	115.4	115.6	115.8	115.9	116.1
	1000	114.1	114.4	114.5	113.7	115.0	115.2	115.3	115.6	115.6	115.8
441	100	114.8	115.2	115.1	115.4	115.5	115.9	116.3	116.6	116.5	116.8
	200	115.1	115.4	115.6	115.8	116.0	116.2	116.7	116.9	117.0	117.2
	300	115.5	115.8	116.4	116.6	116.4	116.7	117.0	117.2	117.2	117.4
	400	**115.8**	**116.1**	**116.6**	**116.8**	**116.8**	**117.1**	**117.3**	**117.5**	**117.7**	**117.9**
	500	115.6	115.9	116.3	116.5	116.7	116.9	117.0	117.3	117.4	117.6
	600	115.3	115.7	116.0	116.2	116.4	116.6	116.8	117.0	117.1	117.4
	700	115.1	115.4	115.8	115.9	116.1	116.3	116.5	116.7	116.8	117.1
	800	114.8	115.1	115.5	115.7	115.8	116.0	116.2	116.4	116.5	116.8
	900	114.5	114.8	115.3	115.5	115.6	115.8	115.8	116.2	116.3	116.6
	1000	114.2	114.6	115.0	115.3	115.4	115.6	115.6	115.9	116.0	116.3
490	100	115.6	115.9	115.8	116.2	116.1	116.4	116.6	116.9	116.8	117.2
	200	115.8	116.2	116.2	116.4	116.5	116.7	117.0	117.2	117.3	117.5
	300	116.2	116.4	116.5	116.7	116.7	116.9	117.2	117.4	117.6	117.8
	400	116.5	116.7	116.7	116.9	117.0	117.2	117.5	117.7	117.8	118.1
	500	**116.7**	**116.9**	**117.0**	**117.2**	**117.2**	**117.5**	**117.7**	**117.9**	**118.2**	**118.4**
	600	116.4	116.6	116.8	117.0	117.0	117.3	117.4	117.6	117.9	118.2
	700	116.2	116.3	116.5	116.7	116.7	117.0	117.2	117.4	117.6	117.9
	800	115.8	116.0	116.2	116.5	116.4	116.7	117.0	117.2	117.4	117.7
	900	115.6	115.8	115.9	116.2	116.1	116.4	116.7	116.8	117.1	117.4
	1000	115.3	115.5	115.7	115.9	115.8	116.1	116.4	116.6	116.8	117.0
539	100	115.8	116.0	116.1	116.4	116.4	116.8	116.8	117.1	117.4	118.0
	200	116.1	116.3	116.5	116.7	116.9	117.1	117.1	117.3	117.7	118.3
	300	116.5	116.7	116.7	116.9	117.1	117.3	117.3	117.5	118.1	118.5
	400	116.8	116.9	117.2	117.4	117.4	117.6	117.7	117.9	118.4	118.7
	500	117.2	117.4	117.5	117.7	117.6	117.9	117.9	118.1	118.6	118.9
	600	**117.4**	**117.6**	**117.7**	**117.9**	**117.9**	**118.1**	**118.3**	**118.5**	**118.8**	**119.0**
	700	117.1	117.3	117.4	117.7	117.5	117.8	118.1	118.2	118.5	118.7
	800	116.7	117.0	117.2	117.4	117.3	117.5	117.8	117.9	118.3	118.4
	900	116.4	116.6	116.8	117.0	117.1	117.3	117.5	117.7	117.9	118.2
	1000	116.2	116.4	116.3	116.7	116.7	117.0	117.3	117.5	117.6	117.9
588	100	116.3	116.7	116.6	116.9	116.8	117.2	117.1	117.4	118.2	118.5
	200	116.7	116.9	117.1	117.3	117.3	117.5	117.4	117.6	118.4	118.6
	300	117.2	117.4	117.4	117.6	117.5	117.7	117.7	117.9	118.6	118.8
	400	117.5	117.6	117.8	118.0	118.0	118.2	118.1	118.3	118.8	119.1
	500	117.7	117.9	118.0	118.2	118.2	118.4	118.3	118.7	119.0	119.2
	600	118.1	118.3	118.4	118.6	118.6	118.8	118.7	118.9	119.6	119.8
	700	**118.6**	**118.8**	**118.7**	**118.9**	**119.1**	**119.3**	**119.2**	**119.5**	**120.0**	**120.2**
	800	118.3	118.6	118.5	118.6	118.7	119.0	118.8	119.2	119.6	119.7
	900	118.1	118.3	118.2	118.4	118.4	118.8	118.5	118.9	119.4	119.4
	1000	117.8	118.1	118.0	118.2	118.2	118.4	118.2	118.6	119.0	119.2

Table 6 A-weighted equivalent continuous sound level at operator's position for rocks at various thrust and air pressures (igneous rock) for threaded drill bit.

Air Pressure (kPa)	Thrust (N)	A-weighted equivalent continuous sound level (dB)									
		Dolerite		Soda granite		Black granite		Basalt		Gabbros	
		Drill bit diameter in (mm)									
		35	38	35	38	35	38	35	38	35	38
392	100	116.4	116.7	116.8	117.2	117.3	117.5	117.6	117.9	117.7	118.1
	200	116.8	117.0	117.3	117.5	117.7	117.9	117.9	118.2	118.2	118.4
	300	117.3	117.5	117.7	117.9	118.0	118.2	118.1	118.4	118.5	118.7
	400	117.6	117.8	118.0	118.2	118.4	118.6	118.6	118.8	118.7	119.0
	500	**118.0**	**118.2**	**118.2**	**118.4**	**118.7**	**118.9**	**118.9**	**119.2**	**119.1**	**119.3**
	600	117.7	117.4	117.9	118.1	118.4	118.5	118.7	118.9	118.9	119.0
	700	117.1	117.1	117.6	117.9	118.2	118.3	118.5	118.6	118.6	118.8
	800	116.8	116.9	117.3	117.6	117.8	118.0	118.2	118.4	118.4	118.6
	900	116.4	116.6	117.2	117.2	117.5	117.8	117.9	118.1	118.1	118.3
	1000	116.2	116.4	116.8	116.9	117.3	117.5	117.7	117.9	117.4	117.9
441	100	116.5	116.9	117.1	117.4	117.3	117.7	117.8	118.0	118.1	118.4
	200	117.1	117.3	117.5	117.7	117.8	118.1	118.0	118.3	118.5	118.7
	300	117.4	117.6	117.9	118.0	118.2	118.4	118.3	118.5	118.7	118.9
	400	117.8	117.9	118.1	118.3	118.5	118.7	118.8	119.0	119.2	119.4
	500	**118.3**	**118.5**	**118.4**	**118.6**	**119.0**	**119.2**	**119.2**	**119.4**	**119.6**	**119.8**
	600	117.9	118.2	118.0	118.4	118.6	118.9	119.0	119.2	119.2	119.5
	700	117.6	117.9	117.8	118.1	118.3	118.5	118.7	118.9	119.0	119.2
	800	117.4	117.6	117.5	117.8	118.0	118.2	118.4	118.6	118.7	119.0
	900	117.2	117.4	117.3	117.5	117.8	118.0	118.2	118.4	118.4	118.7
	1000	117.0	117.1	117.1	117.3	117.5	117.7	118.9	118.0	118.1	118.3
490	100	117.2	117.6	117.6	117.8	117.9	118.2	118.2	118.6	118.4	118.7
	200	117.5	117.9	118.0	118.2	118.2	118.4	118.6	118.8	119.0	119.2
	300	117.8	118.2	118.2	118.4	118.5	118.7	118.8	119.0	119.2	119.4
	400	118.1	118.4	118.4	118.6	118.7	118.9	119.1	119.3	119.4	119.6
	500	118.3	118.6	118.7	118.8	119.1	119.4	119.3	119.5	119.7	119.9
	600	**118.5**	**118.9**	**118.9**	**119.3**	**119.5**	**119.8**	**119.6**	**119.8**	**120.2**	**120.6**
	700	118.2	118.4	118.6	119.0	119.1	119.5	119.4	119.6	119.8	120.3
	800	118.0	118.1	118.3	118.7	118.8	119.2	119.1	119.3	119.5	119.9
	900	117.7	117.9	118.0	118.3	118.6	119.0	118.8	119.0	119.3	119.6
	1000	117.4	117.6	117.8	118.0	118.3	118.6	118.5	118.8	119.0	119.2
539	100	117.7	118.2	118.1	118.5	118.3	118.5	118.6	118.9	118.8	119.0
	200	118.0	118.4	118.5	118.7	118.5	118.8	119.0	119.2	119.3	119.5
	300	118.3	118.7	118.7	118.9	118.7	119.2	119.2	119.6	119.5	119.7
	400	118.5	118.9	119.2	119.4	119.2	119.4	119.6	119.8	120.0	119.2
	500	118.8	119.1	119.4	119.6	119.5	119.7	119.8	120.0	120.2	119.4
	600	119.0	119.3	119.7	119.9	119.7	119.9	120.1	120.3	120.4	119.7
	700	**119.2**	**119.7**	**119.9**	**120.1**	**120.1**	**120.3**	**120.3**	**120.5**	**120.7**	**120.9**
	800	118.9	119.4	119.6	119.8	119.8	120.0	120.0	120.2	120.3	120.6
	900	118.5	119.1	119.2	119.5	119.6	119.8	119.8	120.0	120.0	120.3
	1000	118.2	118.7	118.4	119.2	119.4	119.6	119.6	119.8	119.8	120.0
588	100	118.3	118.7	118.6	119.1	118.8	119.0	119.2	119.5	119.5	119.9
	200	118.6	118.9	119.1	119.3	119.2	119.4	119.5	119.7	120.0	120.3
	300	118.9	119.1	119.4	119.6	119.5	119.6	120.0	120.2	120.3	120.5
	400	119.1	119.3	119.6	119.8	119.7	119.9	120.4	120.6	120.6	120.9
	500	119.4	119.6	119.8	120.2	119.9	120.1	120.6	120.8	121.0	121.2
	600	119.6	120.0	120.2	120.7	120.4	120.6	121.0	121.2	121.2	121.4
	700	120.1	120.4	120.5	120.9	120.7	120.9	121.2	121.4	121.4	121.7
	800	**119.8**	**120.2**	**120.4**	**120.5**	**120.5**	**120.7**	**120.7**	**120.9**	**120.8**	**121.3**
	900	119.5	119.8	120.1	120.3	120.2	120.4	120.4	120.6	120.6	121.0
	1000	119.2	119.5	119.7	120.0	119.9	120.1	120.1	120.3	120.3	120.5

Table 7 A-weighted equivalent continuous sound levels at exhaust for rocks at various thrust and air pressures (sedimentary rock) for threaded drill bit.

Air Pressure (kPa)	Thrust (N)	A-weighted equivalent continuous sound level (dB)									
		Shale		Dolomite		Sand stone		Lime stone		Hematite	
		Drill bit diameter in (mm)									
		35	38	35	38	35	38	35	38	35	38
392	100	115.5	115.8	116.0	116.2	116.0	116.3	116.8	117.1	117.2	117.6
	200	115.9	116.1	116.3	116.5	116.5	116.7	117.3	117.5	117.5	117.7
	300	116.1	116.3	116.6	116.8	117.3	117.5	117.7	117.9	118.0	118.2
	400	**116.4**	**116.6**	**116.9**	**117.1**	**117.5**	**117.7**	**118.1**	**118.3**	**118.4**	**118.6**
	500	116.2	116.3	116.7	116.8	117.4	117.5	117.8	118.0	118.0	118.3
	600	115.9	116.1	116.4	116.6	117.0	117.2	117.4	117.7	117.7	118.1
	700	115.5	115.8	116.0	116.3	116.7	116.8	117.1	117.4	117.5	117.7
	800	115.2	115.4	115.8	115.9	116.4	116.6	116.8	117.0	117.2	117.4
	900	115.0	115.1	115.5	115.7	116.1	116.3	116.5	116.8	116.9	117.1
	1000	114.7	114.9	115.1	115.4	115.8	116.0	116.2	116.5	116.6	116.8
441	100	116.0	116.3	116.3	116.6	116.7	116.9	117.1	117.4	117.5	117.9
	200	116.3	116.5	116.6	116.8	117.0	117.2	117.5	117.7	117.8	118.2
	300	116.7	116.9	116.9	117.1	117.7	117.9	117.9	118.3	118.4	118.6
	400	**117.0**	**117.3**	**117.5**	**117.6**	**118.0**	**118.2**	**118.2**	**118.4**	**118.7**	**118.9**
	500	116.6	117.0	117.2	117.3	117.8	117.8	118.0	118.1	118.3	118.5
	600	116.3	116.6	116.9	117.0	117.4	117.6	117.7	117.7	118.0	118.2
	700	116.1	116.3	116.5	116.8	117.1	117.3	117.4	117.5	117.6	118.0
	800	115.8	116.1	116.2	116.5	116.8	116.9	117.0	117.2	117.3	117.7
	900	115.5	115.9	115.9	116.1	116.6	116.7	116.7	116.9	117.1	117.4
	1000	115.2	115.7	115.6	115.9	116.3	116.5	116.4	116.7	116.7	117.0
490	100	116.7	117.1	117.0	117.3	117.2	117.6	117.7	118.0	118.0	118.5
	200	117.2	117.4	117.3	117.5	117.7	117.9	118.0	118.4	118.3	118.7
	300	117.4	117.6	117.6	117.8	118.0	118.2	118.3	118.6	118.5	118.8
	400	117.6	117.8	117.8	118.0	118.3	118.5	118.5	118.8	119.0	119.2
	500	**117.9**	**118.3**	**118.2**	**118.5**	**118.5**	**118.8**	**118.8**	**119.0**	**119.3**	**119.6**
	600	117.7	118.0	117.8	118.2	118.2	118.4	118.6	118.8	119.0	119.2
	700	117.4	117.6	117.6	117.9	118.0	118.1	118.3	118.5	118.7	118.9
	800	117.0	117.3	117.3	117.6	117.7	117.9	117.9	118.1	118.4	118.6
	900	116.7	117.1	117.0	117.4	117.3	117.6	117.5	117.8	118.1	118.3
	1000	116.5	116.8	116.8	117.0	117.0	117.3	117.2	117.5	117.9	118.0
539	100	117.0	117.3	117.2	117.6	117.6	117.9	118.0	118.2	118.4	119.2
	200	117.3	117.5	117.6	117.8	118.2	118.4	118.3	118.5	118.8	119.5
	300	117.7	117.9	117.9	118.1	118.4	118.6	118.5	118.7	119.1	119.6
	400	118.0	118.2	118.3	118.5	118.6	118.8	118.7	119.0	119.4	119.9
	500	118.4	118.6	118.6	118.8	118.7	119.0	118.9	119.2	119.8	120.0
	600	**118.6**	**118.8**	**118.8**	**119.0**	**119.0**	**119.2**	**119.3**	**119.4**	**120.0**	**120.2**
	700	118.3	118.5	118.4	118.7	118.8	118.9	119.0	119.2	119.6	119.8
	800	117.9	118.1	118.1	118.3	118.5	118.7	118.7	118.9	119.3	119.5
	900	117.6	117.9	117.9	118.0	118.1	118.4	118.4	118.6	119.0	119.3
	1000	117.5	117.6	117.6	117.8	117.8	118.0	118.1	118.3	118.6	119.0
588	100	117.3	117.5	117.6	117.9	118.0	118.4	118.1	118.4	118.7	119.4
	200	117.8	117.9	118.2	118.4	118.4	118.6	118.5	118.6	119.1	119.7
	300	118.1	118.5	118.5	118.7	118.7	118.8	118.7	118.8	119.5	119.9
	400	118.4	118.6	118.8	119.0	119.0	119.2	119.1	119.3	120.2	120.4
	500	118.8	118.9	119.1	119.3	119.3	119.6	119.5	119.7	120.4	120.6
	600	119.2	119.4	119.5	119.7	119.8	119.9	119.7	119.9	120.7	120.9
	700	**119.7**	**119.9**	**120.0**	**120.2**	**120.2**	**120.5**	**120.3**	**120.5**	**121.2**	**121.4**
	800	119.4	119.5	119.7	119.9	119.8	119.9	119.9	120.2	121.0	121.2
	900	119.1	119.3	119.3	119.5	119.6	119.7	119.7	119.8	120.8	120.9
	1000	118.9	118.9	119.1	119.3	119.3	119.5	118.9	119.5	120.6	120.8

Table 7 A-weighted equivalent continuous sound levels at exhaust for rocks at various thrust and air pressures (igneous rock) for threaded drill bit.

Air Pressure (kPa)	Thrust (N)	A-weighted equivalent continuous sound level (dB)									
		Dolerite		Soda granite		Black granite		Basalt		Gabbros	
		Drill bit diameter in (mm)									
		35	38	35	38	35	38	35	38	35	38
392	100	117.5	117.8	117.8	118.2	118.1	118.4	118.3	118.5	118.7	119.0
	200	118.0	118.2	118.3	118.5	118.6	118.8	118.8	119.2	119.3	119.5
	300	118.3	118.5	118.5	118.7	119.0	119.2	119.2	119.5	119.5	119.7
	400	118.6	118.8	118.9	119.2	119.2	119.4	119.5	119.8	120.1	120.3
	500	**118.8**	**119.1**	**119.2**	**119.4**	**119.6**	**119.8**	**119.8**	**120.1**	**120.4**	**120.8**
	600	118.5	118.6	119.0	119.1	119.2	119.6	119.6	119.9	120.0	120.5
	700	118.1	118.4	118.7	118.9	119.0	119.4	119.4	119.6	119.7	120.1
	800	117.8	118.1	118.4	118.6	118.7	119.0	119.1	119.3	119.5	119.9
	900	117.5	117.9	118.0	118.4	118.5	118.8	118.7	118.9	119.2	119.5
	1000	117.1	117.6	117.7	118.1	118.2	118.4	118.5	118.7	118.9	119.2
441	100	117.7	118.0	118.0	118.4	118.3	118.5	118.6	118.9	119.1	119.3
	200	118.1	118.3	118.4	118.6	118.7	118.9	119.0	119.2	119.5	119.7
	300	118.5	118.7	119.1	119.3	119.2	119.4	119.4	119.6	120.0	120.2
	400	119.0	119.2	119.3	119.5	119.5	119.7	119.7	119.9	120.2	120.4
	500	**119.3**	**119.5**	**119.6**	**119.8**	**120.0**	**120.2**	**120.3**	**120.5**	**120.6**	**121.0**
	600	119.1	119.2	119.4	119.5	119.7	120.2	120.0	120.1	120.3	120.6
	700	118.7	119.0	119.1	119.3	119.3	119.7	119.8	119.8	120.0	120.3
	800	118.4	118.7	118.9	119.0	119.0	119.3	119.6	119.5	119.7	120.1
	900	118.2	118.4	118.6	118.8	118.8	119.0	119.2	119.3	119.5	119.7
	1000	117.9	118.0	118.3	118.5	118.5	118.7	119.0	119.0	119.2	119.5
490	100	118.6	118.9	118.8	119.2	119.1	119.4	119.8	120.1	120.0	120.2
	200	119.0	119.2	119.3	119.5	119.4	119.6	120.0	120.4	120.3	120.5
	300	119.2	119.4	119.5	119.7	119.7	119.9	120.4	120.6	120.5	120.8
	400	119.4	119.5	119.7	119.9	120.0	120.2	120.6	120.8	120.7	121.0
	500	119.7	119.8	120.0	120.2	120.2	120.4	120.8	120.9	121.0	121.2
	600	**119.9**	**120.0**	**120.2**	**120.4**	**120.5**	**120.7**	**121.1**	**121.3**	**121.4**	**121.7**
	700	119.6	119.8	120.8	120.1	120.3	120.4	121.7	121.0	121.0	121.4
	800	119.4	119.6	120.4	119.8	120.0	120.0	121.4	120.8	120.7	121.1
	900	119.1	119.2	120.1	119.4	119.6	119.7	121.1	120.5	120.4	120.7
	1000	118.9	119.0	119.8	119.2	119.3	119.4	121.8	120.1	120.0	120.4
539	100	119.0	119.3	119.3	119.7	119.6	119.9	120.0	120.2	120.2	120.4
	200	119.4	119.5	119.9	120.1	120.0	120.3	120.2	120.4	120.6	120.8
	300	119.5	119.7	120.2	120.4	120.3	120.6	120.5	120.9	120.7	121.0
	400	119.8	119.9	120.5	120.7	120.5	120.8	120.8	121.1	121.1	121.3
	500	120.0	120.1	120.7	120.9	120.8	121.0	121.1	121.3	121.4	121.6
	600	120.2	120.3	120.9	121.0	121.0	121.2	121.3	121.5	121.6	121.8
	700	**120.5**	**120.7**	**121.1**	**121.3**	**121.3**	**121.5**	**121.5**	**121.7**	**121.8**	**122.0**
	800	120.1	120.4	120.8	121.1	121.1	121.3	121.0	121.4	121.5	121.7
	900	119.8	120.0	120.5	120.8	120.8	121.0	120.8	121.2	121.3	121.5
	1000	119.6	119.8	120.1	120.4	120.5	120.6	120.5	120.8	121.0	121.3
588	100	119.4	119.7	119.7	120.2	120.0	120.2	120.3	120.6	120.8	121.0
	200	119.7	120.0	120.0	120.5	120.3	120.4	120.6	120.8	121.1	121.3
	300	119.9	120.2	120.2	120.7	120.5	120.7	121.0	121.1	121.3	121.5
	400	120.3	120.5	120.6	120.9	120.8	121.0	121.3	121.4	121.5	121.8
	500	120.5	120.7	120.8	121.1	121.1	121.2	121.5	121.7	121.7	122.0
	600	120.8	120.9	121.0	121.3	121.3	121.4	121.7	121.9	121.9	122.1
	700	121.1	121.2	121.3	121.5	121.5	121.6	121.9	122.0	122.1	122.3
	800	**121.3**	**121.4**	**121.5**	**121.7**	**121.6**	**121.7**	**122.0**	**122.2**	**122.2**	**122.4**
	900	121.0	121.2	121.2	121.4	121.3	121.5	121.6	121.9	122.0	122.1
	1000	120.7	120.9	120.9	121.1	121.0	121.2	121.4	121.6	121.7	121.8

Table 8 A-weighted equivalent continuous sound level near drill bit for rocks at various thrust and air pressures (sedimentary rock) for threaded drill bit.

Air Pressure (kPa)	Thrust (N)	A-weighted equivalent continuous sound level (dB)									
		Shale		Dolomite		Sand stone		Lime stone		Hematite	
		Drill bit diameter in (mm)									
		35	38	35	38	35	38	35	38	35	38
392	100	116.1	116.3	116.2	116.4	116.8	117.0	117.5	117.7	117.8	117.9
	200	116.3	116.5	116.8	116.9	117.1	117.3	118.0	118.1	118.1	118.5
	300	116.9	117.1	117.1	117.3	117.6	117.9	118.2	118.4	118.3	118.6
	400	**117.2**	**117.4**	**117.5**	**117.7**	**118.0**	**118.2**	**118.5**	**118.7**	**118.7**	**118.9**
	500	116.8	117.1	117.2	117.5	117.7	117.9	118.1	118.4	118.4	118.6
	600	116.5	116.8	116.8	117.2	117.5	117.6	117.8	118.0	118.1	118.4
	700	116.3	116.6	116.5	116.8	117.2	117.4	117.6	117.8	117.7	118.0
	800	116.0	116.3	116.2	116.5	117.0	117.2	117.4	117.6	117.5	117.7
	900	115.8	116.1	116.0	116.3	116.7	116.9	117.1	117.3	117.3	117.5
	1000	115.5	115.8	115.7	116.0	116.4	116.6	117.8	117.0	117.0	117.2
441	100	116.5	116.9	116.7	117.0	117.1	117.4	117.8	118.0	118.1	118.4
	200	116.8	117.1	117.2	117.4	117.4	117.6	118.1	118.3	118.5	118.7
	300	117.1	117.3	117.4	117.6	118.1	118.3	118.5	118.7	118.8	119.0
	400	**117.5**	**117.7**	**117.7**	**117.9**	**118.3**	**118.5**	**118.8**	**119.0**	**119.0**	**119.2**
	500	117.2	117.2	117.4	117.7	118.0	118.2	118.4	118.8	118.8	118.9
	600	117.0	116.8	117.2	117.4	117.8	118.0	118.2	118.5	118.6	118.7
	700	116.7	116.6	116.9	117.0	117.6	117.7	117.9	118.1	118.2	118.5
	800	116.4	116.5	116.5	116.8	117.2	117.4	117.6	117.8	117.9	118.2
	900	116.2	116.3	116.3	116.5	117.0	117.2	117.3	117.5	117.7	117.8
	1000	116.0	116.1	116.1	116.3	116.7	116.9	117.1	117.3	117.4	117.6
490	100	117.2	117.4	117.6	117.9	118.0	118.3	118.3	118.7	118.6	118.9
	200	117.6	117.8	118.1	117.3	118.5	118.7	118.7	119.0	119.0	119.2
	300	117.9	118.1	118.4	117.6	118.7	119.2	118.9	119.3	119.3	119.5
	400	118.3	118.5	118.6	117.8	119.2	119.4	119.4	119.6	119.7	119.9
	500	**118.5**	**118.7**	**119.0**	**119.2**	**119.4**	**119.6**	**119.6**	**119.8**	**120.0**	**120.2**
	600	118.3	118.4	118.7	118.9	119.0	119.2	119.3	119.4	119.7	119.9
	700	118.0	118.2	118.5	118.7	118.7	118.9	119.1	119.2	119.4	119.7
	800	117.7	117.9	118.2	118.4	118.4	118.6	118.8	119.0	119.2	119.4
	900	117.3	117.5	118.0	118.2	118.2	118.4	118.4	118.7	118.9	119.0
	1000	117.0	117.3	117.7	117.9	117.9	118.1	118.1	118.4	118.5	118.7
539	100	117.6	117.9	118.1	118.3	118.4	118.7	118.5	118.8	119.5	119.7
	200	117.9	118.1	118.4	118.6	118.8	119.1	119.1	119.3	119.8	119.9
	300	118.3	118.5	118.7	118.9	119.1	119.3	119.3	119.6	120.1	120.2
	400	118.6	118.8	118.9	119.0	119.4	119.7	119.7	119.9	120.5	120.7
	500	119.0	119.2	119.2	119.4	119.8	120.0	120.0	120.2	120.8	120.9
	600	**119.2**	**119.4**	**119.6**	**119.8**	**120.0**	**120.2**	**120.2**	**120.5**	**121.0**	**121.1**
	700	118.7	119.1	119.3	119.6	119.6	119.9	119.9	120.2	120.7	120.9
	800	118.4	118.8	119.0	119.3	119.3	119.6	119.7	120.0	120.4	120.6
	900	118.2	118.5	118.8	119.0	119.1	119.2	119.4	119.7	120.1	120.4
	1000	117.9	118.2	118.5	118.7	118.8	118.9	119.1	119.4	119.7	120.1
588	100	118.0	118.4	118.3	118.5	118.6	118.9	119.0	119.2	119.7	120.0
	200	118.4	118.6	118.6	118.8	119.0	119.3	119.2	119.5	120.0	120.2
	300	118.7	118.9	118.9	119.0	119.3	119.5	119.5	119.8	120.3	120.5
	400	118.9	119.1	119.1	119.3	119.5	119.8	119.7	120.1	120.7	120.9
	500	119.3	119.5	119.4	119.6	119.8	120.2	120.0	120.4	121.0	121.2
	600	119.6	119.8	119.8	119.9	120.0	120.3	120.2	120.6	121.2	121.4
	700	**120.0**	**120.1**	**120.2**	**120.4**	**120.3**	**120.6**	**120.5**	**120.9**	**121.5**	**121.7**
	800	119.7	119.9	120.0	120.2	120.1	120.3	120.3	120.5	121.1	121.4
	900	119.4	119.6	119.7	120.0	119.8	119.9	120.0	120.3	120.9	121.0
	1000	119.1	119.3	119.4	119.7	119.5	119.7	119.7	120.1	120.6	120.8

Table 8 A-weighted equivalent continuous sound level near drill bit for rocks at various thrust and air pressures (igneous rock) for threaded drill bit.

Air Pressure (kPa)	Thrust (N)	A-weighted equivalent continuous sound level (dB)									
		Dolerite		Soda granite		Black granite		Basalt		Gabbros	
		Drill bit diameter in (mm)									
		35	38	35	38	35	38	35	38	35	38
392	100	118.0	118.3	118.2	118.5	118.5	118.9	118.7	118.9	119.2	119.6
	200	118.4	118.6	118.6	118.8	119.1	119.3	119.3	119.5	119.8	120.0
	300	118.7	118.9	119.0	119.2	119.6	119.8	119.7	119.9	120.3	120.5
	400	119.0	119.2	119.4	119.6	119.8	120.0	120.1	120.3	120.6	120.7
	500	**119.4**	**119.8**	**119.7**	**119.9**	**120.2**	**120.4**	**120.4**	**120.6**	**120.8**	**121.0**
	600	119.2	119.6	119.4	119.6	120.0	120.2	120.1	120.3	120.4	120.6
	700	119.0	119.3	119.2	119.3	119.5	119.8	119.7	120.0	120.1	120.3
	800	118.8	119.1	118.9	119.1	119.2	119.5	119.4	119.6	119.8	120.0
	900	118.5	118.8	118.7	118.8	118.9	119.3	119.2	119.4	119.6	119.8
	1000	118.1	118.5	118.4	118.5	118.6	118.0	118.9	119.0	119.3	119.5
441	100	118.5	118.7	118.7	118.9	118.9	119.2	119.1	119.3	119.4	119.7
	200	118.8	118.9	119.0	119.2	119.3	119.5	119.7	119.9	120.0	120.2
	300	119.2	119.4	119.4	119.6	119.7	119.9	120.2	120.5	120.4	120.6
	400	119.4	119.6	119.6	119.8	120.1	120.3	120.5	120.8	120.8	121.0
	500	**119.8**	**119.9**	**120.2**	**120.4**	**120.4**	**120.6**	**120.7**	**121.1**	**121.0**	**121.3**
	600	119.5	119.7	119.7	120.1	120.2	120.3	120.3	120.8	120.7	120.9
	700	119.3	119.4	119.5	119.9	120.0	120.1	`120.0	120.4	120.3	120.6
	800	119.0	119.2	119.2	119.6	119.5	119.7	119.8	120.1	120.0	120.2
	900	118.7	118.9	118.9	119.2	119.2	119.4	119.5	119.8	119.8	120.0
	1000	118.4	118.6	118.7	119.0	118.9	119.1	119.2	119.6	119.5	119.7
490	100	118.9	119.2	119.5	119.7	119.6	119.9	120.0	120.3	120.2	120.6
	200	119.3	119.5	119.8	120.0	120.0	120.2	120.3	120.5	120.7	120.9
	300	119.7	119.9	120.0	120.2	120.3	120.5	120.5	120.8	121.0	121.2
	400	120.1	120.3	120.3	120.5	120.6	120.9	120.7	121.0	121.4	121.5
	500	120.3	120.5	120.6	120.8	120.8	121.2	121.0	121.3	121.8	121.9
	600	**120.6**	**120.8**	**120.8**	**121.2**	**121.1**	**121.4**	**121.3**	**121.5**	**122.0**	**122.2**
	700	120.2	120.5	120.4	120.9	120.8	121.0	121.0	121.2	121.7	121.9
	800	119.9	120.1	120.1	120.5	120.5	120.7	120.7	120.9	121.3	121.5
	900	119.6	119.9	119.8	120.2	120.1	120.3	120.3	120.5	121.0	121.2
	1000	119.4	119.6	119.5	120.0	119.8	120.0	120.0	120.2	120.6	120.8
539	100	119.5	119.8	119.9	120.3	120.0	120.2	120.3	120.6	120.6	121.0
	200	119.9	120.1	120.3	120.5	120.4	120.6	120.8	120.9	121.1	121.4
	300	120.2	120.3	120.6	120.7	120.7	120.8	121.1	121.3	121.3	121.6
	400	120.6	120.7	120.8	120.9	121.0	121.2	121.3	121.5	121.6	121.8
	500	120.9	121.0	121.1	121.3	121.3	121.5	121.5	121.7	121.8	122.0
	600	121.2	121.4	121.4	121.6	121.6	121.8	121.7	121.9	122.0	122.2
	700	**121.4**	**121.7**	**121.6**	**121.9**	**121.8**	**122.1**	**122.0**	**122.3**	**122.2**	**122.4**
	800	121.1	121.3	121.3	121.7	121.7	121.9	121.8	122.1	122.1	122.2
	900	120.9	121.1	121.0	121.4	121.4	121.6	121.6	121.9	121.8	122.0
	1000	120.1	120.9	120.6	121.1	121.0	121.2	121.3	121.4	121.5	121.7
588	100	119.9	120.2	120.1	120.4	120.3	120.6	120.6	120.9	120.9	121.1
	200	120.1	120.4	120.3	120.7	120.6	120.8	121.9	121.1	121.2	121.2
	300	120.4	120.6	120.7	120.9	120.9	121.1	121.1	121.3	121.4	121.4
	400	120.6	120.8	121.0	121.1	121.2	121.4	121.3	121.5	121.5	121.7
	500	120.9	121.1	121.3	121.4	121.5	121.6	121.5	121.7	121.7	121.9
	600	121.1	121.5	121.5	121.6	121.7	121.9	121.8	121.9	121.9	122.1
	700	121.3	121.6	121.7	121.7	121.9	122.0	122.0	121.1	122.0	122.3
	800	**121.6**	**121.9**	**121.8**	**122.1**	**122.0**	**122.2**	**122.1**	**122.4**	**122.4**	**122.6**
	900	121.0	121.3	121.2	121.5	121.4	121.8	121.6	122.1	122.0	122.2
	1000	120.7	120.9	121.0	121.2	121.2	121.5	121.4	121.8	121.7	122.0

Table 9 A-weighted equivalent continuous sound level near drill rod for rocks at various thrust and air pressures (sedimentary rock) for threaded drill bit.

Air Pressure (kPa)	Thrust (N)	A-weighted equivalent continuous sound level (dB)									
		Shale		Dolomite		Sand stone		Lime stone		Hematite	
		Drill bit diameter in (mm)									
		35	38	35	38	35	38	35	38	35	38
392	100	116.3	116.6	116.4	116.7	117.2	117.4	117.6	117.9	118.1	118.3
	200	116.6	116.8	116.8	117.3	117.4	117.6	118.3	118.5	118.5	118.9
	300	117.1	117.4	117.3	117.7	118.0	118.2	118.7	118.9	119.0	119.2
	400	**117.4**	**117.7**	**117.9**	**118.2**	**118.4**	**118.6**	**119.0**	**119.1**	**119.2**	**119.4**
	500	117.1	117.3	117.6	117.8	118.1	118.4	118.6	118.8	118.8	119.0
	600	116.8	117.0	117.2	117.5	117.9	118.1	118.3	118.6	118.5	118.7
	700	116.4	116.8	116.9	117.2	117.6	117.7	118.1	118.3	118.3	118.5
	800	116.2	116.4	116.6	116.8	117.1	117.4	117.8	118.0	118.0	118.2
	900	115.9	116.1	116.3	116.5	116.8	117.1	117.6	117.8	117.8	117.9
	1000	115.7	115.8	116.0	116.3	116.6	116.8	117.2	117.5	117.5	117.7
441	100	116.8	117.2	117.1	117.4	117.4	117.6	118.1	118.3	118.3	118.5
	200	117.2	117.4	117.5	117.7	117.8	117.9	118.6	118.8	119.0	119.2
	300	117.6	117.9	118.1	118.2	118.4	118.6	119.0	119.2	119.2	119.4
	400	**117.2**	**118.4**	**118.5**	**118.7**	**118.7**	**118.9**	**119.3**	**119.5**	**119.6**	**119.8**
	500	117.0	118.1	118.3	118.4	118.5	118.6	119.1	119.2	119.3	119.4
	600	116.7	117.8	118.0	118.2	118.2	118.4	118.8	118.9	119.1	119.2
	700	116.3	117.4	117.7	117.9	117.8	118.0	118.5	118.6	118.8	119.0
	800	116.0	117.1	117.4	117.6	117.6	117.8	118.2	118.4	118.5	118.7
	900	115.7	116.8	117.1	117.4	117.3	117.5	118.0	118.2	118.2	118.4
	1000	116.0	116.4	116.7	117.1	117.0	117.2	117.6	117.8	118.0	118.2
490	100	117.5	117.9	117.7	118.1	117.9	118.4	118.5	118.7	119.0	119.5
	200	118.0	118.2	118.2	118.5	118.4	119.2	119.2	119.4	119.4	119.6
	300	118.2	118.4	118.4	118.7	118.6	119.5	119.4	119.6	119.6	119.8
	400	118.5	118.8	118.7	118.9	119.1	119.8	119.7	119.9	120.1	120.4
	500	**118.8**	**119.0**	**119.1**	**119.3**	**119.5**	**120.2**	**120.1**	**120.2**	**120.3**	**120.5**
	600	118.4	118.7	118.9	119.0	119.3	119.9	119.7	119.8	120.0	120.3
	700	118.1	118.4	118.6	118.8	119.0	119.5	119.4	119.7	119.6	119.9
	800	117.8	118.1	118.4	118.5	118.8	119.2	119.0	119.3	119.3	119.6
	900	117.5	117.9	118.1	118.1	118.4	118.8	118.8	119.0	119.1	119.4
	1000	117.2	117.5	117.8	117.8	118.1	118.6	118.5	118.7	118.7	119.0
539	100	118.0	118.3	118.4	118.6	118.7	119.3	118.9	119.1	119.8	120.0
	200	118.2	118.5	118.6	118.9	119.1	119.6	119.3	119.5	120.1	120.3
	300	118.4	118.8	118.9	119.1	119.5	119.8	119.7	119.7	120.4	120.6
	400	118.9	119.0	119.3	119.4	119.7	120.0	119.9	120.1	120.6	120.8
	500	119.2	119.4	119.5	119.7	120.0	120.4	120.2	120.4	120.9	121.0
	600	**119.5**	**119.7**	**119.7**	**119.9**	**120.2**	**120.6**	**120.4**	**120.6**	**121.0**	**121.2**
	700	119.2	119.5	119.3	119.6	119.8	120.2	120.1	120.3	120.6	120.9
	800	119.0	119.2	119.1	119.3	119.5	119.9	119.7	120.0	120.3	120.5
	900	118.6	118.9	118.7	118.9	119.1	119.6	119.4	119.6	120.0	120.2
	1000	118.3	118.5	118.5	118.7	118.9	119.2	119.1	119.3	119.6	119.9
588	100	118.4	118.7	118.7	118.9	119.1	119.5	119.3	119.5	120.2	120.5
	200	118.8	118.9	119.1	119.3	119.4	119.7	119.7	119.9	120.5	120.7
	300	119.1	119.3	119.4	119.6	119.6	120.0	120.1	120.3	120.8	121.0
	400	119.4	119.6	119.6	119.8	119.8	120.2	120.3	120.5	121.2	121.2
	500	119.7	119.8	119.9	120.1	120.2	120.6	120.6	120.9	121.4	121.4
	600	120.1	120.3	120.2	120.4	120.4	120.8	120.8	121.1	121.6	121.9
	700	**120.3**	**120.5**	**120.5**	**120.7**	**120.8**	**121.0**	**121.1**	**121.3**	**121.8**	**122.4**
	800	119.9	120.1	120.2	120.5	120.5	120.7	120.9	121.0	121.5	121.8
	900	119.6	119.8	119.9	120.3	120.2	120.4	120.5	120.8	121.3	121.6
	1000	119.3	119.5	119.6	119.8	120.0	120.2	120.3	120.6	120.8	121.4

Table 9 A-weighted equivalent continuous sound level near drill rod for rocks at various thrust and air pressures (igneous rock) for threaded drill bit.

Air Pressure (kPa)	Thrust (N)	A-weighted equivalent continuous sound level (dB)									
		Dolerite		Soda granite		Black granite		Basalt		Gabbros	
		Drill bit diameter in (mm)									
		35	38	35	38	35	38	35	38	35	38
392	100	118.2	118.6	118.7	119.0	119.0	119.2	119.2	119.5	119.7	120.0
	200	118.7	118.8	119.1	119.3	119.3	119.5	119.6	119.8	120.1	120.3
	300	119.0	119.4	119.4	119.6	119.7	119.9	120.0	120.2	120.4	120.8
	400	119.5	119.7	119.8	120.0	120.1	120.3	120.3	120.5	120.8	121.0
	500	**119.8**	**119.9**	**120.0**	**120.2**	**120.3**	**120.5**	**120.7**	**120.9**	**121.1**	**121.3**
	600	119.4	119.6	119.8	119.9	119.8	120.1	120.4	120.6	120.9	121.0
	700	119.1	119.4	119.4	119.6	119.6	119.8	120.0	120.3	120.5	120.8.
	800	118.9	119.0	119.1	119.4	119.3	119.4	119.7	120.1	120.2	120.5
	900	118.6	118.8	118.9	119.0	119.0	119.2	119.5	119.7	120.0	120.2
	1000	118.3	118.5	118.6	118.8	118.8	119.0	119.2	119.4	119.6	119.8
441	100	118.4	118.8	119.0	119.3	119.3	119.5	119.5	119.8	120.0	120.2
	200	119.0	119.3	119.2	119.5	119.5	119.7	120.0	120.2	120.4	120.6
	300	119.5	119.7	119.8	120.0	120.2	120.4	120.4	120.6	120.6	120.8
	400	119.7	119.9	120.1	120.3	120.4	120.6	120.7	120.9	121.1	121.3
	500	**120.0**	**120.2**	**120.3**	**120.5**	**120.7**	**120.9**	**121.0**	**121.2**	**121.3**	**121.5**
	600	119.8	119.9	120.0	120.2	120.5	120.6	120.8	120.9	121.0	121.3
	700	119.4	119.6	119.6	120.0	120.2	120.4	120.4	120.7	120.6	121.0
	800	119.1	119.2	119.3	119.6	120.0	120.1	120.2	120.4	120.4	120.6
	900	118.7	118.9	119.0	119.3	119.6	119.8	119.8	120.0	120.1	120.3
	1000	118.4	118.7	118.6	119.0	119.3	119.4	119.6	119.7	119.8	120.0
490	100	119.5	119.8	119.7	120.0	119.9	120.3	120.3	120.5	120.7	1210
	200	120.0	120.2	120.2	120.4	120.3	120.5	120.7	120.9	121.1	121.3
	300	120.1	120.3	120.4	120.5	120.6	120.8	121.0	121.2	121.4	121.6
	400	120.3	120.5	120.7	120.9	120.9	121.1	121.3	121.5	121.6	121.8
	500	120.4	120.7	121.0	121.2	121.1	121.3	121.5	121.7	122.0	122.2
	600	**120.7**	**121.0**	**121.1**	**121.4**	**121.4**	**121.6**	**121.8**	**122.0**	**122.2**	**122.4**
	700	120.3	120.6	120.8	121.0	121.1	121.4	121.6	121.8	121.9	122.0
	800	120.0	120.3	120.5	120.7	120.9	121.0	121.3	121.5	121.5	121.8
	900	119.8	120.1	120.3	120.4	120.6	120.7	120.9	121.1	121.2	121.5
	1000	119.4	119.8	120.0	120.0	120.2	120.3	120.5	120.7	120.8	121.1
539	100	119.8	120.1	120.0	120.4	120.3	120.6	120.7	120.9	121.0	121.4
	200	120.3	120.5	120.5	120.6	120.6	120.9	121.1	121.3	121.5	121.7
	300	120.5	120.7	120.8	121.0	120.9	121.1	121.4	121.6	121.7	121.9
	400	120.8	121.0	121.1	121.3	121.4	121.6	121.8	122.0	122.0	122.2
	500	121.1	121.3	121.3	121.5	121.7	121.9	122.0	122.3	122.2	122.4
	600	121.3	121.4	121.7	121.9	122.0	122.2	122.2	122.5	122.4	122.6
	700	**121.5**	**121.7**	**121.9**	**122.1**	**122.2**	**122.4**	**122.5**	**122.7**	**122.7**	**122.9**
	800	121.2	121.3	121.4	121.8	121.7	122.0	122.0	122.2	122.5	122.7
	900	121.0	120.8	121.1	121.5	121.5	121.7	121.8	122.0	122.2	122.4
	1000	120.3	120.5	120.5	121.2	120.8	121.4	121.5	121.7	122.0	122.2
588	100	120.2	120.5	120.5	120.9	120.8	121.1	121.3	121.5	121.6	122.0
	200	120.6	120.9	120.8	121.2	121.1	121.4	121.7	121.9	122.1	122.3
	300	120.9	121.2	121.2	121.4	121.5	121.7	122.1	122.3	122.4	122.6
	400	121.3	121.4	121.5	121.7	121.8	122.0	122.6	122.8	122.7	122.8
	500	121.5	121.8	121.8	122.0	122.0	122.2	122.8	123.0	122.9	123.1
	600	121.7	122.0	122.0	122.2	122.2	122.5	**123.0**	123.2	123.1	123.3
	700	121.8	122.2	122.2	122.4	122.3	122.7	**123.2**	122.4	123.3	123.5
	800	**122.0**	**122.4**	**122.3**	**122.6**	**122.5**	**122.9**	**123.4**	**123.6**	**123.5**	**123.7**
	900	121.6	121.8	121.8	122.2	122.0	122.3	122.2	122.4	123.0	123.2
	1000	121.3	121.4	121.6	121.9	121.8	122.0	122.0	122.2	122.7	122.9

Table 10 Penetration rate (mm/sec) for rocks at various thrust and air pressures
(sedimentary rock) for threaded drill bit.

Air Pressure (Kpa)	Thrust (N)	A-weighted equivalent continuous sound level (dB)									
		Shale		Dolomite		Sand stone		Lime stone		Hematite	
		Drill bit diameter in (mm)									
		35	38	35	38	35	38	35	38	35	38
392	100	0.37	0.30	0.35	0.27	0.34	0.24	0.32	0.20	0.31	0.18
	200	0.61	0.51	0.58	0.47	0.56	0.44	0.55	0.41	0.54	0.38
	300	0.89	0.77	0.87	0.74	0.84	0.71	0.82	0.68	0.79	0.65
	400	**1.20**	**1.08**	**1.15**	**1.04**	**1.12**	**1.01**	**1.09**	**0.98**	**1.05**	**0.95**
	500	0.91	0.77	0.87	0.71	0.81	0.66	0.75	0.61	0.69	0.57
	600	0.83	0.65	0.79	0.61	0.75	0.57	0.71	0.52	0.63	0.48
	700	0.68	0.49	0.65	0.44	0.50	0.41	0.55	0.37	0.47	0.23
	800	0.47	0.32	0.42	0.28	0.38	0.23	0.33	0.20	0.28	0.18
	900	0.41	0.27	0.38	0.23	0.33	0.19	0.29	0.16	0.21	0.14
	1000	0.33	0.24	0.29	0.20	0.25	0.16	0.21	0.14	0.15	0.12
441	100	0.43	0.33	0.40	0.30	0.37	0.27	0.35	0.24	0.33	0.21
	200	0.68	0.54	0.65	0.51	0.61	0.47	0.58	0.44	0.56	0.41
	300	0.98	0.88	0.95	0.85	0.91	0.82	0.87	0.79	0.83	0.76
	400	**1.38**	**1.31**	**1.28**	**1.26**	**1.21**	**1.24**	**1.21**	**1.15**	**1.11**	**1.09**
	500	1.08	1.03	1.01	0.97	0.96	0.89	0.84	0.80	0.79	0.75
	600	1.01	0.97	0.95	0.91	0.90	0.83	0.77	0.73	0.72	0.69
	700	0.85	0.81	0.78	0.74	0.74	0.65	0.62	0.58	0.46	0.50
	800	0.79	0.74	0.72	0.68	0.67	0.60	0.56	0.52	0.51	0.46
	900	0.64	0.59	0.57	0.53	0.53	0.44	0.39	0.36	0.34	0.30
	1000	0.47	0.41	0.41	0.48	0.47	0.39	0.24	0.21	0.20	0.15
490	100	0.48	0.43	0.45	0.40	0.41	0.37	0.37	0.34	0.35	0.31
	200	0.79	0.71	0.76	0.68	0.72	0.65	0.68	0.61	0.63	0.57
	300	1.31	1.21	1.28	1.17	1.24	1.13	1.21	1.05	1.17	0.98
	400	1.82	1.61	1.76	1.57	1.71	1.52	1.67	1.37	1.62	1.34
	500	**2.18**	**2.00**	**2.10**	**1.96**	**2.01**	**1.92**	**1.98**	**1.88**	**1.93**	**1.64**
	600	1.86	1.76	1.81	1.71	1.76	1.66	1.71	1.63	1.61	1.38
	700	1.75	1.69	1.72	1.64	1.69	1.60	1.65	1.38	1.54	1.31
	800	1.57	1.53	1.51	1.47	1.48	1.43	1.43	1.38	1.38	1.15
	900	1.38	1.34	1.33	1.28	1.29	1.24	1.24	1.19	1.19	0.97
	1000	1.25	1.20	1.20	1.15	1.14	1.10	1.09	1.05	1.03	0.90
539	100	0.56	0.5	0.51	0.48	0.48	0.46	0.44	0.42	0.41	0.39
	200	0.94	0.91	0.91	0.87	0.87	0.84	0.82	0.72	0.79	0.76
	300	1.46	1.41	1.41	1.37	1.38	1.33	1.26	1.20	1.21	1.17
	400	1.88	1.72	1.83	1.69	1.73	1.66	1.69	1.62	1.65	1.58
	500	2.29	2.13	2.25	2.10	2.12	2.08	2.08	2.06	2.04	1.95
	600	**2.59**	**2.48**	**2.53**	**2.45**	**2.42**	**2.40**	**2.35**	**2.32**	**2.27**	**2.19**
	700	2.28	2.21	2.20	2.15	2.15	2.10	2.09	2.03	2.02	1.96
	800	2.16	2.10	2.08	2.06	2.04	2.01	2.00	1.94	1.95	1.89
	900	1.97	1.91	1.92	1.87	1.86	1.80	1.81	1.85	1.75	1.70
	1000	1.77	1.69	1.72	1.63	1.69	1.59	1.62	1.53	1.56	1.47
588	100	0.65	0.58	0.62	0.54	0.59	0.51	0.55	0.47	0.51	0.43
	200	1.18	1.12	1.15	1.09	1.08	1.05	1.03	1.01	0.97	0.94
	300	1.71	1.61	1.67	1.57	1.56	1.52	1.49	1.42	1.39	1.37
	400	2.21	2.19	2.16	2.10	2.12	2.01	2.08	1.92	1.86	1.80
	500	2.61	2.41	2.57	2.37	2.38	2.33	2.32	2.29	2.28	2.05
	600	2.91	2.80	2.88	2.82	2.85	2.81	2.81	2.71	2.65	2.61
	700	**3.19**	**2.97**	**3.15**	**2.92**	**3.11**	**2.87**	**3.08**	**2.83**	**3.02**	**2.79**
	800	2.76	2.72	2.71	2.67	2.67	2.64	2.63	2.55	2.51	2.49
	900	2.41	2.18	2.37	2.14	2.32	2.11	2.07	2.02	2.04	1.98
	1000	1.95	1.89	1.91	1.84	1.83	1.81	1.79	1.61	1.56	1.50

Table 10 Penetration rate (mm/sec) for rocks at various thrust and air pressures (igneous rock) for threaded drill bit.

Air Pressure (kPa)	Thrust (N)	A-weighted equivalent continuous sound level (dB)									
		Dolerite		Soda granite		Black granite		Basalt		Gabbros	
		Drill bit diameter in (mm)									
		35	38	35	38	35	38	35	38	35	38
392	100	0.29	0.15	0.28	0.13	0.23	0.11	0.18	0.09	0.11	0.07
	200	0.50	0.35	0.44	0.31	0.38	0.29	0.33	0.27	0.2	0.18
	300	0.76	0.61	0.72	0.57	0.60	0.53	0.46	0.41	0.33	0.30
	400	0.97	0.92	0.92	0.75	0.80	0.71	0.65	0.61	0.49	0.38
	500	**1.33**	**0.96**	**1.21**	**0.92**	**0.97**	**0.89**	**0.76**	**0.71**	**0.61**	**0.46**
	600	1.01	0.71	0.94	0.65	0.72	0.64	0.51	0.45	0.36	0.24
	700	0.92	0.66	0.84	0.60	0.66	0.58	0.44	0.39	0.31	0.18
	800	0.74	0.48	0.64	0.41	0.51	0.41	0.32	0.22	0.2	0.15
	900	0.57	0.31	0.43	0.26	0.35	0.33	0.27	0.18	0.16	0.12
	1000	0.51	0.25	0.37	0.19	0.27	0.16	0.16	0.10	0.12	0.09
441	100	0.31	0.18	0.29	0.15	0.26	0.12	0.23	0.10	0.12	0.08
	200	0.53	0.38	0.50	0.35	0.41	0.32	0.38	0.29	0.23	0.22
	300	0.79	0.72	0.76	0.62	0.68	0.60	0.57	0.43	0.37	0.35
	400	1.08	1.02	1.04	0.90	0.96	0.78	0.75	0.62	0.52	0.50
	500	**1.35**	**1.29**	**1.25**	**1.16**	**1.18**	**1.05**	**0.93**	**0.72**	**0.63**	**0.61**
	600	1.07	0.98	0.95	0.90	0.85	0.73	0.69	0.48	0.39	0.32
	700	0.98	0.90	0.88	0.81	0.74	0.67	0.61	0.41	0.35	0.25
	800	0.81	0.71	0.72	0.62	0.57	0.52	0.45	0.23	0.24	0.20
	900	0.65	0.56	0.54	0.45	0.41	0.36	0.38	0.15	0.18	0.16
	1000	0.58	0.51	0.47	0.38	0.34	0.37	0.21	0.14	0.16	0.12
490	100	0.33	0.28	0.31	0.25	0.29	0.21	0.25	0.19	0.14	0.12
	200	0.59	0.52	0.56	0.48	0.48	0.46	0.42	0.43	0.25	0.23
	300	1.12	0.94	1.07	0.80	0.75	0.68	0.68	0.65	0.41	0.36
	400	1.57	1.31	1.51	1.02	1.03	1.00	0.94	0.91	0.55	0.53
	500	1.87	1.61	1.75	1.33	1.32	1.30	1.18	1.15	0.72	0.68
	600	**2.12**	**1.89**	**1.99**	**1.53**	**1.68**	**1.49**	**1.44**	**1.37**	**0.82**	**0.78**
	700	1.91	1.64	1.72	1.25	1.18	1.11	1.07	1.00	0.55	0.51
	800	1.81	1.57	1.66	1.18	1.11	1.02	1.01	093	0.48	0.40
	900	1.58	1.39	1.35	0.97	0.95	0.84	0.8	0.77	0.31	0.23
	1000	1.28	1.16	0.94	0.79	0.77	0.68	0.4	0.59	0.19	0.15
539	100	0.37	0.35	0.35	0.33	0.32	0.31	0.29	0.26	0.16	0.13
	200	0.74	0.71	0.71	0.62	0.62	0.61	0.55	0.48	0.27	0.25
	300	1.17	1.07	1.15	0.98	0.93	0.88	0.85	0.77	0.43	0.41
	400	1.61	1.44	1.55	1.35	1.32	1.10	1.03	1.00	0.64	0.57
	500	1.99	1.82	1.88	1.73	1.60	1.41	1.30	1.25	0.73	0.70
	600	2.16	1.97	2.01	1.94	1.88	1.66	1.58	1.44	0.84	0.81
	700	**2.41**	**2.21**	**2.29**	**2.18**	**2.13**	**1.95**	**1.65**	**1.60**	**0.95**	**0.95**
	800	1.98	1.74	1.93	1.71	1.65	1.52	1.15	0.99	0.64	0.63
	900	1.65	1.31	1.51	1.16	1.32	1.21	0.83	0.68	0.48	0.46
	1000	1.47	0.94	1.3	0.89	0.91	0.87	0.64	0.37	0.28	0.25
588	100	0.47	0.40	0.43	0.37	0.40	0.35	0.33	0.29	0.17	0.15
	200	0.93	0.91	0.89	0.72	0.77	0.71	0.58	0.51	0.3	0.28
	300	1.35	1.34	1.29	1.11	1.16	1.08	0.98	0.83	0.48	0.45
	400	1.83	1.81	1.75	1.49	1.70	1.44	1.16	1.11	0.67	0.63
	500	2.21	1.84	2.13	1.81	2.00	1.73	1.52	1.2	0.77	0.73
	600	2.58	2.45	2.52	2.23	2.28	2.14	1.71	1.49	0.87	0.83
	700	2.65	2.51	2.59	2.27	2.30	2.19	1.68	1.45	0.98	0.87
	800	**2.75**	**2.73**	**2.69**	**2.51**	**2.48**	**2.33**	**1.89**	**1.63**	**1.02**	**0.98**
	900	1.96	2.01	1.88	1.75	1.77	1.64	1.22	0.88	0.64	0.60
	1000	1.51	1.26	1.4	1.24	1.27	1.02	0.73	0.52	0.35	0.32
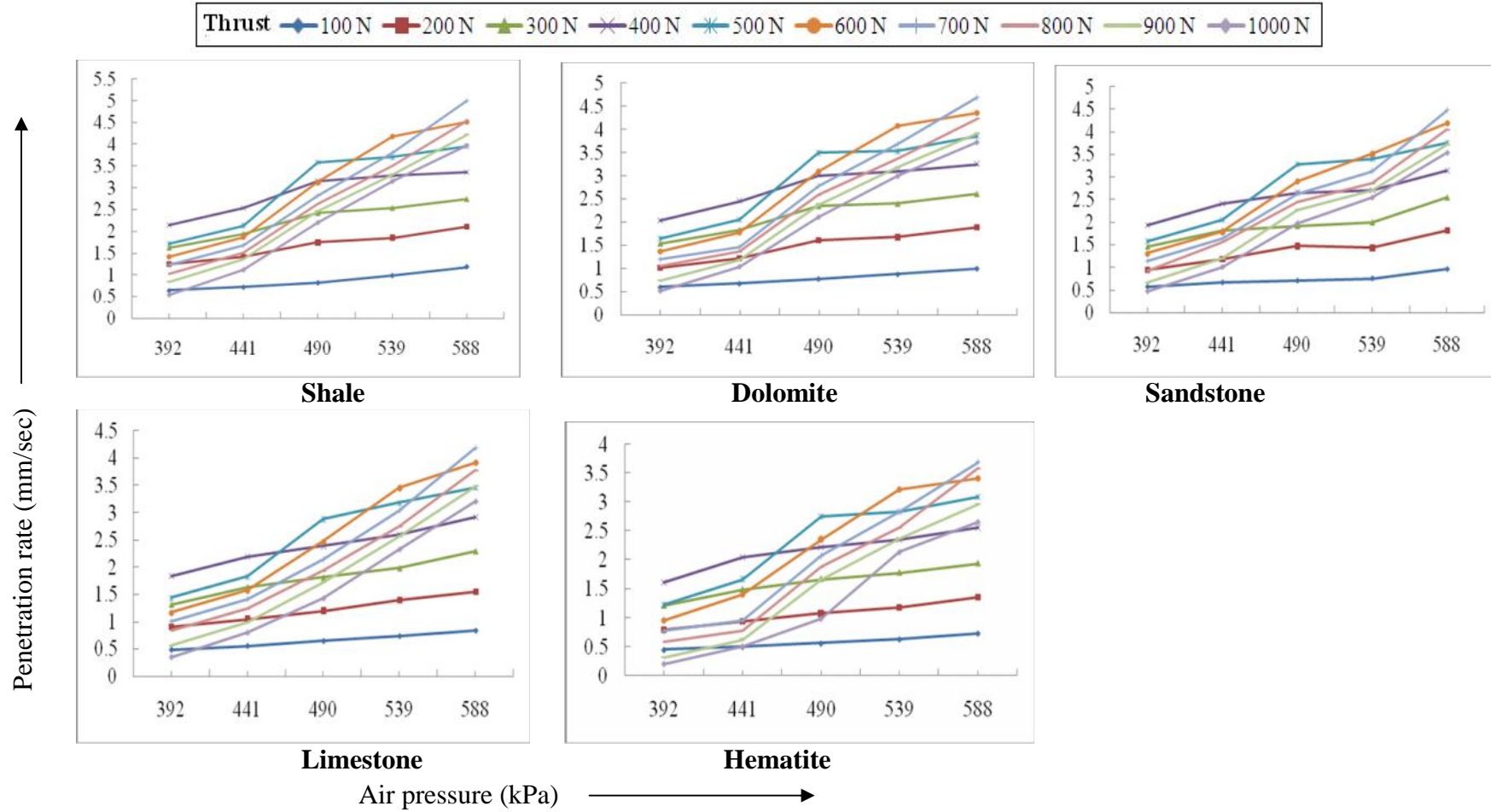
Fig. 5.1a Influence of air pressure on penetration rate for integral drill bit diameter of 30 mm with varying thrust for five different sedimentary rocks

Thrust ◆100 N ■200 N ▲300 N ✕400 N ✳500 N ●600 N ─700 N ─800 N ─900 N ◆1000 N

Dolerite

Soda granite

Black granite

Basalt

Gabbros

Penetration rate (mm/sec)
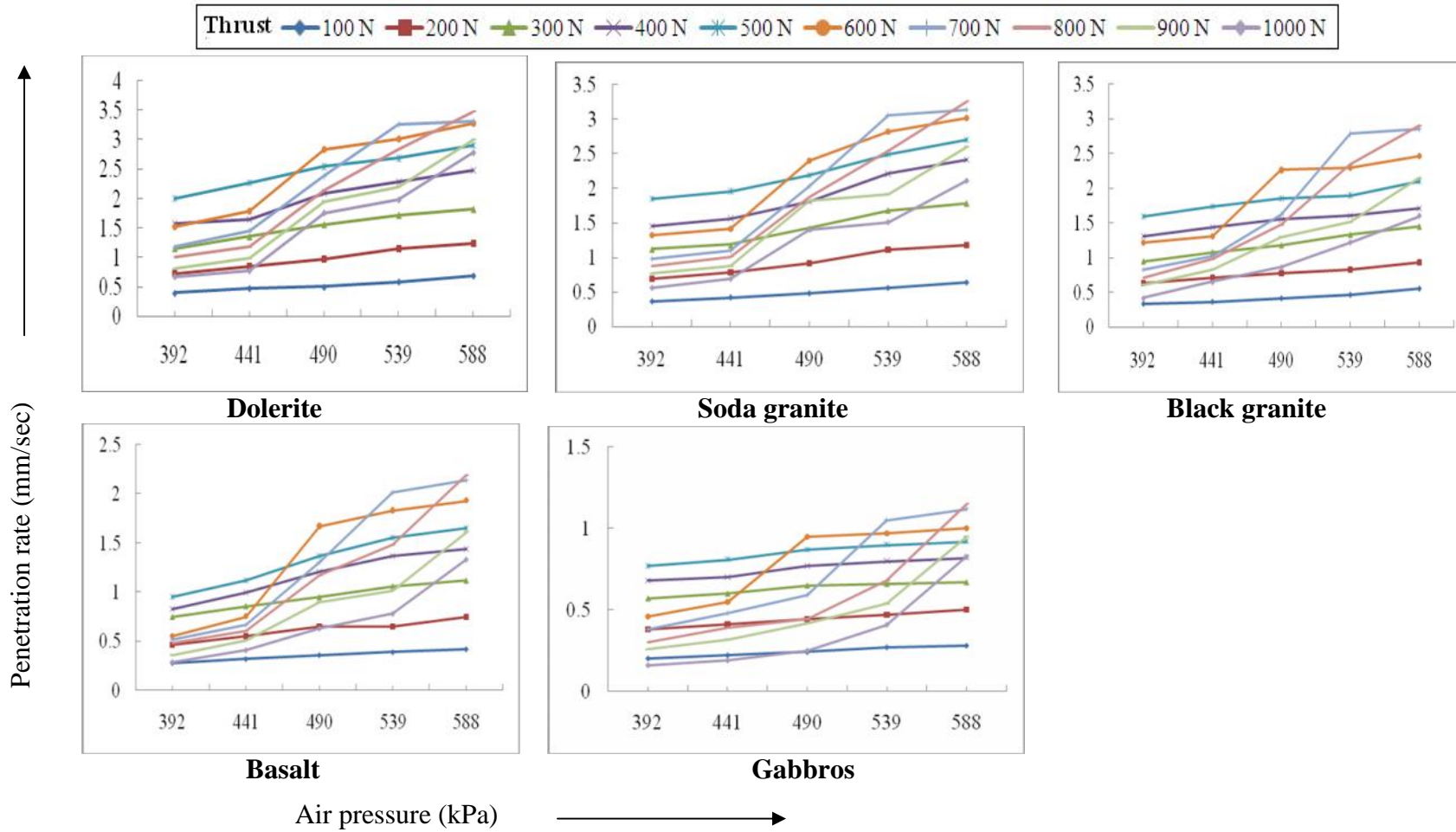
Air pressure (kPa)

Fig. 5.1b Influence of air pressure on penetration rate for integral drill bit diameter of 30 mm with varying thrust for five different igneous rocks

Penetration rate (mm/sec)

Fig. 5.2a Influence of air pressure on penetration rate for threaded drill bit diameter of 35 mm with varying thrust for five different sedimentary rocks

Thrust: —◆— 100 N —■— 200 N —▲— 300 N —✳— 400 N —✳— 500 N —●— 600 N —+— 700 N —— 800 N —— 900 N —◆— 1000 N

Dolerite

Soda granite

Black granite

Basalt

Gabbros
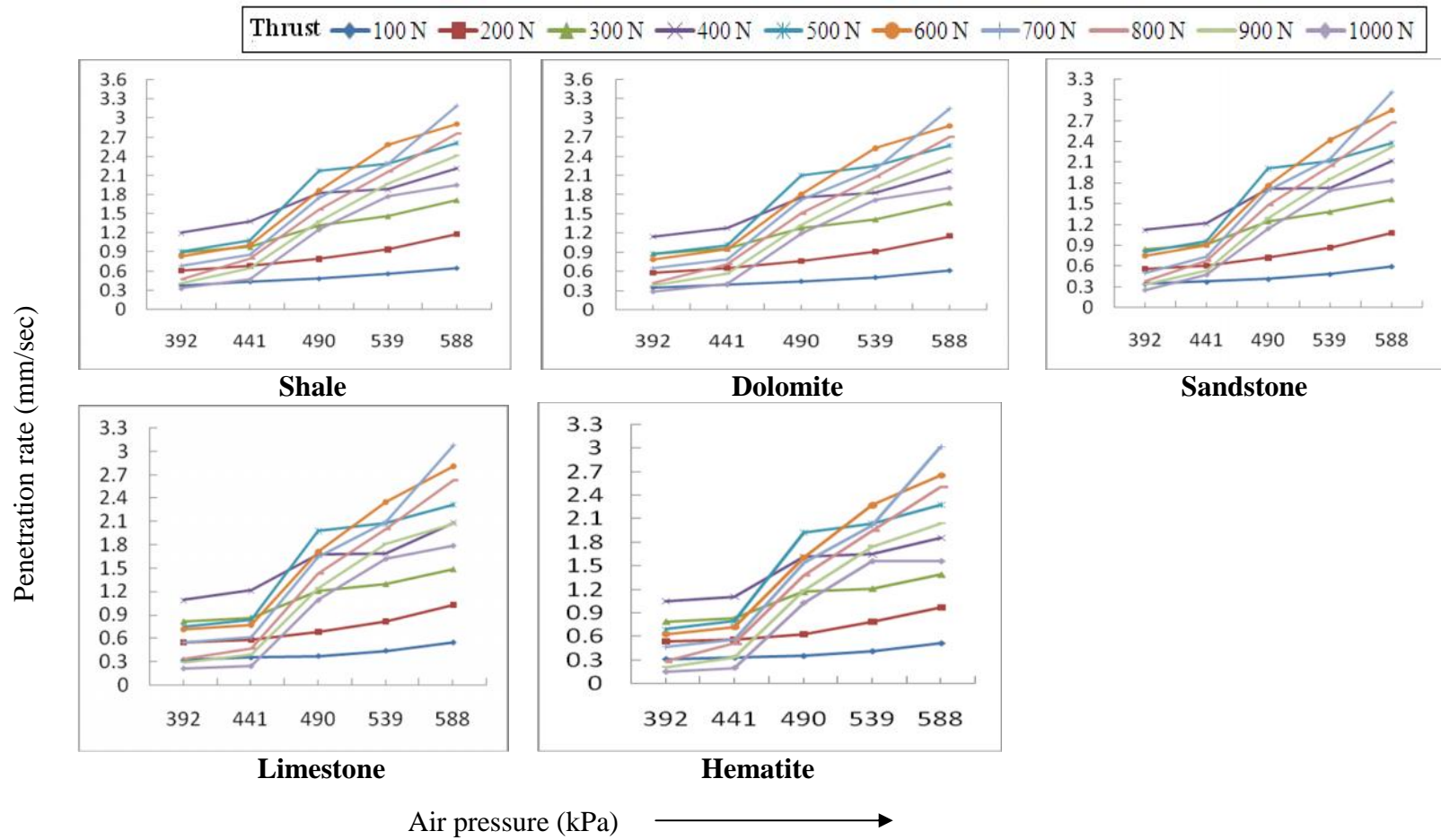
Penetration rate (mm/sec)
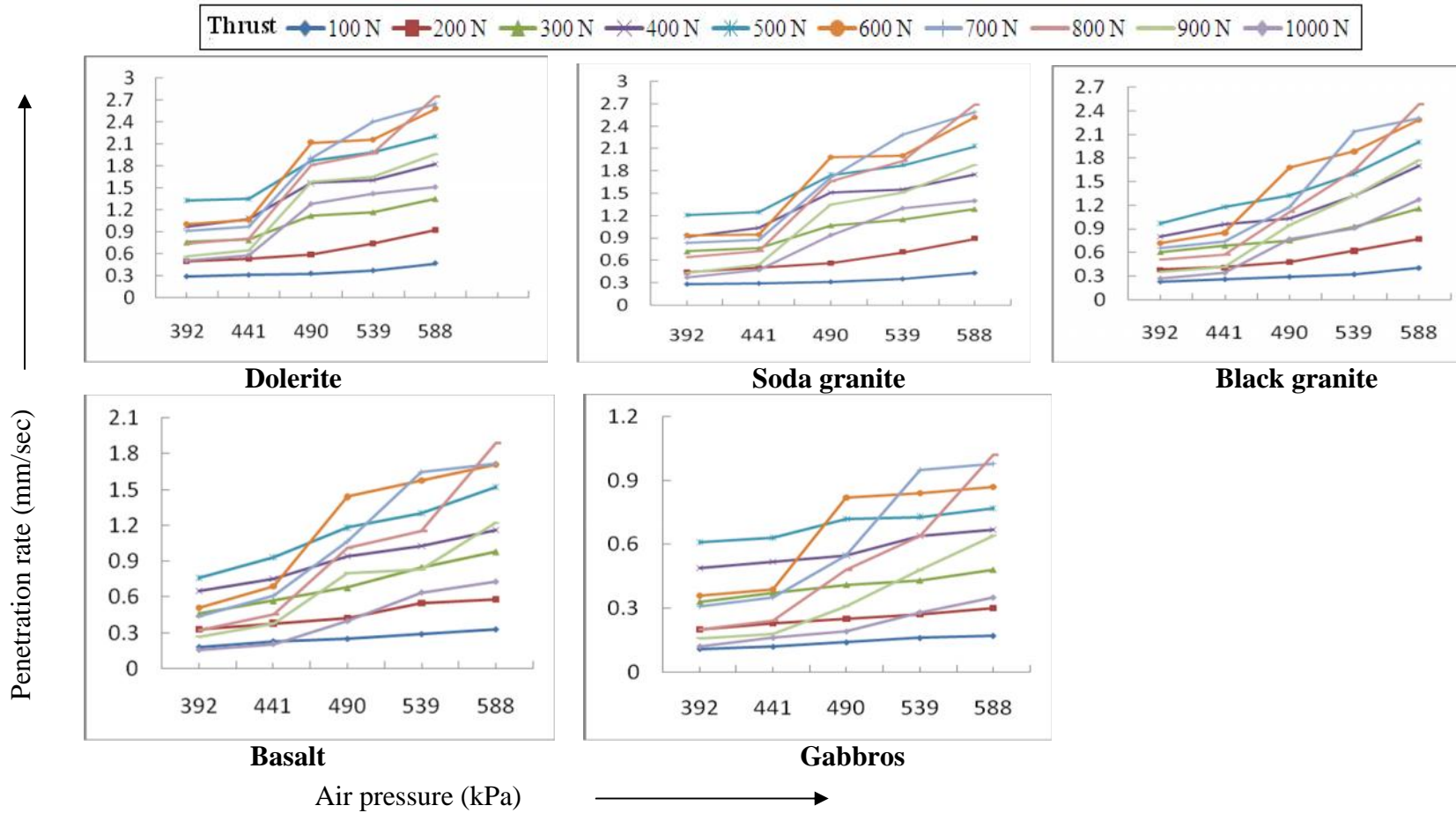
Air pressure (kPa)

Fig. 5.2b Influence of air pressure on penetration rate for threaded drill bit diameter of 35 mm with varying thrust for five different igneous rocks

Fig. 5.3a Influence of thrust on penetration rate for integral drill bit diameter of 30 mm with varying air pressure for five different sedimentary rocks
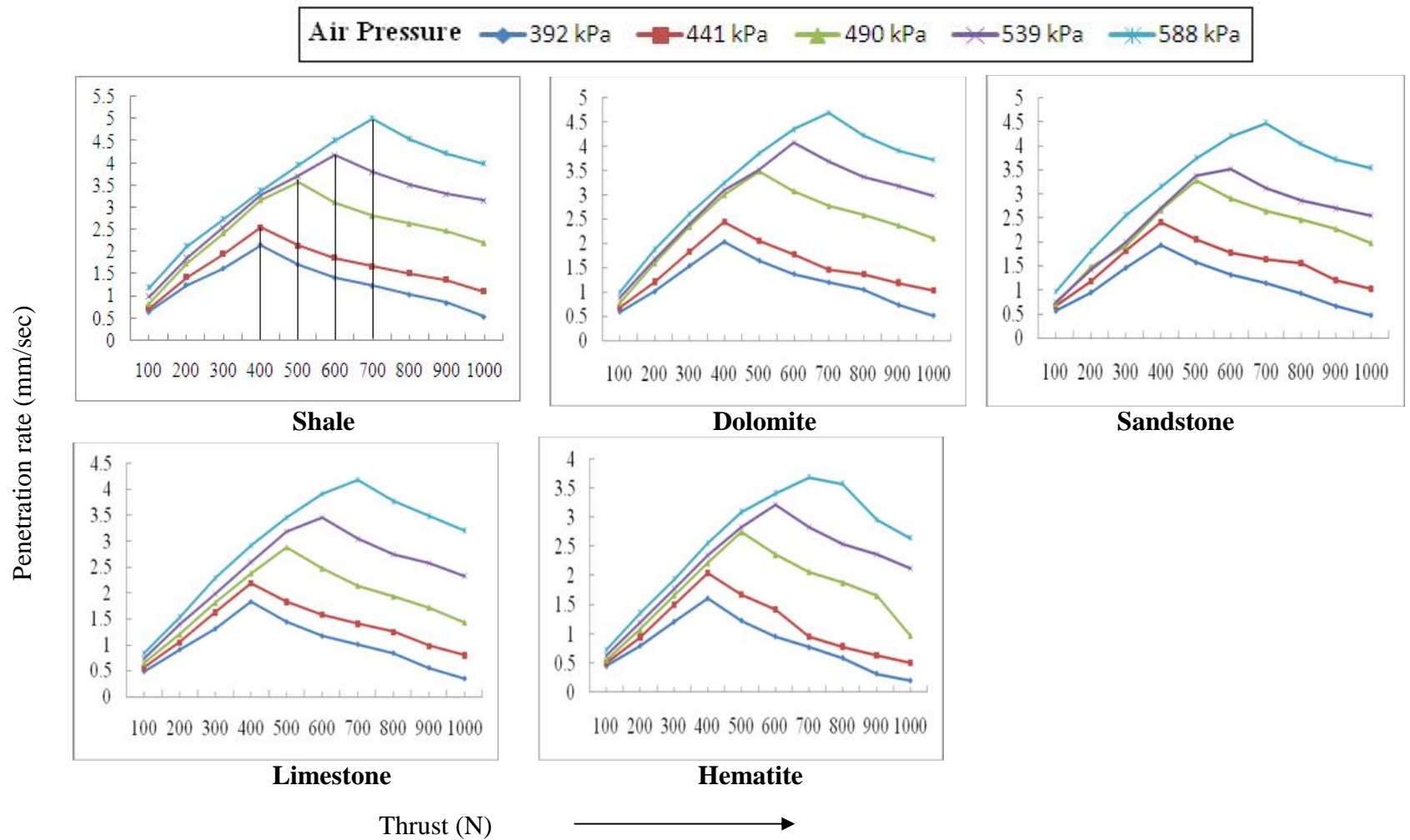
Penetration rate (mm/sec)
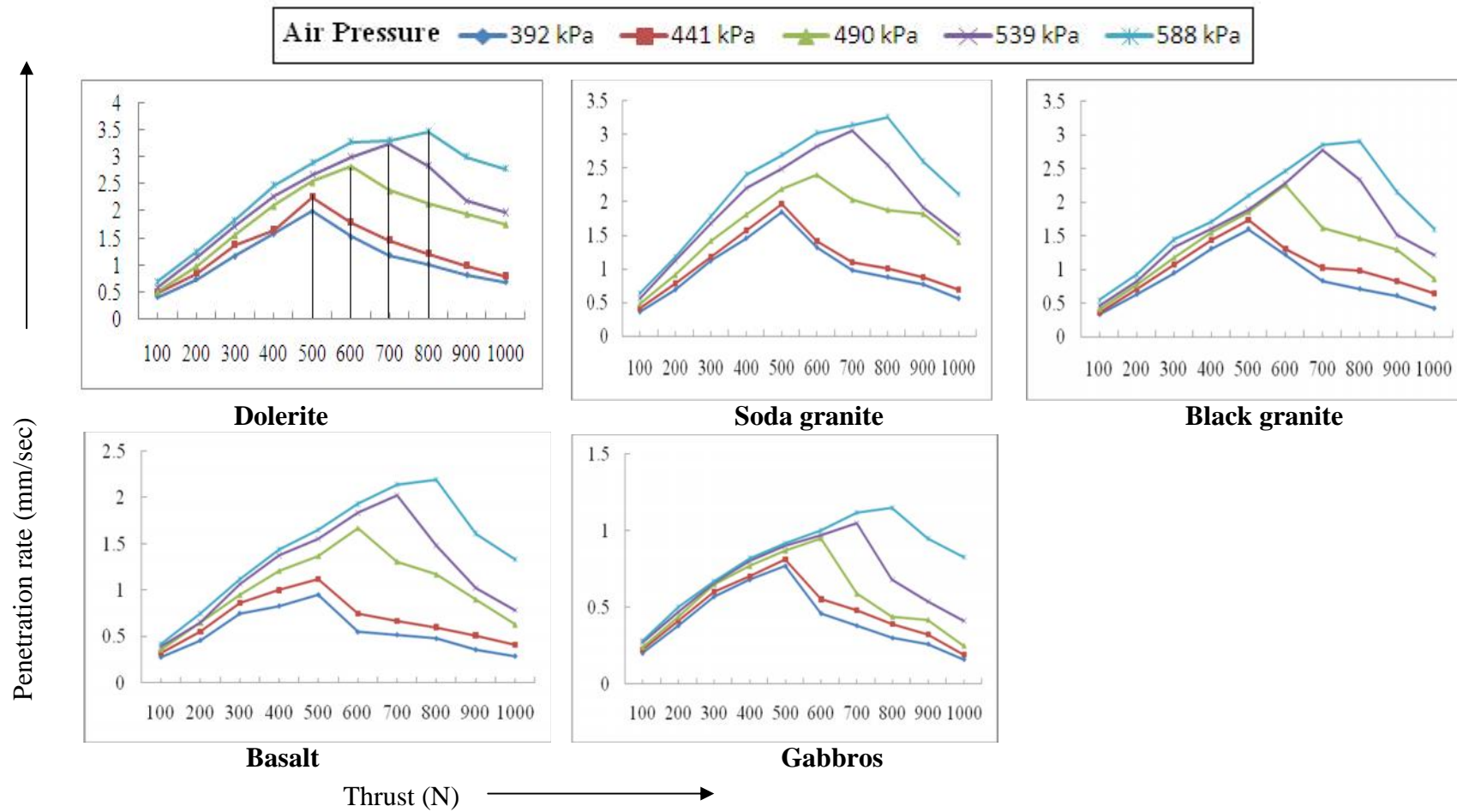
Thrust (N)

Fig. 5.3b Influence of thrust on penetration rate for integral drill bit diameter of 30 mm with varying air pressure for five different igneous rocks

Fig. 5.4a Influence of thrust on penetration rate at air pressure of 588 kPa with varying integral drill bit diameter for five different sedimentary rocks
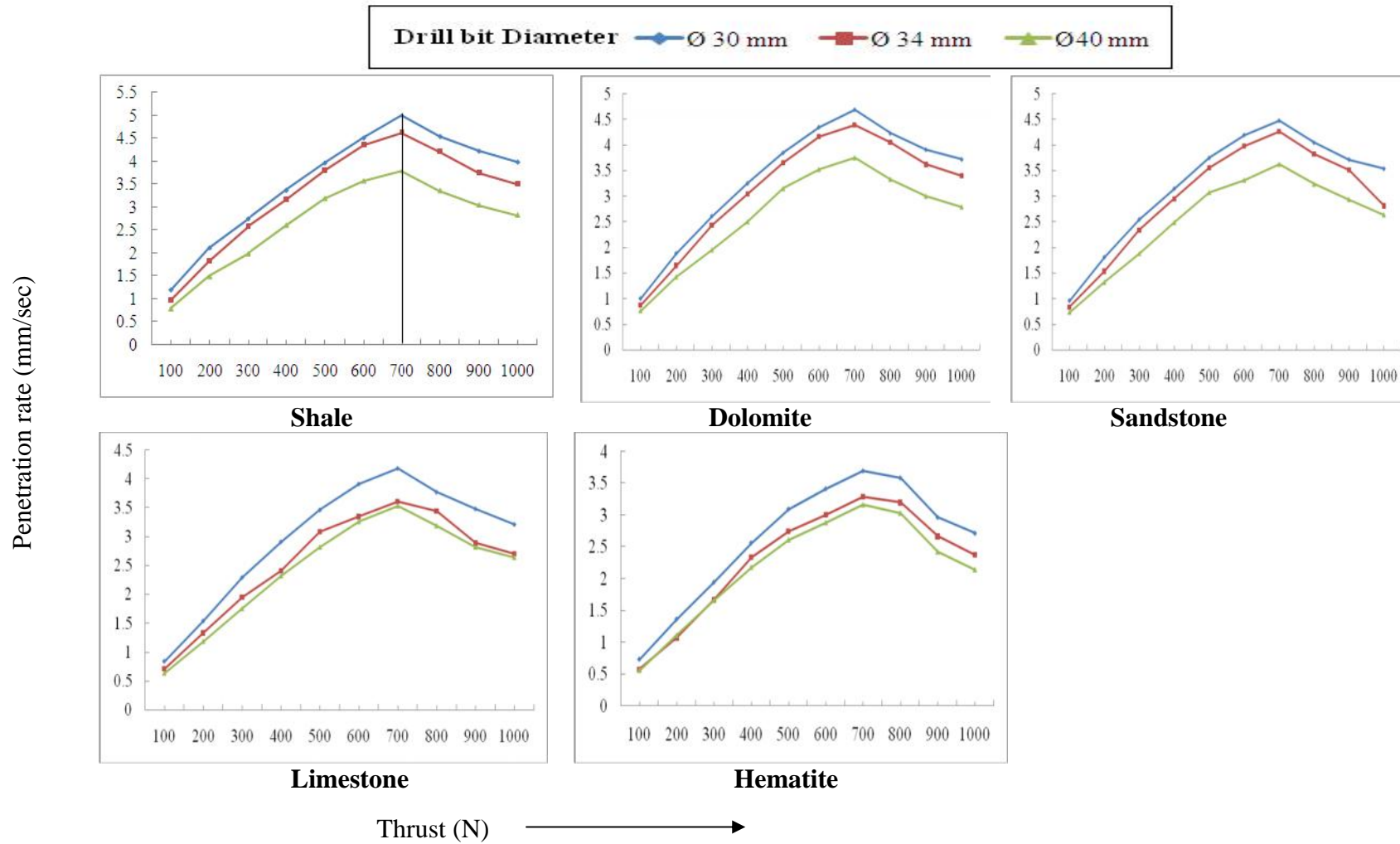
Penetration rate (mm/sec)
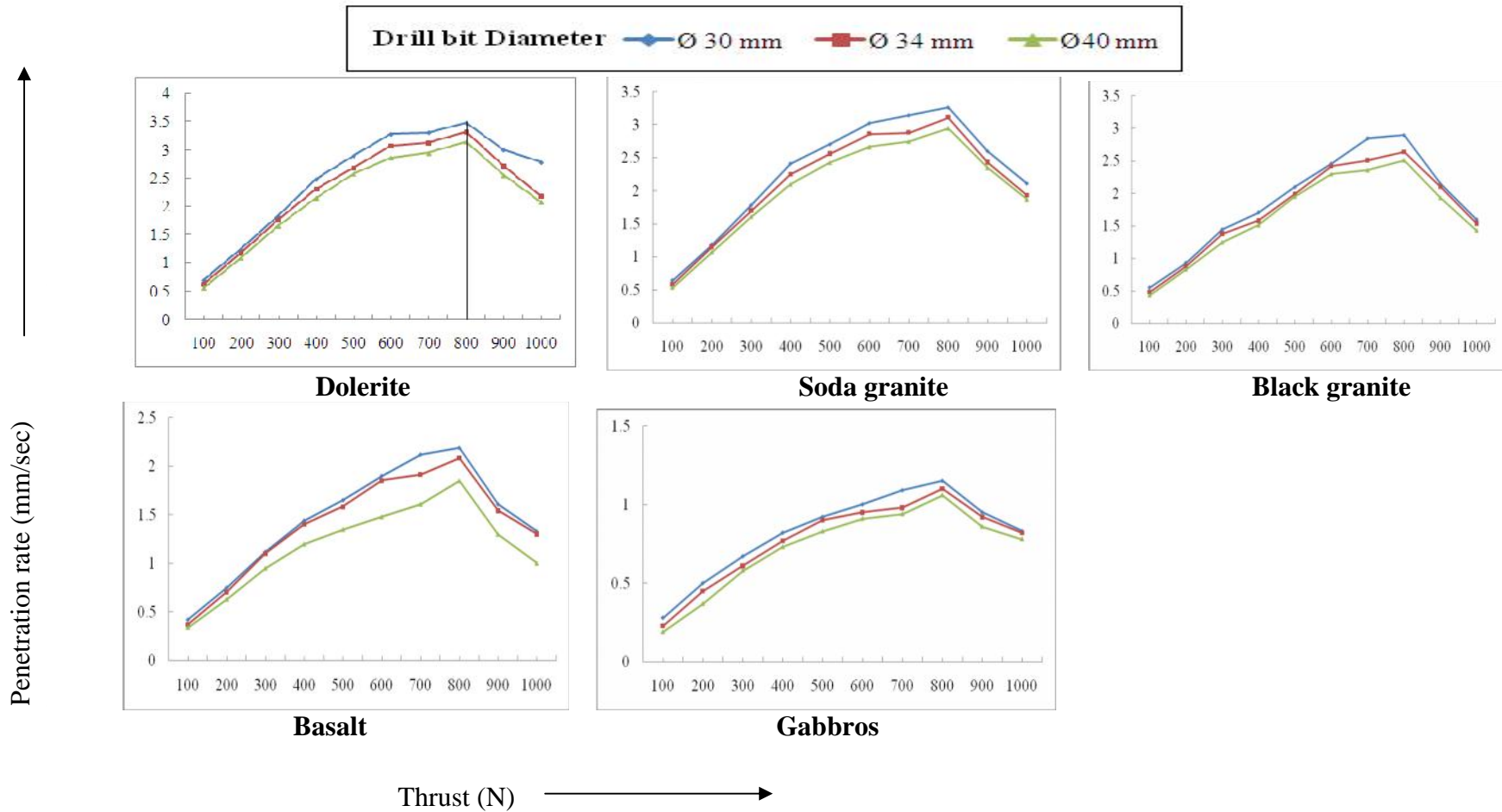
Thrust (N) ⟶

Fig. 5.4b Influence of thrust on penetration rate at air pressure of 588 kPa with varying integral drill bit diameter for next five different igneous rocks

Fig. 5.5a Influence of thrust on penetration rate for integral drill bit diameter of 35mm threaded with varying air pressure for five different sedimentary rocks

Penetration rate (mm/sec)

Thrust (N)

Fig. 5.5b Influence of thrust on penetration rate for integral drill bit diameter of 35mm threaded with varying air pressure for five different igneous rocks

Penetration rate (mm/sec)

Shale

Dolomite

Sandstone

Limestone

Hematite
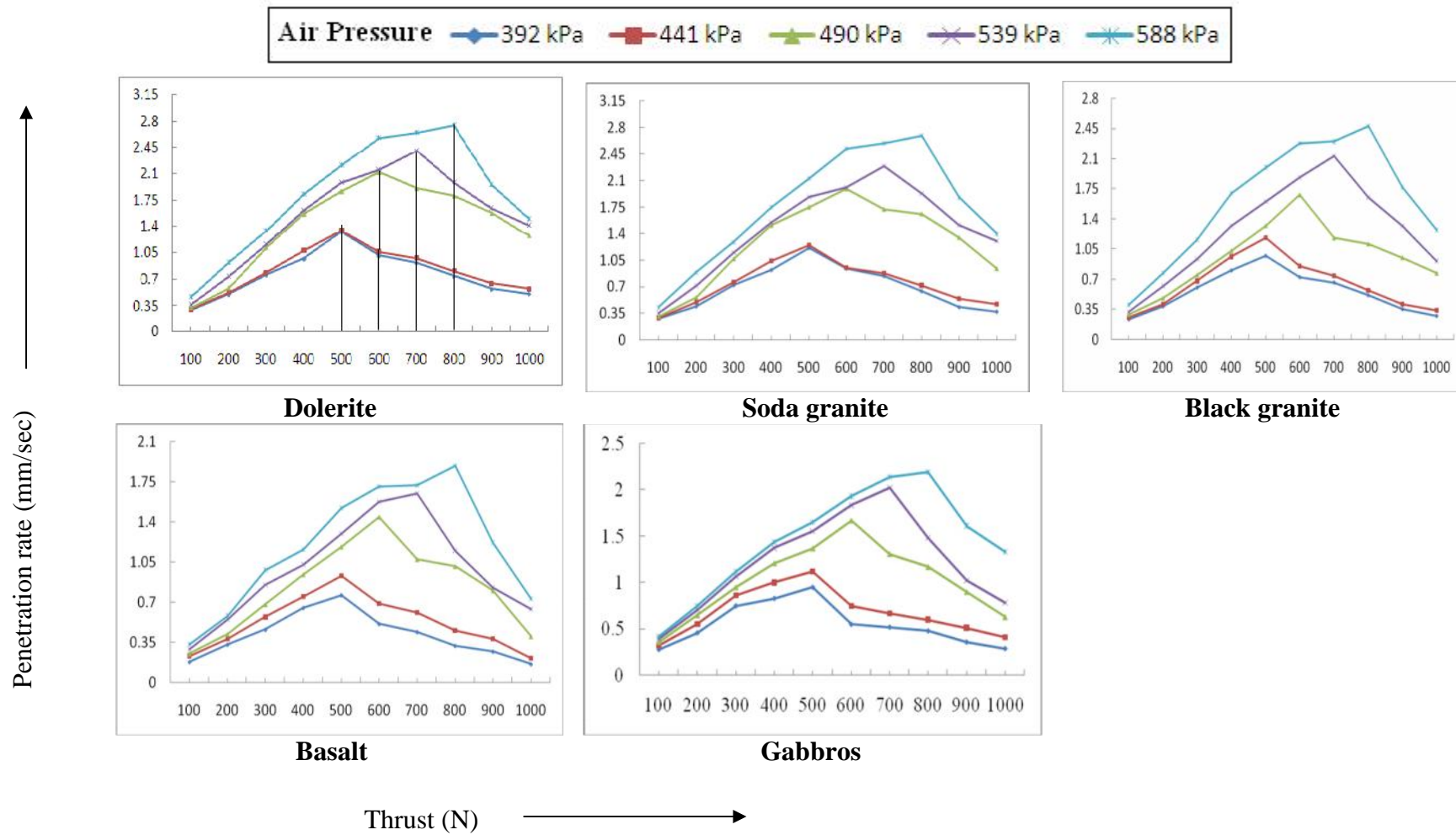
Thrust (N)

Fig. 5.6a Influence of thrust on penetration rate at air pressure of 588 kPa with varying threaded drill bit diameter for five different
sedimentary rocks
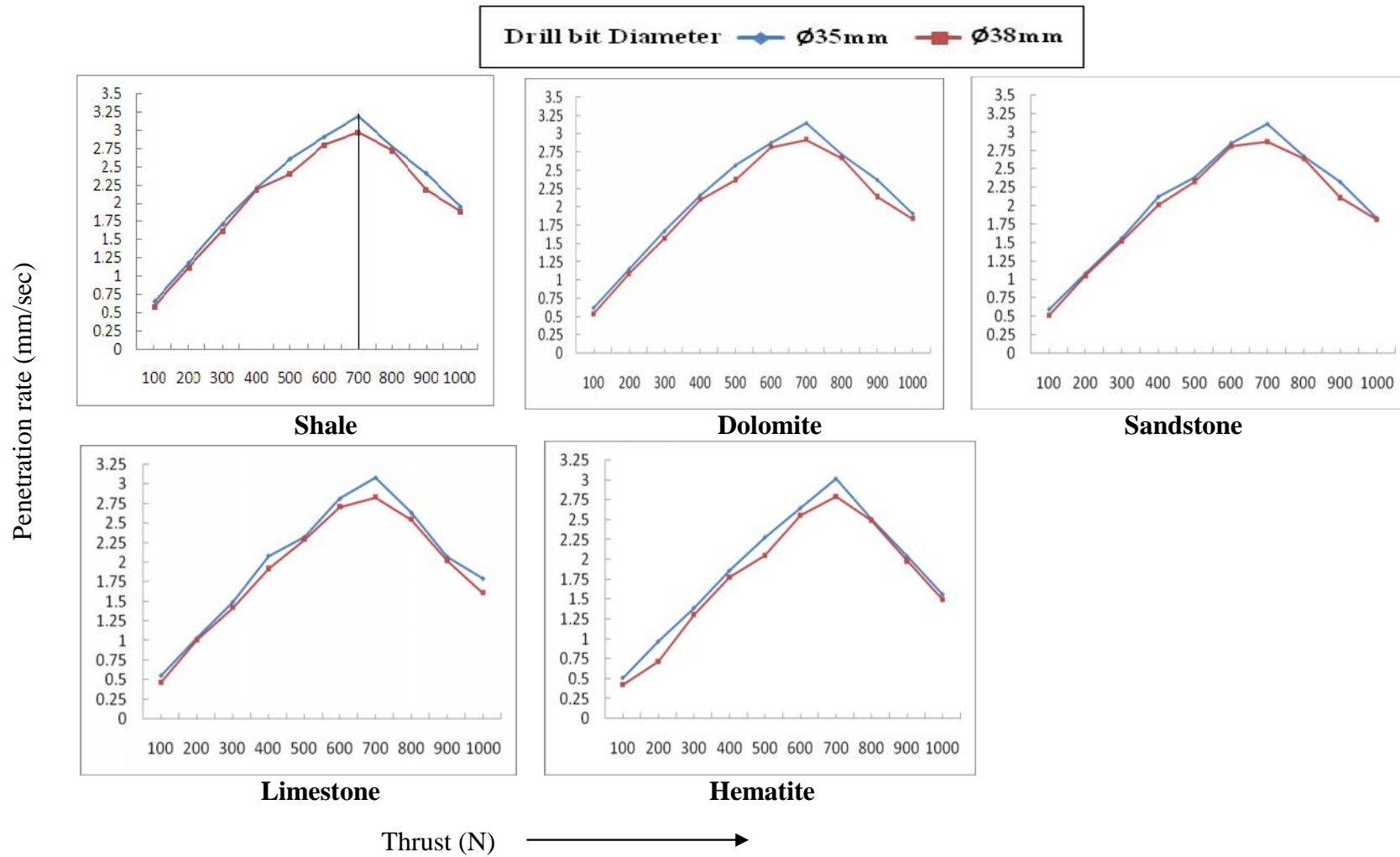
Penetration rate (mm/sec)
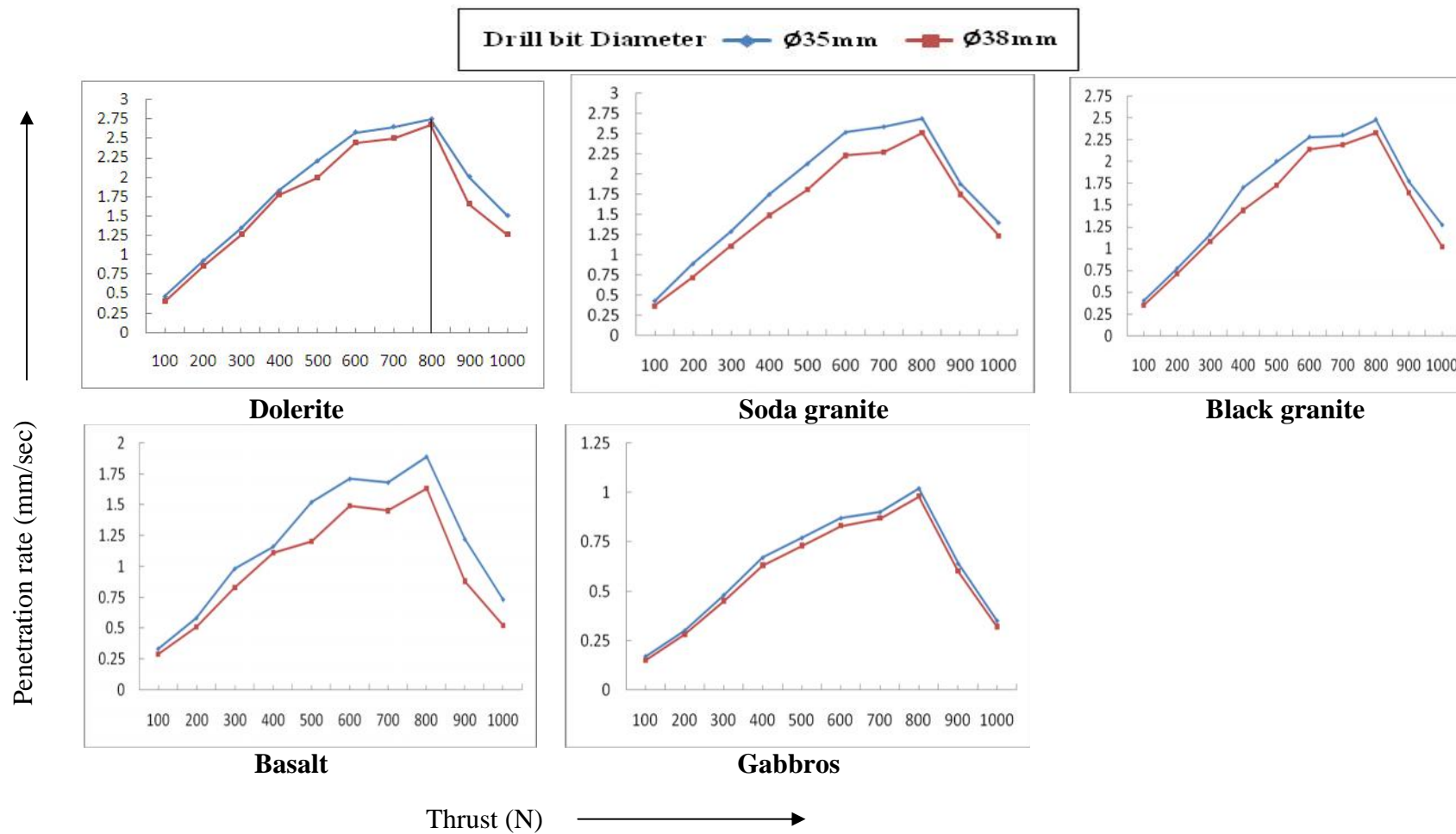
Thrust (N)

Fig. 5.6b Influence of thrust on penetration rate at air pressure of 588 kPa with varying threaded drill bit diameter for five different igneous rocks
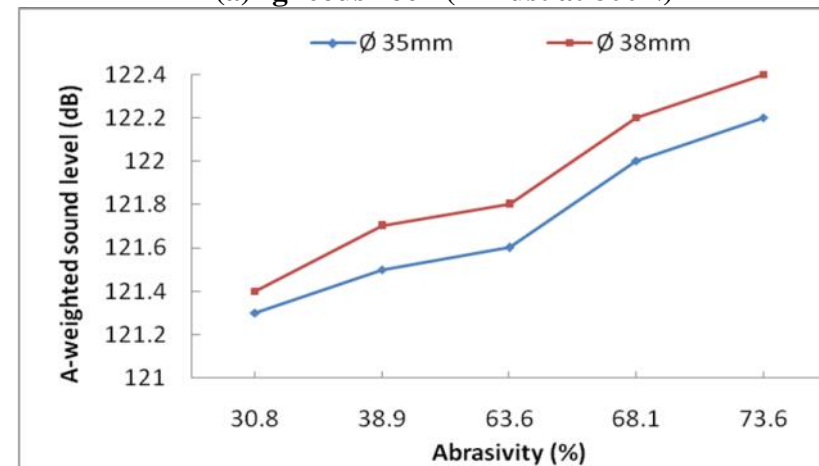
(a) Sedimentary rock (Thrust at 700N)

(a) Igneous rock (Thrust at 800N)

(b) Sedimentary rock (Thrust at 700N)

(b) Igneous rock (Thrust at 800N)

Fig. 5.7 Influence of UCS on penetration rate at air pressure of 588 kPa with (a) Integral and (b) Threaded drill bit diameters for different sedimentary and igneous rocks
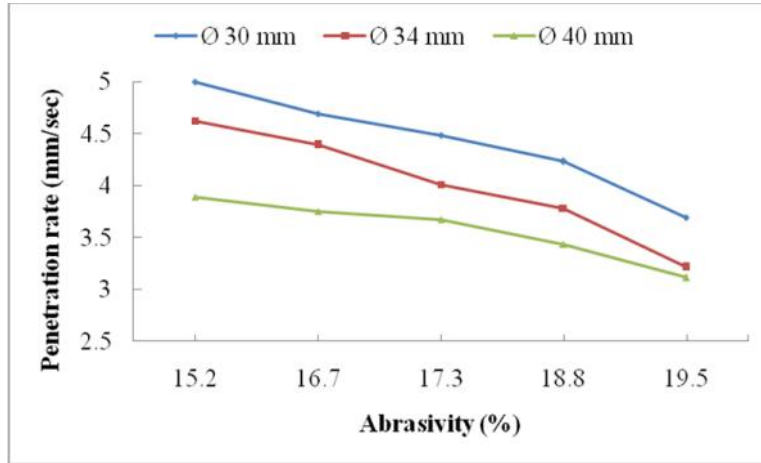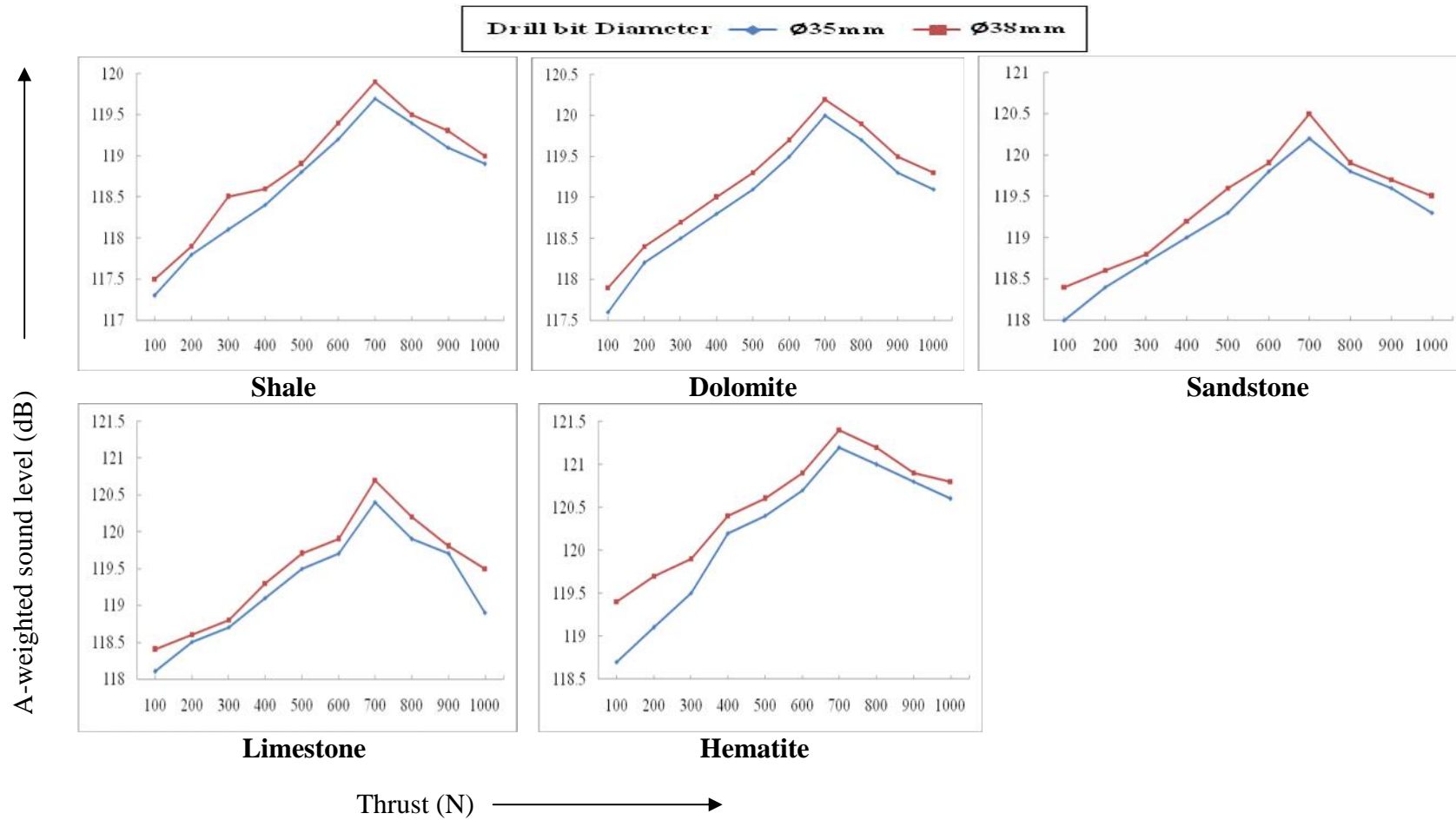
(a) Sedimentary rock (Thrust at 700N)
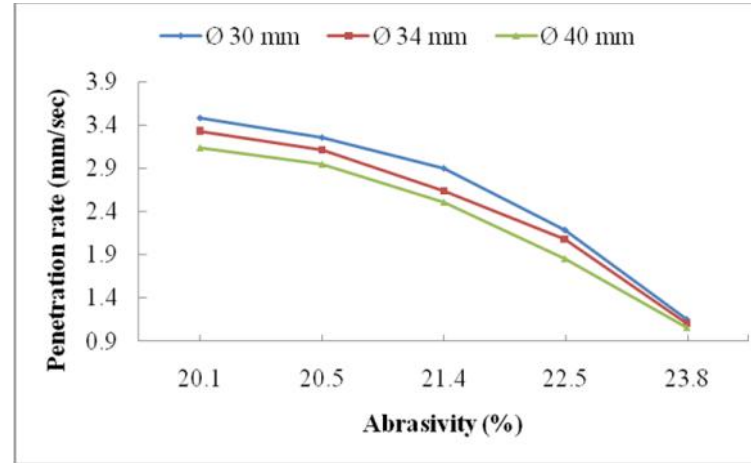
(a) Igneous rock (Thrust at 800N)
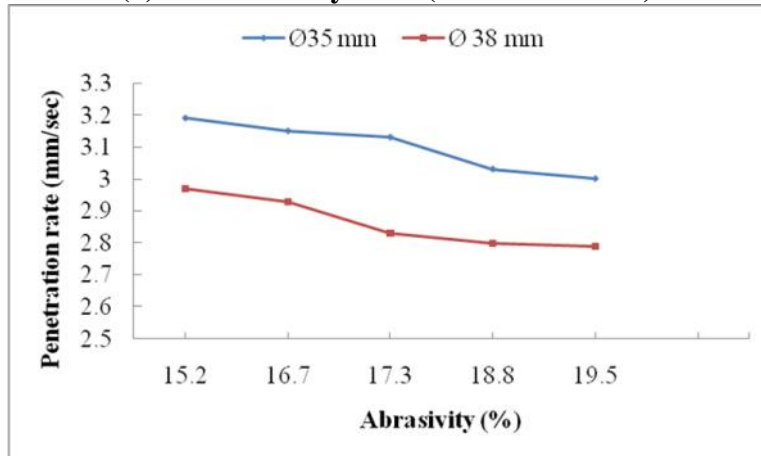
(b) Sedimentary rock (Thrust at 700N)
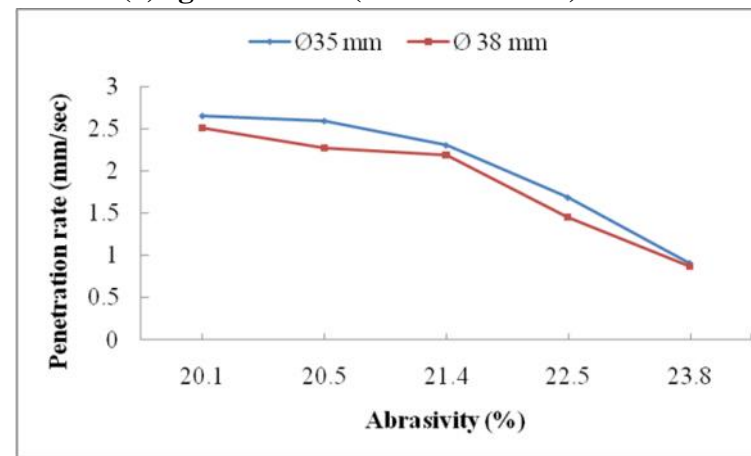
(b) Igneous rock (Thrust at 800N)

Fig. 5.8 Influence of abrasivity on penetration rate at air pressure of 588 kPa with (a) Integral and (b) Threaded drill bit diameters for sedimentary and igneous rocks

Fig. 5.9a Influence of integral bit diameter on penetration rate at air pressure of 588 kPa with varying thrust for five different sedimentary rocks
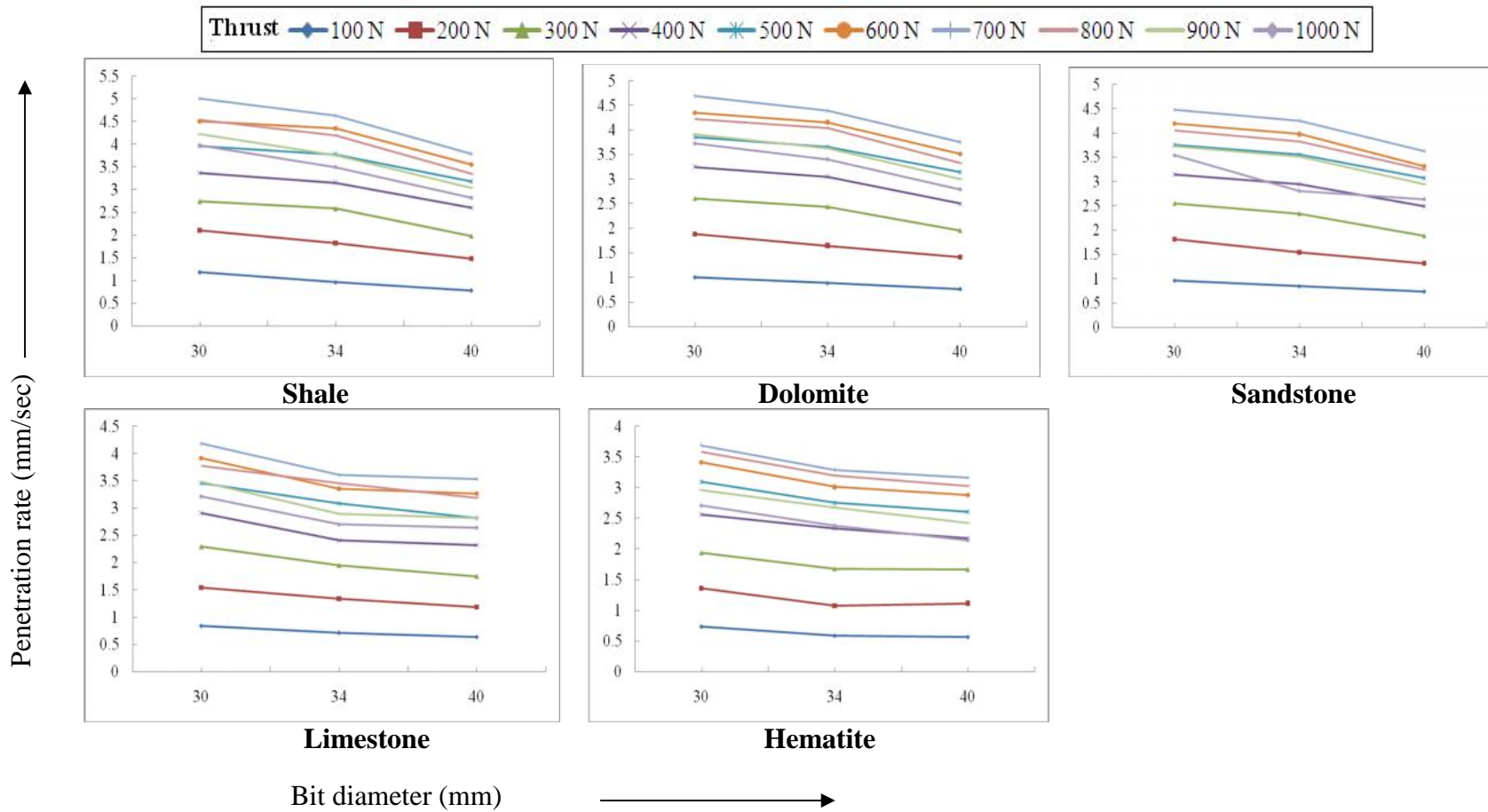
Penetration rate (mm/sec)
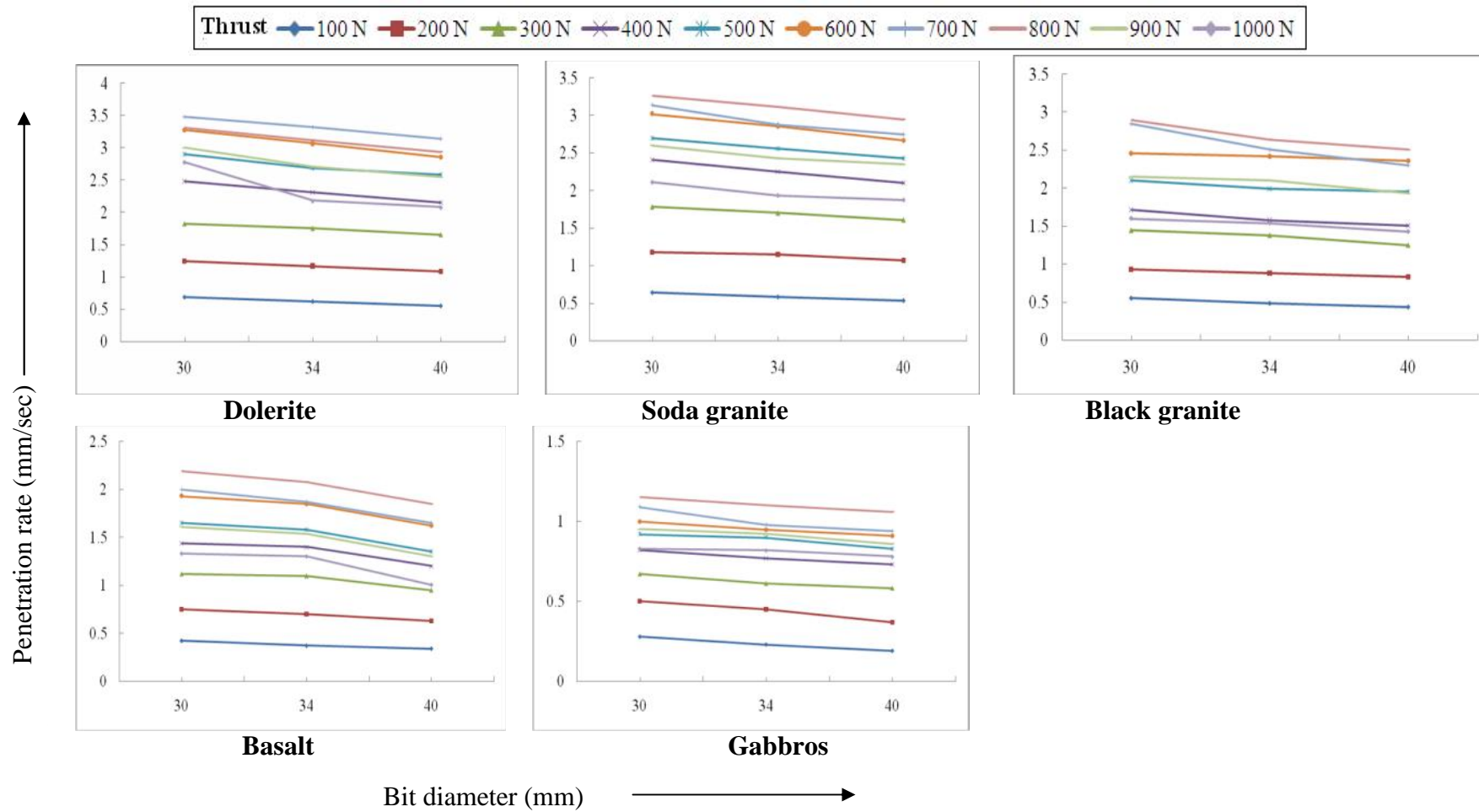
Bit diameter (mm)

Fig. 5.9b Influence of integral bit diameter on penetration rate at air pressure of 588 kPa with varying thrust for five different igneous rocks
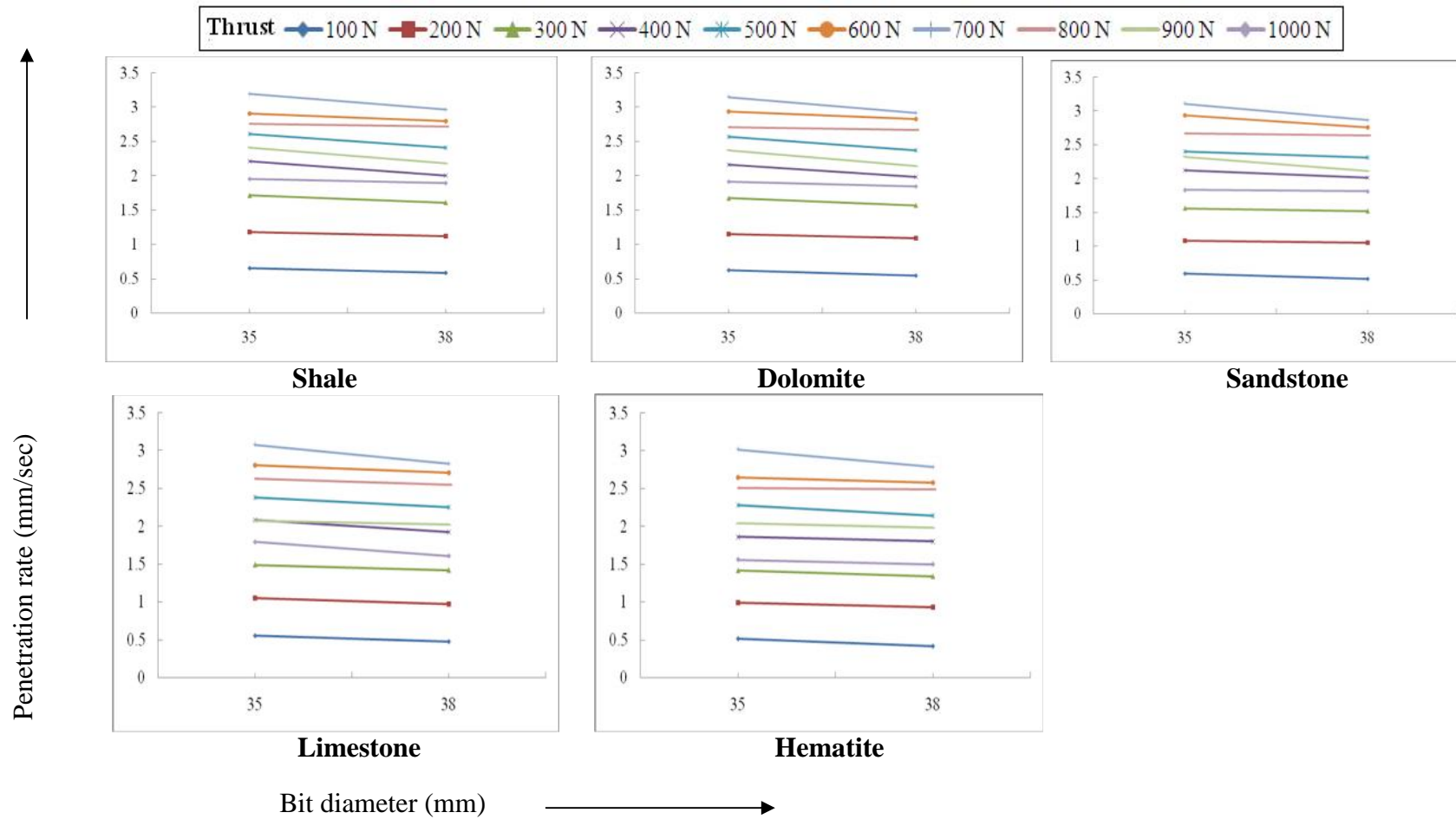
Fig.5.10a Influence of threaded bit diameter on penetration rate at air pressure of 588 kPa with varying thrust for five different sedimentary rocks

Penetration rate (mm/sec)
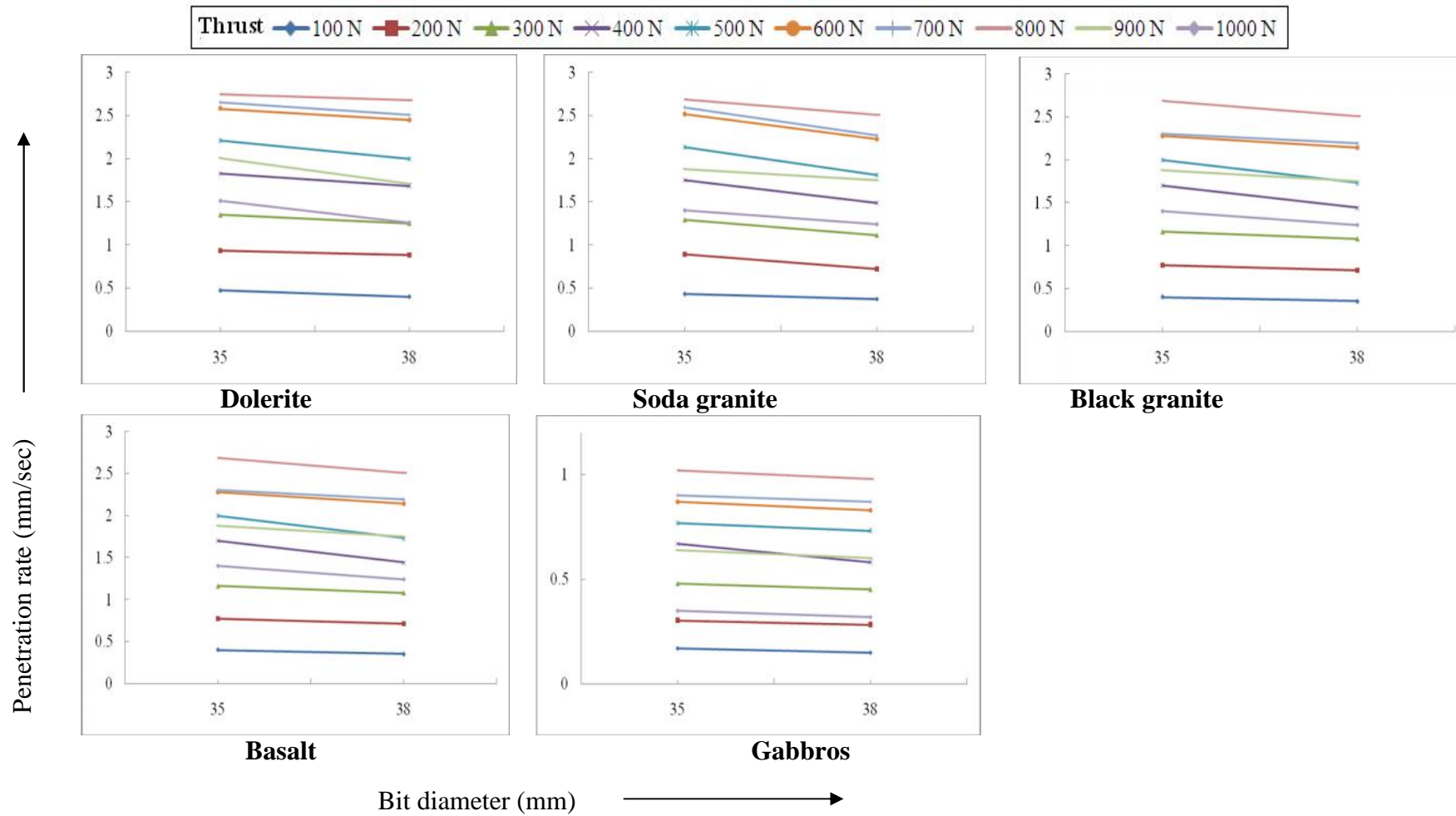
Bit diameter (mm)

Fig. 5.10b Influence of threaded bit diameter on penetration rate at air pressure of 588 kPa with varying thrust for five different igneous rocks
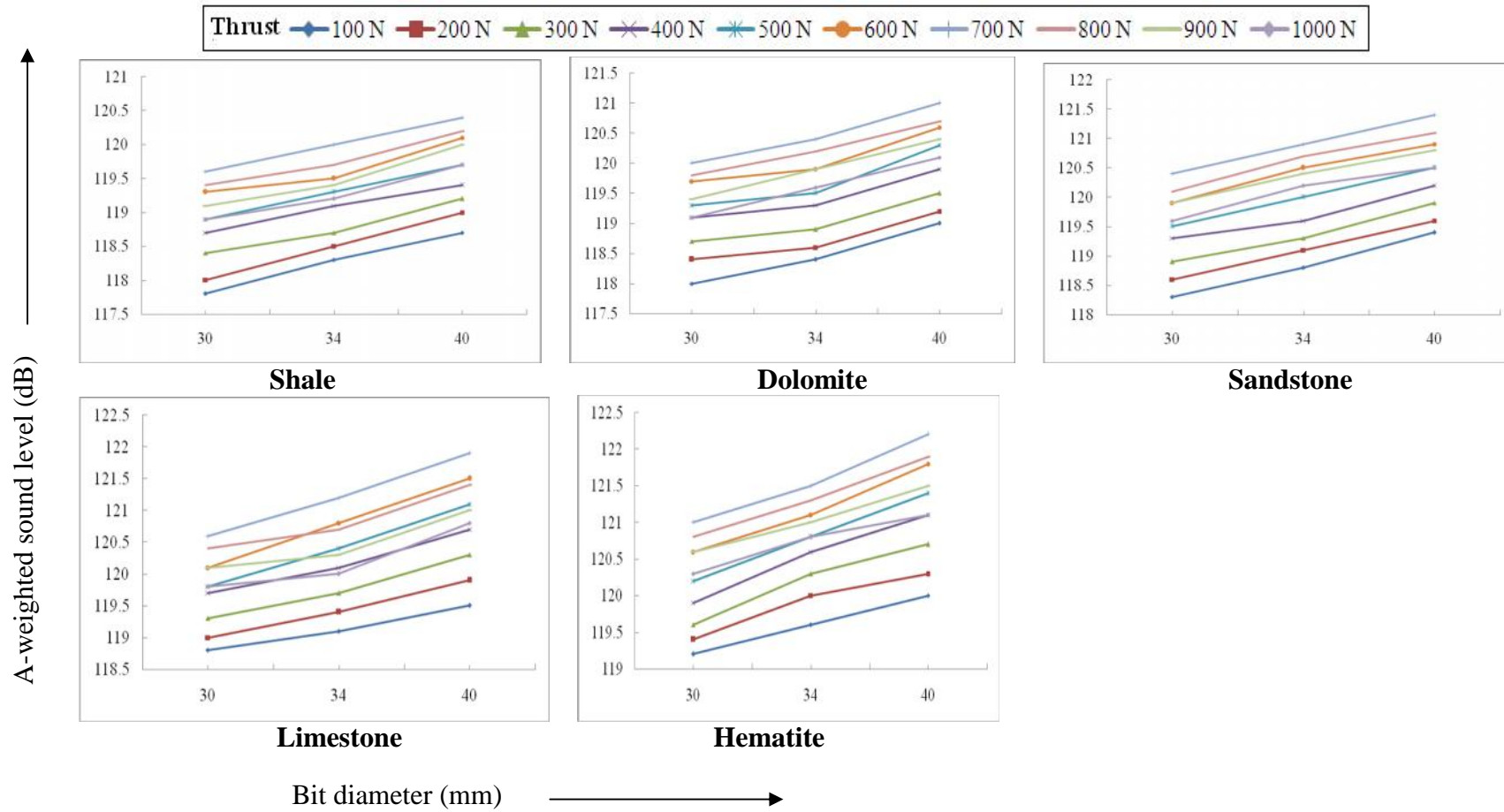
Fig. 5.11a Influence of integral bit diameter on sound level at operator's position at air pressure of 588 kPa with varying thrust for five different sedimentary rocks
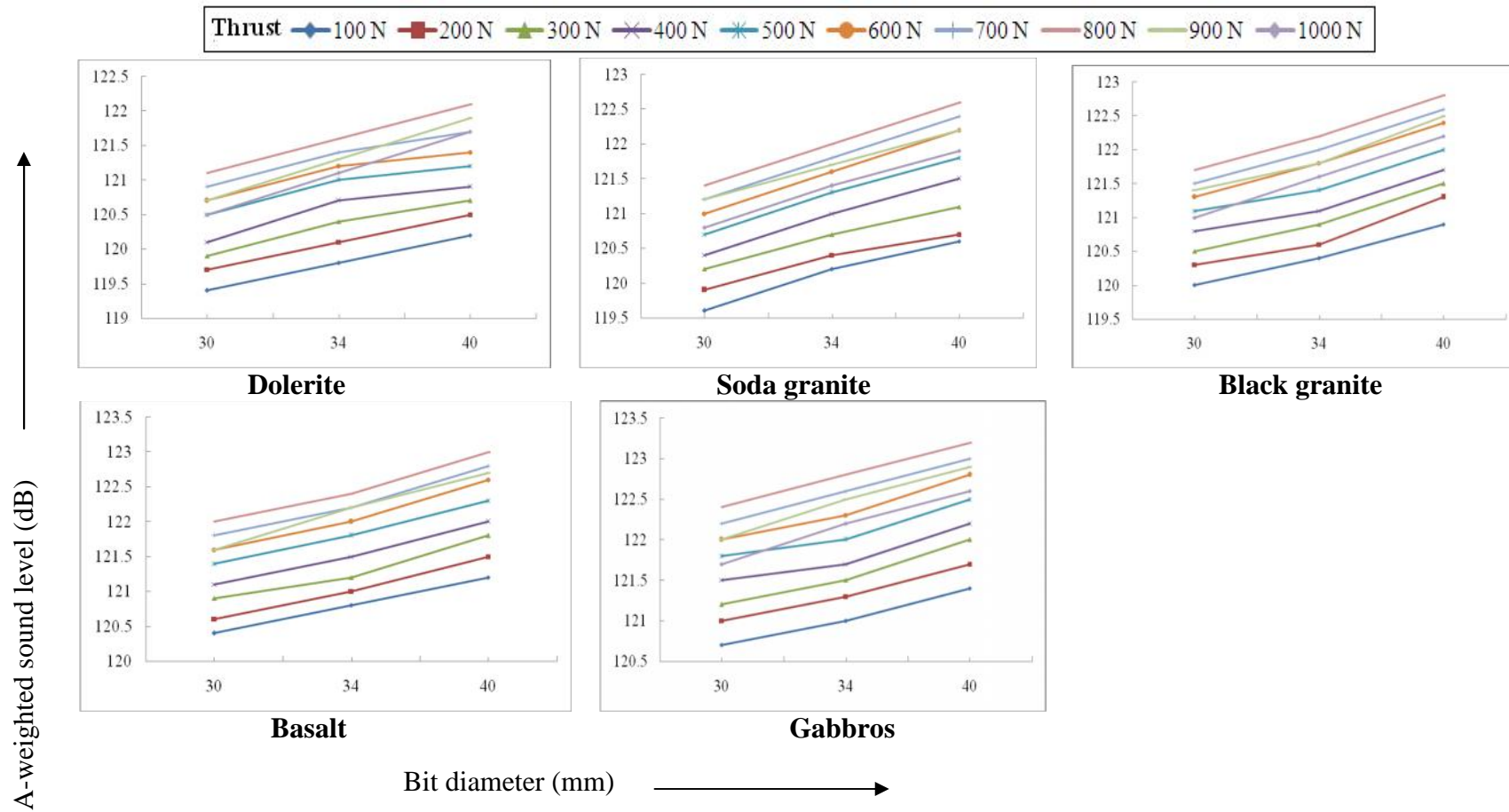
Fig. 5.11b Influence of integral bit diameter on sound level at operator's position at air pressure of 588 kPa with varying thrust for five different igneous rocks
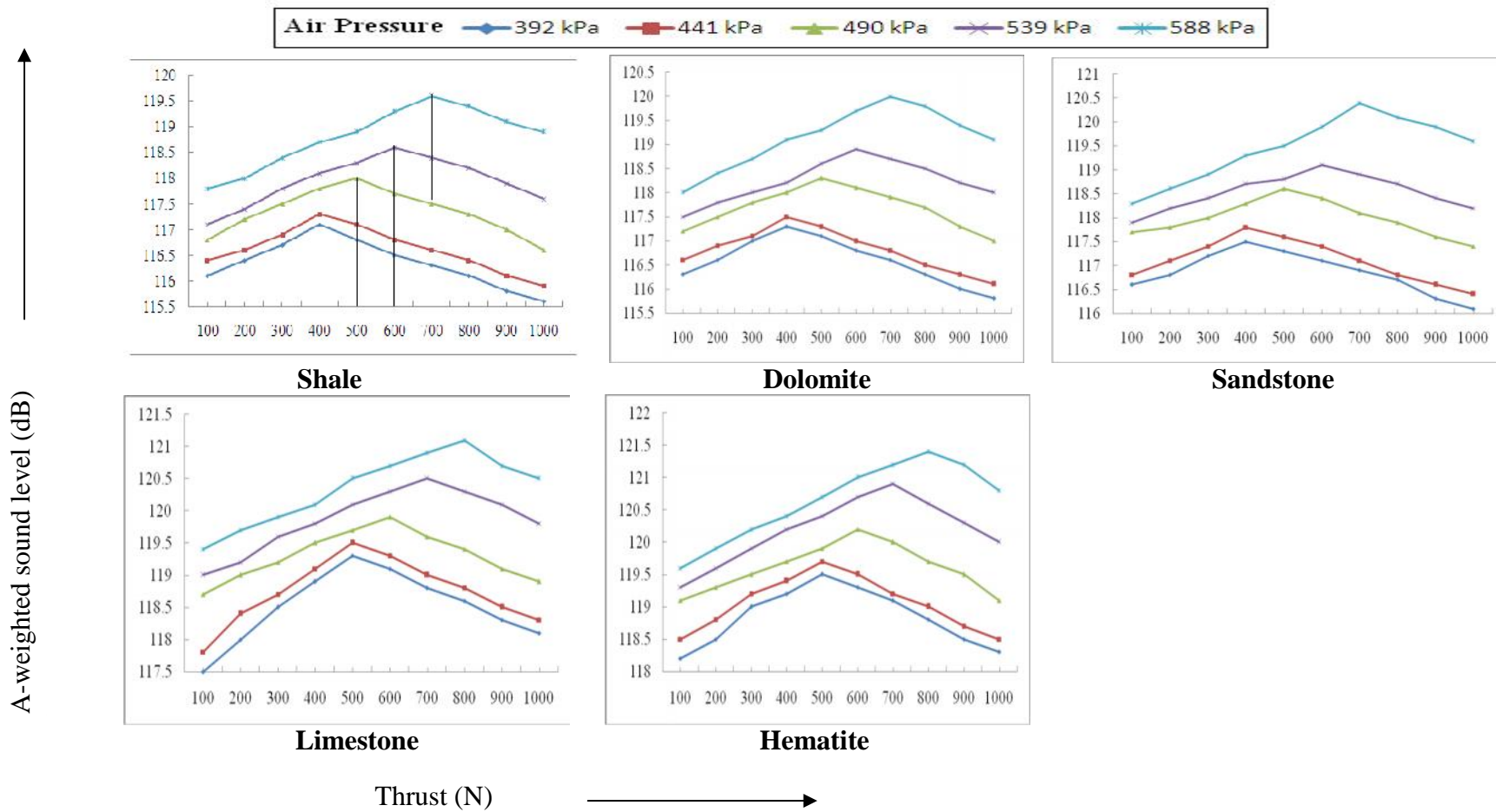
Fig. 5.12a Influence of thrust on A-weighted sound level at operator`s position for integral drill bit diameter of 30 mm with varying air pressure for five different sedimentary rocks
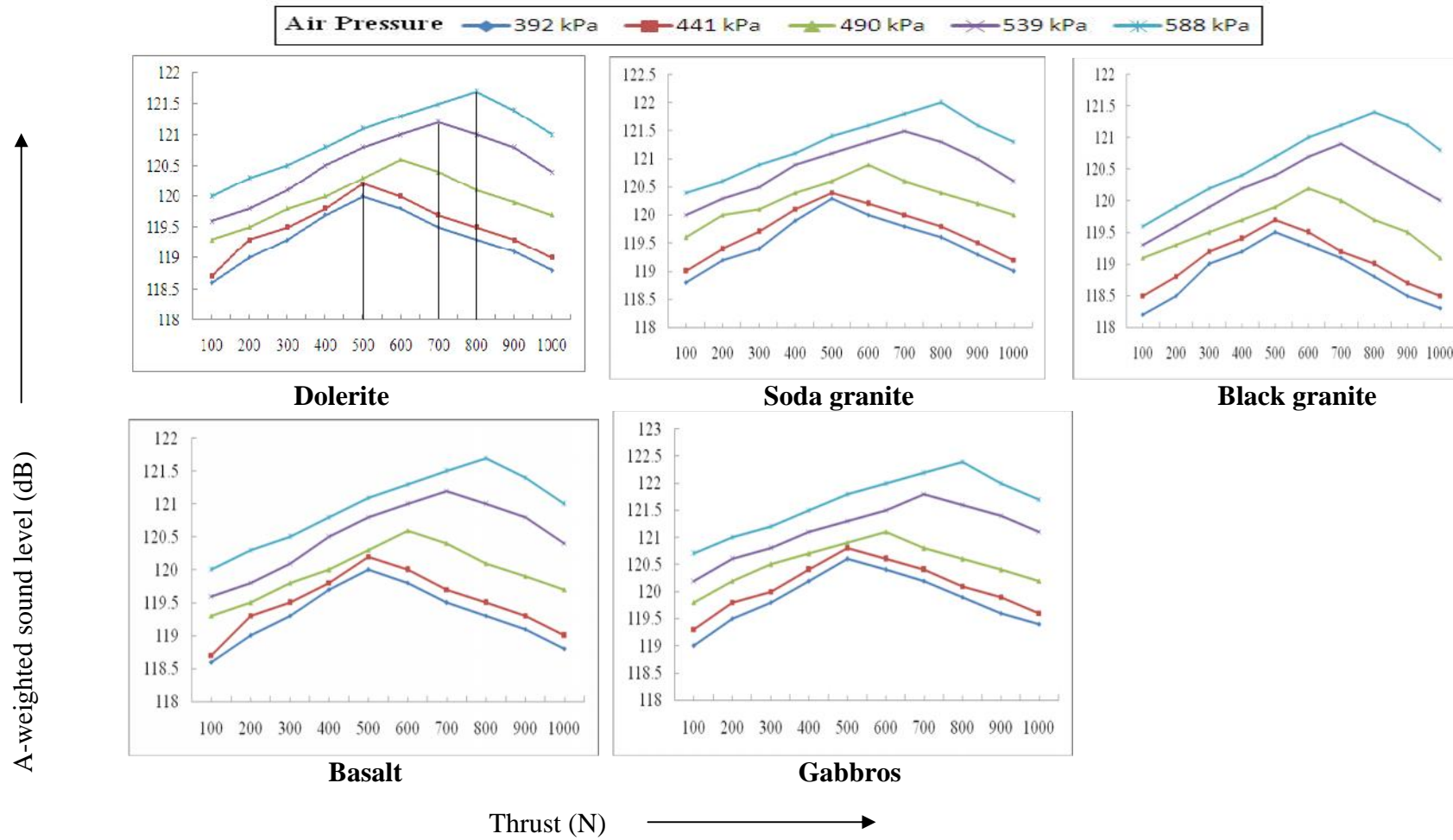
Fig. 5.12b Influence of thrust on A-weighted sound level at operator`s position for integral drill bit diameter of 30 mm with varying air pressure for five different igneous rocks

Fig. 5.13a Influence of thrust on A-weighted sound level at operators position at air pressure of 392 kPa with varying integral bit diameter for five different sedimentary rocks

Drill bit Diameter — Ø 30 mm — Ø 34 mm — Ø40 mm

A-weighted sound level (dB)

Dolerite

Soda granite

Black granite

Basalt

Gabbros
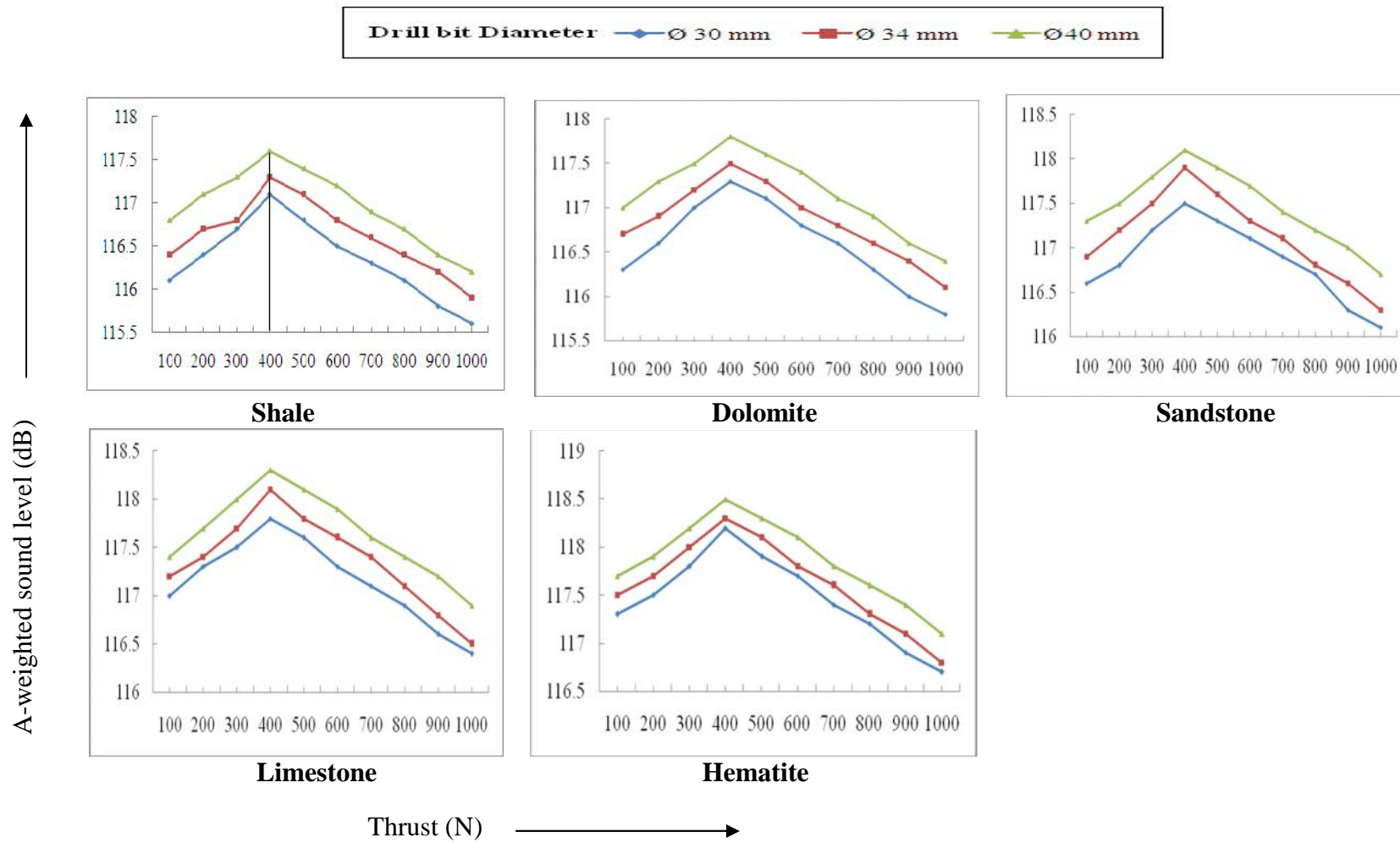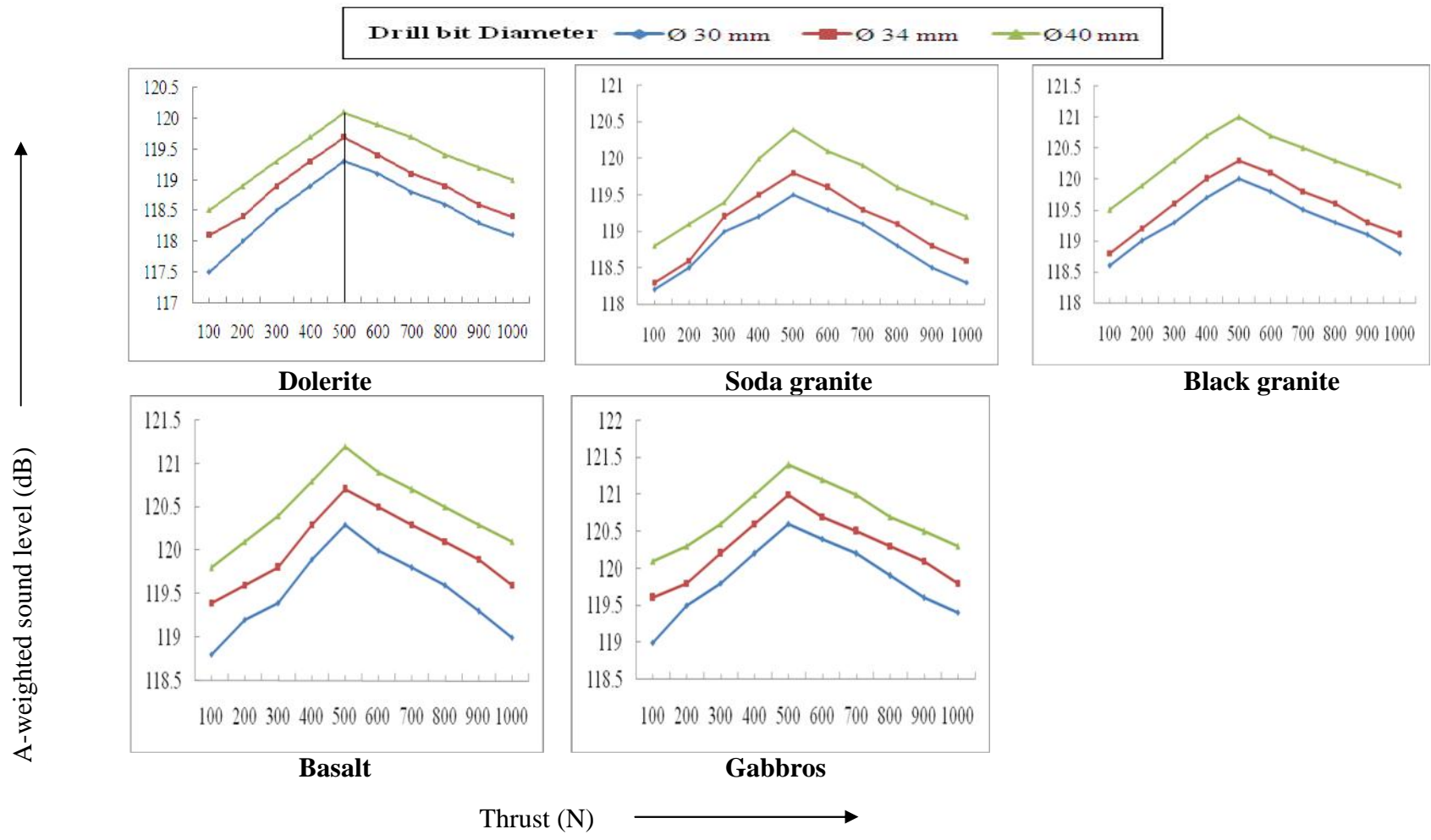
Thrust (N)

Fig. 5.13b Influence of thrust on A-weighted sound level at operators position at air pressure of 392 kPa with varying integral bit diameter for five different igneous rocks
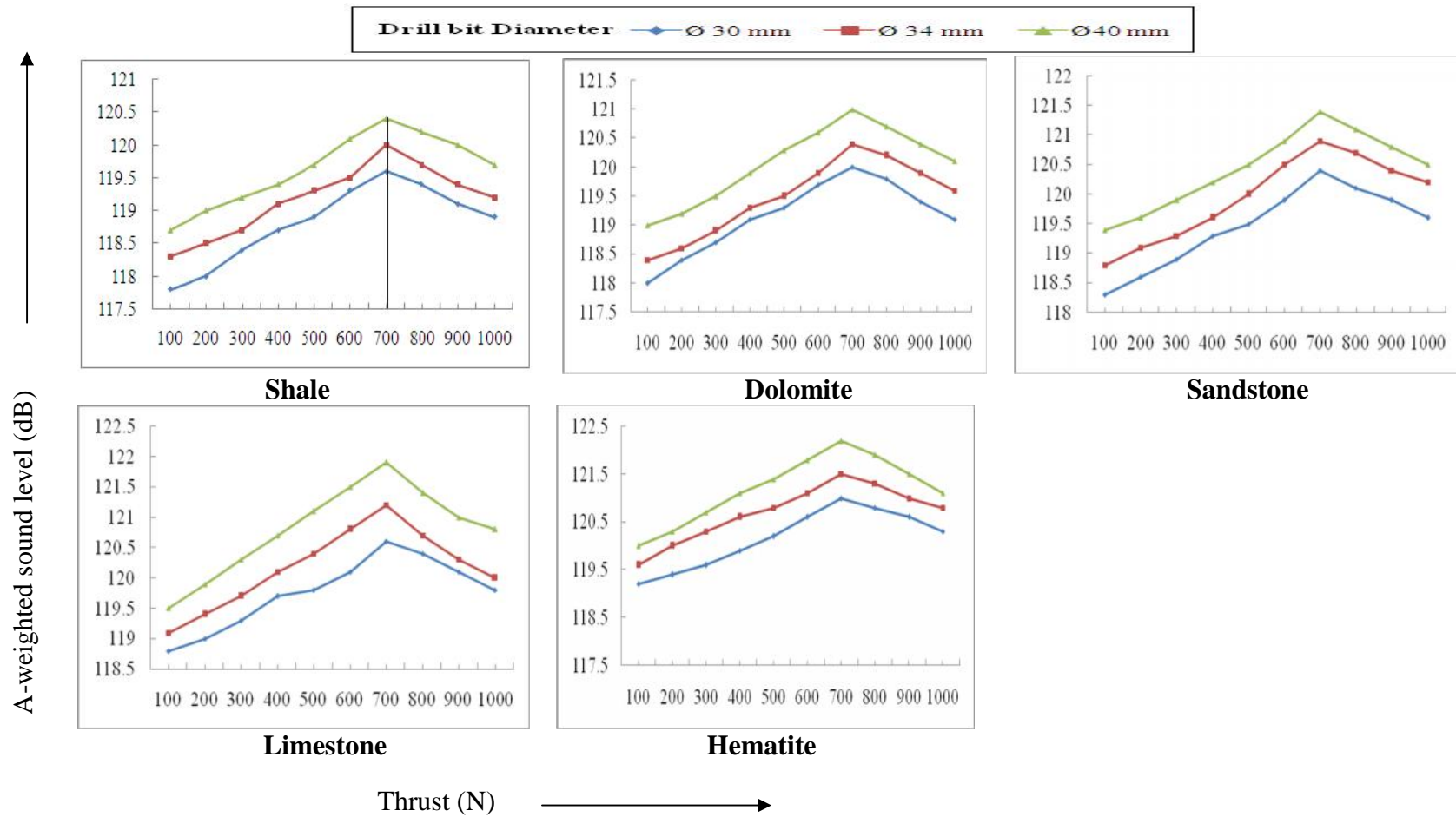
Fig. 5.14a Influence of thrust on A-weighted sound level at operators position at air pressure of 588 kPa with varying integral bit diameter for five different sedimentary rocks
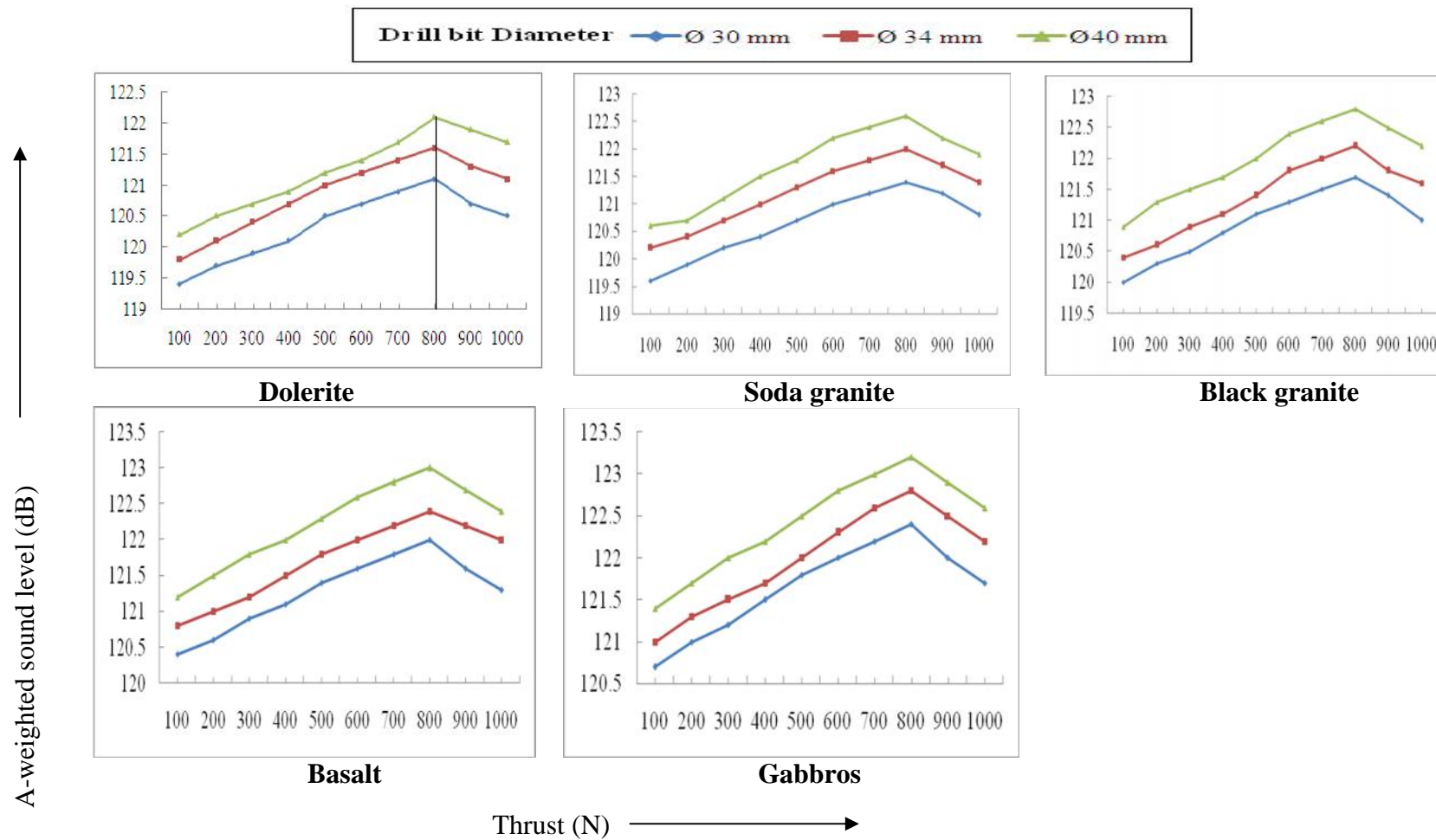
Fig. 5.14b Influence of thrust on A-weighted sound level at operators position at air pressure of 588 kPa with varying integral bit diameter for five different igneous rocks
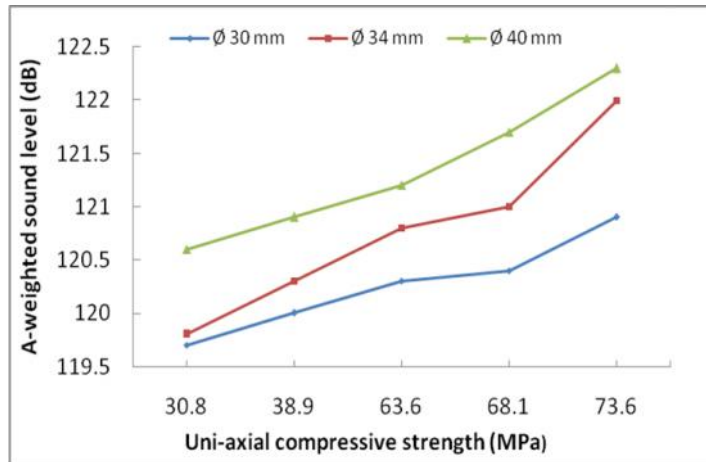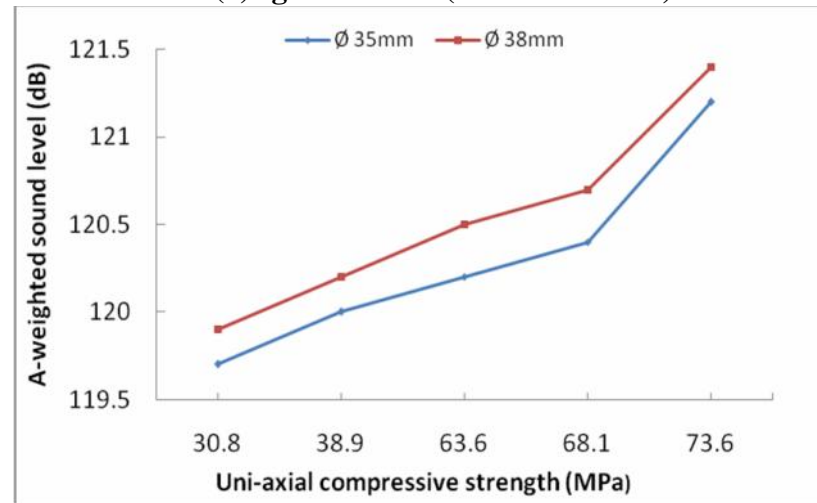
(a) **Sedimentary rock (Thrust at 700N)**
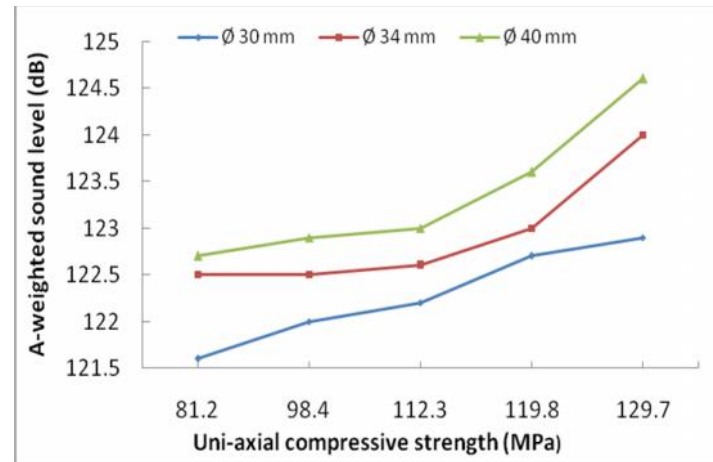
(a) **Igneous rock (Thrust at 800N)**
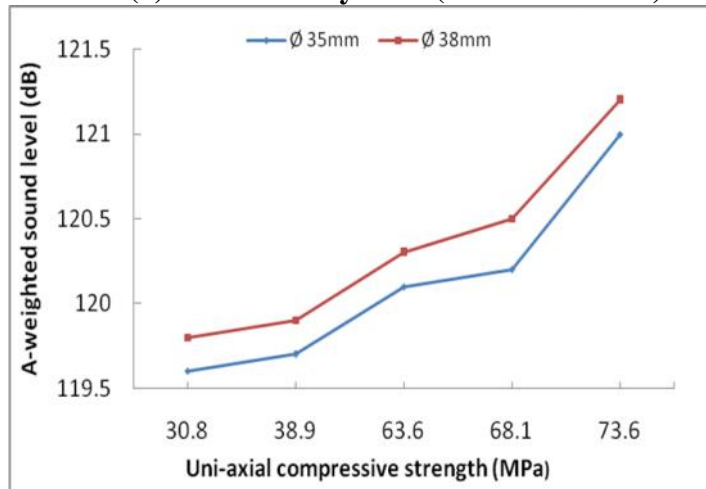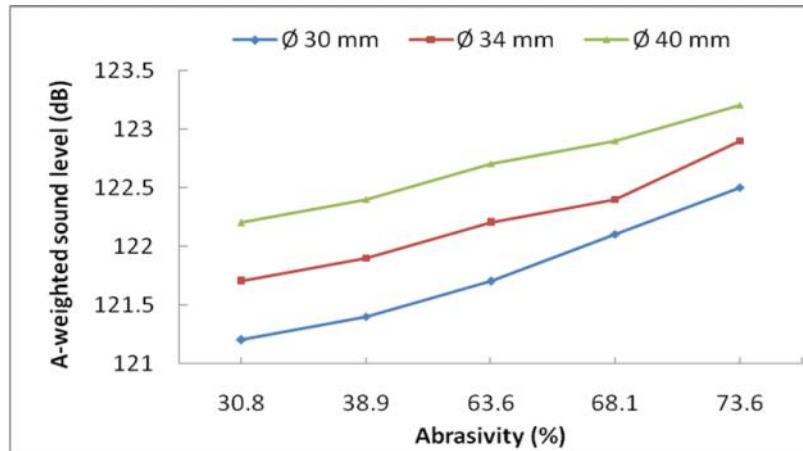
(b) **Sedimentary rock (Thrust at 700N)**
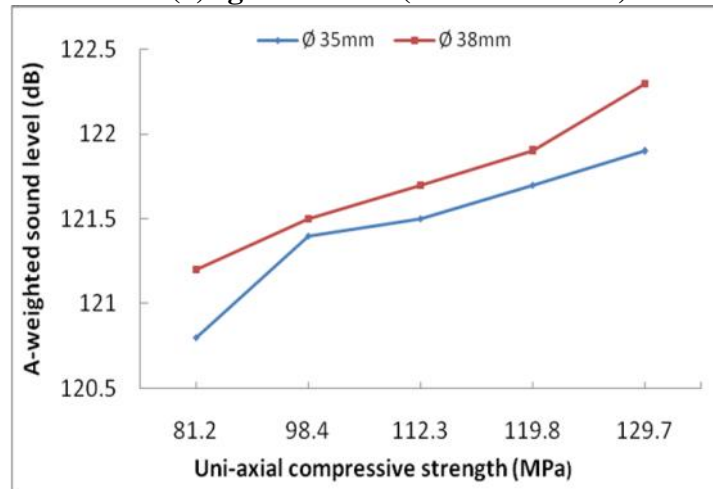
(b) **Igneous rock (Thrust at 800N)**

Fig. 5.15 Influence of UCS on A-weighted sound level at operator's position at air pressure of 588 kPa with varying (a) Integral and (b) Threaded drill bit diameters for different sedimentary and igneous rocks
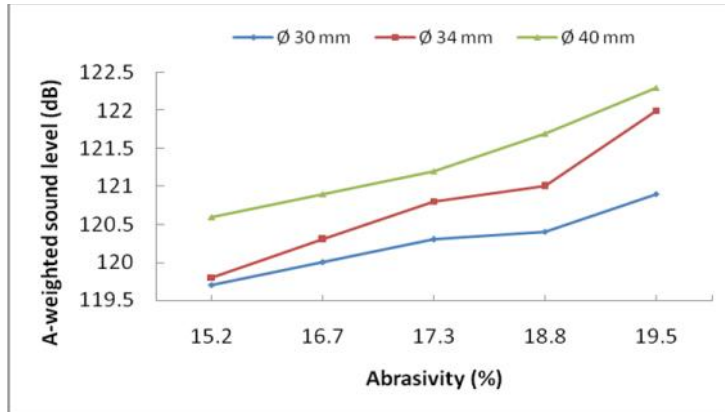
(a) Sedimentary rock (Thrust at 700N)
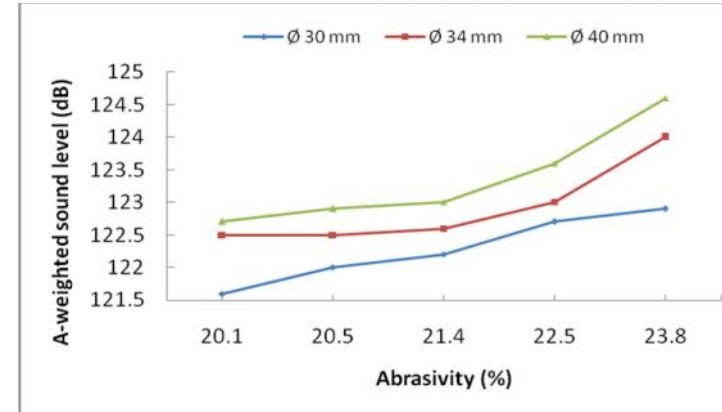
(a) Igneous rock (Thrust at 800N)
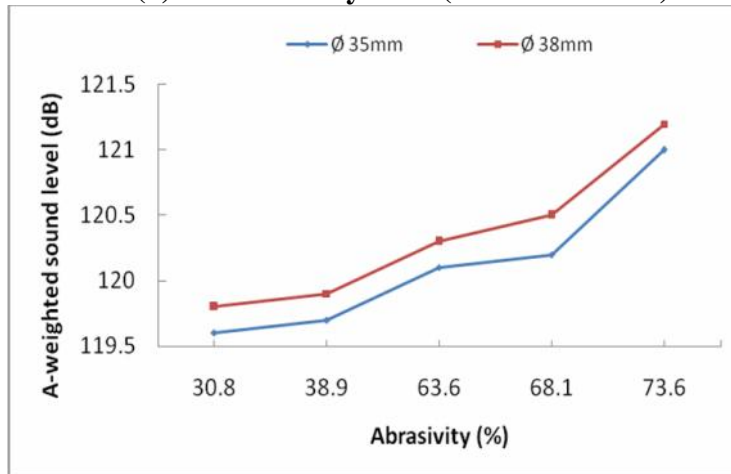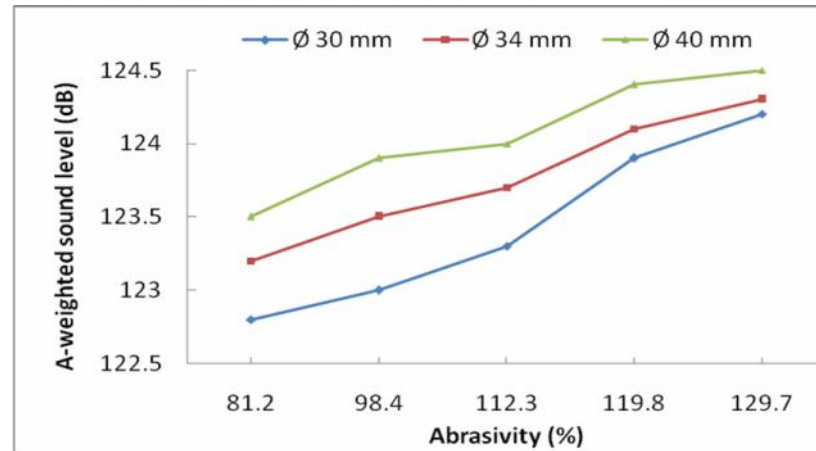
(b) Sedimentary rock (Thrust at 700N)
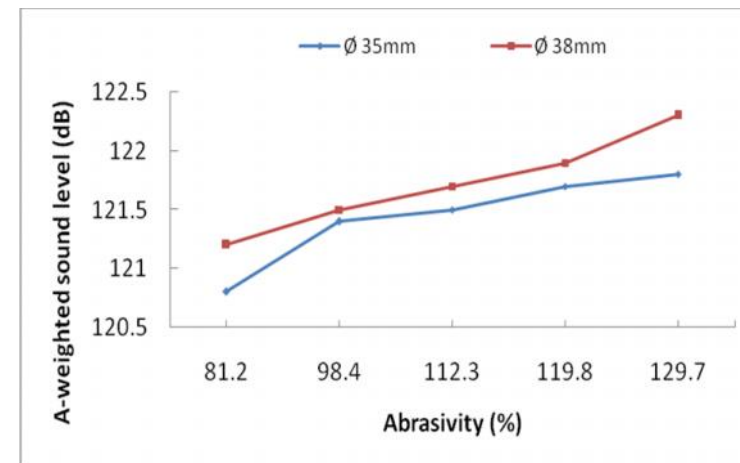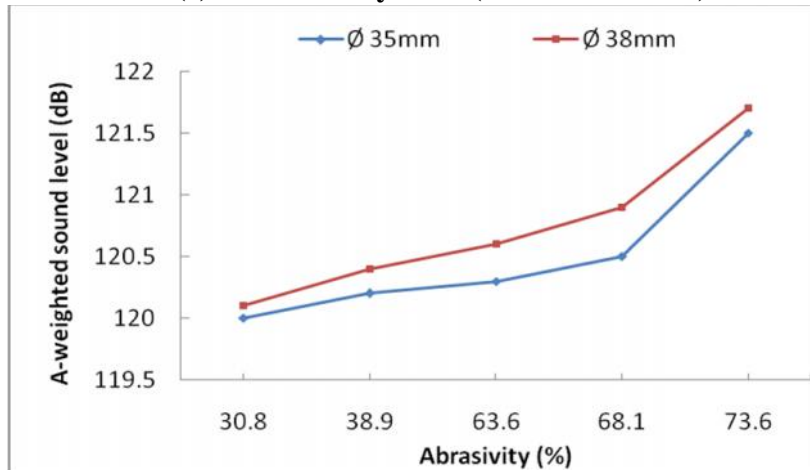
(b) Igneous rock (Thrust at 800N)

Fig. 5.16 Influence of abrasivity on A-weighted sound level at operator's position at given air pressure of 588 kPa with varying
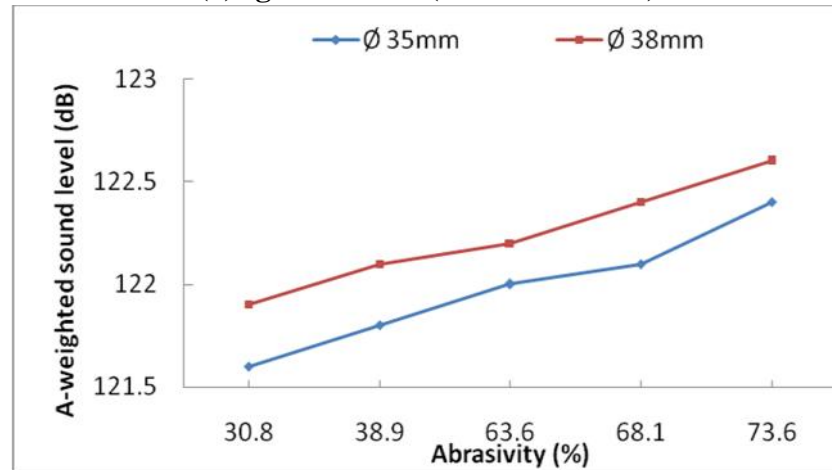(a) Integral and (b) Threaded drill bit diameters for different sedimentary and igneous rocks
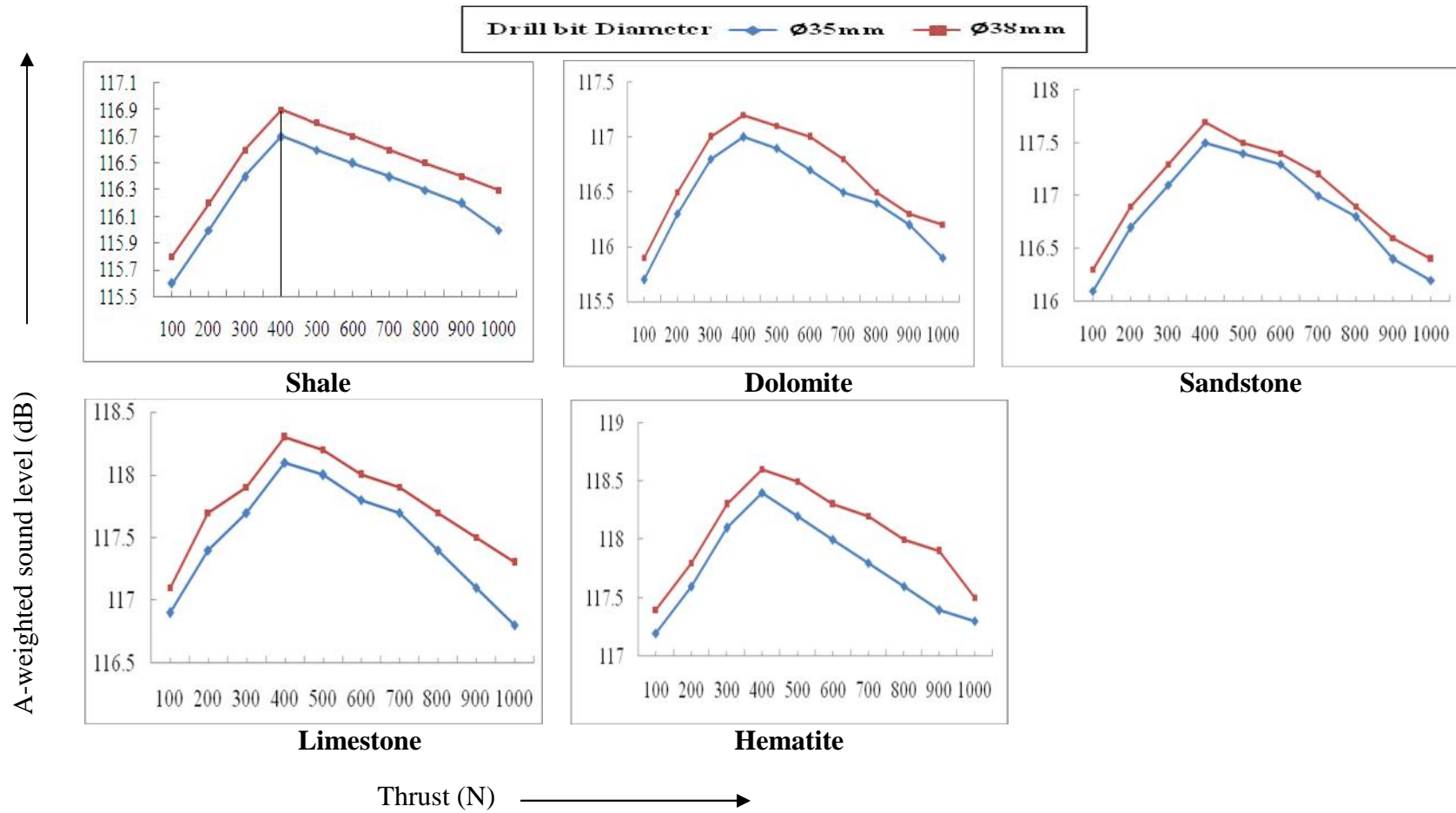
Fig. 5.17a Influence of thrust on A-weighted sound level at operator's position at air pressure of 392 kPa with varying threaded drill bit diameters for five different sedimentary rocks
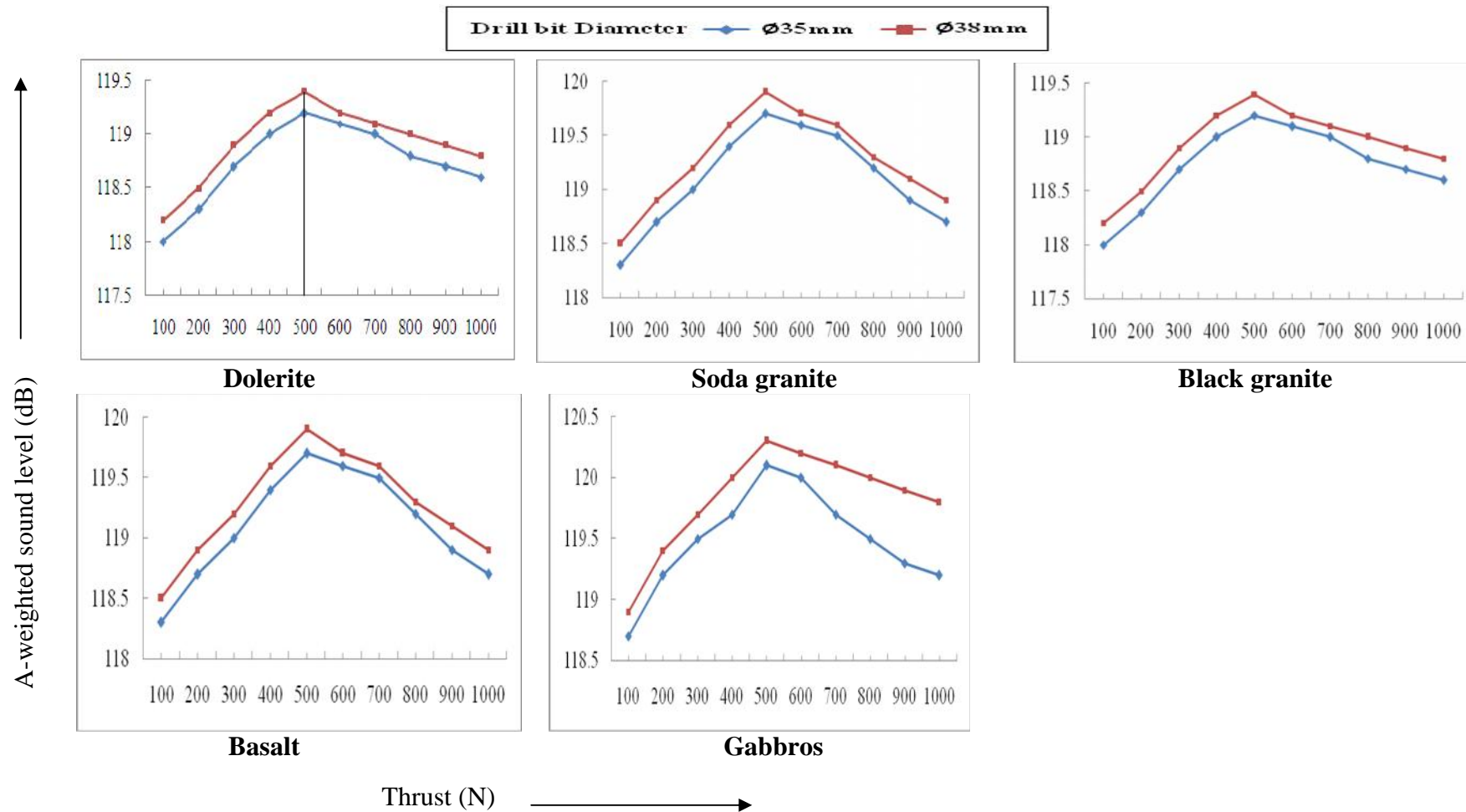
Fig. 5.17b Influence of thrust on A-weighted sound level at operator's position at air pressure of 392 kPa with varying threaded drill bit diameters for five different igneous rocks
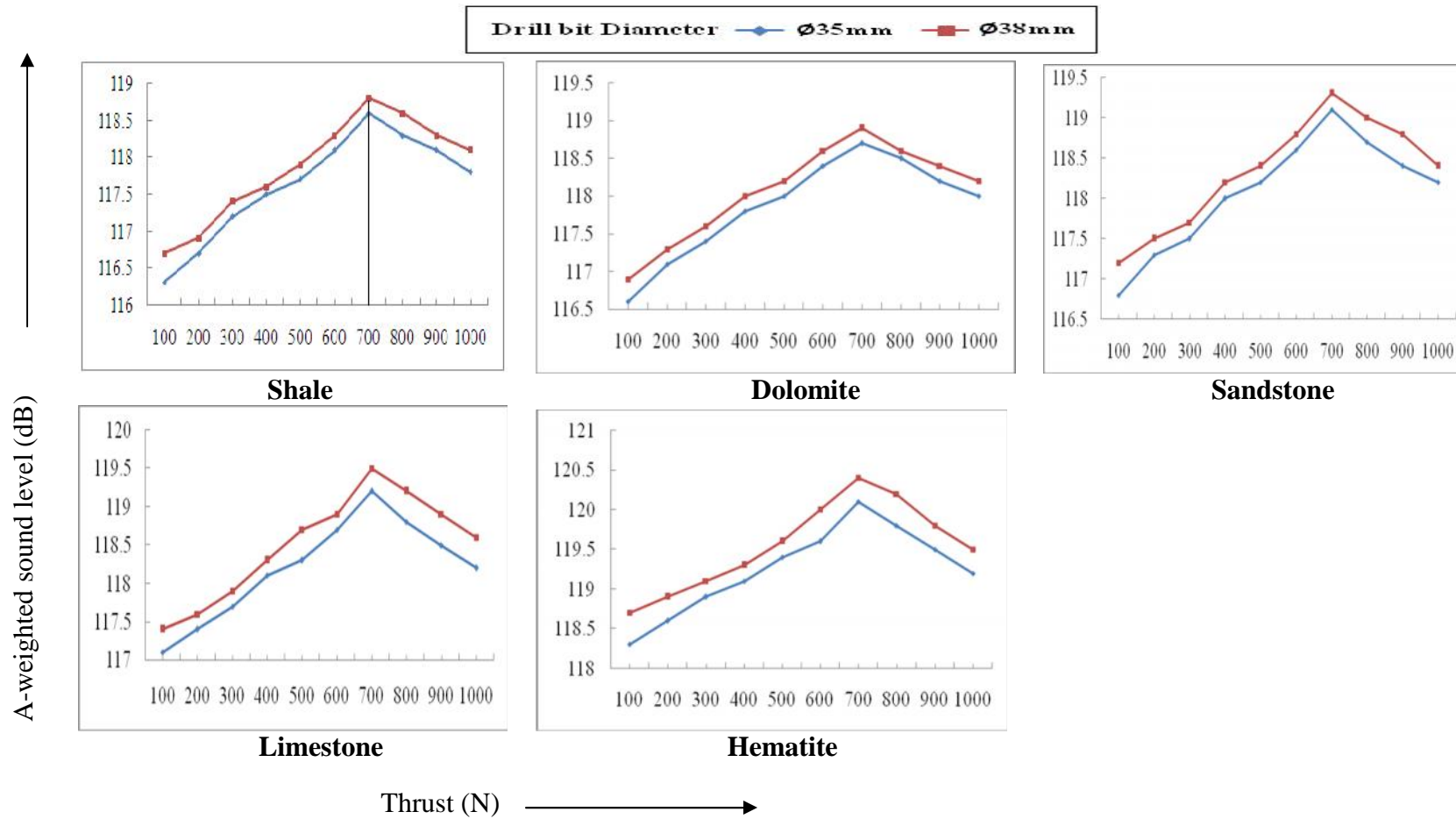
Fig. 5.18a Influence of thrust on A- weighted sound level at operator's position at air pressure of 588 kPa with varying threaded drill bit diameters for five different sedimentary rocks

Fig. 5.18b Influence of thrust on A- weighted sound level at operator's position at given air pressure of 588 kPa with varying threaded drill bit diameters for five different igneous rocks
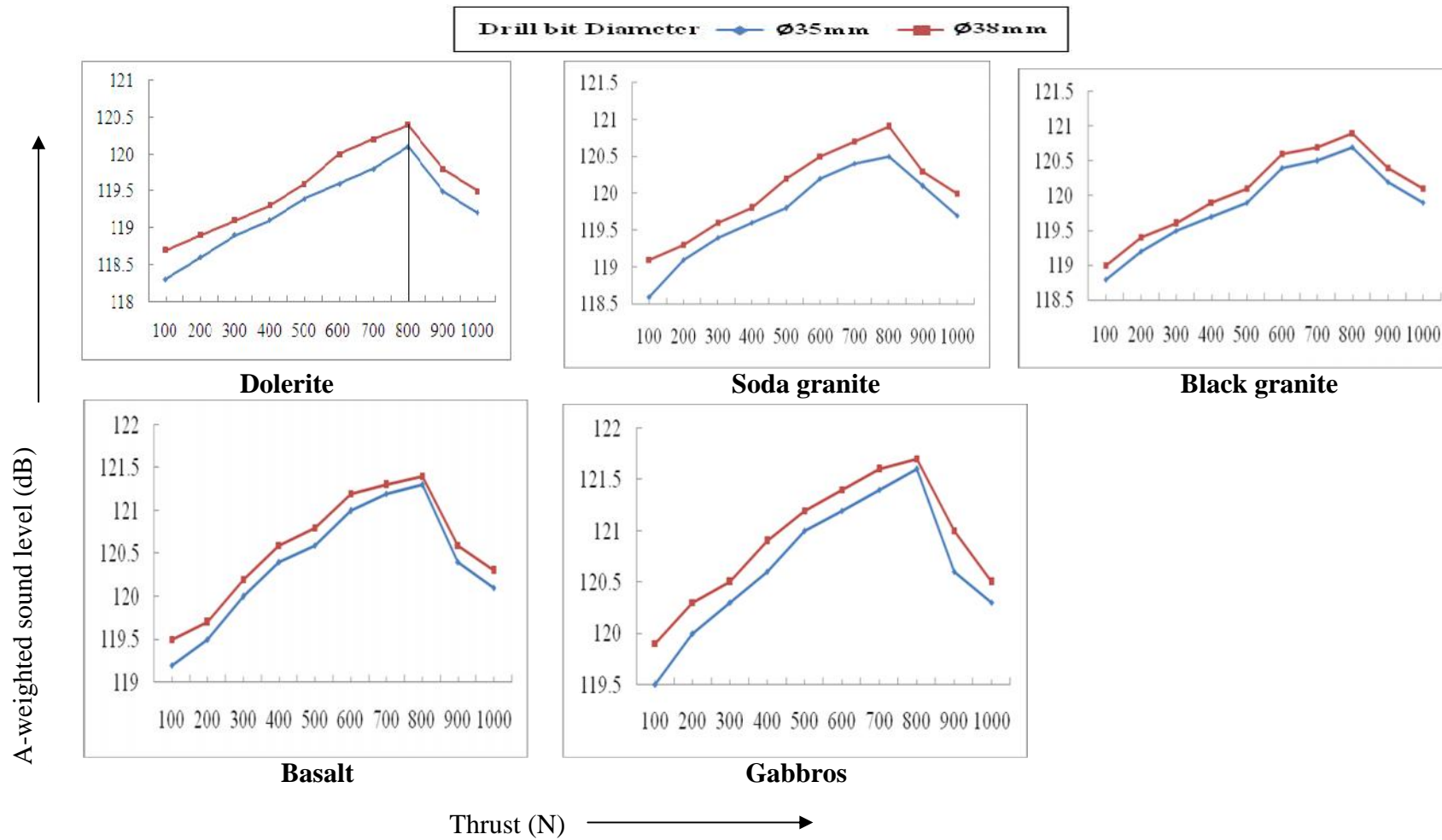
A-weighted sound level (dB)
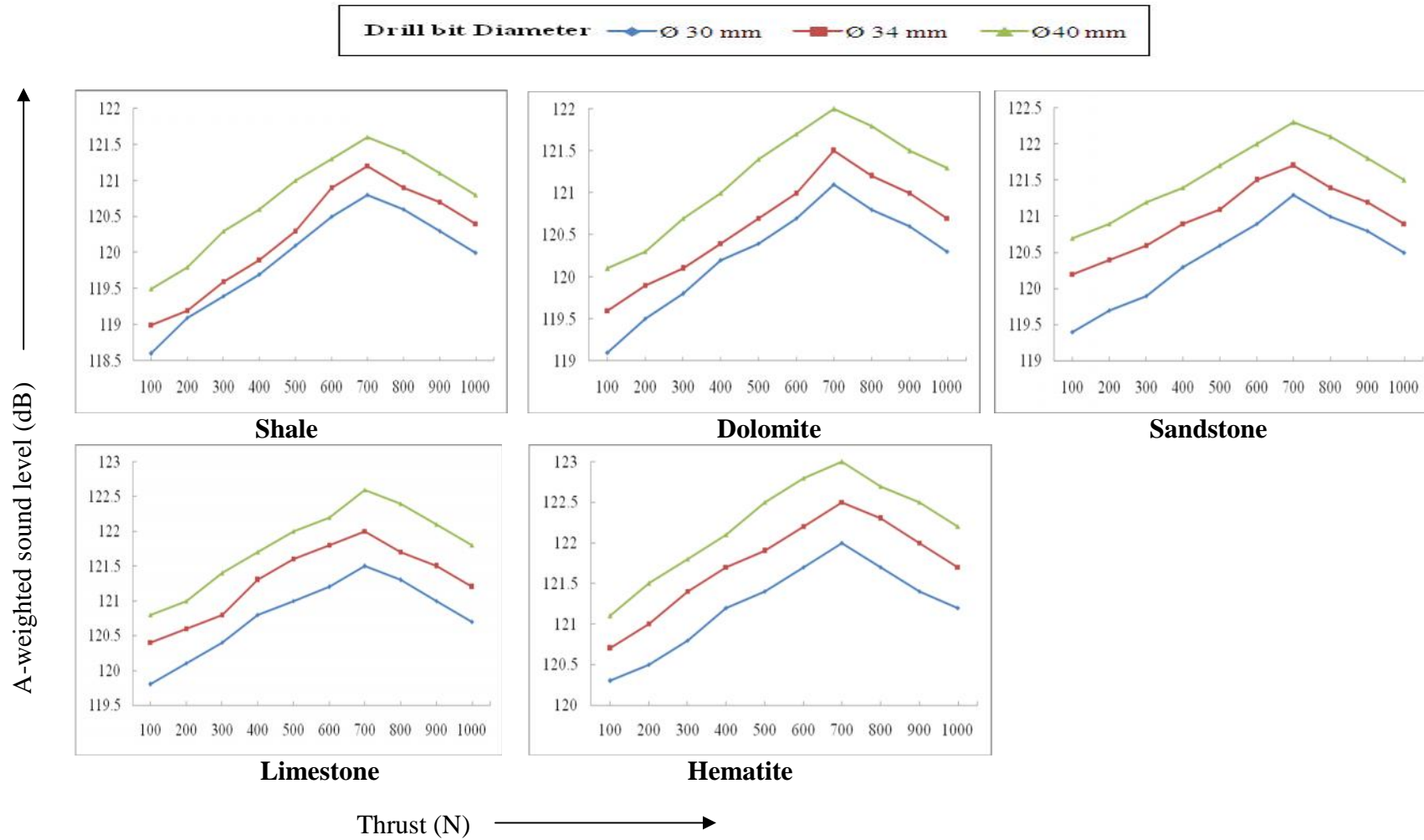
Thrust (N)

Fig. 5.19a Influence of thrust on A-weighted sound level at exhaust position at air pressure of 588 kPa with varying integral bit diameters for five different sedimentary rocks
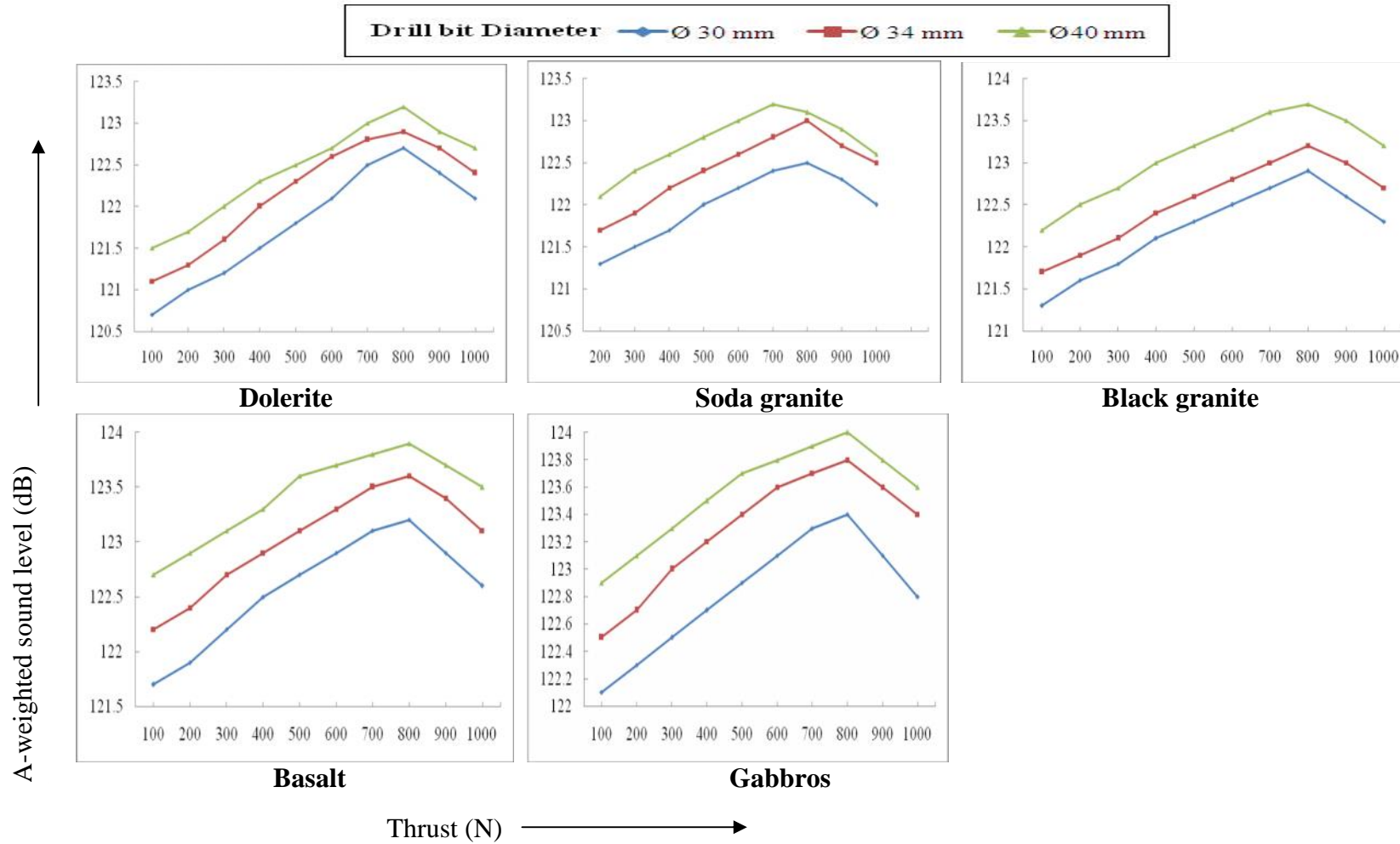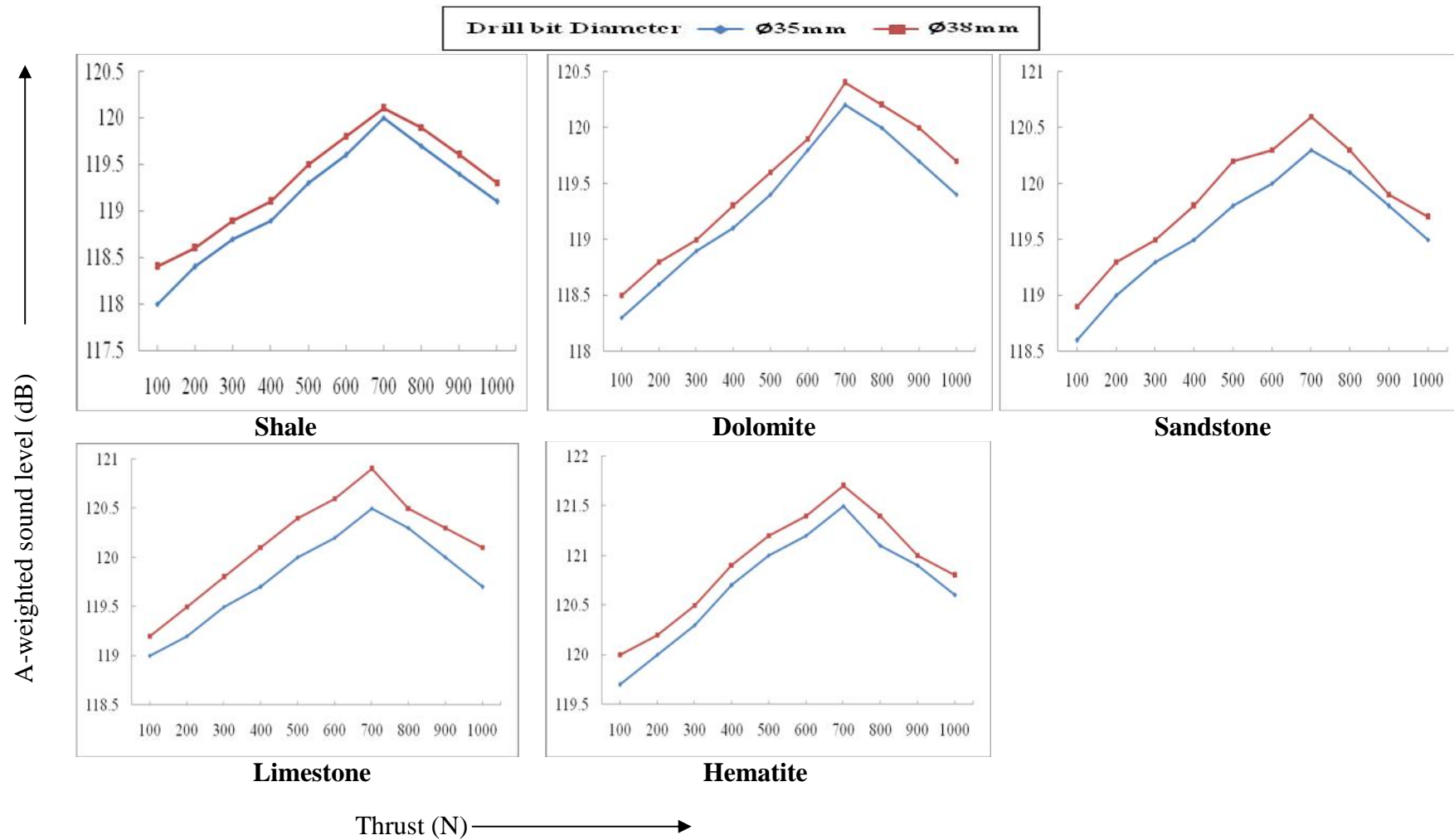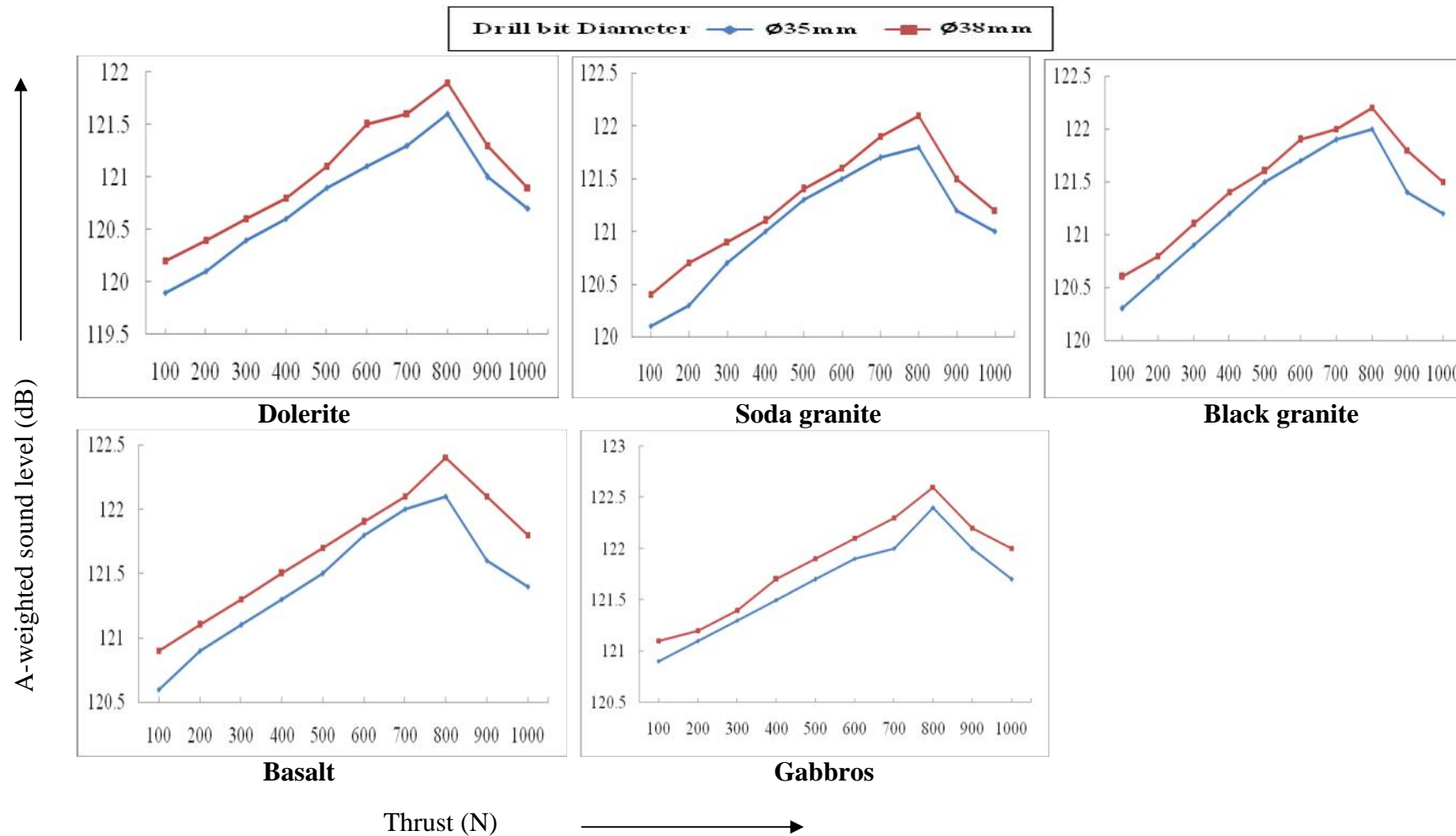
Fig. 5.19b Influence of thrust on A-weighted sound level at exhaust position at air pressure of 588 kPa with varying integral bit diameters for five different igneous rocks
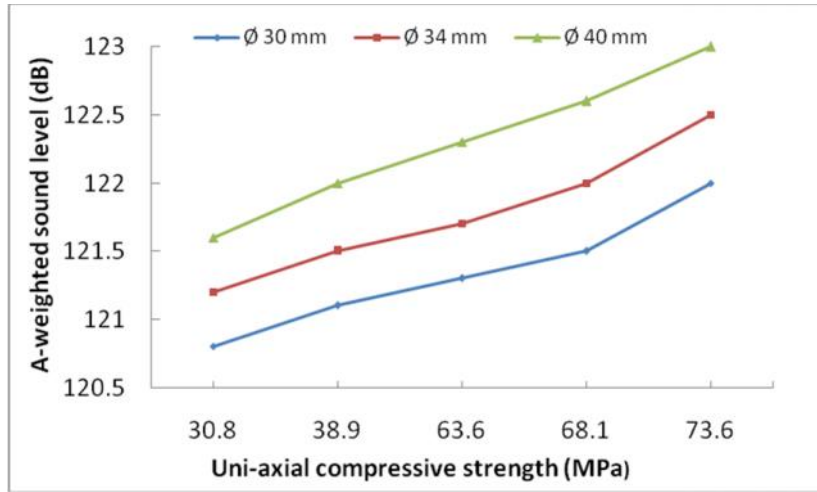
(a) Sedimentary rock (Thrust at 700N)
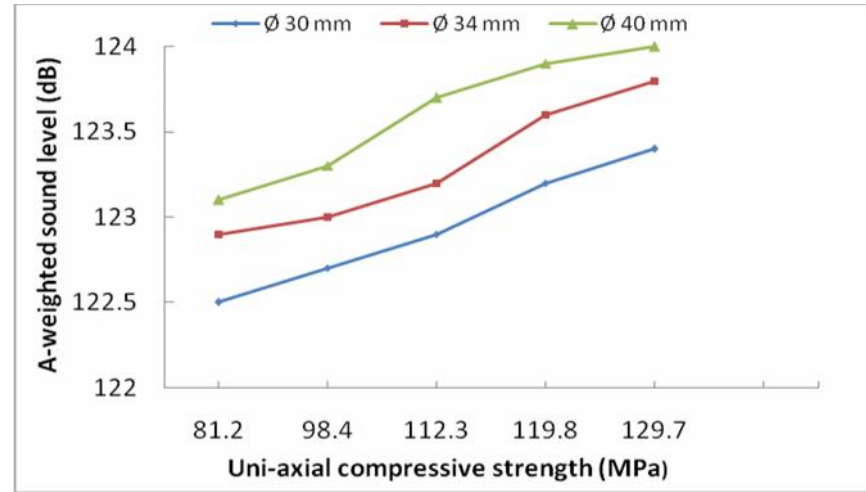
(a) Igneous rock (Thrust at 800N)
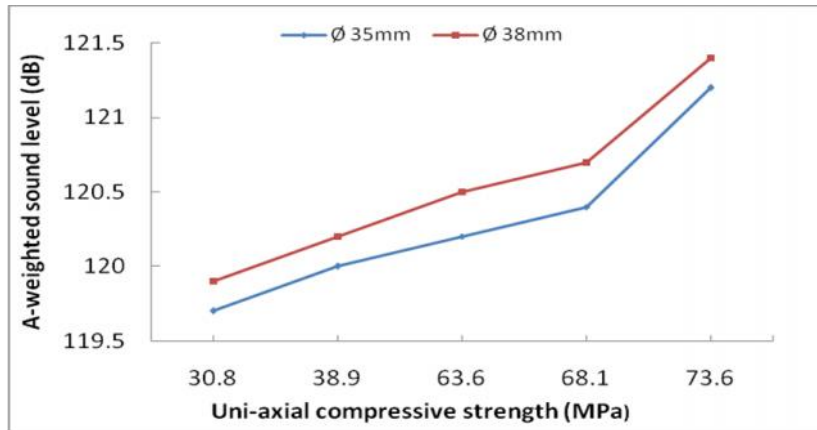
(b) Sedimentary rock (Thrust at 700N)
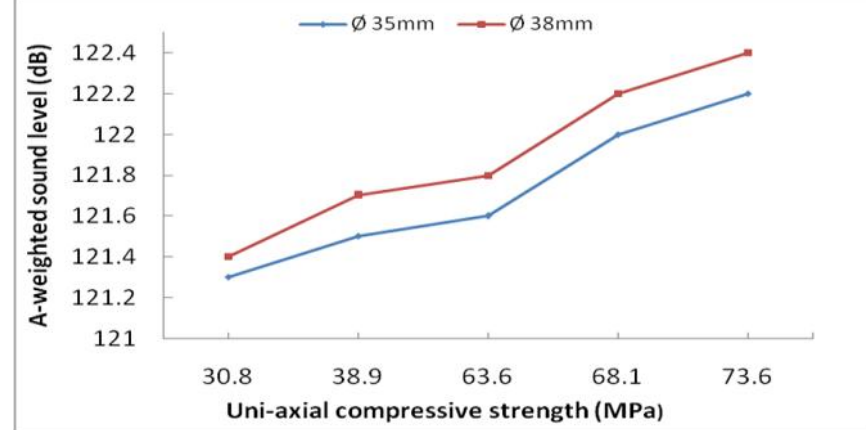
(b) Igneous rock (Thrust at 800N)

Fig. 5.20 Influence of UCS on A-weighted sound level at exhaust position at given air pressure of 588 kPa with (a) Integral and (b) Threaded drill bit diameters for sedimentary and igneous rocks
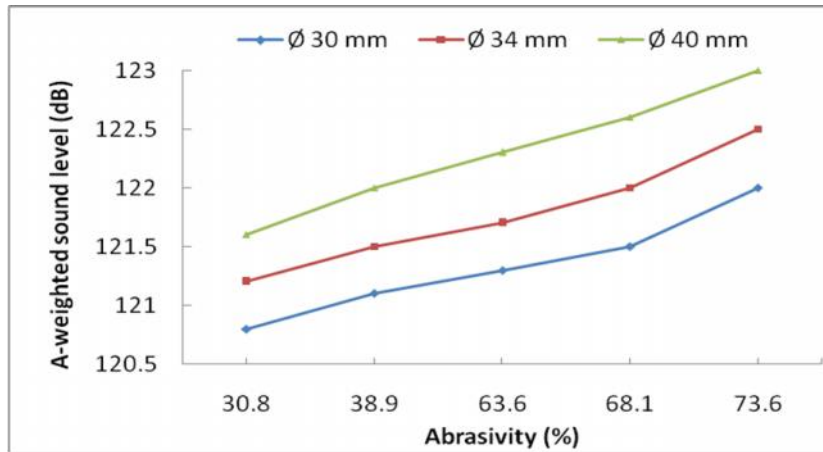
(a) Sedimentary rock (Thrust at 700 N)
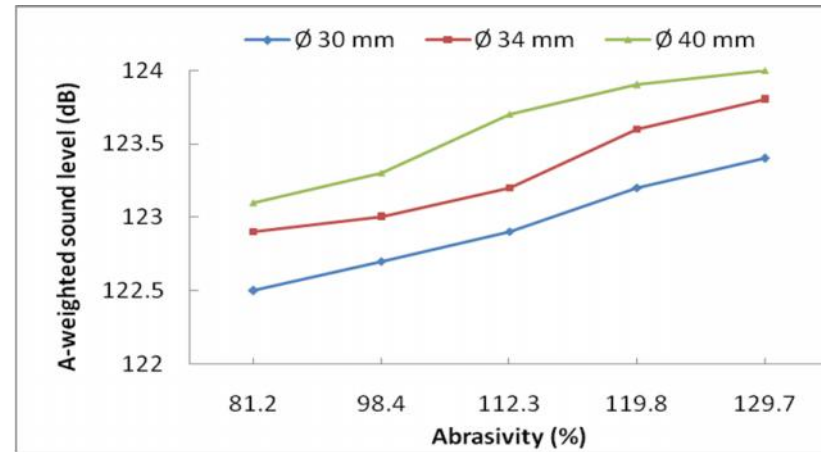
(a) Igneous rock (Thrust at 800N)
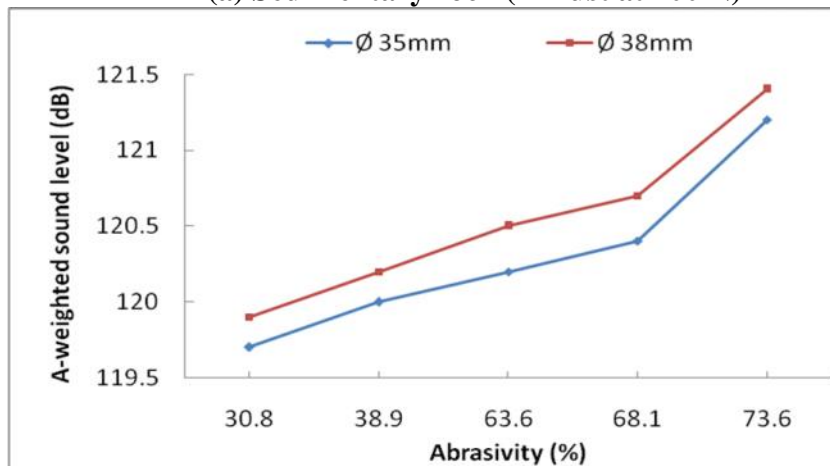
(b) Sedimentary rock (Thrust at 700 N

(b) Igneous rock (Thrust at 800N)

Fig. 5.21 Influence of abrasivity on A-weighted sound level at exhaust position at given air pressure of 588 kPa with (a) Integral and
(b) Threaded drill bit diameters for sedimentary and igneous rocks

Fig. 5.22a Influence of thrust on A-weighted sound level at exhaust position at air pressure of 588 kPa with varying threaded bit diameter for five different sedimentary rocks
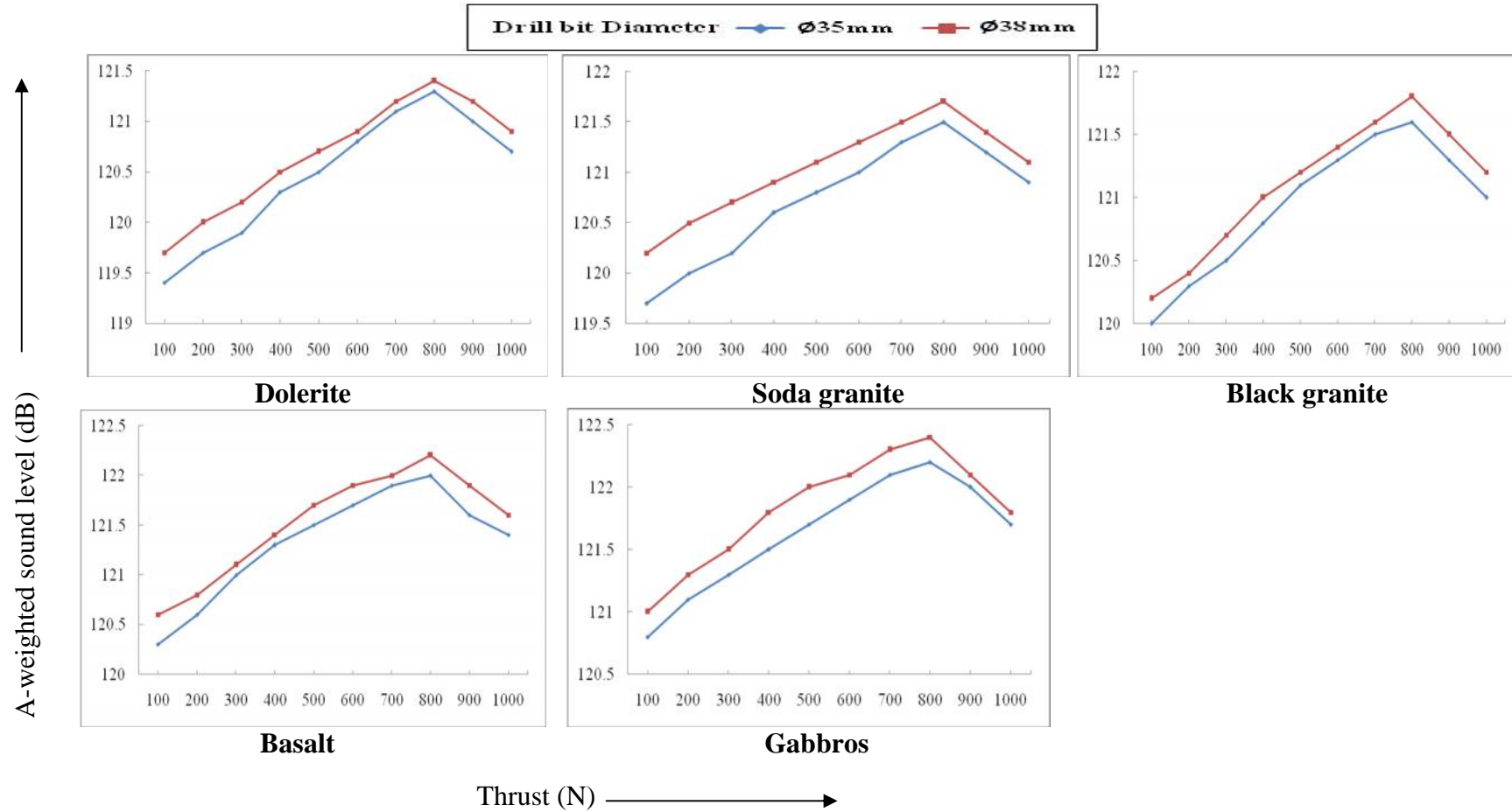
Fig. 5.22b Influence of thrust on A- weighted sound level at exhaust position at air pressure of 588 kPa with varying threaded drill bit diameter for five different igneous rocks
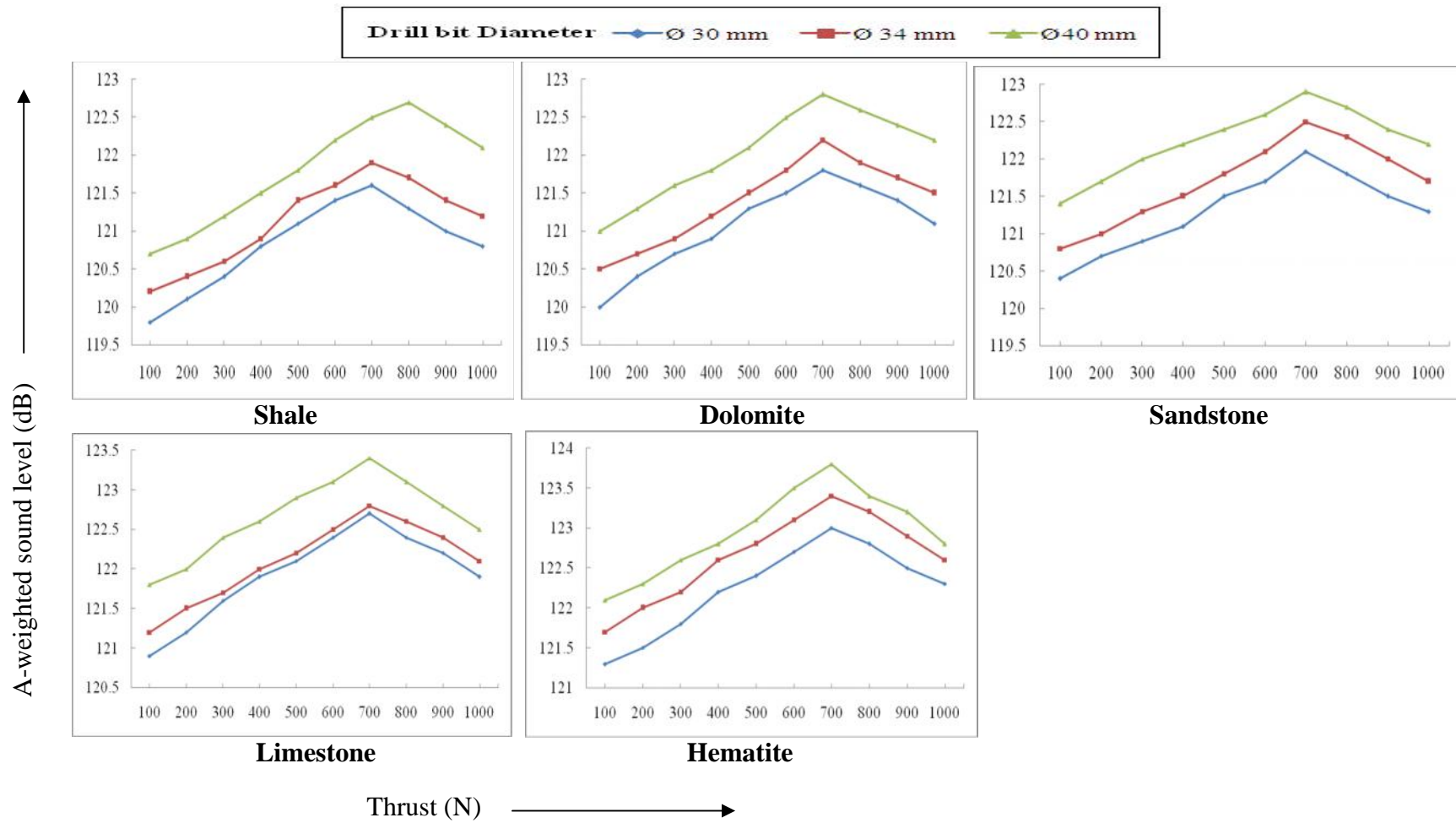
Fig. 5.23a Influence of thrust on A-weighted sound level near drill bit at air pressure of 588 kPa with varying integral bit diameters for five different sedimentary rocks
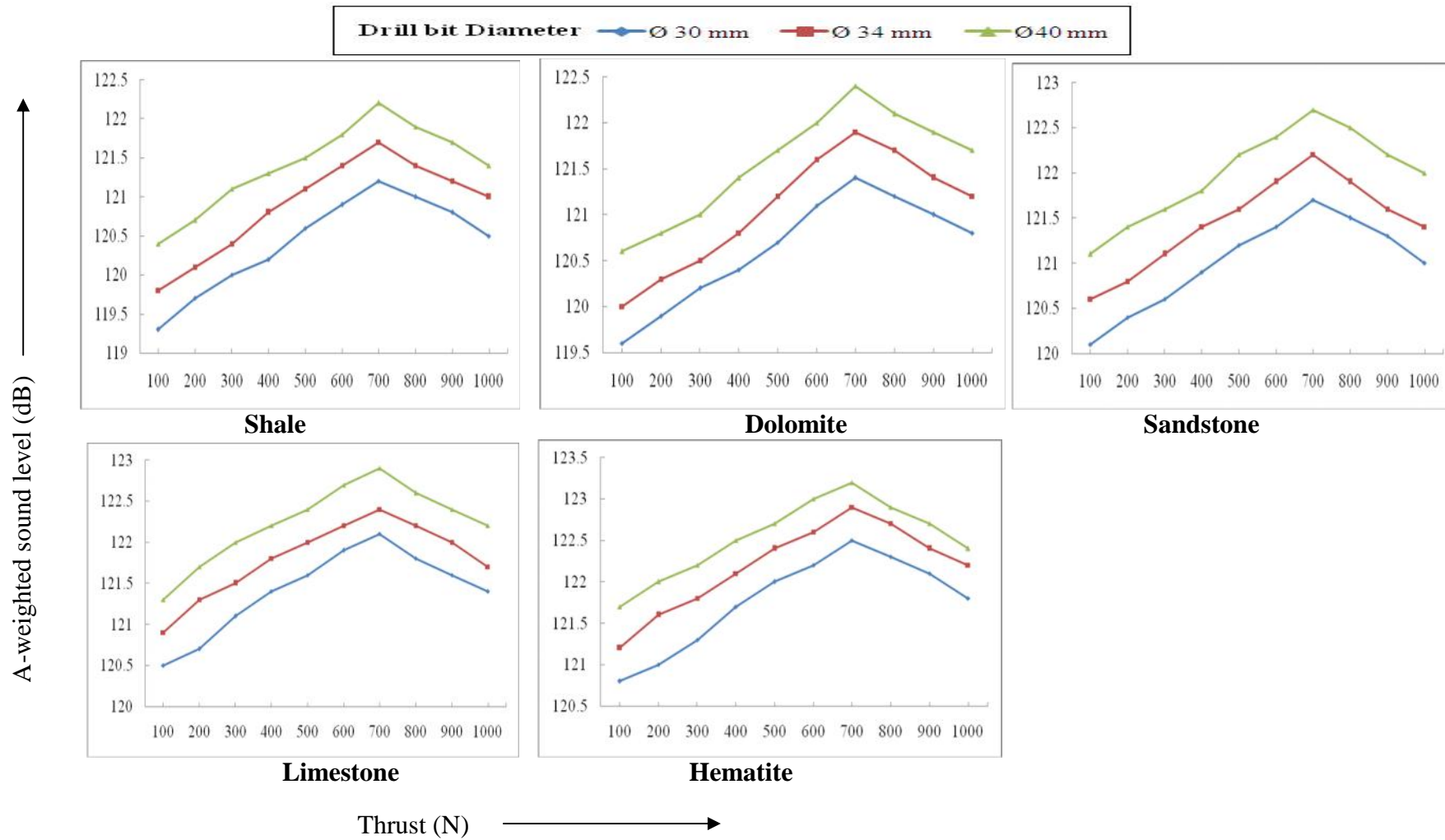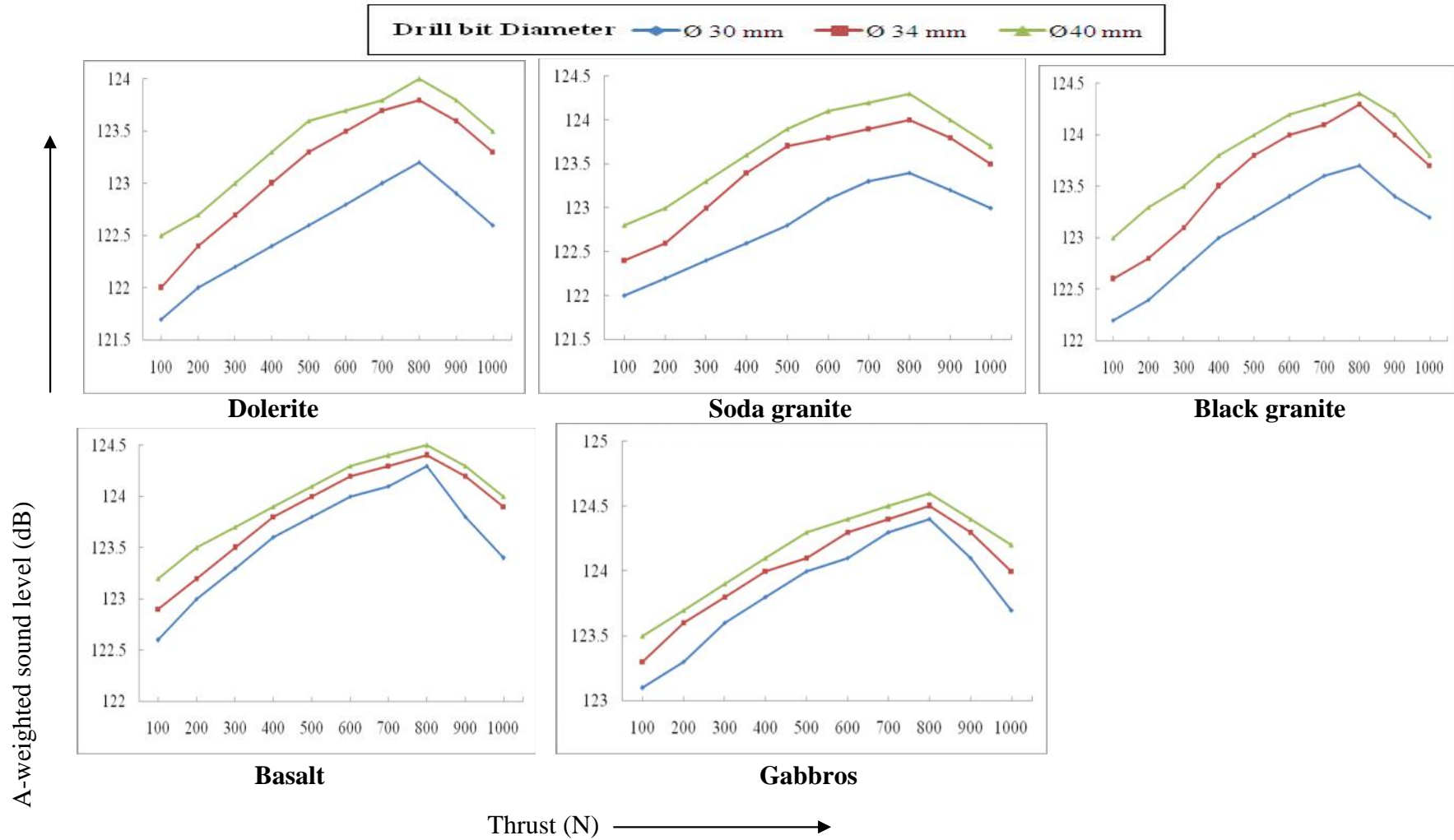
A-weighted sound level (dB)
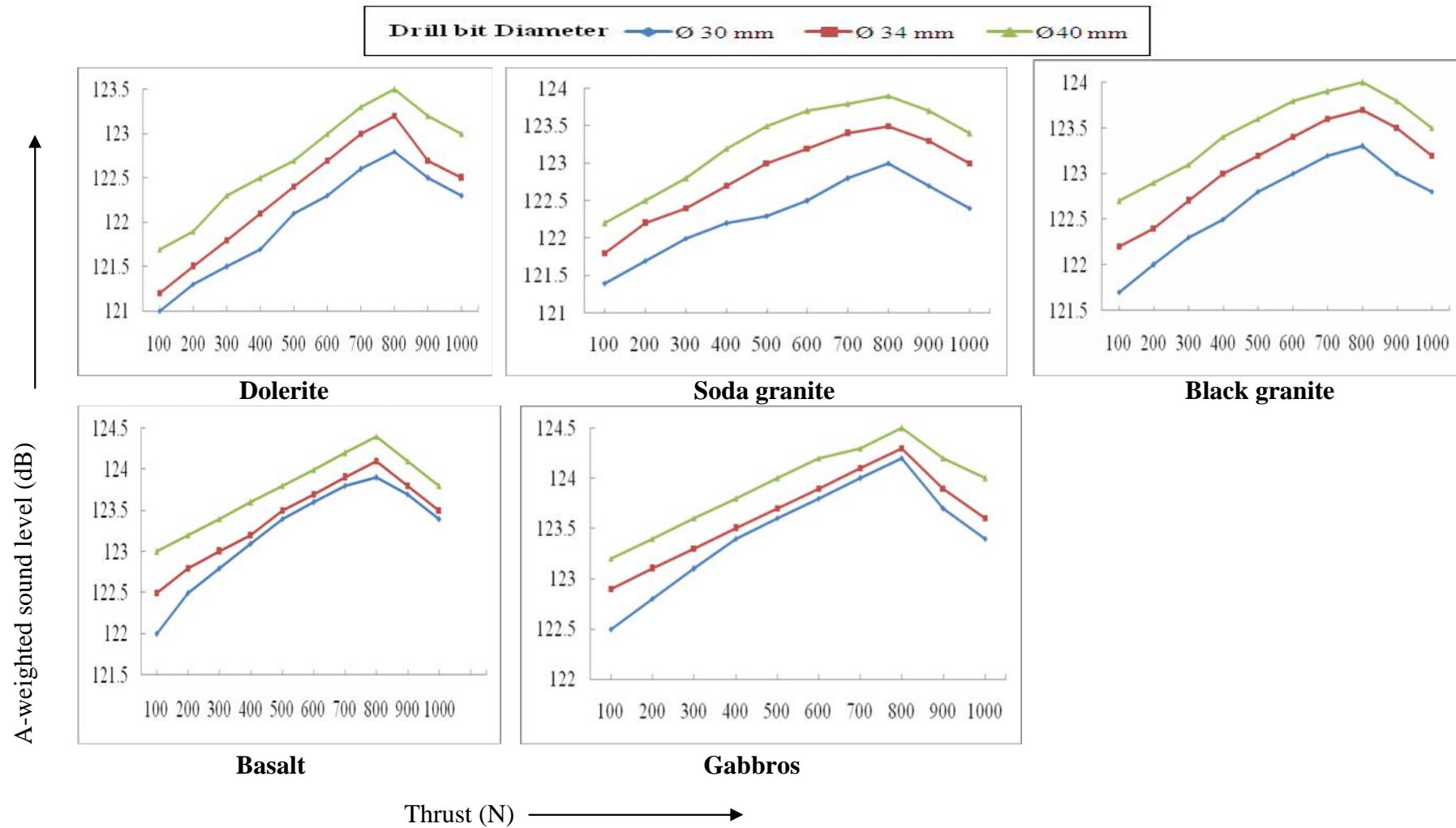
Thrust (N)

Fig. 5.23b Influence of thrust on A-weighted sound level near drill bit at air pressure of 588 kPa with varying integral bit diameters for five different igneous rocks
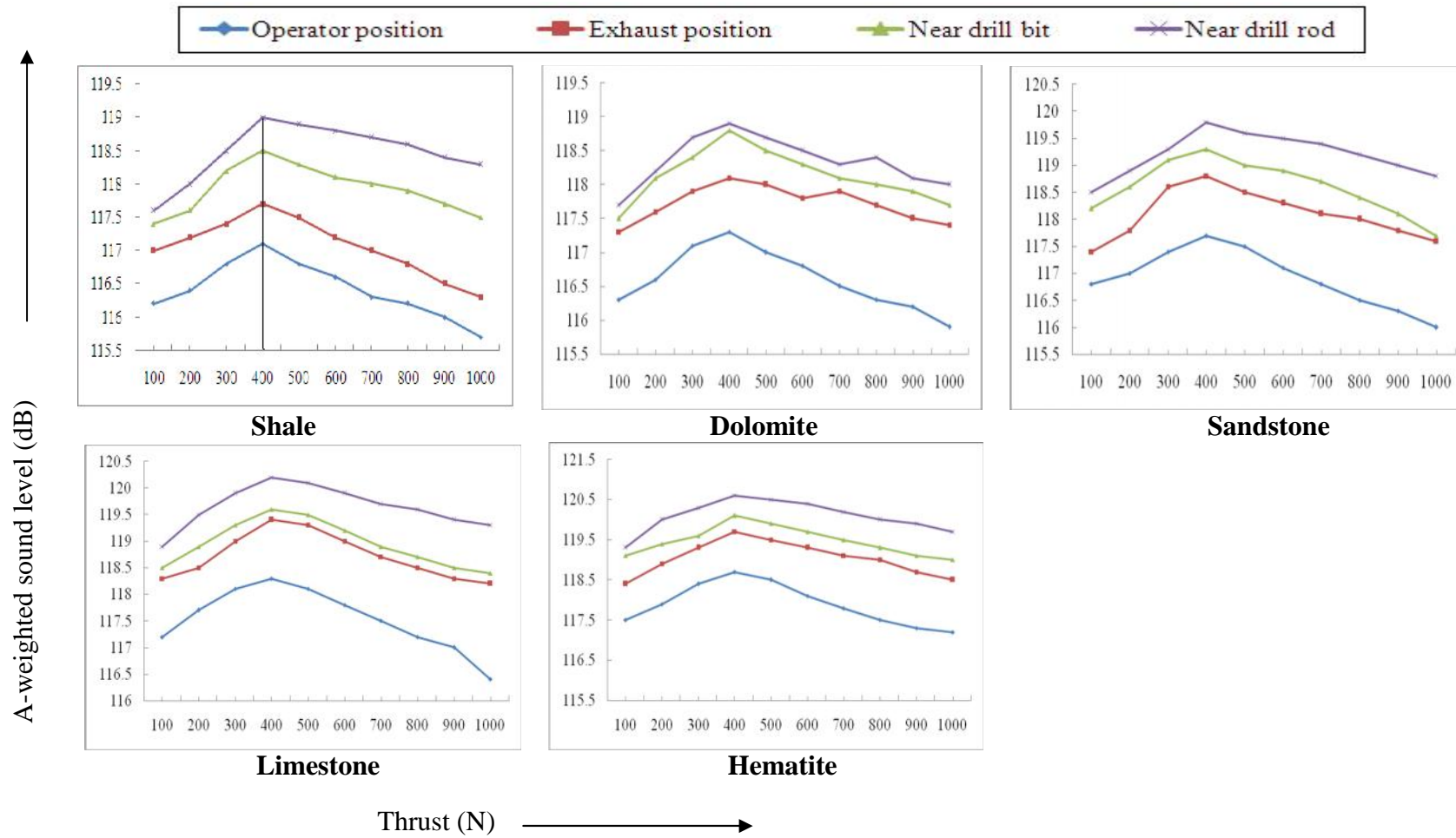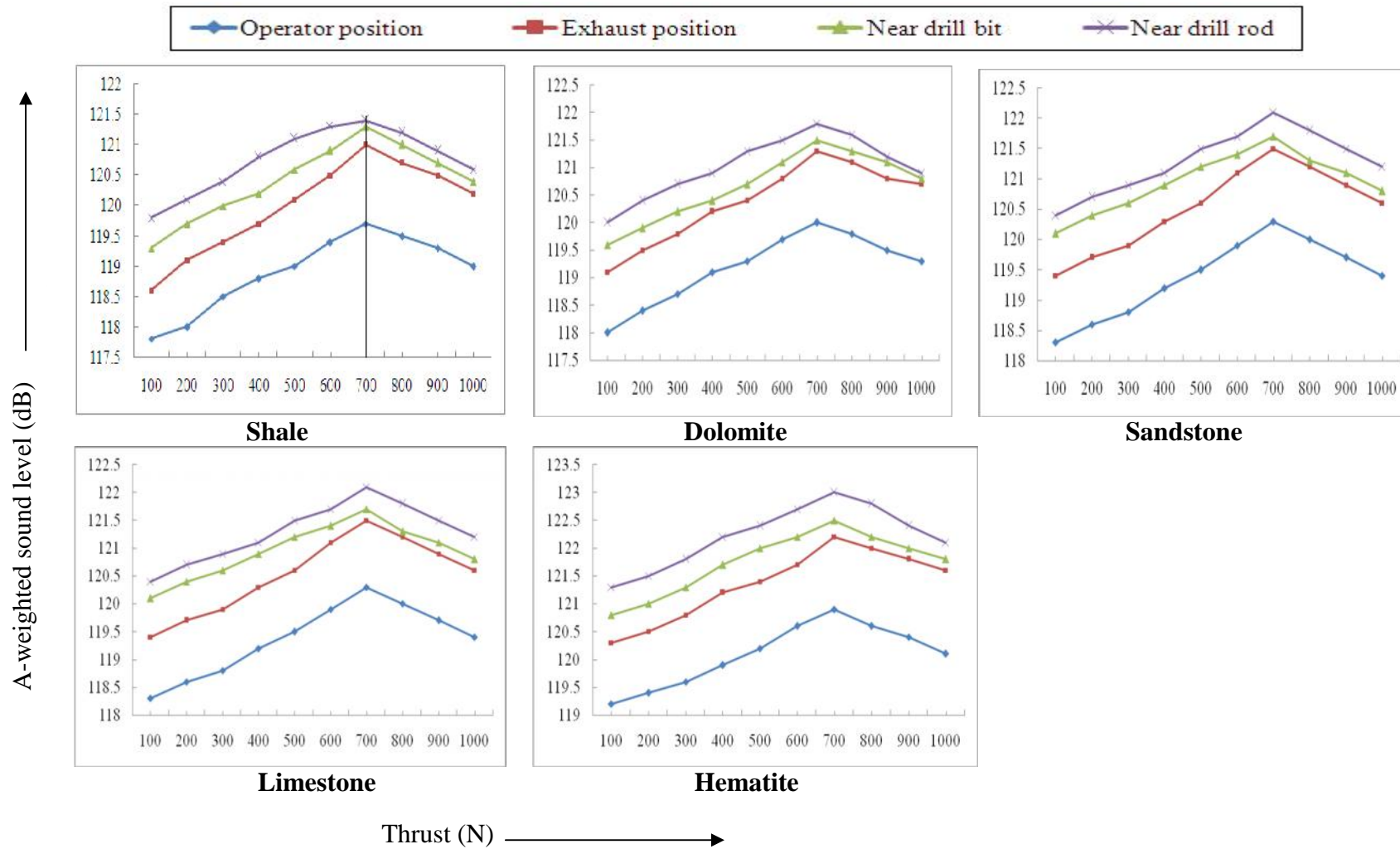
Fig. 5.24a Influence of thrust on A-weighted sound level for integral bit diameter of 30 mm and at air pressure of 392 kPa for five different sedimentary rocks
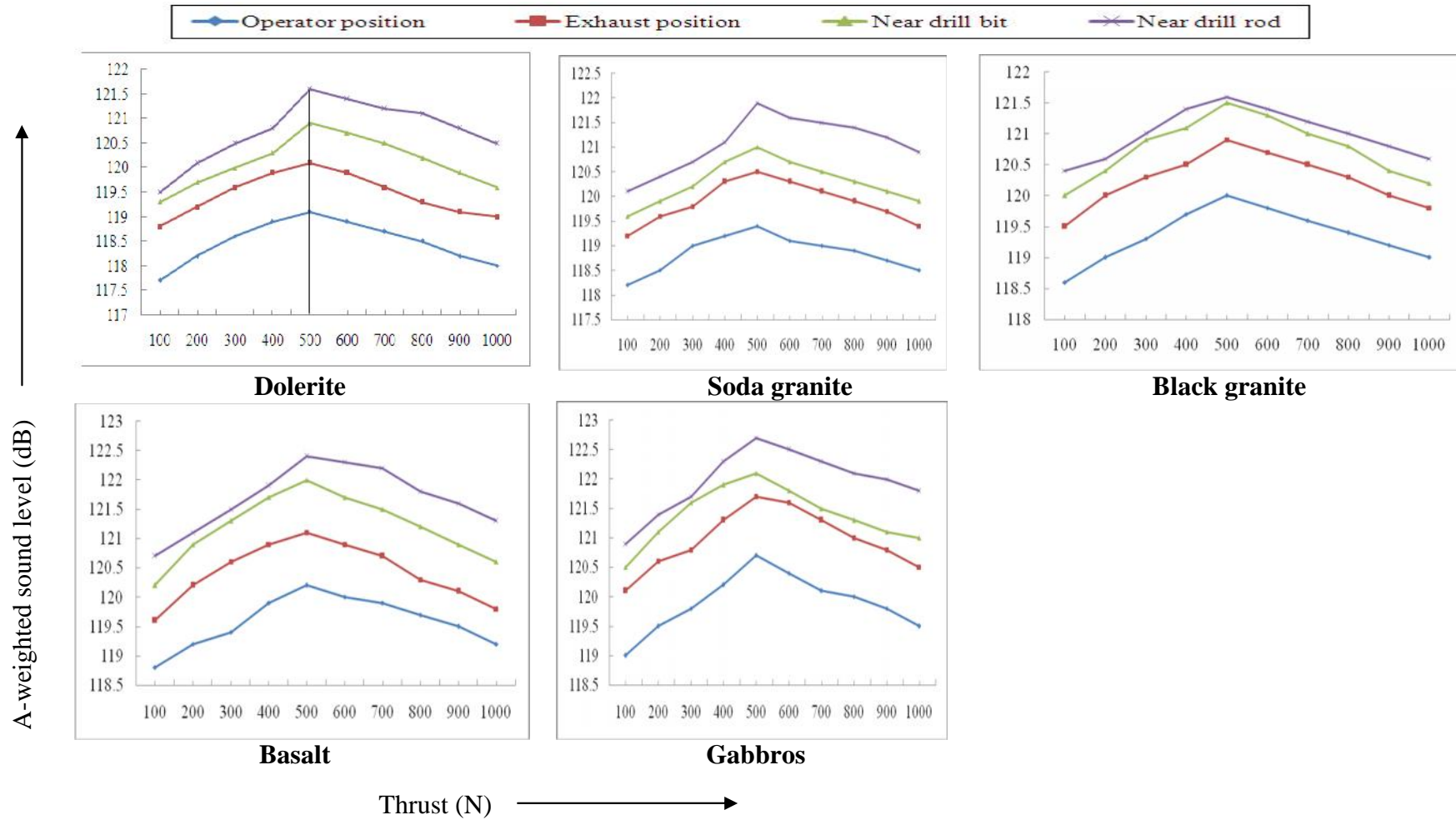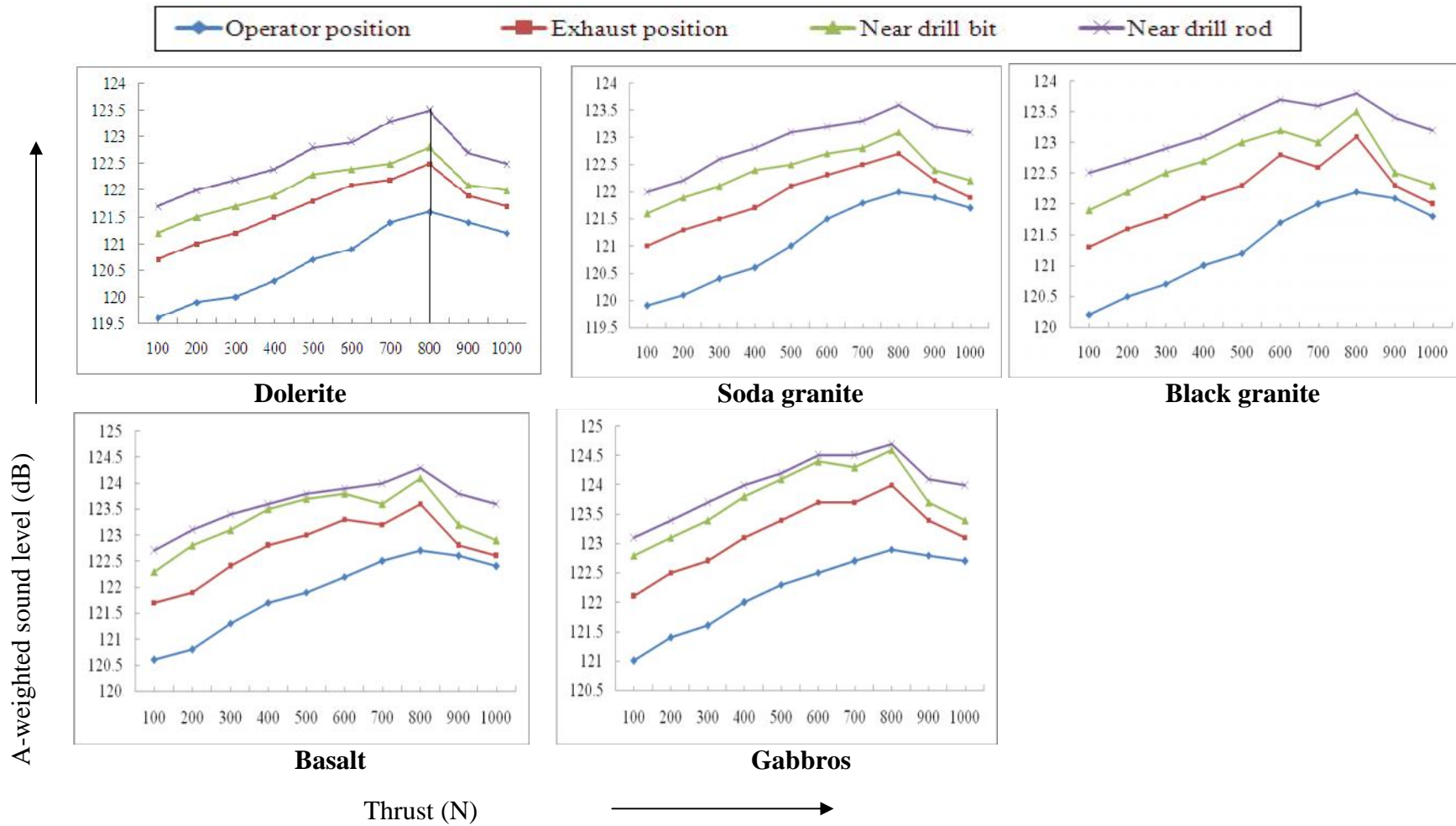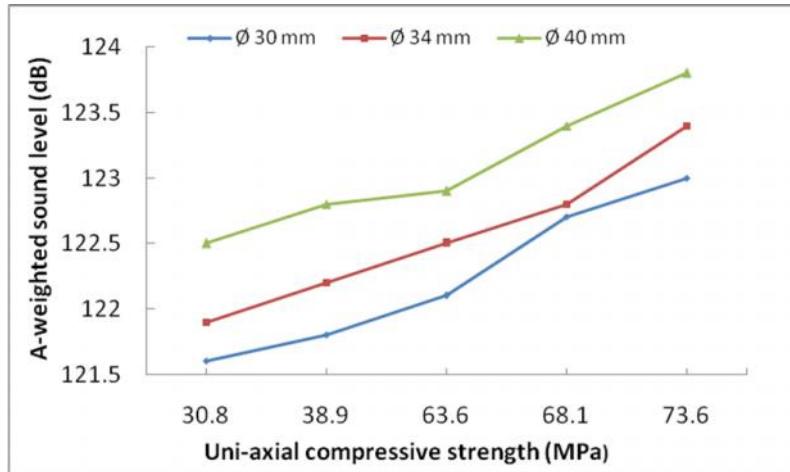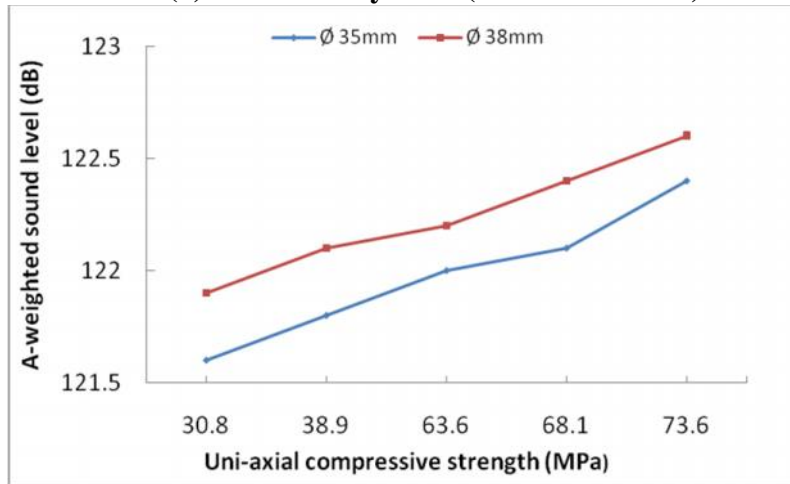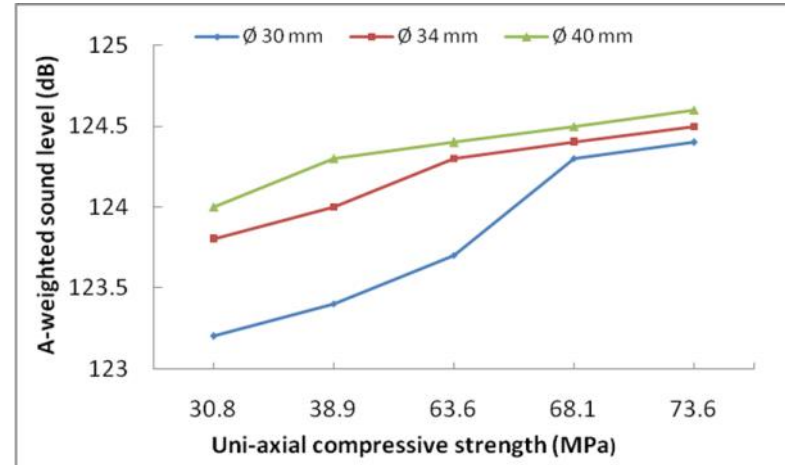
Fig. 5.24b Influence of thrust on A-weighted sound level for integral bit diameter of 30 mm and air pressure of 392 kPa for five different igneous rocks
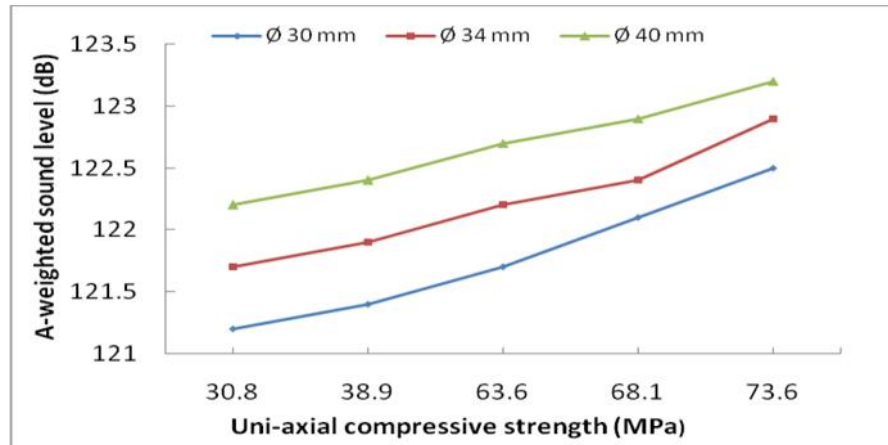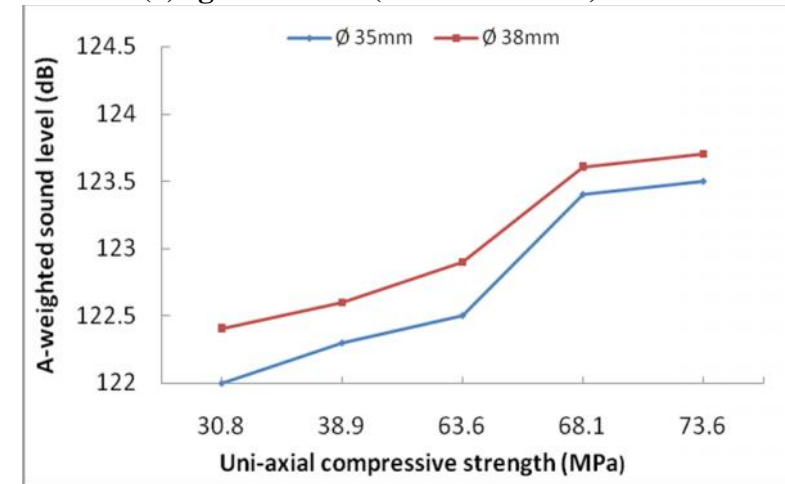
(a) Sedimentary rock (Thrust at 700 N)
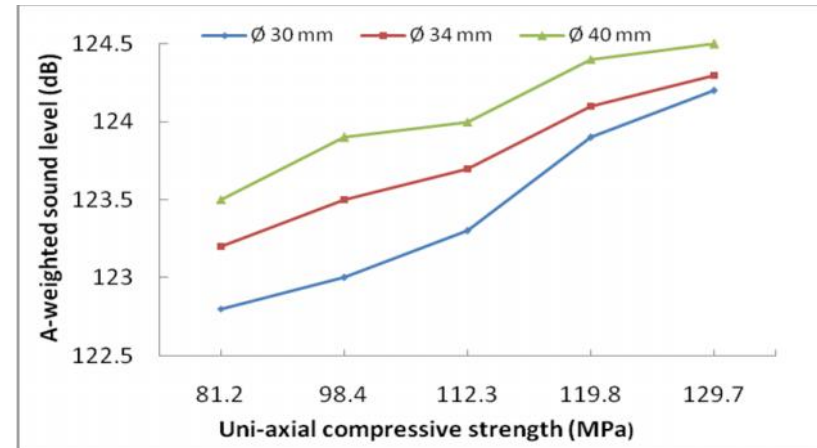
(a) Igneous rock (Thrust at 800N)
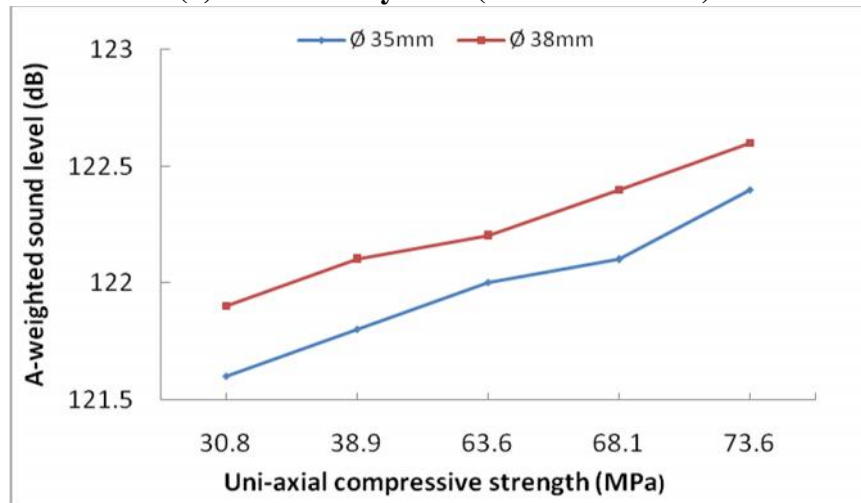
(b) Sedimentary rock (Thrust at 700 N)

(b) Igneous rock (Thrust at 800N)

Fig. 5.25 Influence of UCS on A-weighted sound level near drill bit at given air pressure of 588 kPa with (a) Integral and (b) Threaded drill bit diameters for different sedimentary and igneous rocks

(a) **Sedimentary rock (Thrust at 700 N)**

(a) **Igneous rock (Thrust at 800N)**
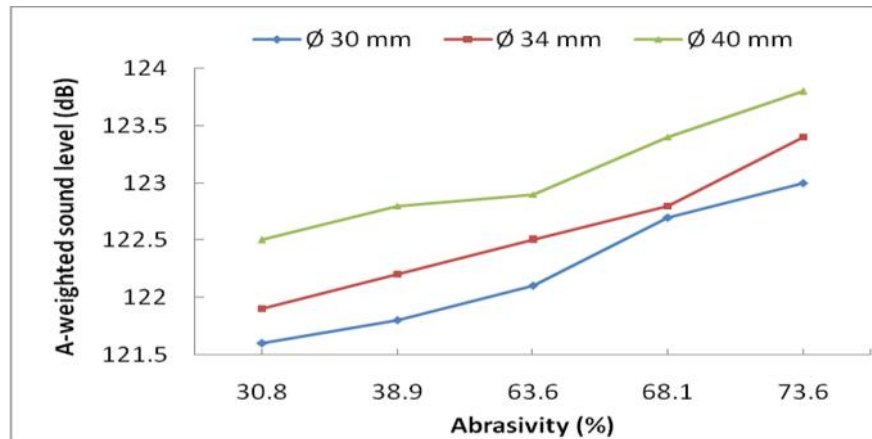
(b) **Sedimentary rock (Thrust at 700 N)**

(b) **Igneous rock (Thrust at 800N)**

Fig. 5.26 Influence of abrasivity on A-weighted sound level near drill bit at given air pressure of 588 kPa with (a) Integral and (b) Threaded drill bit diameters for different sedimentary and igneous rocks

Fig. 5.27a Influence of thrust on A-weighted sound level near drill bit at air pressure of 588 kPa with varying threaded bit diameters for five different sedimentary rocks

Fig. 5.27b Influence of thrust on A-weighted sound level near drill bit at air pressure of 588 kPa with varying threaded drill bit diameters for five different igneous rocks

Fig. 5.28a Influence of thrust on A-weighted sound level near drill rod at air pressure of 588 kPa with varying integral bit diameter for five different sedimentary rocks

Fig. 5.28b Influence of thrust on A-weighted sound level near drill rod at air pressure of 588 kPa with varying integral bit diameter for five different igneous rocks

Fig. 5.29a Influence of thrust on A-weighted sound level for integral bit diameter of 30 mm at air pressure of 588 kPa for five different sedimentary rocks

Appendix-II

Fig. 5.29b Influence of thrust on A-weighted sound level for integral bit diameter of 30 mm at air pressure of 588 kPa for five different igneous rocks

(a) Sedimentary rock (Thrust at 700 N)

(a) Igneous rock (Thrust at 800N)

(b) Sedimentary rock (Thrust at 700 N)

(b) Igneous rock (Thrust at 800N)

Fig. 5.30 Influence of UCS on A-weighted sound level near drill rod at given air pressure of 588 kPa with (a) Integral and (b) Threaded drill bit diameters for sedimentary and igneous rocks
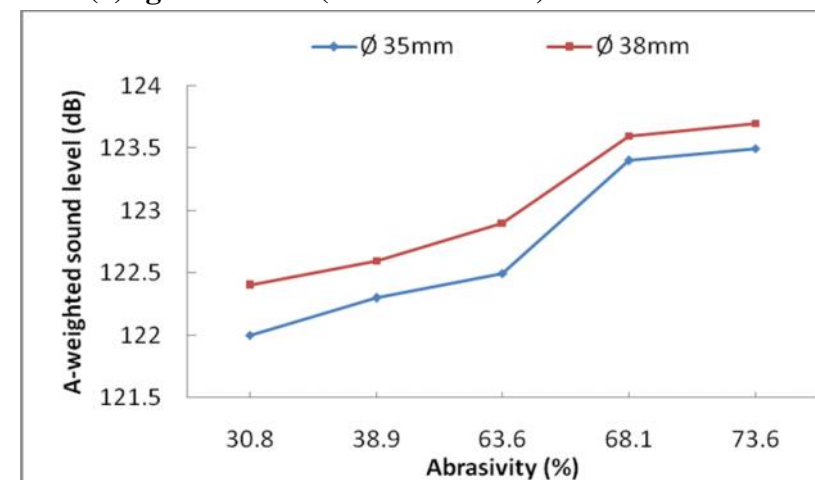
(a) Sedimentary rock (Thrust at 700 N)
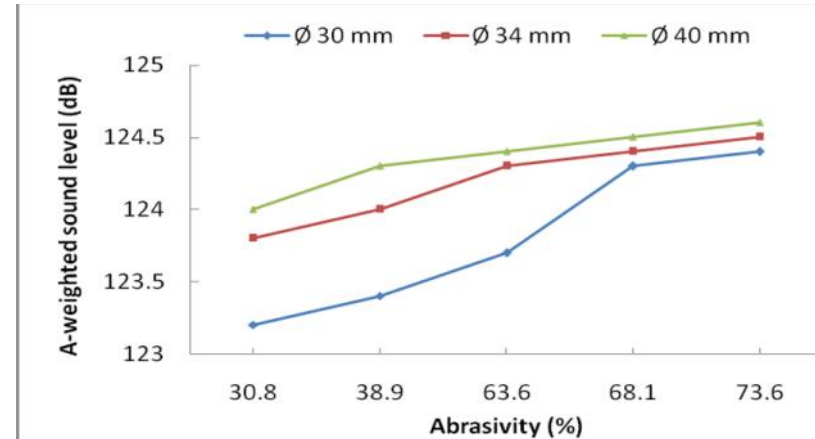
(a) Igneous rock (Thrust at 800N)
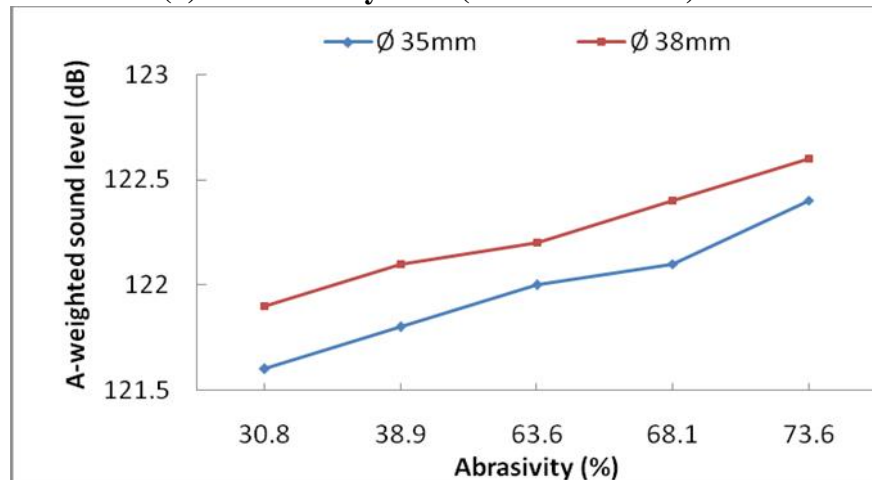
(b) Sedimentary rock (Thrust at 700 N)

(b) Igneous rock (Thrust at 800N)

Fig. 5.31 Influence of abrasivity on A-weighted sound level near drill rod at given air pressure of 588 kPa with (a) Integral and (b) Threaded drill bit diameters for sedimentary and igneous rocks
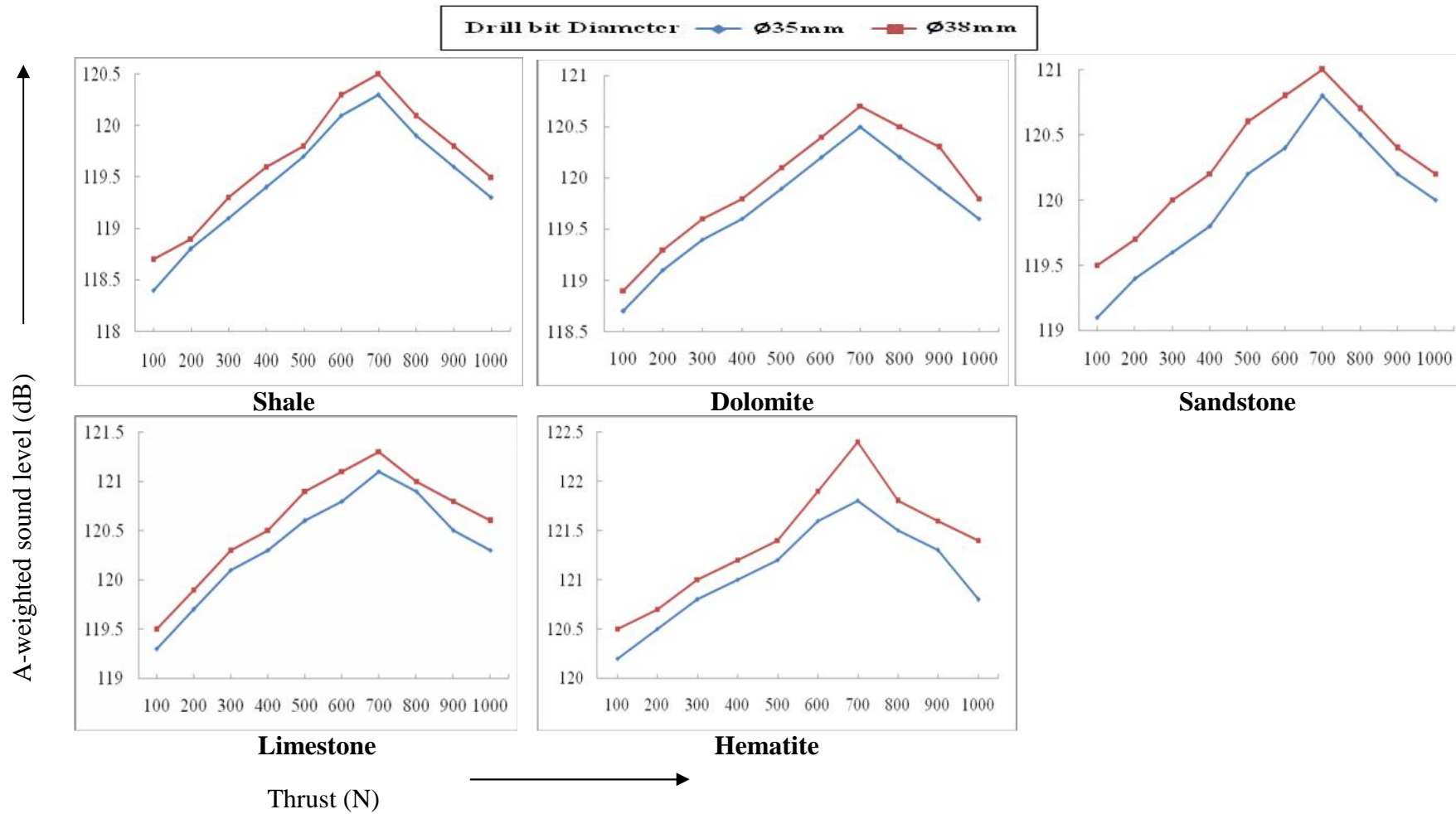
Fig. 5.32a Influence of thrust on A-weighted sound level near drill rod at air pressure of 588 kPa with varying threaded bit diameters for five different sedimentary rocks
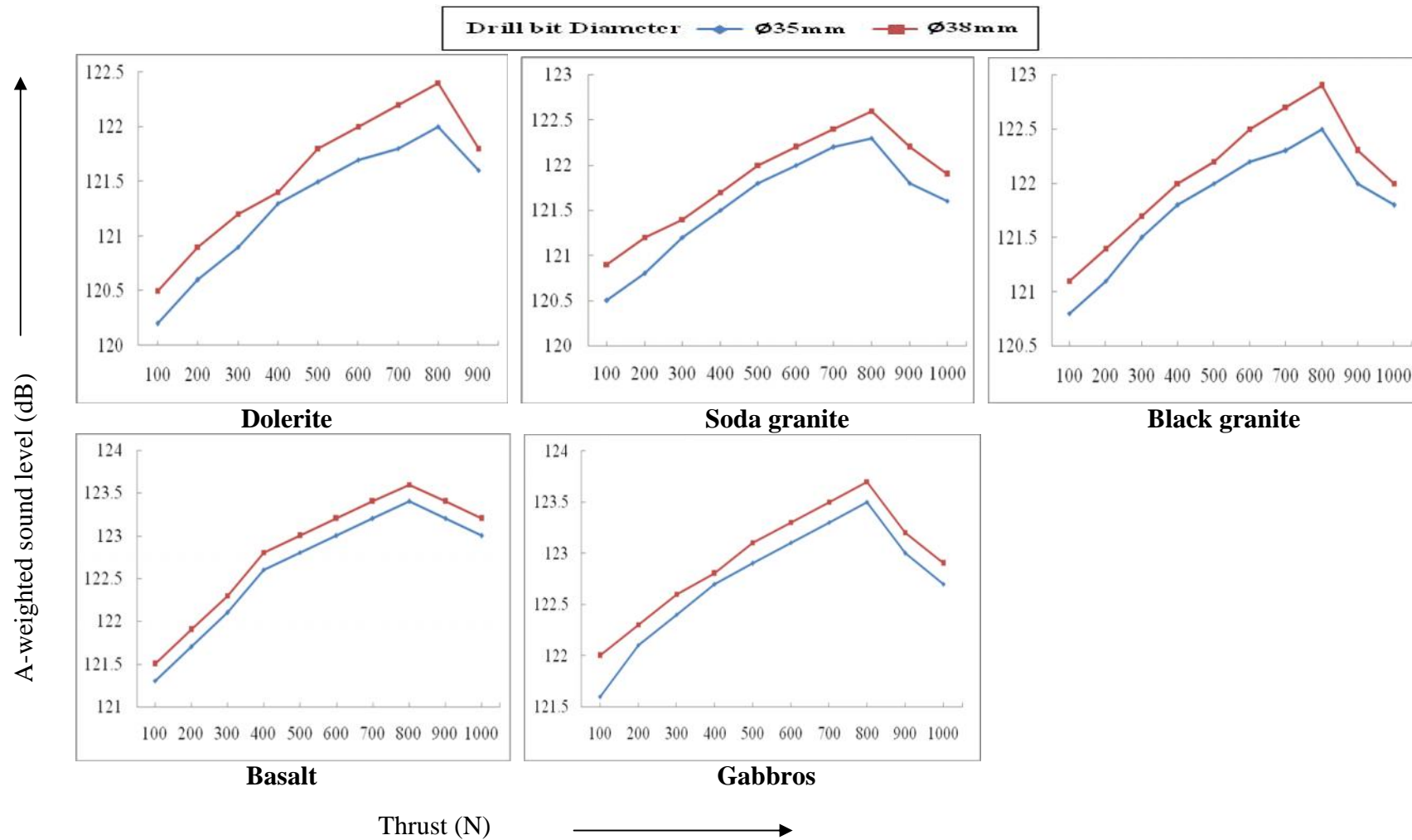
Fig. 5.32b Influence of thrust on A-weighted sound level near drill rod at air pressure of 588 kPa with varying threaded drill bit diameters for five different igneous rocks
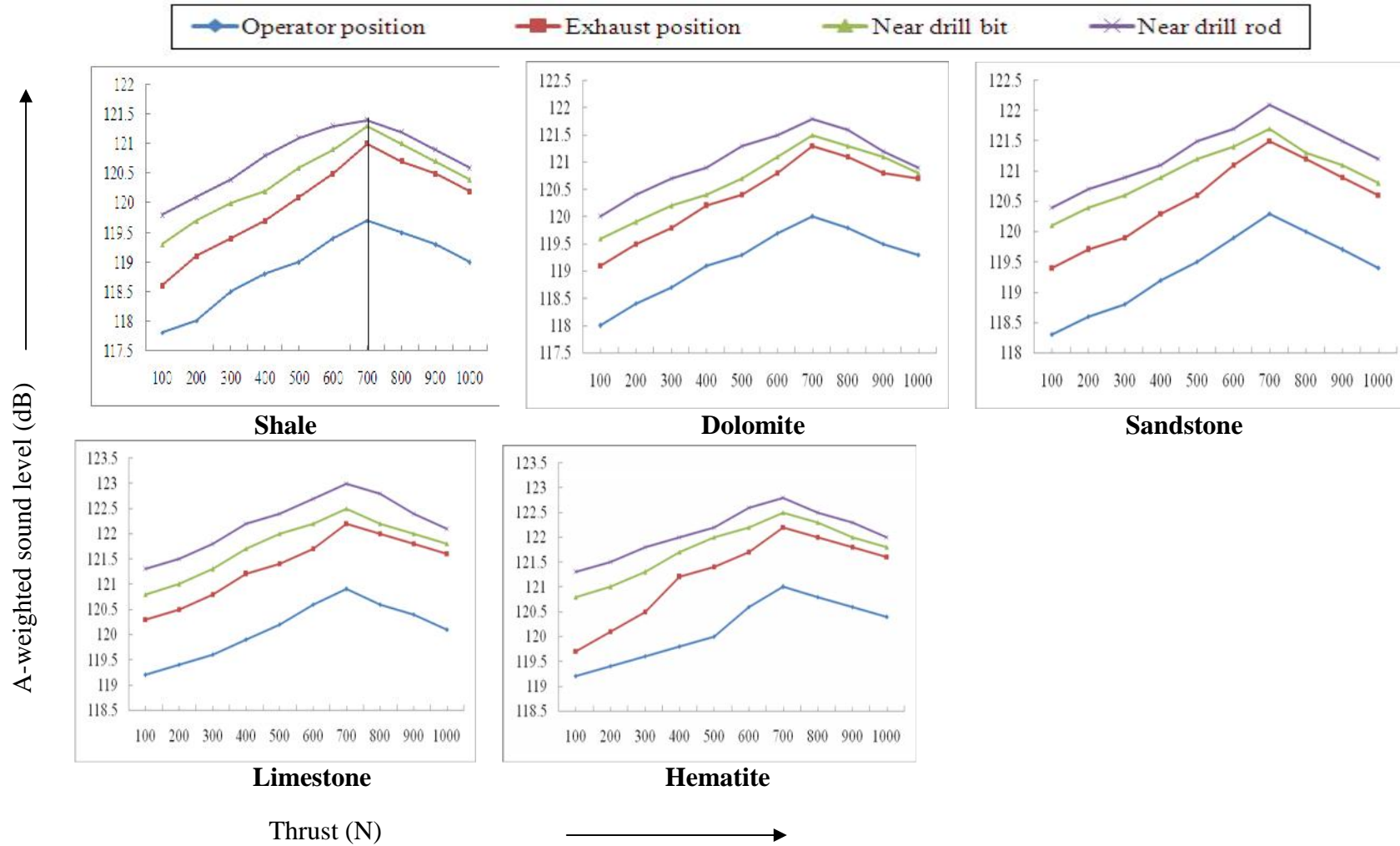
Fig. 5.33a Influence of thrust on A-weighted sound level for threaded bit diameter of 35 mm and air pressure of 392 kPa for five different sedimentary rocks
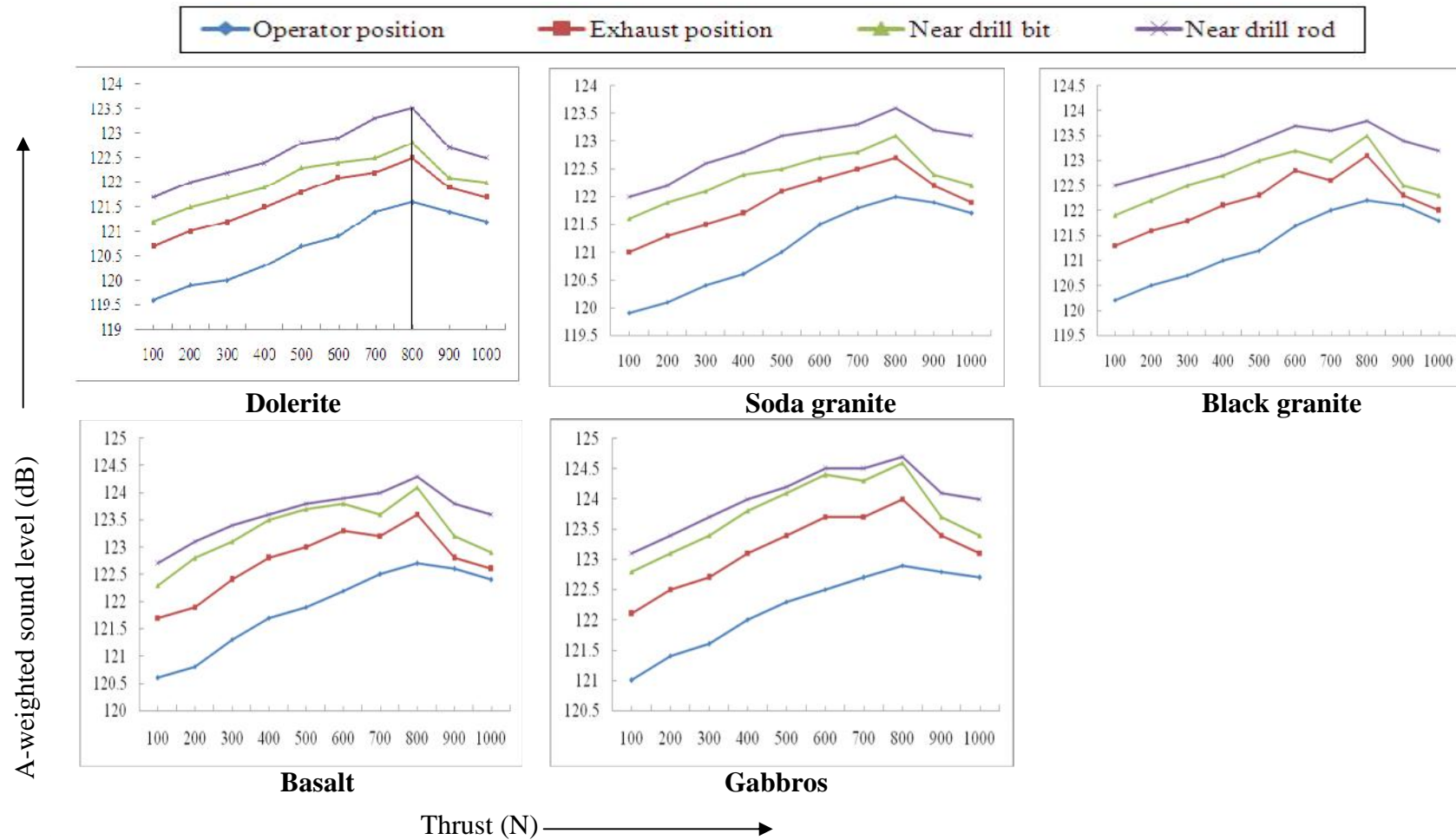
Fig. 5.33b Influence of thrust on A-weighted sound level for given threaded bit diameter of 35 mm at air pressure of 392 kPa for five different igneous rocks

APPENDIX - III

Igneous rock (Integral drill bit)

Table 1a Significance of regression coefficients for estimation of universal compressive strength (UCS)

Model Terms for UCS	Parameter Estimate (Coefficients)	t-value	p-value
Constant	-83527.6	181.728	0.000
A	-12.6430	-18.982	0.000
B	-142.034	-39.948	0.000
C	-0.0536181	-4.234	0.000
D	1449.91	43.164	0.000
E	-514.266	-33.300	0.000
A^2	-0.000799972	-13.172	0.000
B^2	0.0795914	4.760	0.000
C2	0.0000426728	5.933	0.000
D^2	-6.27243	-24.073	0.000
E^2	-3.33338	-7.107	0.000
A×B	-0.00888531	-8.755	0.000
A×D	0.111289	17.873	0.000
A×E	0.0196017	2.981	0.003
B×D	1.14743	15.319	0.000
B×E	-1.17482	-13.590	0.000
D×E	4.41352	8.473	0.000

Table 1b Analysis of variance (ANOVA) for the selected quadratic model for estimation of UCS

Source of variations	Degree of freedom	Sum of squares	Mean Squares	F-Value	P-Value
Model	16	200265	12516.6	590.79	0.000
Linear	5	178723	16714.8	788.95	0.000
Square	5	7848	2940.3	138.79	0.000
Interaction	6	13694	2282.3	107.73	0.000
Residual Error	733	15529	21.2		
Total	749	215794			

Table 1c Model summary for dependent variable (UCS)

R²Value	R² Predicted	R² Adjusted	Standard Error
92.80	92.45	92.65	4.6028

Table 2a Significance of regression coefficients for estimation of abrasivity

Model Terms for Ab	Parameter Estimate (Coefficients)	t-value	p-value
Constant	-3141.22	688.892	0.000
A	-0.574920	-16.982	0.000
B	-4.21367	-47.467	0.000
D	53.8855	49.477	0.000
E	27.4662	-53.357	0.000
A^2	-0.0000511900	-12.251	0.000
B^2	0.00672519	5.951	0.000
D^2	-0.228714	-12.867	0.000
E^2	0.312527	13.400	0.000
A×B	-0.000230658	-3.275	0.001
A×D	0.00507869	11.894	0.000
A×E	0.00464143	12.021	0.000
B×D	0.0303058	6.139	0.000
D×E	-0.264471	-11.093	0.000

Table 2b Analysis of variance (ANOVA) for the selected quadratic model for estimation of abrasivity

Source of variations	Degree of freedom	Sum of squares	Mean Squares	F-Value	P-Value
Model	13	1294.31	99.563	970.76	0.000
Linear	4	1209.30	128.317	1251.12	0.000
Square	4	52.10	12.493	121.81	0.000
Interaction	5	32.91	6.582	64.18	0.000
Residual Error	736	75.49	0.103		
Total	749	1369.80			

Table 2c Model summary for dependent variable (abrasivity)

R²Value	R² Predicted	R² Adjusted	Standard Error
94.49	94.28	94.39	0.3202

Table 3a Significance of regression coefficients for estimation of Tensile Strength

Model Terms for TS	Parameter Estimate (Coefficients)	t-value	p-value
Constant	-2702.98	160.012	0.000
A	-1.17604	-17.673	0.000
B	-12.2593	-36.698	0.000
C	-0.00525244	-3.804	0.000
D	130.415	40.063	0.000
E	-26.1781	-31.190	0.000
A^2	-0.000079859	-12.437	0.000
B^2	0.00926059	5.239	0.000
C^2	0.00000420054	5.530	0.000
D^2	-0.561824	-20.391	0.000
E^2	-0.148447	-2.994	0.003
A×B	-0.000764001	-7.121	0.000
A×D	0.0103484	15.720	0.000
A×E	0.00336702	4.844	0.000
B×D	0.0971597	12.274	0.000
B×E	-0.0874072	-9.565	0.000
D×E	0.214437	3.896	0.000

Table 3b Analysis of variance (ANOVA) for the selected quadratic model for estimation of tensile strength

Source of variations	Degree of freedom	Sum of squares	Mean Squares	F-Value	P-Value
Model	16	2297.83	143.615	606.47	0.000
Linear	5	2103.38	162.019	684.19	0.000
Square	5	88.72	25.310	106.88	0.000
Interaction	6	105.73	17.622	74.41	0.000
Residual Error	733	173.58	0.237		
Total	749	2471.41			

Table 3c Model summary for dependent variable (tensile strength)

R²Value	R² Predicted	R² Adjusted	Standard Error
92.89	92.64	92.82	0.4866

Table 4a Significance of regression coefficients for estimation of Schmidt
Rebound Number (SRN)

Model Terms for SRN	Parameter Estimate (Coefficients)	t-value	p-value
Constant	-4924.01	1105.020	0.000
A	-12.9616	-18.404	0.000
B	-126.432	-46.678	0.000
C	-0.0599892	-4.896	0.000
D	1381.03	51.307	0.000
E	-29.0512	-40.203	0.000
A^2	-0.000978919	-12.698	0.000
B^2	0.130459	6.154	0.000
C^2	0.0000484544	7.415	0.000
D^2	-5.91814	-18.193	0.000
A×B	-0.00753939	-5.828	0.000
A×D	0.114120	14.352	0.000
A×E	0.0625081	12.304	0.000
B×D	0.973851	10.692	0.000
B×E	-0.776766	-10.070	0.000

Table 4b Analysis of variance (ANOVA) for the selected quadratic model for
estimation of SRN

Source of variations	Degree of freedom	Sum of squares	Mean Squares	F-Value	P-Value
Model	14	414412	29600.8	850.92	0.000
Linear	5	386307	77294.0	2221.92	0.000
Square	4	11822	4157.3	119.51	0.000
Interaction	5	16282	3256.4	93.61	0.000
Residual Error	735	25568	34.8		
Total	749	439980			

Table 4c Model summary for dependent variable (SRN)

R²Value	R² Pred.	R² Adj.	Standard Error
94.19	93.95	94.08	5.898

Igneous rock (Threaded R22 type)

Table 5a Significance of regression coefficients for estimation of universal
compressive strength (UCS)

Model Terms for UCS	Parameter Estimate (Coefficients)	t-value	p-value
Constant	-90586.8	246.726	0.000
A	-12.8241	-18.198	0.000
B	-157.149	-20.531	0.000
C	-0.102835	-10.109	0.000
D	1576.58	51.616	0.000
E	-699.382	-23.778	0.000
A^2	-0.00101218	-15.574	0.000
C^2	7.81039E-05	10.434	0.000
D^2	-6.84228	-21.661	0.000
E	-5.99819	-8.072	0.000
A×B	-0.00527630	-2.087	0.037
A×D	0.113476	16.799	0.000
A×E	0.0644915	6.749	0.000
B×D	1.30681	7.131	0.000
B×E	-1.48356	-6.035	0.000
D×E	4.41352	7.565	0.000

Table 5b Analysis of variance (ANOVA) for the selected quadratic model for
estimation of UCS

Source of variations	Degree of freedom	Sum of squares	Mean Squares	F-Value	P-Value
Model	15	136076	9071.7	563.84	0.000
Linear	5	118796	13094.7	813.88	0.000
Square	4	7697	2826.8	175.69	0.000
Interaction	6	9583	1597.1	99.26	0.000
Residual Error	484	7787	16.1		
Total	499	143863			

Table 5c Model summary for dependent variable (UCS)

R²Value	R² Predicted	R² Adjusted	Standard Error
94.59	94.15	94.42	4.011

Table 6a Significance of regression coefficients for estimation of abrasivity

Model Terms for Ab	Parameter Estimate (Coefficients)	t-value	p-value
Constant	-1985.97	677.665	0.000
A	-0.464933	-13.354	0.000
B	-0.196998	-20.817	0.000
D	32.7951	38.666	0.000
E	65.4225	-19.975	0.000
A^2	-6.88005E-05	-13.893	0.000
C^2	5.43476E-06	9.696	0.000
D^2	-0.133516	-5.867	0.000
E^2	0.199613	3.596	0.000
A×D	0.00419554	8.361	0.000
A×E	0.0105524	14.668	0.000
D×E	-0.597676	-10.669	0.000

Table 6b Analysis of variance (ANOVA) for the selected quadratic model for estimation of abrasivity

Source of variations	Degree of freedom	Sum of squares	Mean Squares	F-Value	P-Value
Model	12	867.363	72.2802	767.95	0.000
Linear	5	801.175	52.2520	555.15	0.000
Square	4	39.904	9.3944	99.81	0.000
Interaction	3	26.284	8.7614	93.09	0.000
Residual Error	487	45.837	0.0941		
Total	499	913.200			

Table 6c Model summary for dependent variable (abrasivity)

R²Value	R² Predicted	R² Adjusted	Standard Error
94.98	94.64	94.86	0.3068

Table 7a Significance of regression coefficients for estimation of Tensile Strength

Model Terms for TS	Parameter Estimate (Coefficients)	t-value	p-value
Constant	-3652.91	214.622	0.000
A	-1.15494464933	-16.575	0.000
B	-9.47620	-18.791	0.000
C	-0.0117914	-12.185	0.000
D	125.839	50.645	0.000
E	-3.13058	-24.189	0.000
A^2	-1.06051E-04	-15.325	0.000
C^2	8.95236E-06	12.364	0.000
D^2	-0.539424	-17.280	0.000
E^2	-0.339815	-4.219	0.000
A×D	0.0101286	14.167	0.000
A×E	0.0107874	13.826	0.000
B×D	0.0765331	5.025	0.000
B×E	-0.0880001	-3.541	0.000

Table 7b Analysis of variance (ANOVA) for the selected quadratic model for estimation of tensile strength (TS)

Source of variations	Degree of freedom	Sum of squares	Mean Squares	F-Value	P-Value
Model	13	1555.67	119.667	632.60	0.000
Linear	5	1398.62	271.856	1437.12	0.000
Square	4	82.46	25.888	136.85	0.000
Interaction	4	74.59	18.648	98.58	0.000
Residual Error	486	91.94	0.189		
Total	499	1647.61			

Table 7c Model summary for dependent variable (tensile strength)

R^2Value	R^2 Predicted	R^2 Adjusted	Standard Error
94.42	94.05	94.27	0.4349

Table 8a Significance of regression coefficients for estimation of Schmidt Rebound
Number

Model Terms for SRN	Parameter Estimate (Coefficients)	t-value	p-value
Constant	-2905.42	1272.894	0.000
A	-11.4728	-14.622	0.000
B	-69.8878	-20.447	0.000
C	-0.136037	-11.033	0.000
D	1388.40	45.152	0.000
E	477.532	-20.201	0.000
A^2	-0.00129593	-13.851	0.000
C^2	0.000103554	11.333	0.000
D^2	-4.81711	-10.859	0.000
A×D	0.101723	10.666	0.000
A×E	0.161958	13.032	0.000
B×D	0.546060	2.973	0.003
D×E	-4.80393	-4.469	0.000

Table 8b Analysis of variance (ANOVA) for the selected quadratic model for
estimation of SRN

Source of variations	Degree of freedom	Sum of squares	Mean Squares	F-Value	P-Value
Model	12	276790	23065.8	679.56	0.000
Linear	5	254314	30343.0	893.96	0.000
Square	3	11048	4414.0	130.04	0.000
Interaction	4	11429	2857.1	84.18	0.000
Residual Error	487	16530	33.9		
Total	499	293320			

Table 8c Model summary for dependent variable (SRN)

R²Value	R² Predicted	R² Adjusted	Standard Error
94.36	94.01	94.23	5.826

Table 9a Significance of regression coefficients for estimation of sound level

Model Terms for sound level	Parameter Estimate (Coefficients)	t-value	p-value
Constant	112.712	4262.421	0.000
A	0.00848458	37.724	0.000
B	0.0907237	19.671	0.000
C	0.00589917	15.985	0.000
C^2	-0.00000588889	-22.576	0.000
A×C	0.00000333354	3.501	0.000

Table 9b Analysis of variance (ANOVA) for the selected quadratic model for estimation of sound level

Source of variations	Degree of freedom	Sum of squares	Mean Squares	F-Value	P-Value
Regression	5	697.155	139.431	517.50	0.000
Linear	3	556.524	185.508	688.51	0.000
Square	1	137.329	137.329	509.69	0.000
Interaction	1	3.302	3.302	12.25	0.000
Residual Error	744	200.459	0.269		
Total	749	897.614			

Table 9c Model summary for dependent variable (sound level)

R^2 Value	R^2 Predicted	R^2 Adjusted	Standard Error
95.99	95.86	95.93	0.2208

Table 10a Significance of regression coefficients for estimation of penetration rate

Model Terms for Penetration rate	Parameter Estimate (Coefficients)	t-value	p-value
Constant	1.32215	61.968	0.000
A	0.000985088	14.585	0.000
B	-0.0272657	-6.112	0.000
C	0.00399512	17.223	0.000
C^2	-4.95972E-06	-19.659	0.000
A×C	5.22404E-06	5.672	0.000

Table 10b Analysis of variance (ANOVA) for the selected quadratic model for estimation of penetration rate

| Source of variations	Degree of freedom	Sum of squares	Mean Squares	F-Value	P-Value
Regression	5	243.312	48.6624	193.07	0.000
Linear	3	137.792	45.9307	182.23	0.000
Square	1	97.411	97.4112	386.48	0.000
Interaction	1	8.109	8.1087	32.17	0.000
Residual Error	744	187.524	0.2520		
Total	749	430.836			

Table 10c Model summary for dependent variable (penetration rate)

R^2 Value	R^2 Predicted	R^2 Adjusted	Standard Error
86.47	85.86	86.18	0.5020

Table 11a Significance of regression coefficients for estimation of sound level

Model Terms for sound level	Parameter Estimate (Coefficients)	t-value	p-value
Constant	109.413	433.640	0.000
A	-0.00115996	83.840	0.000
B	0.0736	13.562	0.000
C	0.00652005	37.534	0.000
D	0.324432	-4.033	0.000
E	1.17027	5.407	0.000
F	0.684527	4.080	0.000
A^2	0.00000105908	5.227	0.000
C^2	-0.00000547045	-48.831	0.000
D^2	-0.002179	-4.526	0.000
A×C	0.00000114533	2.800	0.005

Table 11b Analysis of variance (ANOVA) for the selected quadratic model for estimation of sound level

Source of variations	Degree of freedom	Sum of squares	Mean Squares	F-Value	P-Value
Regression	10	480.488	48.0488	1450.16	0.000
Linear	6	399.640	66.4772	2006.34	0.000
Square	3	80.588	26.8627	810.74	0.000
Interaction	1	0.260	0.2598	7.84	0.005
Residual Error	489	16.202	0.0331		
Total	499	496.690			

Table 11c Model summary for dependent variable (sound level)

R^2 Value	R^2 Predicted	R^2 Adjusted	Standard Error
96.74	96.60	96.67	0.1820

Table 12a Significance of regression coefficients for estimation of penetration rate

Model Terms for Penetration rate	Parameter Estimate (Coefficients)	t-value	p-value
Constant	1.45923	1.962	0.050
A	0.032553	19.246	0.000
B	-0.0424973	-8.076	0.000
C	0.00927668	19.992	0.000
D	-0.175622	2.708	0.007
E	0.257183	-3.694	0.000
F	-0.696171	-2.514	0.012
C^2	-0.00000407355	-37.499	0.000
D^2	0.00123892	2.654	0.008
A×C	0.00000556811	14.040	0.000
A×D	0.0000524761	2.583	0.010
A×E	-0.00172338	-6.759	0.000
C×D	-0.0000425462	-2.199	0.028
C×E	-0.000341721	-3.822	0.000
C×F	0.000522208	2.357	0.019

Table 12b Analysis of variance (ANOVA) for the selected quadratic model for estimation of penetration rate

Source of variations	Degree of freedom	Sum of squares	Mean Squares	F-Value	P-Value
Regression	14	168.448	12.0320	386.21	0.000
Linear	6	110.388	10.0093	321.29	0.000
Square	2	44.027	22.0136	706.61	0.000
Interaction	6	14.033	2.3388	75.07	0.000
Residual Error	485	15.110	0.0312		
Total	499	183.557			

Table 12c Model summary for dependent variable (penetration rate)

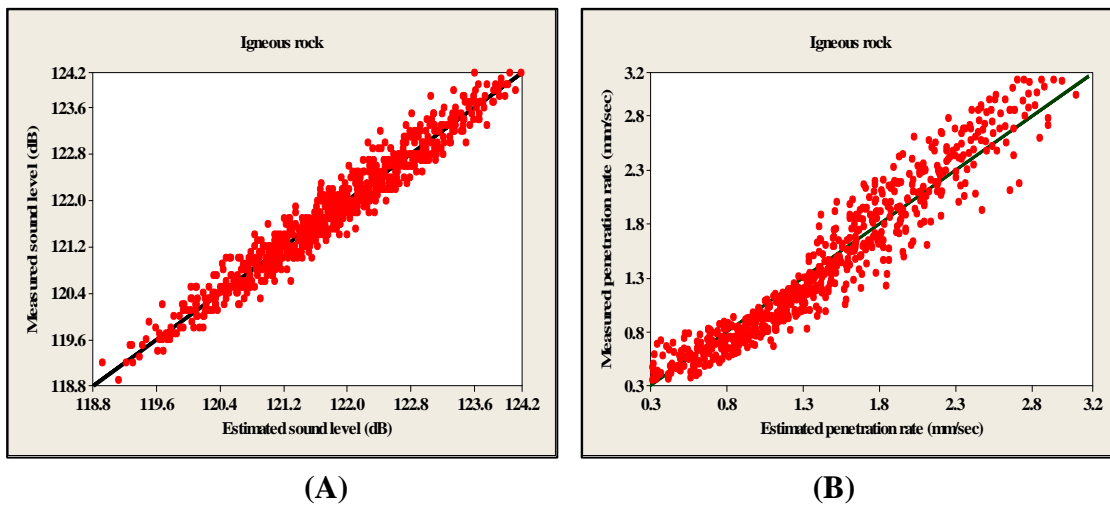| R^2 Value	R^2 Predicted	R^2 Adjusted	Standard Error
91.77	91.21	91.43	0.1765
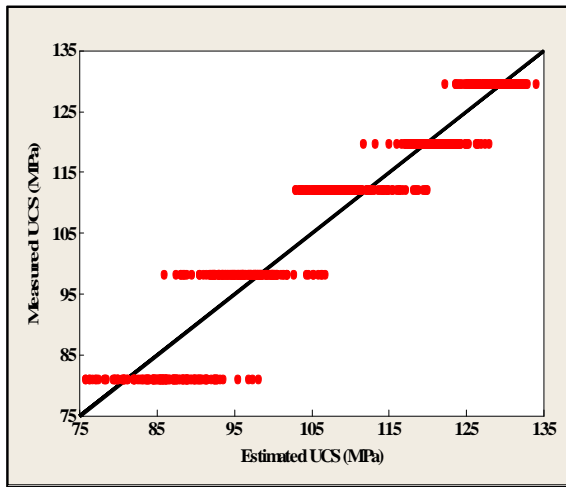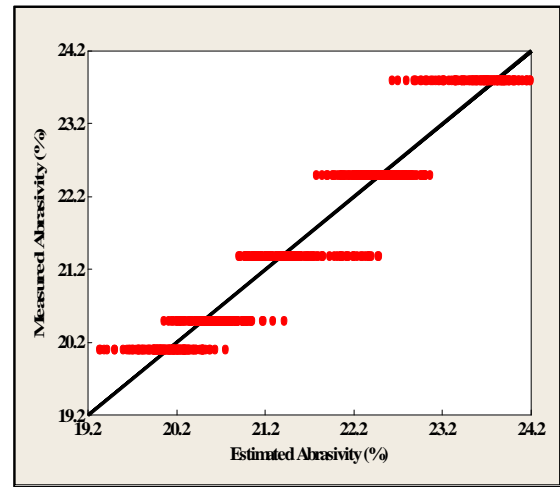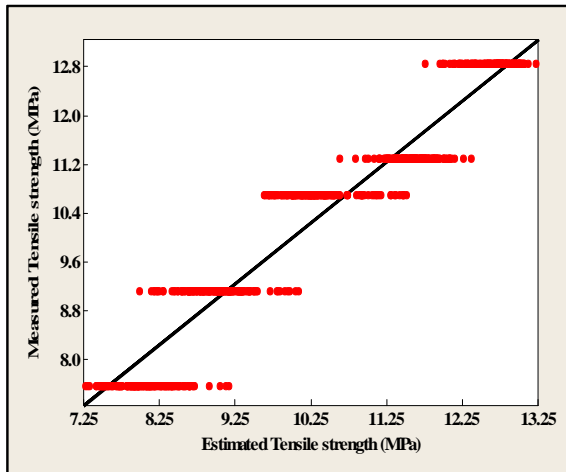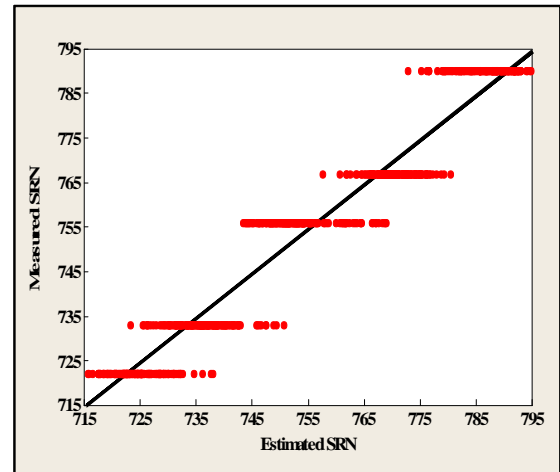
Fig. 1 Cross correlation graph between predicted and measured for sedimentary rocks
using integral drill bit
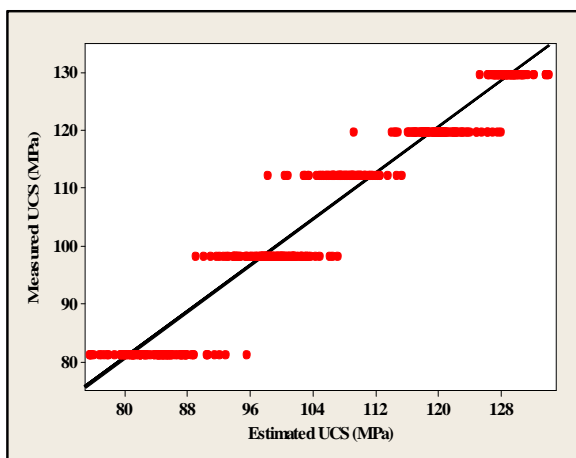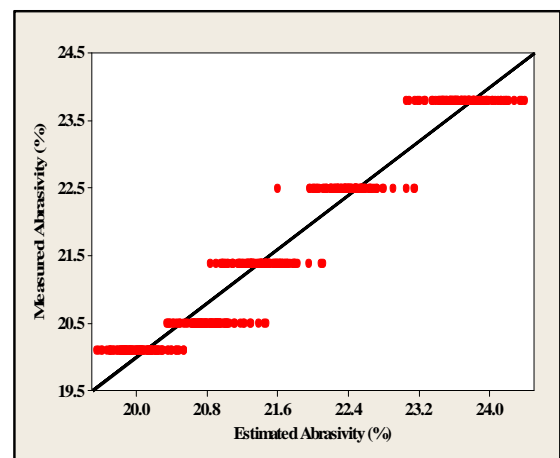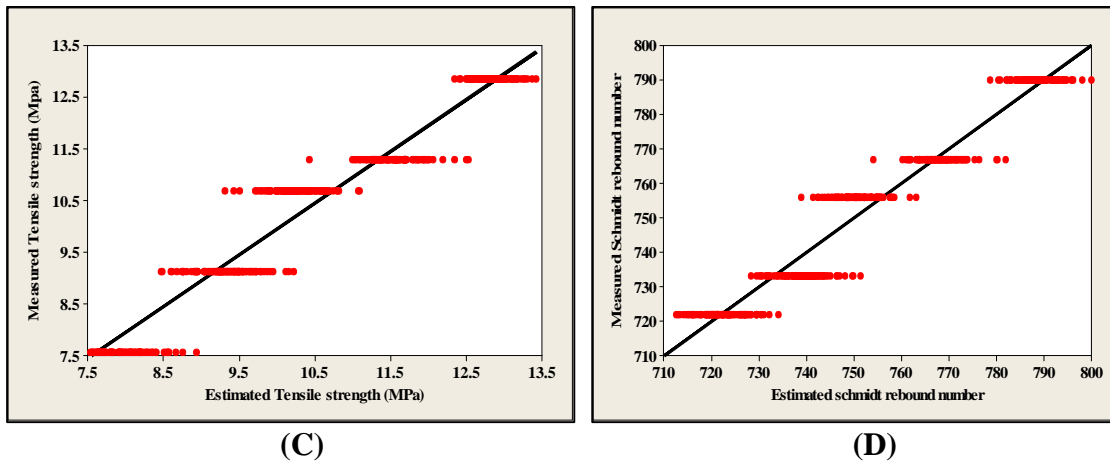
Fig. 2 Cross correlation graph between predicted and measured for sedimentary rocks using threaded drill bit

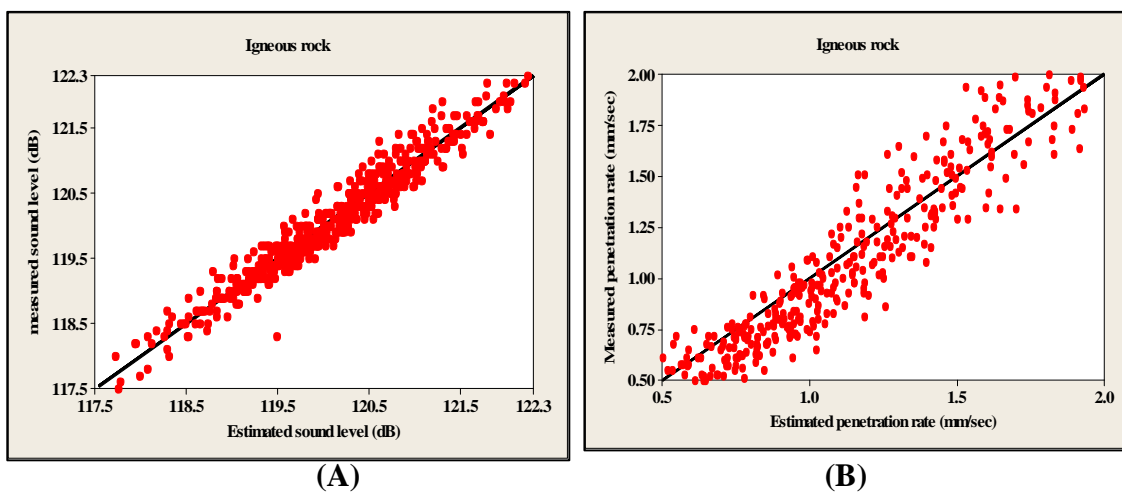**Fig. 3** Cross correlation graph between predicted and measured for sedimentary rocks using integral drill bit

Fig. 4 Cross correlation graph between predicted and measured for sedimentary rocks using threaded drill bit

APPENDIX - IV

Table 1a Performance prediction indices of different training algorithms for
igneous rock using integral drill bit

			UCS	Abrasivity	Tensile strength	SRN
traingda	Training data	VAF	87.691	86.192	89.276	83.859
		RMSE	4.285	2.091	2.173	2.962
		MAPE	12.309	13.808	10.724	16.141
	Testing data	VAF	85.256	84.056	86.675	81.587
		RMSE	5.314	2.498	3.634	4.678
		MAPE	14.744	15.944	13.325	20.413
trainrp	Training data	VAF	89.827	88.293	90.697	85.568
		RMSE	0.2434	0.0531	0.0213	2.132
		MAPE	10.173	11.707	9.303	14.432
	Testing data	VAF	89.189	86.329	89.980	83.475
		RMSE	0.4843	0.1891	0.0385	4.243
		MAPE	10.811	13.671	10.020	16.525
trainscg	Training data	VAF	90.756	91.245	91.356	86.579
		RMSE	0.2239	0.0526	0.0267	2.1301
		MAPE	9.244	8.755	8.644	13.241
	Testing data	VAF	89.274	89.738	90.186	84.430
		RMSE	0.3483	0.07695	0.05482	4.796
		MAPE	10.726	10.262	9.814	15.570
trainlm	Training data	VAF	96.765	95.842	97.152	94.73
		RMSE	0.1423	0.0321	0.0154	1.456
		MAPE	3.235	4.158	2.848	5.27
	Testing data	VAF	92.675	92.243	93.532	91.371
		RMSE	0.1731	0.0547	0.0178	4.870
		MAPE	7.325	8.757	6.468	9.629

Table 1b Performance of different training algorithm for igneous rock using
integral drill bit

Training algorithm	Network architecture	Number of epochs	Time taken for convergence (sec)	Mean square error
trainrp	5,13,10,7,4	94	04	0.00000965
trainlm	5,13,10,7,4	10	02	0.00000894
trainscg	5,13,10,7,4	908	23	0.00000973
traingda	5,13,10,7,4	2000	29	0.00676

Table 2a Performance prediction indices of different training algorithms for
igneous rock using threaded drill bit

			UCS	Abrasivity	Tensile strength	SRN
traingda	Training data	VAF	84.175	84.398	87.172	83.565
		RMSE	4.99	2.345	2.987	3.231
		MAPE	15.825	15.602	12.828	16.435
	Testing data	VAF	83.762	83.893	85.845	81.762
		RMSE	6.435	3.675	4.823	5.972
		MAPE	16.238	16.107	14.155	18.238
trainrp	Training data	VAF	86.234	85.137	87.175	83.123
		RMSE	0.2435	0.0635	0.0243	2.317
		MAPE	13.766	14.863	12.825	16.877
	Testing data	VAF	85.125	84.246	86.098	82.967
		RMSE	0.4434	0.2130	0.0548	5.465
		MAPE	14.875	15.754	13.902	17.033
trainscg	Training data	VAF	87.325	88.545	89.128	84.237
		RMSE	0.2412	0.0675	0.0298	2.2187
		MAPE	12.675	11.455	10.872	15.763
	Testing data	VAF	86.698	87.173	88.217	83.043
		RMSE	0.4833	0.0956	0.0529	5.69
		MAPE	13.302	12.827	11.783	16.957
trainlm	Training data	VAF	93.275	93.678	94.534	93.768
		RMSE	0.1651	0.0387	0.0189	1.786
		MAPE	6.725	6.322	5.466	6.232
	Testing data	VAF	91.432	92.238	92.876	91.154
		RMSE	0.1932	0.0385	0.0123	5.123
		MAPE	8.568	7.762	7.124	8.846

Table 2b Performance of different training algorithm for igneous rock (threaded bit)

Training algorithm	Network architecture	Number of epochs	Time taken for convergence (sec)	Mean square error
trainrp	5,13,10,7,4	81	2	0.00000987
trainlm	5,13,10,7,4	6	1	0.00000625
trainscg	5,13,10,7,4	1492	27	0.00000994
traingda	5,13,10,7,4	2000	22	0.00417

Table 3a Performance prediction indices of different training algorithms for
igneous rock using integral drill bit

			Penetration rate	Sound level
traingda	Training data	VAF	87.324	89.758
		RMSE	2.013	2.237
		MAPE	12.676	10.242
	Testing data	VAF	85.705	87.154
		RMSE	2.564	3.421
		MAPE	14.295	12.846
trainrp	Training data	VAF	88.654	90.096
		RMSE	0.0458	0.0359
		MAPE	11.346	9.904
	Testing data	VAF	86.391	87.364
		RMSE	0.2397	0.0297
		MAPE	13.609	12.636
trainscg	Training data	VAF	90.784	91.983
		RMSE	0.0437	0.314
		MAPE	9.216	8.017
	Testing data	VAF	88.527	89.894
		RMSE	0.0672	0.0572
		MAPE	11.473	10.106
trainlm	Training data	VAF	95.337	96.767
		RMSE	0.0234	0.0174
		MAPE	4.663	3.233
	Testing data	VAF	93.162	94.142
		RMSE	0.0496	0.0193
		MAPE	6.838	5.858

Table 3b Performances of different training algorithm for igneous rock (integral bit)

Training algorithm	Network architecture	Number of epochs	Time taken for convergence (sec)	Mean square error
trainrp	4,13,10,7,2	252	03	0.0000131
trainlm	4,13,10,7,2	09	01	0.0000121
trainscg	4,13,10,7,2	2000	47	0.0000143
traingda	4,13,10,7,2	2000	27	0.0000631

Table 4a Performance prediction indices of different training algorithms for
igneous rock using threaded drill bit

			Penetration rate	Sound level
traingda	Training data	VAF	85.324	87.758
		RMSE	2.199	2.176
		MAPE	14.676	12.242
	Testing data	VAF	83.705	85.954
		RMSE	4.129	3.926
		MAPE	16.295	14.046
trainrp	Training data	VAF	85.654	88.096
		RMSE	0.0627	0.0698
		MAPE	14.346	11.904
	Testing data	VAF	84.391	87.364
		RMSE	0.2397	0.0412
		MAPE	15.609	12.636
trainscg	Training data	VAF	93.184	93.983
		RMSE	0.0437	0.0342
		MAPE	6.816	6.017
	Testing data	VAF	91.527	91.894
		RMSE	0.0893	0.0812
		MAPE	8.473	8.106
trainlm	Training data	VAF	94.337	96.767
		RMSE	0.0437	0.0295
		MAPE	5.663	3.233
	Testing data	VAF	92.162	93.142
		RMSE	0.0369	0.0268
		MAPE	7.838	6.858

Table 4b Performances of different training algorithm for igneous rock (Threaded bit)

Training algorithm	Network architecture	Number of epochs	Time taken for convergence (sec)	Mean square error
trainrp	4,13,10,7,2	59	02	0.00000909
trainlm	4,13,10,7,2	08	01	0.00000660
trainscg	413,10,7,2	471	10	0.000012
traingda	4,13,10,7,2	2000	25	0.0000399

Table 5a. Comparison of performance of the developed model of MRA and ANN for sedimentary rock using integral drill bit

|	Rock properties	RMSE	VAF	MAPE
MRA	Uniaxial compressive strength	4.56	95.350	4.65
	Abrasivity	0.3172	94.650	5.35
	Tensile strength	0.4811	96.720	3.28
	Schmidt rebound number	5.8574	93.55	5.45
ANN	Uniaxial compressive strength	0.1423	96.765	3.235
	Abrasivity	0.0321	95.842	4.158
	Tensile strength	0.0154	97.152	2.848
	Schmidt rebound number	1.456	94.730	5.27

Table 5b Comparison of performance of the developed model of MRA and ANN for sedimentary rock using threaded drill bit

	Rock properties	RMSE	VAF	MAPE
MRA	Uniaxial compressive strength	7.50	92.69	7.31
	Abrasivity	0.3028	93.678	6.322
	Tensile strength	0.4318	94.534	5.466
	Schmidt rebound number	5.75	93.768	6.232
ANN	Uniaxial compressive strength	0.1651	93.275	6.725
	Abrasivity	0.0387	93.978	6.022
	Tensile strength	0.0189	94.843	5.157
	Schmidt rebound number	1.786	93.897	6.103

Table 5c. Comparison of performance of the developed model of MRA and ANN for sedimentary rock using integral drill bit

		RMSE	VAF	MAPE
MRA	Sound level	0.4200	94.64	5.36
	Penetration rate	0.2380	95.106	4.894
ANN	Sound level	0.0174	96.767	3.233
	Penetration rate	0.0234	95.337	4.663

Table 5d. Comparison of performance of the developed model of MRA and ANN for sedimentary rock using threaded drill bit

		RMSE	VAF	MAPE
MRA	Sound level	0.4200	94.638	5.362
	Penetration rate	0.2870	94.175	5.825
ANN	Sound level	0.0295	96.767	3.233
	Penetration rate	0.0437	94.337	5.663
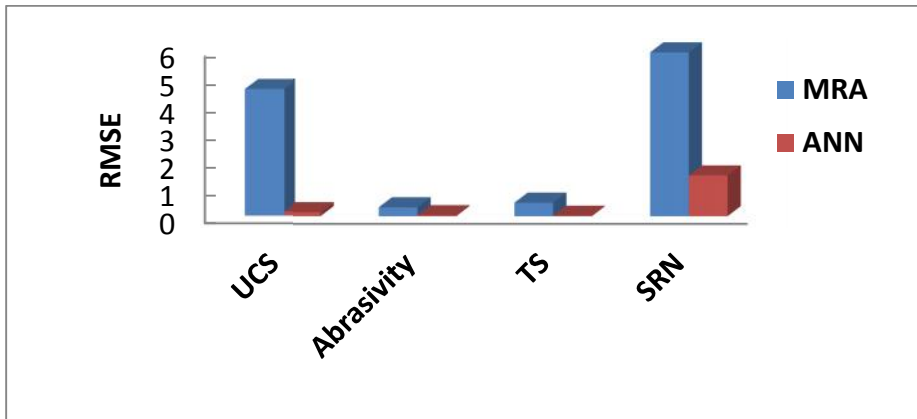
(A)
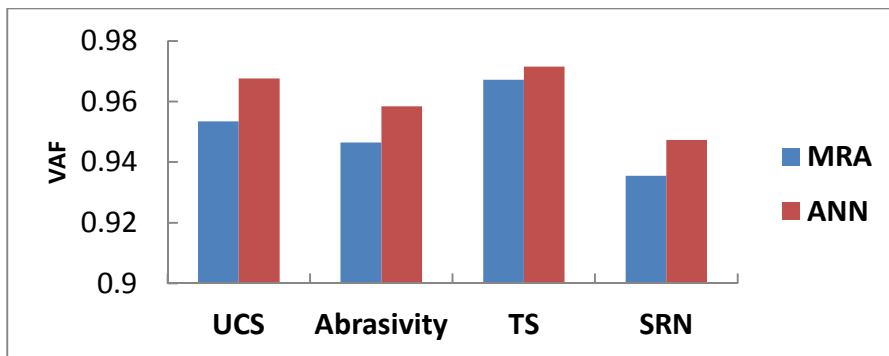
(B)
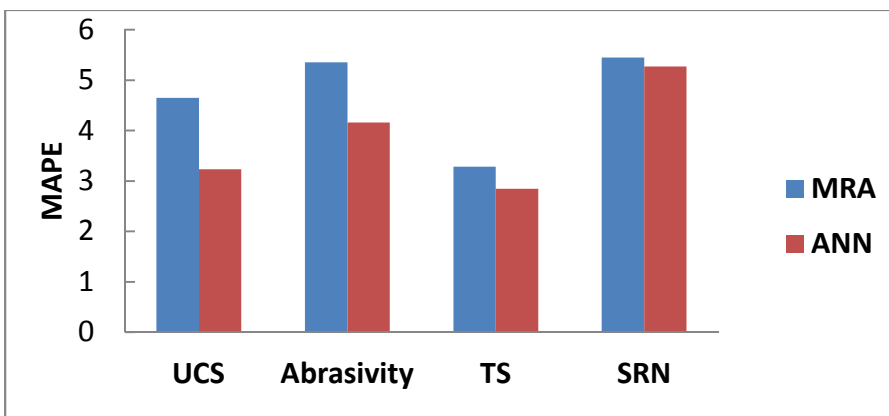
(C)

Fig. 1 Performance indices (a) RMSE (b) VAF and (c) MAPE values of MRA and ANN for Igneous rock using integral drill bit
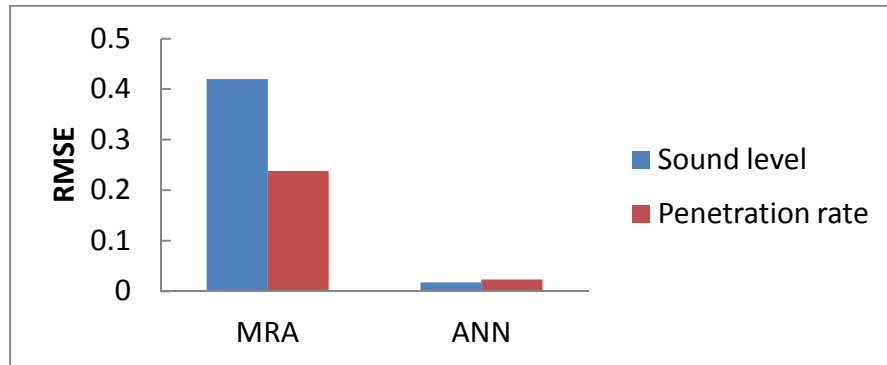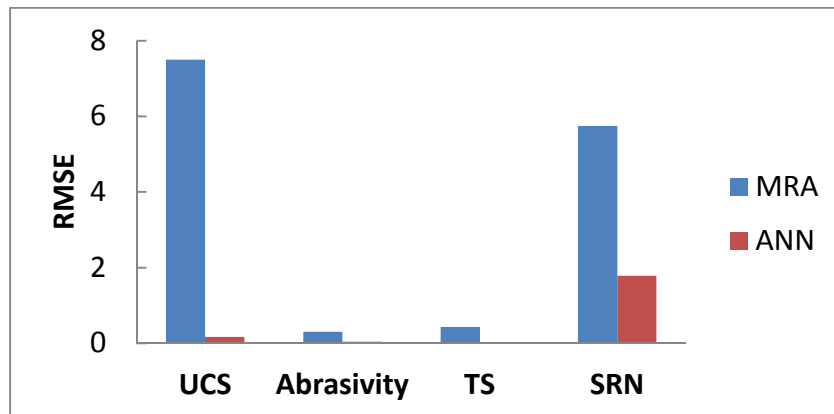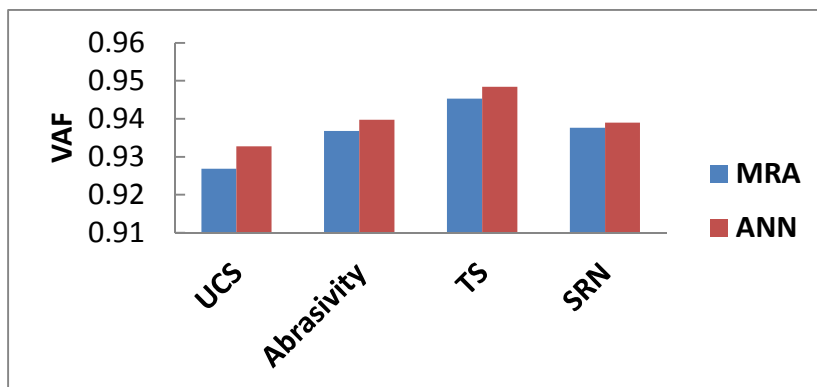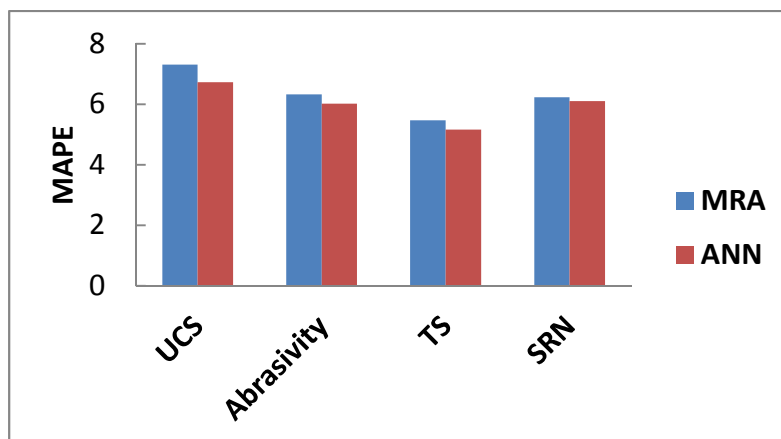
(A)
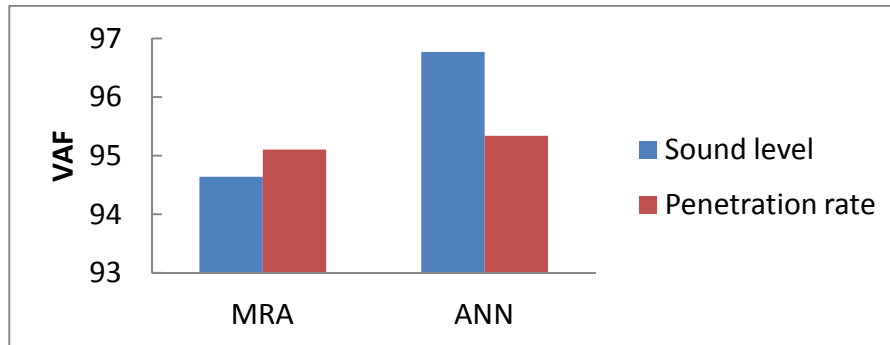
(B)
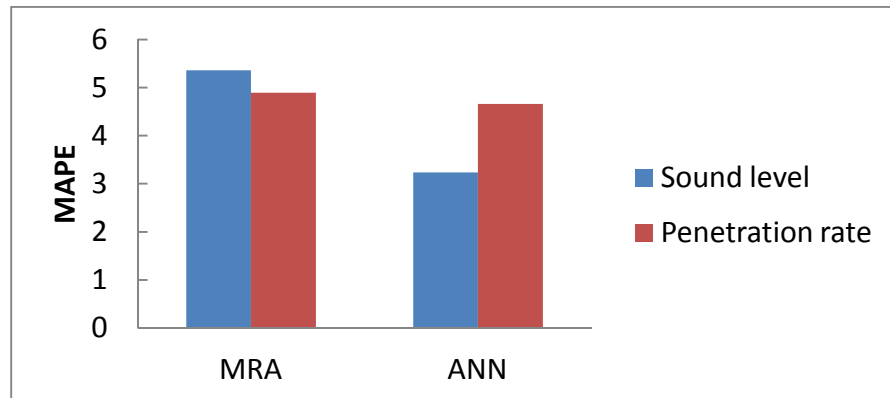
(C)

Fig. 2 Performance indices (A) RMSE (B) VAF and (C) MAPE values of MRA and ANN for igneous rock integral drill bit

(A)

(B)
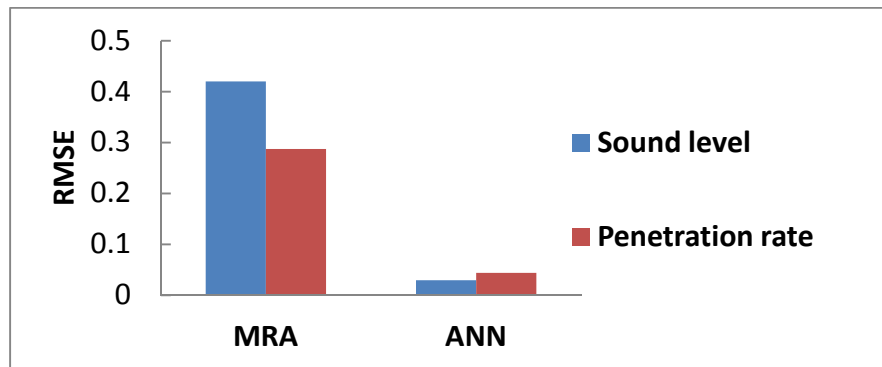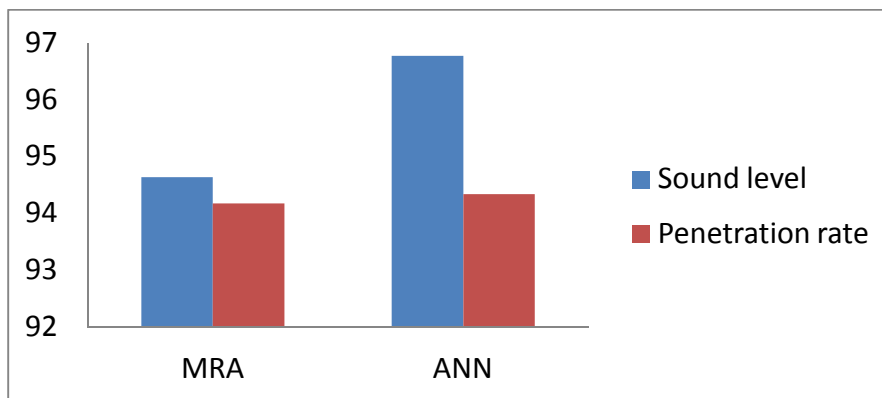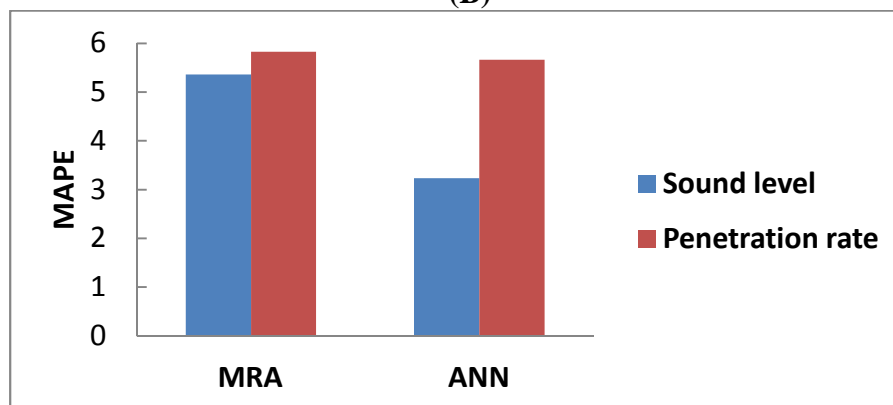

(C)

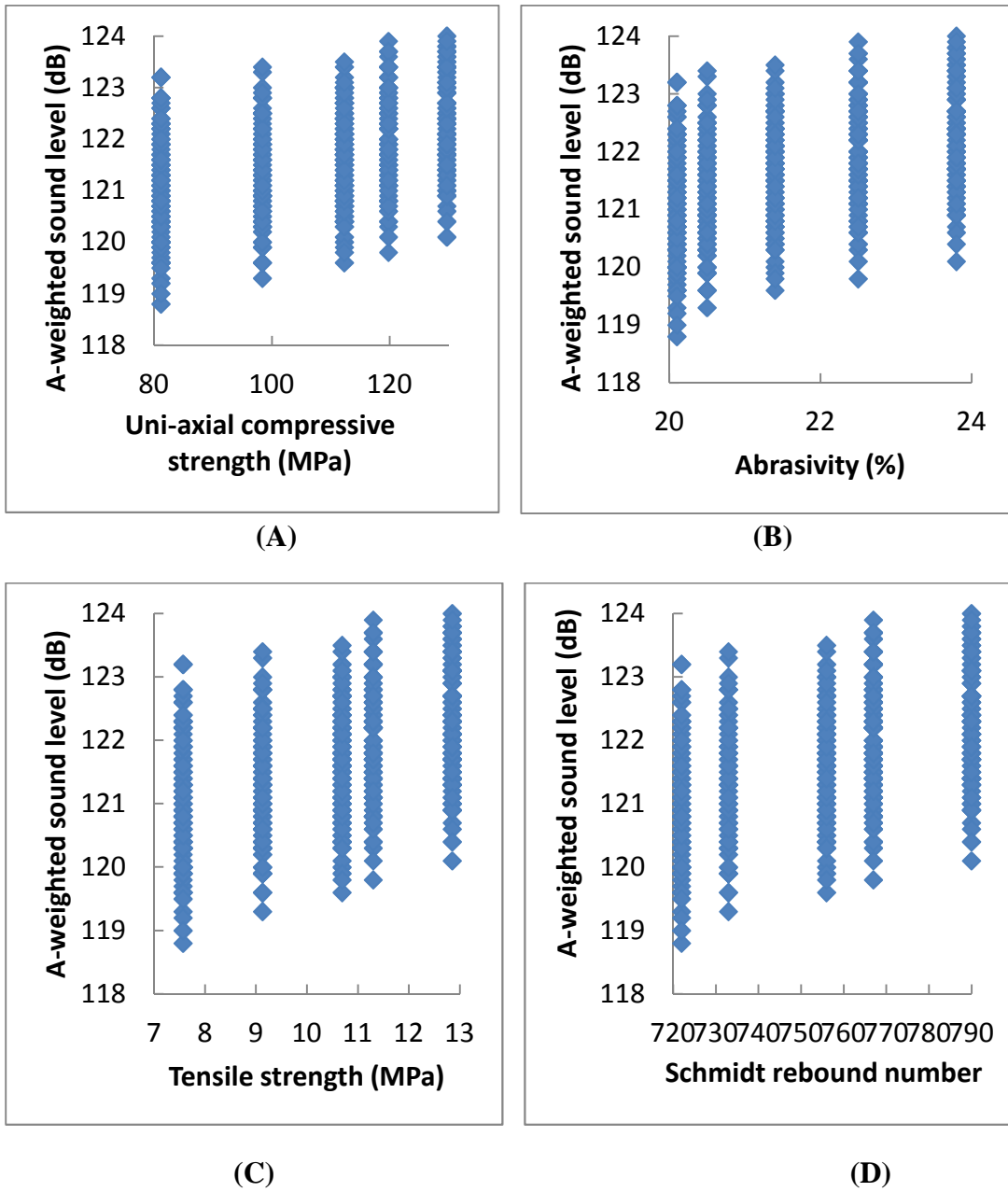**Fig. 3** Performance indices of (A) RMSE (B) VAF and (C) MAPE of MRA and ANN for igneous rock using threaded drill bit.

(A)

(B)

(C)

Fig. 4 Performance indices of (A) RMSE (B) VAF and (C) MAPE of MRA and ANN for igneous rock using threaded drill bi

Fig. 5 Variation of sound level with various rock properties of sedimentary rocks using integral drill bit diameters of 30, 34 mm

(A)

(B)

(C)

(D)
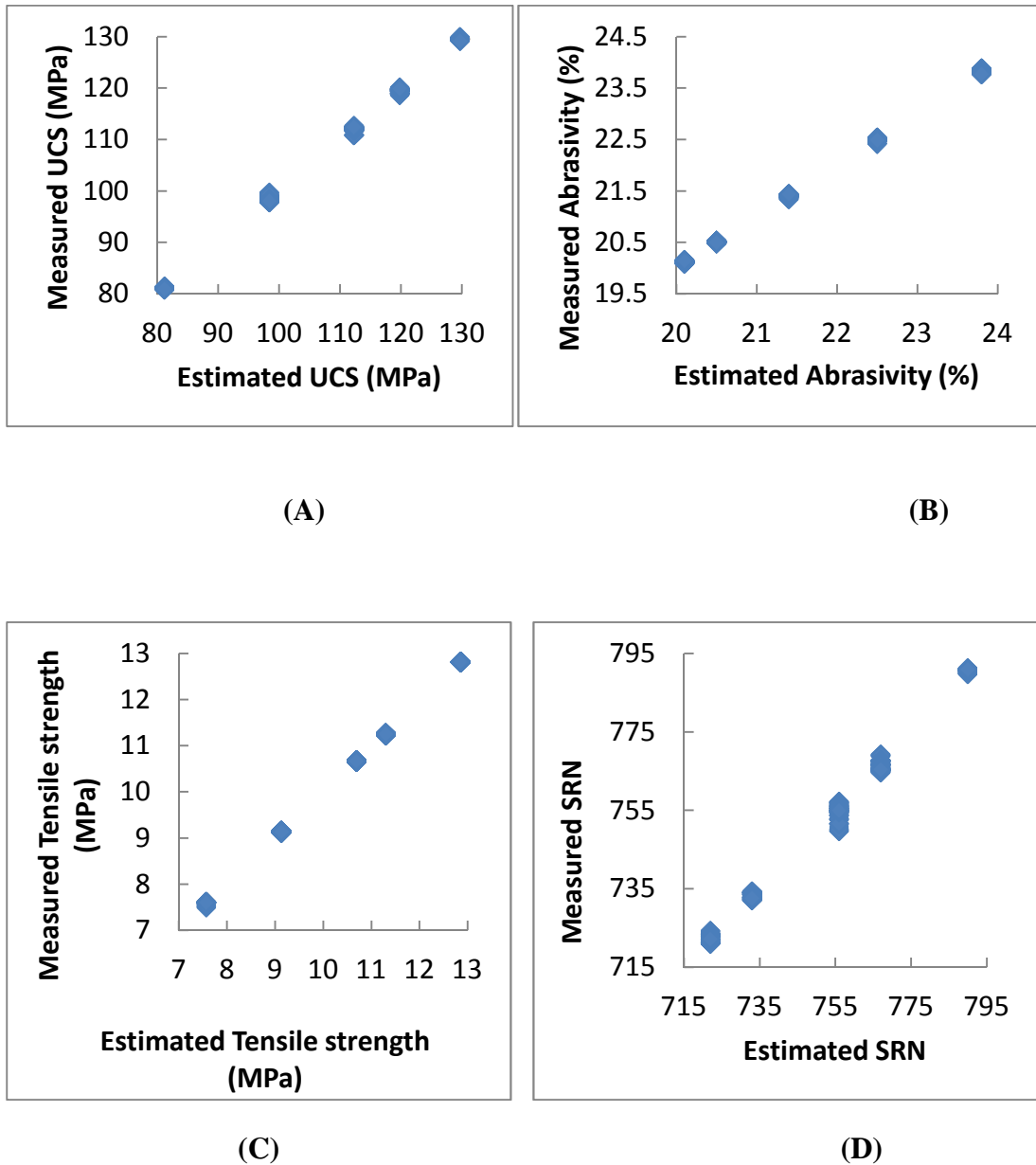
Fig. 6 Experimental mean values and ANN predicted mean values using trainlm algorithm for igneous rock using integral drill bit.

REFERENCES

Aljoe, W.W. (1984). "Quieted percussion drills." Proc.*, Bureau of Mines Technology Transfer Seminars*, Pittsburgh, PA, July 24 and Denver, Co. July 26, U.S. Bureau of Mines - Report of Information Circular No.8986, 75-89.

Aljoe, W.W., Stein, R.R. and Bartholomae, R.C. (1987). "Test apparatus for measuring sound power level of drills." *U.S. Bureau of Mines,* Information Circular No. 9166, 1-35.

Alvarez Grima, M. and Babuska, R. (1999). "Fuzzy model for the prediction of unconfined compressive strength of rock samples." *Int. J. Rock. Mech. Min. Sci.*36, 339–349.

Arzum C.E and Yalcin, K (2007). "Evaluating and forecasting banking crises through neural network models: An application for Turkish banking sector." *Expert Syst. Appl.*, 33, 809-815.

ASTM, (1984); "American Society for Testing and Materials standard test method for unconfined compressive strength of intact rock core specimens." Soil and Rock, Building Stones: *Annual Book of ASTM Standards*, 4.08. Philadelphia.

Bartholoame, R.C. and Stein, R.R. (1988). "Noise reducing technologies for newly designed mining percussion drills." *Proc. Noise-control* 88, 123-128.

Bartholomae, R. (1994). "Small Diameter In-the-Hole Percussion Drilling Tool for Percussion Drill Noise Control." *Proc. National Conference on Noise Control Engineering*, 175-180.

Barton, N. and Choubey, V. (1977). "The shear strength of rock joints in theory and practice." *Rock Mech.* 10, 1-54.

Beste, U. Jacobson, S. and Hogmark, S. (2007). "Rock penetration into cemented carbide drill buttons during rock drilling." *Wear,* 264, 1142-1151.

Bilgin, N (1983). "Prediction of roadheader performance from penetration rates of percussive drills some applications to Turkish coalfields." *Proc. of Eurotunnel 83 Conferences,* 111-114.

Boillat, P., Deqet, G, Drot, H, Marchal, J.P. (1993). "Les differentes techniques de-foration. Mines et Carrieres; *Les Techniques,* 36-70.

Bor-Ren L, Hof RG (2003). "Neural networks and fuzzy logic in power electronics." *Control Eng. Pract.,* 2, 113-121.

Brown E.T. (1981). "Rock characterization testing and monitoring." *International Society of Rock Mechanics (ISRM)* suggested methods. Oxford: Pergamon.

Cargill, J.S. and Shakoor, A. (1990). "Evaluation of empirical methods for measuring the uniaxial strength of rock." *International Journal of Rock Mechanics and Mining Sciences and Geomech. Abstr.,* 27(6), 495-503.

Champoux, Y., Oddo, R., Guigou, C. and Atalla, N. (1994). "On the Noise of Percus s ion Drill Steel Rods." *Proc. National Conference on Noise Control Engineering*, 169-174.

Chau, K.T. and Wong, R.H.C. (1996). "Uniaxial compressive strength and point load strength of rocks." *Int. J. of Rock Mech. and Min. Sci. and Geomech. Abstr.,* 33(2), 183-188.

Cheginia, G. R, Khazaeia J, Ghobadianb B, Goudarzic A. M. (2008). "Prediction of process and product parameters in an orange juice spray dryer using artificial neural networks." *J. Food Eng.,* 84, 534-543.

Chester, J. W, Dewoody, R. T, and Miller, W. C. (1964). "Noise from pneumatic rock drills-shape and exit noise of an exhaust muffler." U.S. Bureau of Mines - Report of Investigation No. 6450, 1-12.

Cohen, S. and Intrator, N. (2002). "Automatic model selection in a hybrid perceptron / radial network Information Fusion." *Special Issue on Multiple Experts,* 3(4), 259-66.

Cohen, S. and Intrator, N. (2003). "A study of ensemble of hybrid networks with strong regularization." *Multiple Classifier Systems*, 227–235.

Dewoody, R.T., Chester, J.W. and Miller, W.C. (1964). "Noise from pneumatic rock drills Analogy Studies of muffler Designs." *U. S. B. M,* Report of Investigation No. 6345, 1-12.

Dutta, P.K. (1972). "A theory of percussive drillbit penetration." *Int. J. Rock Mech. Min. Sci.,* 9, 543-67.

Finol, J., Guo, Y.K. and Jing, X.D. (2001). "A rule based fuzzy model for the prediction of petrophysical rock parameters." *Journal of Petroleum Science and Engineering,* 29, 97–113.

Fischer, H.C. (1962). "Noise control of pneumatic mining equipment." *Canadian Mining Journal,* 83, 75-85.

Fish, B. G. (1961). "The basic variables in rotary drilling". *Mine Quarry Eng.,* 27(1), 29-34.

Gehring, K.H. (1997). "Classification of drillability, cuttability, boreability and abrasivity." *In Tunn. Felsbau,* 15, 183-191.

Gokceoglu, C., (2002). "A fuzzy triangular chart to predict the uniaxial compressive strength of the Ankara Agglomerates from their petrographic composition." *Engineering Geology,* 66, 39-51.

Gorden, J. E. (1963). "Noise Suppression on rock drills." *Canadian Mining and Metallurgical Bulletin,* 56, 835-838.

Hakalehto, K.O. (1972). "Energy required to break rock by percussive drilling". *Proc. of the 14th Symposium on Rock Mechanics,* Pennsylvania State University, 613-21.

Harper, G.S. and O'Brien, T.M. (2006). "The prediction of underground drilling noise." *Journal of the South African Institute of Mining and Metallurgy*, vol.106, 533-543.

Hawkes, I. and Burks, J. A. (1979). "Investigation of noise and vibration in percussive drill rods." *International Journal of Rock Mechanics, Mineral Sciences and Geomechanics Abstracts,* 16, 363-376.

Hawkes, I., Wright, D.D.and Dutta, P. K. (1977a). "Development of a quiet rock drill.Volume 1: Evaluation of design Concepts." *Technical report 77-1 U.S. Bureau of Mines.*

Haykin S (1994). "Neural Networks: A Comprehensive Foundation." New York MacMillan.

Holdo, J. (1958). "Energy Consumed by Rock drill Noise." *The Mining Magazine*, 73-76.

Howarth, D.F. and Rowland, J.C. (1987). "Quantitative assessment of rock texture and correlation with drillability and strength properties." *Rock Mech. Rock Eng.* 20, 57-85.

Howarth, D.F. (1986). "Correlation of model tunnel boring and drilling machine performance with rock properties." *Int. J. Rock Mech. Min. Sci.*, 23, 171–5.

Huang N, Tan, K.K. and Lee T.H. (2008). "Adaptive neural network algorithm for control design of rigid-link electrically driven robots." *Neurocomputing,* 71, 885-894.

Hustrulid, W. A. and Fairhurst, C. (1971a). "A theoretical and experimental study of the percussive drilling of rock. Part I Theory of percussive drilling." *Int. J. Rock Mech. Min. Sci,.* 8, 11–33.

Hustrulid, W. A, and Fairhurst, C. (1971b). "A theoretical and experimental study of the percussive drilling of rock. Part II force penetration and specific energy determination." Int. J. Rock mech. Min. Sci., 8, 35-36.

Hustrulid, W. A, and Fairhurst, C. (1972a). "A theoretical and experimental study of the percussive drilling of rock. Part III Experimental verification of the mathematical theory." *Int. J. Rock Mech. Min. Sci.,* 9, 417–29.

Hustrulid, W. A. and Fairhurst, C. (1972b). "A theoretical and experimental study of the percussive drilling of rock. Part VI Application of the model to actual percussive drilling." *Int. J. Rock Mech. Min. Sci.,* 9, 431-49.

Jensen, J. W. and Visnapuu, A. (1972). "Progress in suppressing the noise of the pneumatic rock drill." *In Proc. Inter-Noise, 72,* 282-287.

Kahraman, S., Bilign, N. and Feridunoglu, C. (2003). "Dominant rock properties affecting the penetration rate of percussive drills." *Int. J. Rock. Mech. Min.Sci.,* 40, 711-723.

Kahraman, S. and Mulazimoglu, A. (1999). "The performance analysis of drill rigs used in the construction of Pozanti-Tarsus crossing motorway." *Madencilik..* 38(2-3), 31-35.

Kahraman, S., Balchi, C., Yazichi, S. and Bilgin, N. (2000). "Prediction of the penetration rate of rotary blast hole drills using a new drillability index." *Int. J. Rock Mech. Min. Sci.,* 37, 729-743.

Kahraman, S. (2001). "Evaluation of simple methods for assessing the uniaxial compressive strength of rock." *International Journal of rock Mechanics and Mining Sciences.,* 38, 981-994.

Kahraman, S. (1999). "Rotary and percussive drilling prediction using regression analysis." *Int. J. Rock Mech. Min. Sci.,* 36, 981-989.

Kahraman, S. (2002). "Correlation of TBM and drilling machine performances with rock brittleness." *Eng. Geol.,* 65, 269-283.

Kalogeria, S. (2000). "Applications of artificial neural networks for energy systems." *Appl Energy,* 67(2), 17-35.

Katz. O, Reches, Z. and Roegiers, J.C. (2000); "Evaluation of mechanical rock properties using a Schmidt Hammer." *Int. J. Rock. Mech. Min. Sci.,* 37, 723-728.

Kennedy, B. A. and Bruce A. Kennedy. (1990). "Mine Operations." *In Surface Mining,* 2nd Edition, 513-522.

Kenneth, J., Wernter, S. and MacInyre, J. (2001). "Knowledge extraction from radial basis function networks and multi layer perceptrons." *International Journal of Computational Intelligence and Applications,* 1(3), 369-382.

Kolaiti, E., Papadopoulus, Z. (1993). "Evaluation of Schmidt rebound hammer testing: a critical approach." *Bull. Int. Assoc. Eng. Geol. IAEG.,* 48, 69-76.

Koncagul, E.C. and Santi, P.M. (1999). "Predicting the unconfined compressive strength of the Breathitt shale using slake durability, shore hardness and rock structural properties." *Int. J. Rock. Mech. Min. Sci.,* 36(2), 139-153.

Lee, K., Booth, D. and Alam, P.A. (2005). "Comparison of Supervised and Unsupervised Neural Networks in Predicting Bankruptcy of Korean Firms." *J. Expert Systems with Applications,* 29, 1-16.

Leighton, J.C., Brawner, C.O. and Stewart, D. (1982). "Development of a correlation between rotary drill performance and controlled blasting powder factors." *Can. Inst. Min. Bull.* 844, 67-73.

Lemay, G. (1972). "Campaign quiets worst noise offenders." *Canadian Mining Journal,* 93, 59-60.

Lesage, C., Oddo, R., Champoux, Y. and Attalla, N. (1997). "Experimental Characteri zation of the Noise Generation Mechanism of Percussion Drill Rods." *CIM Bulletin,* 90(1010), 65-69.

Loh, W. and Tim, L. (2000). "A comparison of prediction accuracy, complexity, and training time of thirty three old and new classification algorithm." *Machine Learning,* 40(3), 203-238.

Lu, Y. (2005). "Underground blast induced ground shock and its modeling using artificial neural network." *Comput Geotech.* 32, 164-78.

Lundberg, B. (1982). "Microcomputer simulation of stress wave energy transfer to rock in percussive drilling." *Int. J. Rock Mech. Min. Sci.,* 19, 229-39.

Lundberg, B. (1985). "Microcomputer simulation of percussive drilling." *Int. J. Rock Mech. Min. Sci.,* 22, 237-49.

Magali, R.G.M. and Paul, E.M.A. (2003). "A comprehensive review for industrial applicability of artificial neural networks." *IEEE Trans. Ind. Electron.,* 50(3), 585-601.

Majdi, A., Beiki, M. (2010). "Evolving neural network using a genetic algorithm for predicting the deformation modulus of rock masses." *Int. J. Rock Mech. Min. Sci.,* 47 (2), 246-253.

Majors M., Stori, J. Dongil C (2002). "Neural network control of automotive fel-injection systems." *Control Syst. Mag. IEEE,* 14, 31-36.

McGregor, K. (1967). "The drilling of rock." *C.R. Books Ltd.,* London. Milette, L. (1989). "Bialan comparative du bruit emis par differents types de foreuses bequilles. *Rapport de I'* Universite de Sherbrooke.

Miller, R.P. (1965). "Engineering classification and index properties for intact rock." *Ph.D. Thesis,* University of Illinois.

Miller, W.C. (1963). "Noise from pneumatic rock drills-measurements and significance." U. S. Bureau of Mines-Report of Investigation No. 6165, 1-30.

Milette, L. (1989); "Bialan comparative du bruit emis par differents types de foreuses bequilles. Rapport de I' Universite de Sherbrooke, September.

Miranda. A, and Mello-Mendes, F. (1983). "Drillability and drilling methods." *In: Proc. of the Fifth Congress International Society on Rock Mechanics,* Melbourne, 5, 195-200.

Myer, R. and Montgomery, D.C. (2002). "Response surface methodology." *John Wiley,* New York.

Niyazi Bilim (2011). "Determination of drillability of some natural stones and their association with rock properties." *Scientific Research and Essays* Vol. 6(2), 382-387.

Onan, M, and Muftuoglu, Y.V. (1993). "A study of drill parameters and penetration rates relationships in Gelik–44 borehole." 13th *Mining Congress* of Turkey, 221-234.

Palchik, V. (1999). "Influence of porosity and elastic modulus on uniaxial compressive strength in soft brittle porous sandstones." *Rock Mech. Rock Eng.* 32(4), 303-309.

Pandey, A.K., Jain, A.K. and Singh, D.P. (1991). "An investigation into rock drilling." *Int. J. Surface Min. Recl.,* 5, 139-141.

Paone, J. and Madson, D. (1966). "Drill ability studies: Impregnated Diamond Bits." *U. S. Bureau of Mines* Report of Investigations, RI 6776, 16.

Paone, J. D. Madson, and Bruce, W. E. (1969); "Drill ability studies-Laboratory percussive drilling." *Bu. Mines RI* 7300, 22.

Pathinkar, A G., and Misra, G. B. (1976). "A Critical Appraisal of the Protodyakonov Index." *International Journal of Rock Mechanics and Mineral Sciences,* 13, 249-251.

Pathinkar, A. G. and Misra, G. B. (1980). "Drill ability of rocks in percussive drilling from energy per unit volume as determined with a microbit." *Min. Eng.* 32, 1407-10.

Peranbur N.S, Preechayasomboon, A. (2002). "Development of a neuroinference engine for ADSL modem applications in telecommunications using an ANN with fast computational ability." *Neurocomputing,* 48, 423-441.

Powell, W. H. (1956); "The assessment of noise at collieries", *Transactions of the Institution of Mining Engineers,* 116, 22-42.

Protodyaknov, M.M. (1962). "Mechanical properties and drillability of rocks." *Proce. of the Fifth symposium on Rock Mechanics,* Minneapolis, MN: University of Minnesota, 103-18.

Rabia, H. and Brook W. (1980). "An Empirical Equation for Drill Performance Prediction." *Proc. of the 21st U.S. Symposium on Rock Mechanics,* University of Missouri.

Rajesh Kumar, B., Vardhan, H. and Govindraj, M. (2010). "Estimating rock properties using sound level during drilling: Field investigation." *International Journal of Mining and Mineral engineering*. 2(3), 169-184.

Rajesh Kumar, B., Vardhan, H. and Govindraj, M. (2011). "Prediction of uniaxial compressive strength, tensile strength and porosity of sedimentary rocks using sound level produced during rotary drilling." *Rock Mechanics and Rock Engineering,* 1-8.

Reeves, E. R. (2005). "Assessment of noise controls commonly used on Jumbo drills and Bolters in Western United States Underground metal mines." *Mining Engineering* (USA), 41-47.

Reynolds, J. W. (1964). "Noise control at the Sullivan Mine." *The Canadian Mining and Metallurgical Bulletin.* LXV11, 13-16.

Rumelhart, D. and McClelland, J. (1986). "Parallel distributed processing: explorations in the microstructure of cognition." *Bradford books*, MIT Press, Cambridge.

Savich, M.U. and Wylie, J. (1975). "Noise attenuation in rock drills." *Canadian Mining journal,* 96, 39-42.

Savich, M.U. (1982). "Abatement of noise and Vibration in the Canadian Mining Industry." *Canadian Mining Journal*, 103, 31-38.

Schliesing, (1978). "Noise reduction in roadway drivage." Gluckauf, Vol. 114, 524-525.

Schmidt, E. (1951). "A non-destructive concrete tester." *Concrete* 59(8), 34-35.

Schmidt, R.L. (1972). "Drillability studies-Percussive drilling in the field." U.S.B.M. RI 7684.

Schneider, H. (1988), "Criteria for selecting a boom-type roadheader." *Min.Mag.,* 183-187.

Selim, A. and Bruce, W.E. (1970). "Prediction of penetration rate for percussive drilling." *U.S.B.M.* R.I. 7396

Simpson, P. K. (1990). "Artificial neural system foundation, paradigm, application and implementation." *Pergamon Press,* New York.

Singh, D. P. (1969). "Drillability and Physical Properties of Rocks." *Proc. of the Rock Mechanics Symposium*, University of Sydney.

Singh, T. N., Kanchan, R., Verma, A. K., Singh, S. (2003). "An intelligent approach for prediction of triaxial properties using unconfined uniaxial strength." *Min. Eng. J.* 5, 12-16.

Singh, V. K., and Singh, D. P. (1993). "Correlation between point load index and compressive strength for quartzite rocks." *Geotech. Geol. Engineering,* 11(4), 269-272.

Srivastava, M. S. (2002). "Methods of multivariate statistics". John Wiley, New York, 728.

Stein, R. R. and Aljoe, W. W. (1989). "Noise Test Report: Handheld Pneumatic Rotary Drill." *U. S. Bureau of Mines* Report of Investigation No. 9269, 1-11.

Tadanand, S and Unger, H. F. (1975). "Drillability determination - A drillabilty index of percussive drills." *U. S. B. M.* RI 8073.

Thuro, K. and Pliinninger, R. J. (1999). "Predicting roadheader advance rates." *Tunnels Tunn. Int.,* 36-39.

Tu J.V. (1996). "Advantages and disadvantages of using artificial neural networks versus logistic regression in predicting medical outcomes." *J. Clin. Epidemiol,* 49, 1225-1231.

Tugrul, A. and Zarif, I. H. (1999). "Correlation of mineralogical and textural characteristics with engineering properties of selected granitic rocks from Turkey. *Engineering Geology,* 51(4), 303-317.

Turner. S. K. (1986). "Noise control in the South Midlands Area." *The Mining Engineer,* Paper No. 5030, 289-294.

Vallejo, L. E., Welsh, R. A., and Robinson, M. K. (1989). "Correlation between unconfined compressive and point load strengths for Appalachian rocks." *In: Proc. 30ᵗʰ U. S. Symposium on Rock Mechanics* as a Guide for Efficient Utilization of Natural Resources, Morgantown, 461-468.

Vardhan, H., Adhikari, G. R. and Govnda Raj, M. (2009). "Estimating rock properties using sound levels produced during drilling." *International Journal of rock mechanics and Mining sciences,* 46 (3), 604 - 612.

Vardhan, H. and Murthy, Ch. S. N., (2007). "An experimental investigation of Jack Hammer drill noise with special emphasis on drilling in rocks of different compressive strength." *Noise control Engineering Journal,* 55(3)*,* 282-293.

Venkatesan, P. and Anitha, S. (2006). "Application of a radial basis function neural network for diagnosis of diabetes mellitus." *Current Science,* 91 (9), 1195-1199.

Visnapuu, A. and Jensen, J. W. (1975). "Noise reduction of a pneumatic rock drill." *U. S. Bureau of Mines*-Report of Investigation No. 8082, 1-23.

Walker, A. (1963). "Noise-Its effect and control in mining operations." *The Mining and Metallurgical Bulletin,* November, 820-834.

Wallace, A.W. (1964). "Rock drill noise-an approach." *Canadian Mining and Metallurgical Bulletin,* 57, 1038-1041.

Xiaotian Z, Hong Wang X, Li L, Li H (2008). "Predicting stock index increments by neural networks: The role of trading volume under different horizons". *Expert Syst. Appl.,* 34, 3043-3054.

Xu, G., Grasso, P., and Mahtab, A. (1990). "Use of Schmidt hammer for estimating mechanical properties of weak rock." *In Proc. of 6ᵗʰ Int. IAEG Congress*, ed. Price, D.G., 511-519. Rotterdam: Balkema.

Yenice, H., Ozfirat, M.K., Karaca, Z. (2009). "Investigation of the parameters effecting drilling rate index (DRI) of marbles." *Proc. of the 2nd Mining Machinery Symposium* of Turkey, 4-6 November, 233-246.

Yilmaz, I., and Yuksek, A.G. (2009). "Prediction of the strength and elasticity modulus of gypsum using multiple regression, ANN, ANFIS models and their comparison." *International Journal of Rock Mechanics and Mining Sciences,* 46(4), 803–810.

Yilmaz, I. and Yuksek, A.G. (2008). "An example of artificial neural network application for indirect estimation of rock parameters." *Rock Mechanics and Rock Engineering,* 41(5), 781-795.

Yılmaz, I., Sendir, H. (2002). "Correlation Schmidt hardness with unconfined compressive strength and Young's modulus in gypsum from Sivas (Turkey)." *Eng. Geol.* 666, 211–219.

Zhang L, Jiang JH, Liu P, Liang YZ, Yu RQ (1997). "Multivariate nonlinear modeling of fluorescence data by neural network with hidden mode pruning algorithm." *Analytica Chimica Acta*, 344, 29-39.

LIST OF PUBLICATIONS

RESEARCH PUBLICATIONS (International/National journals):

1. Kivade, S. B., Murthy, Ch. S. N., Harsha Vardhan (2012), " Prediction of penetration rate and sound level produced during percussive drilling". International Journal of Mining and Mineral Processing. Vol. 3, No. 1, pp: 13-20

2. Kivade, S. B., Murthy, Ch. S. N., Harsha Vardhan (2012), "The use of dimensional analysis and optimization of pneumatic drilling operations and operating parameters". Journal of the Institution of Engineers (India) Series-D 93(1):31–36. (Springer).

3. Kivade, S. B., Murthy, Ch. S. N., Harsha Vardhan (2012), "Prediction of penetration rate and sound level produced during percussive drilling using regression and artificial neural network". International Journal of Earth Science and Engineering. ISSN 0974-5904, Vol. 05, No. 06, pp. 1639-164

4. Kivade, S. B., Murthy, Ch. S. N., Harsha Vardhan (2012), "Central composite design in optimization of the pneumatic drilling operations and operating parameters". International Journal of Mining and Mineral Processing. Vol. 3, No. 1, pp: 21-27.

5. Kivade, S. B., Murthy, Ch. S. N., Harsha Vardhan (2011), "Assessment of noise and effect of thrust on penetration rate in percussive drilling". The Institution of Engineers India. Volume-91, pp. 3-7.

6. Kivade, S. B., Murthy, Ch. S. N., Harsha Vardhan (2011), "Study of noise sources in pneumatic rock drills-its effect and control a critical review". The Indian Mining and Engineering journal. Vol .50, No. 01. pp. 12-23.

7. Kivade, S. B., Ch.S. N. Murthy, and Harsha Vardhan: "Investigation of noise level and penetration rate of pneumatic drill vis-à-vis rock compressive strength and abrasivity". Journal of the South African Institute of Mining and Metallurgy. (Accepted for Publication).

8. Kivade, S. B., Murthy, Ch. S. N., Harsha Vardhan "Laboratory investigations on percussive drilling". Journal of the Institution of Engineers (India) Series-D (Springer Accepted for Publication)

PUBLICATIONS IN CONFERENCE /SYMPOSIUM:

9. Kivade, S. B., Murthy, Ch. S. N., Harsha Vardhan, "Rock Drill Noise and its Control", Institute of Engineers (India) (Mysore local centre) Modern Trends in Mechanical Engineering MTME–2010 held during 24th-25th September 2010, Pp.337-344.

10. Kivade, S. B., Murthy, Ch. S. N., Harsha Vardhan, "Assessment and Control of Noise in Pneumatic Drills". International Symposium on Emerging Trends in Environment, Health and Safety Management in Mining and Mineral Based Industries" held during 21st - 22nd August, 2010, PP. 356-361.

11. Kivade, S. B., Murthy, Ch. S. N., Harsha Vardhan, "A Critical Review on Assessment and Control of Noise in Percussive drilling" National Seminar on Synergy in Mineral Sector for Sustainable Development-Vision 2020 held during 4th -5th Oct 2008, PP.132-139.

CURRICULUM VITAE

CAREER VISION: To work in a challenging environment demanding all my skills and efforts to explore and adapt myself in different fields and realize my potential where I get the opportunity for continuous learning.

NAME	: SANGSHETTY B. KIVADE

PERMANENT ADDRESS   : C/o S. V. Patil

                                             H. No. 8-9-91, Trupti Nivas

                                             Jail Colony, Udgir Road,

                                             Bidar-585 401

                                             Karnataka, India

                                             Mobile No.: 09449577015,

                                             Email: sbkivade@gmail.com,

DATE OF BIRTH   : 07/06/1970

ACADEMIC QUALIFICATIONS:

1. M.Tech (Production Management), Basveshwar Engineering College Bagalkot (KS), 2001, Visvesvaraya Technological University, Belgaum.

2. Bachelor of Engineering (I & P), P. E. S. College of Engineering Mandya, 1993, Mysore University, Mysore

RESEARCH PUBLICATIONS (International/National journals):

1. Kivade, S. B., Ch. S. N. Murthy, and Harsha Vardhan: "Prediction of penetration rate and sound level produced during percussive drilling". International Journal of Mining and Mineral Processing. Vol. 3, No. 1, Jan-June 2012. pp: 13-20

2. Kivade, S. B., Ch. S. N. Murthy, and Harsha Vardhan: "Central composite design in optimization of the pneumatic drilling operations and operating parameters:. International Journal of Mining and Mineral Processing. Vol. 3, No. 1, Jan-June 2012 pp: 21-27.

3. Kivade, S. B., Ch. S. N. Murthy, and Harsha Vardhan: "Prediction of penetration rate and sound level produced during percussive drilling using regression and artificial neural network". International Journal of Earth Science and Engineering. ISSN 0974-5904, Vol. 05, No. 06, December 2012 pp. 1639-164

4. Kivade, S. B., Ch. S. N. Murthy, and Harsha Vardhan: "Investigation of noise level and penetration rate of pneumatic drill vis-à-vis rock compressive strength and abrasivity". Journal of the South African Institute of Mining and Metallurgy. (Accepted for Publication).

5. Kivade, S. B., Ch. S. N. Murthy, and Harsha Vardhan: "The use of dimensional analysis and optimization of pneumatic drilling operations and operating parameters". Journal of the Institution of Engineers (India) Series-D (April-Sept.2012) 93 6(1):31–36. (Springer)

6. Kivade, S. B., Ch. S. N. Murthy, and Harsha Vardhan: "Study of noise sources in pneumatic rock drills-its effect and control a critical review". The Indian Mining and Engineering journal. Vol .50, No. 01. January 2011. pp. 12-23.

7. Kivade, S. B., Ch. S. N. Murthy, and Harsha Vardhan: "Assessment of noise and effect of thrust on penetration rate in percussive drilling". The Institution of Engineers India. Volume-91, February 2011.pp. 3-7.

8. Kivade, S. B., Ch. S. N. Murthy, and Harsha Vardhan: "Laboratory investigations on percussive drilling". Journal of the Institution of Engineers (India) Series-D (Springer Accepted for Publication)

PUBLICATIONS IN CONFERENCE /SYMPOSIUM:

9. Kivade, S. B., Ch. S. N. Murthy, and Harsha Vardhan "Rock Drill Noise and its Control", Institute of Engineers (India) (Mysore local centre) Modern trends in Mechanical Engineering MTME–2010 held during 24th-25th September 2010, Pp.337-344.

10. Kivade, S.B., Ch. S. N. Murthy, and Harsha Vardhan "Assessment and control of

Noise in Pneumatic Drills". International Symposium on Emerging Trends in Environment, Health and Safety Management in Mining and Mineral Based Industries" held during 21st - 22nd August, 2010, PP. 356-361.

11. Kivade, S. B., Ch. S. N. Murthy, and Harsha Vardhan "A Critical Review on Assessment and Control of Noise in Percussive drilling" National Seminar on Synergy in Mineral Sector for Sustainable Development-Vision 2020 held during 4th-5th Oct 2008, PP.132-139.

Place: Basavakalyan   **Yours Sincerely**

                                           SANGSHETTY KIVADE

232